CAUSES AND CONSEQUENCES OF GENOMIC INSTABILITY IN PROSTATIC CARCINOGENESIS

By

Anthony Michael Joshua

A thesis submitted in conformity with the requirements for the degree of

Doctor of Philosophy

Graduate Department of Medical Biophysics

University of Toronto

CAUSES AND CONSEQUENCES OF GENOMIC INSTABILITY IN PROSTATIC CARCINOGENESIS

By Anthony Michael Joshua

Doctor of Philosophy

2009

Department of Medical Biophysics

University of Toronto

ABSTRACT

The evolution of prostate cancer from normal epithelium via the preneoplastic lesion of high-grade prostatic intraepithelial neoplasia to invasive carcinoma is characterised by a number of particular genomic abnormalities that are predominantly generated in the preneoplastic phase. Whilst there are numerous candidates for the cause of these alterations, telomere dysfunction is thought to be a major contributor. Telomeres are the terminal ends of human chromosomes, and when dysfunctional can lead to break-fusion-bridge cycles and multi-polar mitoses that generate numerical and structural chromosomal instability.

The results presented reinforce the association of telomere dysfunction with the generation of certain markers of genomic instability such as abnormalities of the arms of chromosome 8. Furthermore, this work clarifies that the TMPRSSS2-ERG aberrations are not telomere related phenomena and are associated with a genomic deletion in a proportion of cases. Similarly, the *PTEN* microdeletions did not appear to have an association with telomere attrition. A previously unrecognised association between the telomere length in various types of prostatic epithelia and

adjacent stroma is defined, suggesting evidence of a micro-environmental field effect in the generation of prostatic neoplasia. Finally, when examined retrospectively, it appears that telomere attrition, both in the HPIN epithelium and the stroma has independent prognostic value in the diagnosis of prostate cancer after a previous diagnosis of HPIN.

Taken together, the research presented suggests important avenues for further research to determine the nature of barriers to the evolution of prostatic carcinogenesis such as oncogene- and telomere-induced senescence that may be exploited for therapeutic gain. These understandings may also help tailor management for prostate cancer such as risk stratification for men with HPIN and the use of targeted agents such as AKT inhibitors and telomerase inhibitors. In more advanced disease, translational application of this work has enabled a clinical trial of cytarabine in the treatment of metastatic hormone refractory prostate cancer.

ACKNOWLEDGEMENTS

My first extension of gratitude is to my wonderful wife, Elly. I am dependent on her companionship, thoughtfulness, love and encouragement. We reach greater heights together than we ever could apart, and I can't imagine not having you by my side forever.

My parents have devoted incredible time and effort into preparing me for my ongoing education and professional career. Your guidance and love were very much appreciated.

I would like to acknowledge the supervision, contribution and diligence of my supervisor, Dr Jeremy Squire in the preparation of this thesis and the task of moulding me into a scientist. The assistance and advice of Dr Maria Zielenska was also invaluable over the last 4 years. My committee members Dr Ian Tannock, Dr Lea Harrington and Dr Mona Gauthier have been instrumental in guiding this work to its completion.

I would also like to thank my colleagues Dr Bisera Vukovic, Dr Maisa Yoshimoto, Jane Bayani, Paula Marrano, Dr Shamini Selvarajah, Ilan Braude, Jana Paderova, Dr Georges Maire, Dr Khaldoun Alromiah, Dr Bekim Sedokovic and Olga Ludkovski for their advice and support.

Finally, I would like to thank the Department of Medical Oncology for its generous support throughout my fellowship.

TABLE OF CONTENTS

LIST of TABLES

LIST OF FIGURES

LIST OF ABBREVIATIONS

Abbreviation	Expansion
aCGH	Array Comparative Genomic Hybridization
AMACR	Alpha-methylacyl-CoA racemase
APC	Adenomatous Polyposis Coli
AR	Androgen Receptor
BFB	Break-Fusion-Bridge
BPH	Benign Prostatic Hyperplasia
BRFS	Biochemical Recurrence Free Survival
CaP	Carcinoma of the Prostate
CAV1	Caveolin 1
CCND2	Cyclin 2
CDH1	E-Cadherin
CDH13	Cadherin 13
CDKN2A	Cyclin Dependent Kinase Inhibitor
CEP	Centromere Specific FISH probe
CGH	Comparative Genomic Hybridization
CIC	Cancer Initiating Cell
CRBP1	Cellular retinol binding protein
Cy	Cyanine
CZ	Central Zone
DAB2IP	DAB2 interacting protein
DAPI	4',6-diamidino-2-phenylindole
DAPK1	Death Associated Protein Kinase 1
DCIS	Ductal Carcinoma In Situ
DNA	Deoxyribonucleic Acid
EDNRB	Endothelin Receptor B
EMT	Epithelial to Mesenchymal Transition
EPCA	Early Prostate Cancer Antigen
ESR	Estrogen Receptor
FISH	Fluorescence In-Situ Hybridization
FTIC	Fluorescein isothiocyanate
GSTP1	Glutathione S-transferase pi 1
HPIN	High-Grade Prostatic Intraepithelial Neoplasia
HRPC	Hormone Refractory Prostate Cancer
LAMA3	Laminin, alpha 3
LAMB3	Laminin, beta 3
LAMC2	Laminin, gamma 2
LCM	Laser Capture Microdissection
LGPIN	Low-Grade Prostatic Intraepithelial Neoplasia
LOH	Loss of Heterozygosity
MGMT	O-6-methylguanine-DNA

	methyltransferase
mRNA	messenger Ribonucleic Acid
OIS	Oncogene Induced Senescence
PAP	Prostatic Acid Phosphatase
PCR	Polymerase Chain Reaction
PIA	Prostatic Inflammatory Atrophy
PNA	Peptide Nucleic Acid
PSA	Prostate Specific Antigen
PZ	Peripheral Zone
qFISH	Quantitative Fluorescence In-Situ Hybridization
RARB	Retinoic acid receptor Beta
RARRES	Retinoic acid receptor responder
RASSF1	RAS association domain family protein
RNA	Ribonucleic Acid
SKY	Spectral Karyotyping
STELA	Single Telomere Length Analysis
TMA	Tissue Microarray
TMS1	Target of methylation-induced silencing
TRF	Terminal Restriction Fragment
TZ	Transition Zone
UPA	Urokinase
XAF1	XIAP associated factor-1

1. BACKGROUND

SUMMARY

Prostate cancer is a heterogeneous neoplasm both with regard to its development, molecular abnormalities and clinical course. Here, we summarise novel understandings of the early molecular events in prostatic carcinogenesis that may underlie both the molecular and clinical heterogeneity. Issues covered include those related to stem cells and embryonic signalling, oncogene/tumor suppressor abnormalities, androgen signalling, apoptosis and the nature of tumor-stromal interactions. Emphasis is placed on signalling pathway abnormalities, their causation, consequences and interactions. For example, genomic abnormalities involving the *TMPRSS2-ETS* and *PTEN* loci and the resulting signalling effects suggest the importance of genomic instability as a crucial factor in the emergence of this neoplasm. Together with new insights into signalling pathways consequent to abnormalities such as these, a greater understanding of the pathophysiology involved in prostatic carcinogenesis will lead to targeted approaches for both therapy and chemoprevention in the future.

BASED ON WORK IN;

Joshua AM, Evans A, Van der Kwast T, Zielenska M, Meeker AK, Chinnaiyan A, Squire JA., Prostatic preneoplasia and beyond., Biochim Biophys Acta. 2008 Apr;1785(2):156-81.

1.1 Introduction

Prostate cancer is the most commonly diagnosed malignancy in men in North America, with over two hundred thousand cases expected to be diagnosed in 2008 alone (1, 2). It is also a heterogeneous neoplasm with regard to its development, molecular abnormalities and clinical course. For example, in western populations, 1 in 6 men are diagnosed with prostate cancer whilst only 1 in 34 die of metastatic disease (3). Understanding the basis of this clinical heterogeneity is of fundamental importance as if detected while still organ-confined, prostate cancer can be potentially cured by either a surgical procedure (radical prostatectomy) or radiotherapy. However, not all men require curative treatments due to the frequent slow course of this disease and competing morbidity and mortality. Therefore, there is a clear need for further research to discover the pathological mechanisms behind prostatic carcinogenesis that may lead to improved prognostic and predictive biomarkers that will amy lead to tailored treatment for the men who suffer from this disease.

1.2 Histology and Neoplastic pathology of the prostate gland

The prostate is a walnut-sized glandular structure, whose main function relates to the secretion of fluid to provide nutritional support to semen. The prostatic epithelium is made up of four major cell types; secretory, basal, transient amplifying (an intermediate between the previous two (4) and neuroendocrine cells. The secretory cells line the prostatic glands and ducts and are responsible for the physiological secretions of the gland. The basal cells are much less abundant and rest on the basement membrane adjacent to the basal aspect of the secretory cells. Their absence is a useful marker of prostate cancer. Neuroendocrine cells are scattered throughout the gland and are believed to be involved in the regulation of prostatic secretory

activity and cell growth. The prostate is supported by a stroma composed of smooth muscle cells, fibroblasts, lymphocytes and neurovascular tissue in a supporting extra-cellular matrix.

There are three anatomical prostatic glandular zones: the peripheral (PZ), the transitional (TZ), and the central zone (CZ). Benign prostatic hypertrophy (BPH) occurs almost exclusively within the TZ of the prostate, and up to 80% of men aged 70–80 years have histological evidence of BPH (5). Most prostate cancers occur in the PZ, at the dorsal and dorso-lateral side of the prostate; only <30% of prostate cancers consist of TZ tumors, they have lower biochemical recurrence rates and are less malignant than tumors originating in the PZ (6).

1.3 Preneoplastic lesions of the prostate

Currently, high-grade prostatic intra-epithelial neoplasia (HPIN) is considered most likely to represent a forerunner to prostate cancer (CaP) on the basis of pathological (7), epidemiological (8, 9) and cytogenic (10) evidence.

HPIN is characterised by architecturally benign prostatic acini and ducts, lined by cytological atypical cells. The cytological changes are characterized by prominent nucleoli in a substantial proportion (≥5%) of cells, nuclear enlargement, nuclear crowding, an increased density of the cytoplasm, and variation in nucleolar size. HPIN lesions can be subdivided into four different architectural patterns; tufted, micropapillary, flat and cribiform (11). Unlike CaP, however, HPIN is confined to the gland by intact basement membrane and a well-defined basal cell layer.

Pathologically, HPIN and CaP are correlated; HPIN can be found in up to 70-80% of prostate glands that show presence of carcinoma (12). The volume of HPIN in a prostate is related to tumor stage and Gleason grade (7) as well as the risk of relapse (13, 14). HPIN is multifocal and situated mainly in the PZ of the gland (7, 8, 12, 15). Additionally, there are

similarities in their epidemiology; the incidence of HPIN is found to increase with age and to precede cancer initiation by at least 5 years. It is theorised that about 1/3 of cases with HPIN will progress to CaP within 10 years(16).

Analyses of co-existent HPIN and prostate cancer demonstrate similar chromosomal abnormalities such as the characteristic loss of chromosome 8p and gain of chromosomes 8q, 7, 10q and Xq (17, 18). Indeed, recent microarray evidence has suggested that the majority of the alterations in expression of genes that occur during disease progression occur in the transition from benign epithelium to HPIN rather then from HPIN to prostate cancer (19) (see Figure 1.3).

An alternative, possibly earlier, precursor of CaP is proliferative inflammatory atrophy (PIA). PIA is defined by discrete foci of proliferative glandular epithelium with the morphological appearance of simple atrophy (20) or postatrophic hyperplasia (21) occurring in association with inflammation. The key features of this lesion are the presence of two distinct cell layers, mononuclear and/or polymorphonuclear inflammatory cells in both the epithelial and stromal compartments, and stromal atrophy with variable amounts of fibrosis. PIA is proposed to be a common proliferative response to environmental damage such as inflammation and oxidant stress in aging men. Subsequently, HGPIN and prostate cancer lesions are thought to arise as a consequence of the genome damage (22, 23). Pathological evidence linking CaP and HPIN with PIA are mixed (24-30). Recent expression array profiling suggested that PIA may only be a very early precursor, or unrelated, to prostate cancer development (19). However, PIA does express molecular signals of early neoplastic transformation such as GSTP1 hypermethylation (31), increased GSTA1 and COX-2 (32, 33), reduced NKX3.1 expression (34), early chromosomal abnormalities (35), elevated Bcl-2 (36) and telomere shortening (37). Thus, although both the aetiological and pathological observations suggest the involvement of PIA in prostatic carcinogenesis, further study is needed.

1.4 Morphological context of carcinogenesis within the prostate

Originally proposed in the context of oral cancer by Slaughter *et al*., (38) field carcinogenesis describes a concept whereby clinically occult multifocal preneoplastic foci emerge within the epithelium of an anatomic region exposed to the same carcinogen(s). These lesions may not be apparent at histological examination but molecular techniques for detecting carcinogenic alterations such as p53 loss, loss of heterozygosity and microsatellite instability have found evidence of such change in a variety of epithelial neoplasms and surrounding epithelia (39, 40). Notably, such a concept is often absent in discussion about the nature of prostatic carcinogenesis despite the fact that 80% of radical prostatectomy specimens demonstrate more than one (average five) neoplastic foci (41, 42) and the occurrence of multicentric HPIN in approximately 70% of radical prostatectomies (7). There is strong evidence to suggest that prostate cancer is not derived from a single precursor cell; both markers of allelic imbalance (43) (44-46)and more recently analyses of *TMPRSS2-ETS* fusion genes suggest the emergence of independent foci throughout the peripheral zone in multiple studies(47, 48).

As with other neoplasms, these foci of genetic change may extend further from a preneoplastic or neoplastic focus than can be appreciated by traditional histology; markers associated with neoplastic progression such as AMACR (49, 50), EPCA (51), Akt-1 (52), GST-Pi, telomerase (53), altered proliferation/ apoptosis (54) and nuclear morphology (53, 55) have all been found to be altered in normal epithelium surrounding a neoplastic focus. Indeed, expression microarray studies have found 70% similarity in the genetic profile between tumor samples and prostatic tissue adjoining the tumors (49).

Traditionally, field carcinogenesis referred only to the epithelial component of the relevant organ, however, there is emerging evidence that prostatic stroma is affected by the

prostatic milieu either as a primary or secondary phenomena; For example, hypermethylation of GSTPi and RARB2 were found in a subset of histologically normal appearing stroma from radical prostatectomy specimens (56).

The above findings suggests that the PZ of the prostate is likely subject to multiple etiological factors leading to the emergence of a field effect of carcinogenesis. The selective nature of the carcinogenic insult that leads to effects predominantly in the PZ remain unclear; however regional differences in sex steroid metabolism (57), dietary carcinogen and inflammation localisation (22) or a differential between proliferative and apoptotic indices have been suggested(58).

1.5 Prostate Cancer and Stem Cells

Traditional stochastic theories of carcinogenesis predicted that every cell within a tumor can form a new primary tumor, and this understanding formed the basis for most tumor therapies to the present day (59). Recently, more interest has been placed on the stem cell model of carcinogenesis that predicts that only a subset of tumor cells have replicative potential that are often defined on their ability to repopulate tumor growth in serial transplantation models (60). This cancer stem cell hypothesis represents a modern-day interpretation of the proposal made by pathologists such as Rudolph Virchow and Julius Cohnheim 150 years ago that cancer results from the activation of dormant embryonic-tissue remnants (61, 62). This idea, subsequently refined by Till and McCulloch (63), and experimentally verified by Dick and colleagues (64), suggests that these self-renewing cancer “stem cells” or cancer initiating cells (CICs) are organ-specific cells that have the biologic property of self-renewal and with each division to produce both progenitor cells and at least 1 offspring that maintains the stem cell phenotype in a regulated manner.

Whilst stem cell research is most developed in hematologic malignancies, recent identification of putative CICs in various solid malignancies (65-68) has been reported. Several lines of evidence suggested the normal prostate stem cell lies within the basal compartment (69), and a recent candidates for a murine prostate CIC has recently been identified (70) as a Lin(-)Sca-1(+)CD133(+)CD44(+)CD117(+) cell. Ultimately, the characterisation of CICs and the nature of their involvement in human prostatic carcinogenesis hold great potential for understanding carcinogenesis but much validation remains to be done (recently reviewed in (71-73)).

1.6 PRO-CARCINOGENIC FACTORS

1.6.1 Embryonic signalling cascades

The regulation of stem cells and in particular their dysregulation in prostate cancer is thought to occur through a relatively small number of signalling pathways such as Hedgehog and Wnt (74). These pathways are all likely to be co-regulated to maintain stem cell homeostasis and their dysregulation may be crucial to the emergence of a dedifferentiated phenotype (75-77).

1.6.1.1 Hedgehog

The "Hedgehog" proteins are highly hydrophobic secreted proteins that are encoded by 3 signalling genes Shh (Sonic Hedgehog), Ihh (Indian Hedgehog) and Dhh (Desert Hedgehog). Shh binds to the specific receptor Ptc (Patched) on the cell surface. It ultimately activates an intracellular signal transduction pathway activating the Gli (GLIoma-associated oncogene homolog) family of transcription factors. This family of transcription factors has multiple oncogenic effects; (1) stimulation of proliferation by activation of regulators of G1/S and G2/M phase progression: (2) inhibition of apoptosis by direct induction of Bcl-2 expression and (3)

enhancement of invasiveness and metastasis by direct activation of epithelial to mesenchymal transition (EMT)-promoting factors such as Snail (78, 79).

The expression of these hedgehog proteins is high in the fetal human prostate and decreases to low levels in adult prostate tissue (80) where it is thought to regulate prostatic epithelial homeostasis (81, 82) by inhibiting proliferation and promoting terminal differentiation of ducts (83). Despite initial studies (84) suggesting a critical role of Hedgehog proteins in the development of prostate cancer and metastases, an adequate understanding of the pathway is yet to be realised (85). Indeed, only recently has the paracrine requirement for hedgehog signalling been clarified in cancer (86). Several studies suggest that high levels of Shh and Gli1 expression are found in localised prostate cancer as well as adjacent normal tissue in the same gland, and further increases occur in advanced prostate cancer. The mechanisms for these changes is unknown although loss of the suppressor protein SuFu has been proposed, especially as it is found at 10q24, a region with frequent LOH in prostate cancer (87 , 88). An alternative mechanism may involve the recently identified GLI modulator ZIC2 that is overexpressed in progressive disease (19).

1.6.1.2 Wnt

Similar to the Hedgehog pathway, the Wnt pathway is implicated in directing embryonic growth, and governing processes such as cell specificity, proliferation, polarity, response to androgen and migration (89). The canonical Wnt pathway is characterised by binding of Wnt proteins, through transmembrane receptors (90), to ultimately form a complex with Axin (91). Axin acts as a scaffold protein for a complex involving the APC gene and Beta-catenin, facilitating phosphorylation of both APC and Beta-catenin (92). Consequently, cytoplasmic Beta-catenin is translocated to the nucleus (93), where it associates with the T-cell factor (Tcf) and lymphoid enhancer (LEF) family of transcription factors (94). The B-catenin/ Tcf/ LEF

complex activates transcription of target genes with relevance to carcinogenesis including those that regulate cellular proliferation (C-MYC (95), C-JUN (96), Cyclin D1 (97), cellular migration (uPA, CD44, MMP-7) and cellular differentiation (FGF2, PPAR-gamma).

There are multiple levels of evidence suggesting a role of Wnt signalling in prostatic carcinogenesis. For example, expression of a stable Beta-catenin in a mouse model produces lesions with similar appearance to HPIN, as early as 10 weeks of age, but these do not progress to invasion or metastases in animals up to 5 months (98). Beta-catenin nuclear immunohistochemical staining was found in 28 of 122 (23%) radical prostatectomy specimens in one study (99) and 25 of 49 (51%) specimens in another (100) with both studies showing an increase of 20-30% of immunopositive cases in more advanced metastatic lesions

1.6.2 Epigenetics

Epigenetic changes are important in causing changes in gene expression in prostate cancer. They occur with advancing age in the prostate (101), early in prostatic carcinogenesis (102) and co-ordinately throughout the genome (103) however their cause remains obscure. Some evidence suggests that epigenetic regulatory mechanisms are sensitive to external influences such as diet and oxidative stress, and therefore may act as interpreters of the effect of these environmental stimuli in prostatic carcinogenesis (104-106).

1.6.2.1 DNA Methylation

Along with most neoplasms a global decrease in genomic hypomethylation is noted in prostate cancer (107), which has been associated with the emergence of chromosome instability both in mouse (108) and man (109). However, it is the focal hypermethylation of critical genes that appears to be more important. Genes commonly found to be methylated in prostate cancer

affect diverse cellular processes, many of which have roles in tumor processes such as hormonal response (AR, ESR1/2, RARB, RARRES1), cell cycle control (CCND2, CDKN2A), tumor invasion/ architecture (APC, CAV1, CD44, CDH1, CDH13, LAMA3, LAMB3, LAMC2), repair of DNA damage (GSTP1, MGMT), apoptosis (XAF1, CRBP1, TMS1) and signal transduction (DAB2IP, DAPK1, EDNRB, RASSF1) (110). Conversely, other genes are demethylated e.g. UPA (111) and heparanase (112) which may have functional importance for the invasive phenotype. These methylation changes have been reviewed extensively (113, 114) although three genes in particular are worthy of further mention given their importance to early carcinogenesis.

1.6.2.1.1 GST-Pi

GSTpi is a member of a family of enzymes that play an important role in reducing oxidative stress (23) by detoxification and catalyzing the conjugation of many hydrophobic and electrophilic compounds with reduced glutathione. It is hypermethylated and silenced in more than 90% of prostate cancers, as well as HPIN, PIA, tumor associated stroma and associated endothelial cells (56, 115). Interestingly, in other malignancies, this gene is often upregulated and thought to contribute to drug resistance (116). Therefore it is perplexing that this enzyme and indeed glutatione metabolism in its entirety is downregulated in prostatic carcinogenesis (19).

1.6.2.1.2 14-3-3σ (SFN, HME1)

The expression of 14-3-3σ is decreased in over 90% of HPIN and prostate cancer samples (117), often by promoter methylation (118). The importance of this p53 dependent gene is twofold; it has a role in mitotic translational machinery (119) and inhibits Akt(120). Thus cells with inactive 14-3-3σ, through either defects in p53 or promoter methylation, are likely to

have greater phosphorylation of Mdm2 (121), with G1/S and G2/M progression as well as p27 nuclear export and degradation (122).

1.6.2.1.3 E-cadherin

E-cadherin (CDH1) is a critical gene involved in the maintenance of normal tissue architecture and cell adhesion and is thought to have a role as a metastases suppressor gene, with subsequent repression promoting cell survival in metastases (123). Its reduced expression appears to be predominantly due to promoter methylation (124) and has prognostic importance in prostate cancer (125 , 126). Additionally, decreased E-cadherin augments androgen receptor signalling (127) by releasing B-catenin from intracellular sequestration to augment ligand-dependent signalling of the androgen receptor.

1.6.2.2 Histone Acetylation

There is increased expression of the family of histone deacetylase enzymes in prostate cancer (128) and a renewal of interest in the importance of histone modification following the discovery of the association between histone deactylase 1 (HDAC1) activity and the occurrence of ETS fusion genes (see section 1.6.3.1.1). Strong to moderate HDAC1 overexpression is evident in malignant human prostate tissue examined with immunohistochemistry (129). HDAC1 target genes include Bax, $p21^{WAF1/CIP1}$, p27, CK18 (cytokeratin 18) as well as the androgen receptor, p53 and maspin (130-135).

1.6.2.3 Histone Methylation

Histone methyltransferase enzymes are altered in prostate cancer with the most prominent example being the EZH2 complex, which is a critical component of a complex that methylates lysine 27 on histone H3. Expression of EZH2 decreases with aging (136), is

increased by AKT (137), represses the INK4a/ARF complex (138), is involved in stem cell differentiation (139) and is regulated by a microRNA (140). It appears to increase the risk of a number of adverse clinical outcomes in prostate cancer, and is generally associated with poor prognosis or advanced disease (139, 141).

1.6.3 Chromosomal Instability and Recurrent genomic rearrangements

Genomic instability is a general term to describe the overall processes that increase the rate of mutation, enabling cells to develop new and aggressive phenotypes, and to adapt to changing selection pressures. Mechanisms of instability fall into two broad groups: microsatellite or chromosomal (142). Microsatellite instability involves simple DNA base changes in short, tandomly repeated nucleotide sequences known as microsatellite regions. Due to their repetitive nature, they are a common site of replication errors or defects in the DNA repair processes including base excision repair (BER), mismatch repair (MMR) and nucleotide excision repair (NER) (143, 144). Chromosomal instability describes the cellular processes that increase the rate that whole chromosomes, or large portions of chromosomes are gained, lost or rearranged in tumors (145) and is thought to be due to specific acquired defects in cellular mechanisms that maintain genomic stability (see Figure 1.1). It can be further subclassified into structural and numerical instability. A consequence of chromosomal instability is simultaneous growth of diverse tumor subpopulations (146). Indeed, the majority of aberrations during tumorigenesis do not persist and are transient (non-clonal). By definition, a tumour exhibiting chromosomal instability should be expected to present intra- and inter-sample genomic heterogeneity (146), phenomena that are present in both local and advanced prostate cancer (147, 148).

Analysis of the cytogenetics and genomics of prostate cancer and precursor lesions such as PIN have shown that specific chromosomal alterations are recurrent and take place early in

the malignant process (18, 149). Previous studies have suggested that several common genomic loci are either gained (7q22, 8q21-qter, 16p12-13) or lost in a high proportion of HPIN (6q16, 8q21-qter, 10q22-23, 13q13-26, 16q22-qter). Recently reviewed by Saramaki and Visakorpi (150) a few trends from these analyses are evident; (i) Losses tend to predominate earlier in carcinogenesis, suggesting haploinsufficency (consequences secondary to the absence of the full gene dosage) as a likely phenomenon that contributes to transformation (110, 151). (ii) The rate of evolution of genomic instability is higher in HPIN and proportionally less in more advanced stages of prostate cancer. This is consistent with a mechanism of telomere generated chromosomal instability (152) although other mechanisms such as centrosome defects (153, 154), DNA repair defects (155 , 156) and checkpoint defects (157) found in prostate cells are possible (158). (iii) The aberrations found give insight into genetic loci that have functional importance in the cancer phenotype. For example, initial comparative genomic hybridisation studies (CGH) studies lead to the identification and verification of NKX3.1 (8p21.2), *PTEN* (10q23.3), E-cadherin (16q22.1) and gain of EZHZ2 (7q36.1), and Xq12 (AR) in prostatic carcinogenesis.

Additionally, novel loci identified on the basis of higher resolution technologies are also of increasing interest such as losses of MXI1 (10q25.2) (a MYC antagonist), FOXO1A (13q14.11) (an inhibitor of AR signalling), ATBF1 (16q22.3) (transactivator of the CDKN1A cyclin-dependent kinase inhibitor) and gains of MCM7 (7q21.3) (part of a complex that binds DNA origins and prepares them for initiation of replication).

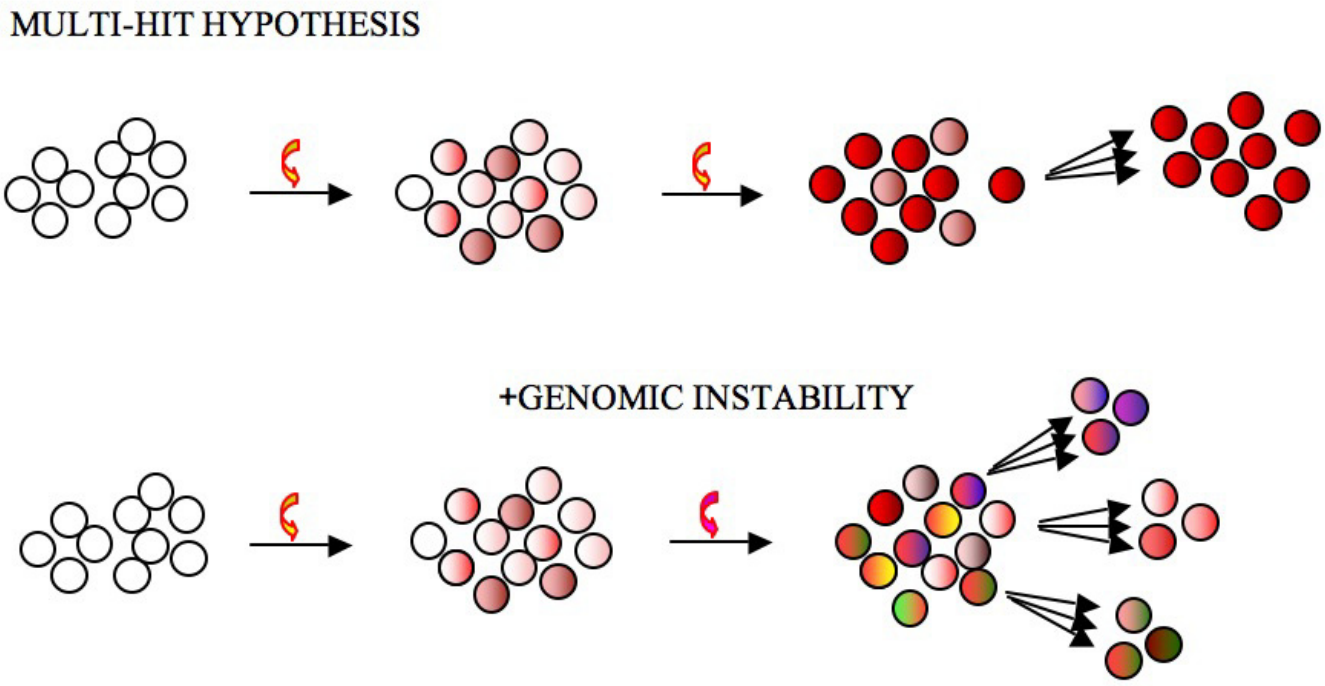

Figure 1.1: Genomic instability in prostatic carcinogenesis**.** Depicted is a concept of a genetic hit that confers an advantage for growth and survival leading to clonal outgrowth of cells harboring the mutation. Accumulation of these random genetic hits in cells over time leads to emergence of malignant cells that proliferate to give rise to a tumor. Proliferation of cells with aberrant genomic stability mechanisms results in genotypically heterogeneous population of cells, acquiring genetic mutations at an accelerated rate. Consequently, multiple malignant outgrowths, genotypically distinct from each other and from the original progenitor cells may arise. This hypothesis is in keeping with the characteristic multifocal and genetically heterogeneous appearance of prostate cancer.

1.6.3.1 "Outlier" based classification of Prostate Cancer

1.6.3.1.1 *TMPRSS2-ETS* family translocations

Undoubtedly, the greatest breakthrough in the understanding of prostatic carcinogenesis within the last decade has been the discovery of the role of the ETS family of oncoproteins in prostate cancer. These genetic translocations and microdeletions were originally described on the basis of novel microarray meta-analysis based on an "outlier profiling" technique and confirmed with RACE, RT-PCR and FISH (159 , 160). The findings were subsequently confirmed by several groups (161 , 162 , 163). Conceptually, they provide the important link between androgen signalling in prostatic carcinogenesis and key pathways of oncogenic over-expression necessary for malignant transformation.

The fusion genes are generated when aberrant genetic translocations generate a fusion between various partner sequences (most commonly an androgen dependent serine protease called TMPRSS2 (21q22.3)) and one of a family of the ETS transcription factors (e.g. ERG (21q22.3), ETV1 (7p21.2), ETV4 (17q21.31)) (159 , 164 , 165)). To date, the *TMPRSS2-ERG* fusions appear to account for the majority of occurrences (50-80%), with ETV1 accounting for up to 20% (166). The resulting fusion transcript generates multiple mRNA products by both alternative splicing and variant breakpoints within a multi-focal tumor, the majority of which are thought to lead to translated protein (167). The cause of these translocations is unknown but homology between repetitive elements such as Alu repeat sequences has been suggested (168, 169).

Currently, the known fusion genes are thought to occur in up to 60-70% of clinically localised prostate cancers. The pattern of rearrangement of the most common TMPRSS2- ERG gene fusion is rather complex. Both genes have the same transcriptional orientation, separated by 2.9 Mb of genomic sequence, and 5' *TMPRSS2* fuses in-frame with 3' *ERG*. Thus the

TMPRSS2-ERG fusion must either be accompanied by a small hemizygous interstitial deletion at 21q22 or undergo a more complex rearrangement to generate a fusion gene. It has been shown that about 50% of *TMPRSS2-ERG* fusions undergo concomitant microdeletion (161 , 170 , 171). The nature of the rearrangement in the remainder is unknown but may involve complex or variant translocations (172, 173). More studies have recently clarified the genomic abnormalities found with the ETV1 gene (174). Surprising fusion partners were detected in prostate tumors with ETV1 outlier expression including untranslated regions from androgen-induced genes (SLC45A3, ACSL3) (175) an endogenous retroviral element (HERV-K_22q11.23), a prostate-specific androgen *repressed* gene (C15*orf*21) and a strongly expressed house-keeping gene (HNRPA2B1).

It is now becoming clear that ETS fusion gene rearrangements are also present in a subset of ~25% (176) of HPIN (hypothesised to be those destined to progress to prostate cancer) and occasional LGPIN (177). Interestingly, despite the relative absence of fusions in HPIN, expression profiling suggests that ETS targets are over expressed in this lesion (19). This suggests that there maybe other genes with overlapping targets/ secondary effects on ETS gene, such as C-MYC, or alternatively that as yet undefined feedback control is exerted over these targets in HPIN which is overcome once *TMPRSS2-ETS* fusions occur.

Insight into the effect of the *TMPRSS2-ETS* fusions can be gleaned from a number of sources. In general, the ETS family of proteins are known to be important in several oncogenic pathways (178); ERG is known to have roles in histone methylation (179), apoptosis (180) and displays transforming abilities (181). Bioinformatic analyses of microarrays suggest that ETS overexpressing tumors compared to non-ETS overexpressing tumors have relative over-expression of WNT, MAPK and FAS signalling pathways as well as the aforementioned histone deacetylase 1 (HDAC1) (182). More recent data about the functional effect of ETV1 and ERG overexpression in cell lines suggests that they promote the expression of genes relevant to the

metastatic phenotype such as the MMP family (166, 183), which lead to increased invasiveness in *in vitro* models (184, 185). *In vivo* mouse modelling has noted the appearance of HPIN in mouse models with ETV1 and ERG overexpression (174). Interestingly, ERG knockdown in VCaP cells (a cell line known to contain the translocation) also induces a transcriptional program consistent with prostate differentiation (186, 187).

Intuitively, the existence of a fusion gene would suggest a poor prognosis, but their clinical importance was initially unclear as early studies suggested that ERG overexpression was a positive prognostic factor for a number of clinical variables such as time to PSA recurrence (188). Subsequently, Wang *et al*., analysed mRNAs from 35 tumors containing the *TMPRSS2-ERG* fusion and found 8 types of mRNA fusion transcripts, and multiple fusion mRNAs in approximately 50% of them. They found that expression of fusion mRNAs containing the native translocation initiation codons in frame with the ERG protein, particularly TMPRSS2 ATG, is associated with aggressive disease. Conversely, in those cases without the native translocation initiation codon, the fusion transcripts were expressed at generally higher levels, perhaps compensating for their lower activity. Thus, when looking at overall expression levels, the tumors with higher levels of ERG mRNA may appear to have a better prognosis. As retrospective and prospective studies become more mature, this issue will be clarified; current reports of the relationship between ETS fusion and prognosis is inconsistent (188-191) although larger studies suggest association with a poorer prognosis (192) especially in tumors with a duplication of the TMPRESS2-ERG fusion (193).

Two further ETS family members with tumour suppressive properties have been described recently to have a role in the evolution of prostate cancer; PDEF and ESE-3. Therefore, it may be that the balance between the ETS family members present is crucial in determining the overall effect on the cellular phenotype (186). For example, PDEF is a transcription factor that interacts with the androgen receptor, NKX3.1, TGF-B and Wnt

pathways and may have a critical role in suppressing epithelial-mesenchymal transition (EMT) and cellular proliferation (194, 195, 196 , 197).

Decreased expression of ESE-3 is found in 80% of prostate cancer and when reexpresed in prostatic cell lines it inhibits clonogenic survival and induces apoptotic death by increasing the levels of procaspase-3 (198). It has also been suggested to have an effect on epithelial differentiation (199).

1.6.3.1.2 SPINK1 overexpressing prostate cancer

The discovery of a subgroup of ETS rearrangement-negative prostate cancers has been reported recently on the basis of further bioinformatic-based "outlier" analysis. This subset, which is believed to compromise 10% of prostate cancer is characterised by the late overexpression of the SPINK1 gene (serine protease inhibitor, Kazal type 1, chr 5q32). The aetiology of the overexpression is not clear. Nevertheless, preliminary experiments suggest that SPINK1 expression is an independent predictor of biochemical recurrence after resection and SPINK1 knockdown in a model cell line attenuates invasion, paralleling the role of the ETS family of proteins(200).

1.6.3.2 Telomere Mediated Instability

Telomeres are the terminal ends and associated nucleoprotein complexes of eukaryotic chromosomes which contain up to two thousand repeats of the sequence, TTAGGG (201). Their primary role is to ensure chromosomal integrity by preventing recognition of chromosome ends as DNA double strand breaks thereby preventing degradation and recombination (202). Telomeres have a unique structure whereby the terminal end of the DNA loops back and inserts itself into the terminal telomeric repeat sequence, known as the "t-loop" (203) via a short 3' overhang. Telomere shortening and dysfunction may be due to several mechanisms such as

oxidative stress (204, 205), stochastic deletion (206) or the "end-replication" problem of chromosomal ends (207).

This latter phenomenon is due to the DNA replication machinery using short RNA primers during lagging-strand synthesis. After their removal, the machinery is unable to fill in the gap created at its 5' end (208, 209) which results in telomere shortening at a rate of around 50-150bp per cell division (208). This latter phenomena is believed to provide the cell with a tumor suppressor mechanism by acting as a "mitotic clock" to limit cellular proliferation likely in a p53 dependent manner. However, following malignant alterations, such as p53 loss, cells continue to proliferate in the presence of shortening and dysfunctional telomeres (see Figure 1.3), there is thought to be unravelling of the loop structure and loss of protective cap function. Thus the open chromosome ends are "sticky" and facilitate end-to-end fusion (often to the sister chromatid), with formation of dicentric chromosomes and anaphase bridges. These anaphase bridges facilitate chromosomal instability with fusion and rearrangements through "break-fusion-bridge cycles" (BFB) (210, 211). Characteristic chromosomal abnormalities found include large terminal deletions, double minutes, multipolar mitoses and inverted repeats (212) (see Figure 1.2). The BFB cycle has been reported to be responsible for genetic intratumor heterogeneity (213, 214) . Support for a model in prostatic carcinogensis similar to Figure 1.3 comes from previous work in our lab by Al-Maghrabi *et al* (215) and Vukovic *et al*, (216) who defined the extent of telomere shortening and chromosomal instability in HPIN and the subsequent prognosis of HPIN.

1.6.3.3 Telomerase Actions

Whilst rearrangements are likely to lead to cell death due to mitotic catastrophe, surviving populations of genomically unstable cells may emerge that eventually stabilise both their telomere lengths and the level of instability through re-expression of an ribonucleoprotein

enzyme called telomerase (217) that adds telomeric sequence DNA to the chromosomes. These additional sequences are thought to reduce, although not abolish, the rate of emergence of genomic instability (152) (see Figure 1.3). Intriguingly, a number of ETS transcription factors such as ESE-3 have been associated with the induction of cellular senescence from a number of stimuli including oxidative stress, oncogene activation and telomere shortening, thus provocatively linking alteration in ETS transcription factors to the emergence from senescence (218).

Another model (219) proposes an additional protective function of hTERT (or telomerase) at telomeres, independent of its effect on bulk telomere length. Evidence supporting this model comes from; the finding that a hypomorphic hTERT did not extend bulk telomere length but significantly prolonged human primary cell life span (220, 221). Second, knockdown of hTERC in human cancer cells caused rapid growth inhibition before any detectable bulk telomere shortening (222). Third, further knockdown of the low endogenous hTERT in primary human fibroblasts attenuated their DNA damage response (223). Fouth, mouse TERT overexpression in a transgenic mouse model induced proliferation of hair follicle stem cells even in TERC-deleted animals (224).

Finally, despite the presence of active telomerase, a distinct class of extremely short telomeres, "t-stumps" are present in a number in human cancer cell lines with a defect in checkpoint pathways. These t-stumps contain arrangements of telomeric repeat variants and a minimal run of seven canonical telomeric TTAGGG repeats, but all bind at least one TRF1 or TRF2 protein *in vitro*. Whilst the abundance of these t-stumps can be altered by manipulating hTERT levels in cancer cells, the exact mechanisms of this are unclear. Nevertheless, the above results suggest that in the setting of active telomerase and compromised checkpoints characteristic of human cancer cells, hTERT (or telomerase) may have as yet undefined roles in telomere protection although this has not been validated in prostatic tissue to date.

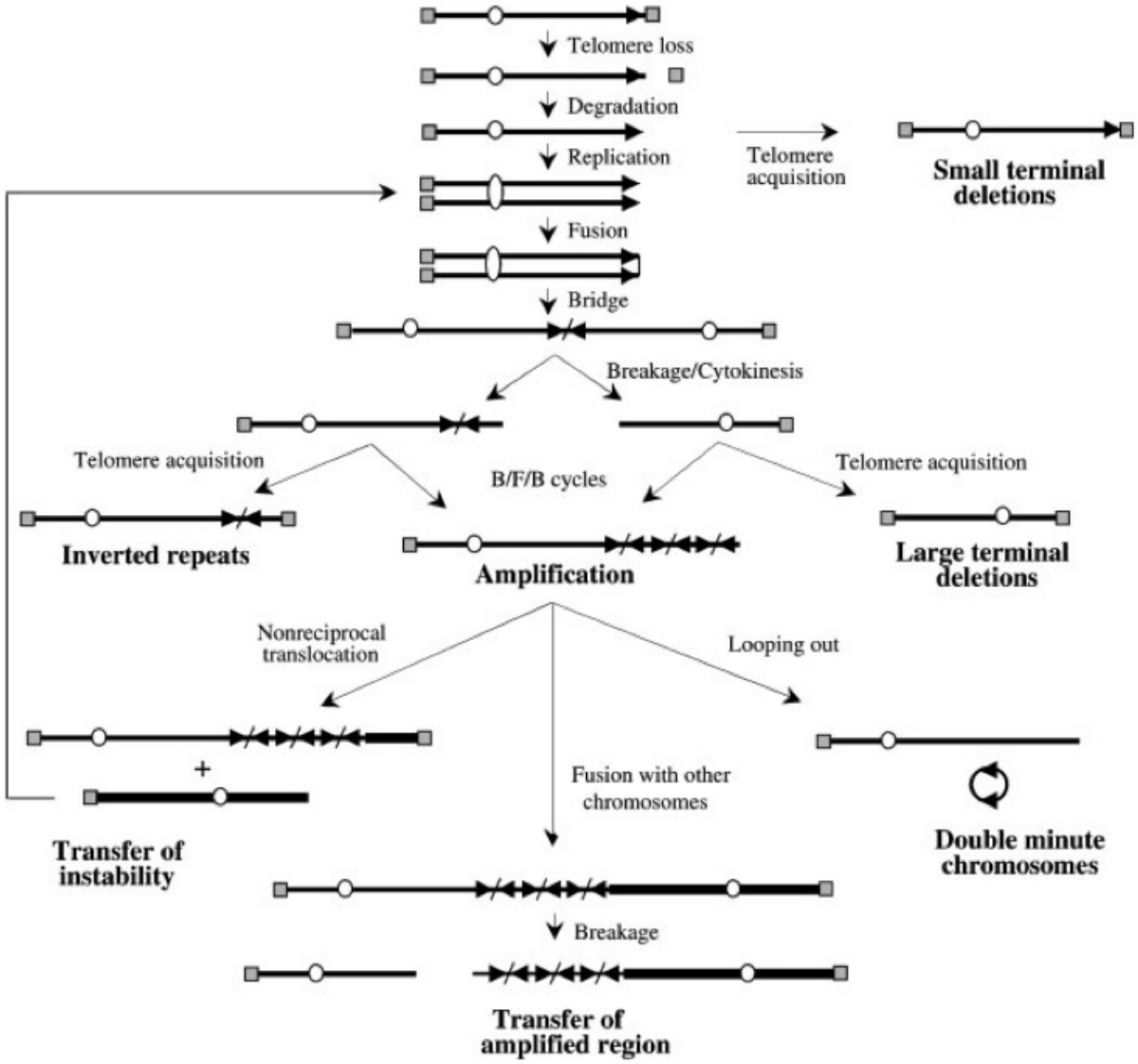

Figure 1.2 The first event following telomere attrition is loss of the end of the chromosome, which is followed by either the addition of a new telomere producing a small terminal deletion, or fusion of chromatids (often sister chromatids after DNA replication). With two centromeres attached to one another, the fused sister chromatids then bridge during anaphase and break, leading to inverted repeats in one daughter cell and a terminal deletion in the other. If the chromosome fails to acquire a new telomere, there will be additional BFB cycles and further DNA amplification. BFB cycles can lead to nonreciprocal translocations, which result in the loss of the telomere on the donor chromosome, transferring the BFB cycles to these chromosomes. Looping out of the amplified DNA as a result of the inherent instability of inverted repeats can also lead to the formation of DM chromosomes that can be involved in high-copy gene amplification. Multipolar mitosis may also arise following telomere attrition, giving rise to unpredictable genomic instability. Reproduced from Murnane JP, Sabatier L., Chromosome rearrangements resulting from telomere dysfunction and their role in cancer. Bioessays; 26(11):1164-74. 2004

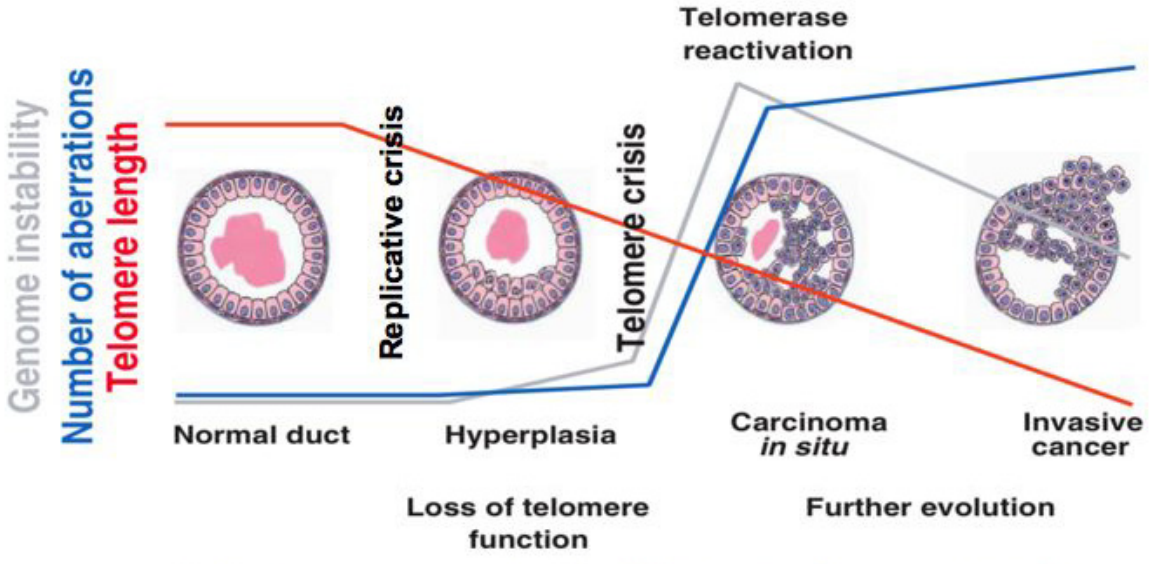

Figure 1.3 As discussed, telomere shortening has been documented in a number of human preneoplastic lesions and their corresponding carcinomas. The mechanism of shortening is displayed above; progressive shortening occurs concurrently with proliferation in the preneoplastic stage. Subsequently, when the telomeres are critically short (and the cells at "crisis"), there is a dramatic increase in genomic instability which is diminished by the re-expression of telomerase. This role of the telomere is in contrast to its purported role in early disease where they may elicit a DNA damage response and therefore act as a tumor suppressor mechanism. Replicative crisis refers to Oncogene induced senescence (see section 1.7.1). Modified from Chin *et al*., In Situ analyses of genome instability in breast cancer, Nature Genetics, 2004 36 (9), 984-8.

1.6.4 Androgen Signalling

Androgen and the androgen receptor (AR) (located on Xq11.2) are fundamental to both prostatic development and prostatic carcinogenesis(225). The AR partly mediates its effects through androgen responsive stroma (226-229) which in turn secretes paracrine mediators such as KGF (230) whilst in contrast, the luminal cell androgen receptor is responsible for regulating function such as secretion.

The AR is dependent on co-regulatory proteins to modulate gene expression; coactivators (e.g. NCOA1, NCOA2, NCOA3, PCAF, CBP, TIP60 and p300) facilitate transcription by recruiting protein complexes to DNA that alter the chromatin structure to a more transcriptionally active form, and co-repressors (e.g. retinoid and thyroid (SMRT) hormone receptors, nuclear receptor co-repressor (NCOR) mediate chromatin condensation and silence transcription (231, 232).

AR-regulated genes have multiple actions in the prostate that may contribute to carcinogenesis. For example, in addition to the ETS fusion genes, androgen action also stimulates production of the Wnt-induced secreted protein-2 (WISP-2), a secreted growth factor that binds and activates integrins and stimulates mitosis. Additionally, apoptosis is decreased through the production of the anti-apoptosis protein c-FLIP and caspase-2 is decreased (233). There are also data to indicate that androgens can function nongenomically through AR action in the cytoplasm through the mitogen-activated protein kinase (MAPK) signal cascade (234).

1.6.5 NF-KB

The role of NF-KB signalling has been under appreciated in early prostatic carcinogenesis. Prostate cancer cells have been reported to have constitutive NF-kappaB activity due to increased activity of the IkappaB kinase complex (235). NF-kappaB may promote cell growth and proliferation in prostate cancer cells by regulating expression of genes such as C-MYC, Cyclin D1, and IL-6 (235). Additionally, NF-KappaB-mediated expression of the AR (236, 237) as well as genes involved in angiogenesis (IL-8, VEGF), invasion and metastasis (MMP9, uPA, uPA receptor) may further contribute to the progression of prostate cancer (235).

1.6.6 C-MYC

The C-MYC oncogene has been long suspected to be involved in prostatic carcinogenesis on the basis of the amplification of the 8q24 cytoband. It is part of a larger family of transcription factors (such as MAX, MAD, MXI-1) that work in recognising a DNA-binding element known as an E-box (238). Transfection experiments both *in vivo* and *in vitro* have demonstrated that C-MYC is sufficient to cause neoplastic development (239-241). The mechanisms by which C-MYC causes this transformation or contributes to the malignant phenotype are unclear but decreased *PTEN* and NKX3.1 expression (239, 242) as well as increased telomerase (hTERT) and TMPRSS2 expression have been suggested (243) . Given these findings, it is not surprising that the expression of C-MYC is also prognostic and correlates with histological grade (244-246). The frequency of C-MYC amplification in primary prostate cancer tumours ranges from 0-44% (245, 247-249), and until recently the timing of its overexpression was controversial (250). The most recent, and accurate analyses of C-MYC protein expression suggest that it is an early change in prostatic carcinogenesis, overexpressed in

70-80% of HPIN and prostate cancer lesions, with trends to decreased expression in higher Gleason grade lesions. Interestingly, there appears to be no relationship between 8q24 copy number and MYC protein staining, suggesting that other genes in 8q24 may have pathological significance. Recent data implicate 2 loci with unknown function adjacent to the C-MYC position on 8q24 as important risk factors for prostate cancer (251, 252); it is provocative to speculate that these variants could affect C-MYC (~260 kb telomeric), although this remains unproven (252). Additional loci, identified on the basis of their involvement in Burkitts lymphoma, extend 400kb telomeric to C-MYC (within the PVT1 locus) and are thought to contain microRNAs that influence C-MYC expression. For example, the microRNA closest to C-MYC, *hsa-miR-1204* leads to increased expression of C-MYC when experimentally overexpressed and importantly, high levels of expression of the *hsa-miR-1204* precursor is also seen in several epithelial cancer cell lines such as breast and colon with MYC/PVT1 coamplification, suggesting an emerging role for these miRNAs in tumorigenesis (253, 254). Their role in prostatic carcinogenesis remains unexplored, although this region has been noted to be amplified in studies CGH and aCGH studies of prostate cancer (255).

1.7 BARRIERS TO TUMORIGENESIS

1.7.1 Oncogene Induced Senescence

Oncogene induced senescence (OIS) is a phenomenon, originally described in the context of ras transfection (256), which acts as a barrier to precancerous evolution likely due to a DNA damage checkpoint, secondary to oncogene induced replication fork collapse (257). Unique markers for the identification of this senescent state remain unclear but a number of candidates have been proposed (see section 5.2). OIS has been suggested to occur in numerous solid neoplasms including prostate (258) (see Figure 1.3), although verification is required.

Telomere dysfunction leading to a DNA damage signal is another cause of senescence that might occur after OIS (259-261).

1.7.2 Tumor Suppressor Genes

1.7.2.1 P53

P53 and its related pathways play critical roles in directing the cellular responses to DNA damage and oncogenic stress. Canonical DNA damage signals are thought to signal through ATM and Chk1/2 kinases to activate p53, leading to the up-regulation of p21 and inhibition of cell cycle progression via binding to and inhibiting the activity of cyclin-CDK2 or -CDK4 complexes. An alternative arm of the pathway involves p14ARF, which acts to block the ability of MDM2 to degrade p53 (262, 263).

Unlike other neoplasms, p53 abnormalities are thought to appear only late in prostate cancer progression. This view however, warrants re-evaluation due to advances in immunohistochemistry and sequencing methodologies (264). In modern studies, abnormal p53 staining is seen in at least 1/3 of early stage tumors (265-273) which is higher than the levels reported a decade previously (274-278). Indeed, levels may even be higher due to issues relating to heterogeneity within the tumour (279), sampling (268), "silent" mutations (280) and effects of post-translational regulation (281, 282). Functional impairment may also be present, as up-regulation of MDM2 expression has also been found in up to 40% of prostatectomy specimens (283). Finally, functional studies of primary cell cultures derived from radical prostatectomies fail to elicit a p53 response to radiation (284). These effects on inappropriate cell cycle progression may be compounded by a constitutional checkpoint defect in normal prostatic epithelium at the CDK1/2-Tyr15 phosphorylation step by the Wee1A tyrosine kinase(157).

1.7.2.2 RB

The retinoblastoma (Rb) pathway acts primarily to regulate the progression of cells from the G1 phase of the cell cycle to the initiation of DNA replication in S phase. The pathway is centred on regulation of the protein product of the retinoblastoma gene and its interaction with the E2F transcription factor family in order to activate the transcription of virtually the entire group of initiation factors that participate in DNA replication. Additionally, at least 3 cyclin-CDK complexes target RB during cell cycle progression. Cyclin D/CDK4/6 phosphorylates RB during early G1, cyclin E-CDK2 is responsible for late G1 Rb phosphorylation, whereas cyclin A-CDK2 maintains hyperphosphorylation of RB during S phase (285). In turn, these cyclin/CDK complexes are regulated prominently by p16 and p27.

The role of the RB pathway in prostatic development is suggested by mouse models (286 , 287) but relatively little work has been done to detail the extent of biallelic loss of RB in prostate cancer samples. Nevertheless, studies of chromosomal markers by CGH have found that deletions are evident at the RB1 locus on chromosome 13q21 in at least 30% of prostate tumours (88) with estimates of 10% biallelic loss.

The RB pathway can also be downregulated through abnormalities of the regulators of the pathway. Whilst abnormalities of cyclin D/CDK4 and E2F are found uncommonly, the two other members of the pathway, p16 and p27 appear to be of particular importance.

Paradoxically, p16 appears to be overexpressed in up to 80% of prostate cancers (288-290) as well as HPIN and PIA (30). Indeed most studies have suggested that it is associated with a poor prognosis (290) even when found in surrounding HPIN (289). The reason for the over-expression is unclear; but, it may involve uncharacterised changes in binding proteins that regulate p16 function such as BMI-1 (291). In normal tissues, transient p16 overexpression is seen in response to cellular stress including telomere dysfunction, HPV infection and aberrant

mitogenic signals (292). Therefore its continued presence in a proportion of prostate cancers may be an indication that other permissive changes in the pathway have taken place to allow bypass of senescence and efficient replication to take place (293).

P27 is a critical regulator of cyclin E/CDK2 activity and of the G1 checkpoint downstream of RB, and as such may be a gatekeeper for the inactivation of the RB pathway in prostate tumors. It may also possess tumor suppressive activity independent of its role in the Rb pathway (294) possibly by increasing either directly or indirectly, the levels of genomic instability in the tumors. Reduced p27 expression is characteristic of prostate cancer, and associated with a poor prognosis (295, 296) as well as being found in HPIN and PIA (297) where it may act as a barrier to senescence (298).

1.7.2.3 *PTEN*

The phosphatase and tensin homologue (*PTEN*) is the second most frequently mutated human tumor suppressor gene (299) and maps to the 10q23 locus that is a common target for deletion in prostate cancer (300). *PTEN* functions as a lipid and protein phosphatase. However its lipid phosphatase activity on phosphotidylinosital-3,4,5-triphosphate (PIP_3), inhibiting PI3Kinase (301) is thought to be more important. Briefly, PI3K is activated after upstream receptor tyrosine kinase growth factor receptors become activated and bind to the p85 subunit. This component binds to the catalytic component (p110) and activates PI3K. PI3K then phosphorylates the inositol ring of PI4P or PI4,5P2 to generate PI3,4P2 and PI3,4,5P3, which act as secondary messengers (302). These specialised phospho-lipids recruit proteins such as AKT, PDK1 and JNK (303) to the plasma membrane. After phosphorylation and activation, AKT dissociates from the plasma membrane and phosphorylates multiple proteins with functions relevant to carcinogenesis such as apoptosis (BAD (304), CASP3, CASP9 (305)), cell cycle regulation (MDM2 (306), p27 (307)), cell growth/proliferation (mTOR (308), IkB kinase

(309)) cellular homeostasis (Wnt (310), and DNA repair/instability (CHK1 (311)). Recent evidence also suggets that PTEN (via AKT and the transcription factor E2F) may regulate the expression of Cdc6 and cyclin E2, two proteins associated with cell cycle progression through the G1S barrier and with prostate metastases *in vivo* (312).

The importance of *PTEN* has been rekindled with an increased appreciation of the effects it has alone, independent of Akt inhibition including; (1) Direct association with p53, increasing its stability, protein levels and transcriptional activity, (2) Regulation of cell cycle arrest via protein phosphatase-dependent interaction with cyclin D, (3) Maintenance of chromosomal stability by associating with the centromeric protein CENP-C and increasing the levels of the homologous repair protein RAD51 (313, 314), (4) Action on other protein substrates such as FAK, ETS-2 and Sp1(315).

Multiple lines of evidence attest to the importance of *PTEN*/Akt in the development of prostate cancer but evidence from murine modelling in particular is persuasive. Whilst conventional deletion of both alleles of *PTEN* leads to developmental defects and early death, *PTEN* heterozygous mice develop HPIN, but without progression to invasive cancer (316, 317). Importantly, heterozygous or homozygous loss of p27 (318), NKX3.1 (319) and INK4A/p19 (320) all exacerbate the phenotype whilst prostate-specific homozygous deletion leads to invasive cancer with 100% penetrance (321). With the development of therapeutics targeting this pathway, relevant cellular and mouse modelling suggest that it is the Akt1 isoform (322) and mTOR activation that are the primary effectors responsible for the neoplastic phenotype and that the effect of mTOR inhibitors can be inhibited by BCL-2 overexpression.

At least 4 mechanisms are involved in *PTEN* inactivation in human cancer; chromosome deletion or loss of heterozygosity, somatic mutations, oxidation (323) and methylation. Whilst early studies of *PTEN* in human prostate tissues suggested that *PTEN* deletion was a late event in carcinogenesis, it appears that a substantial proportion of both HPIN and prostate cancer

lesions in human tissue contain abnormalities of *PTEN*, in particular if haploinsufficency is important as suggested by murine models (324). In addition, the lack of *PTEN* (in particular homozygous deletions) either alone or in association with high levels of phospho-AKT appear to portend a number of poor clinical outcomes (325-330).

1.7.2.4 NKX3.1

NKX3.1 is a prostate specific homeobox gene whose relevance to prostatic carcinogenesis was described originally on the basis of a loss of heterozygosity of chromosome 8p21.2 in 50-85% of prostate cancer cases (88, 331). Murine models suggest both a haploinsufficient effect on carcinogenesis and both haploinsufficent and homozygous synergy with *PTEN* and CDKN1B/P27 (332 , 333). Expression in human prostate tissue correlates with the degree of gene inactivation by deletion, methylation or both (334). NKX3.1 staining intensity is significantly diminished in PIA and PIN lesions compared with normal epithelium (34). In more advanced prostate cancer, there is an association between 8p deletions and NKX3.1 expression suggesting that genetic deletions may be more important in the progression of invasive disease whilst decreased NKX3.1 expression is more important in initiation of disease (335).

NKX3.1 mutant mice display deregulated expression of several oxidation related enzymes with concomitant increased levels of oxidative damage in prostatic preneoplastic lesions, which accumulate in overt carcinoma (336). Finally, NKX3.1 appears to have a central role as an integrator of multiple signal pathways including the AR, *PTEN* and p53 that may have relevance in the initiation of prostatic carcinogenesis (337).

1.7.3 Stromal Dependence

Investigating the contribution of the cellular microenvironment and the tumor-stromal interaction to the generation of prostatic preneoplasia is critical in developing a greater understanding of prostate cancer causation. Phenomena such as the inhibition of prostate cancer growth when co-inoculated with normal prostatic fibroblasts (338), the stimulation of prostate cancer growth with cancer-associated or spontaneously-immortalised fibroblasts (339 , 340) and the dependence on orthotopic (rather than ectopic) sites for metastatic ability (341) suggest that the stroma must co-evolve with the neoplastic epithelium to maintain its neoplastic phenotype (342-344). Prevailing theories of carcinogenesis describe the development of an "activated" tumor-associated stroma with the expression of myofibroblastic markers such as increased vimentin and actin (345, 346). The best characterised molecules that may affect both afferent and efferent interactions are TGF-Beta, the androgen receptor and the insulin growth factor family (reviewed in (342)).

1.7.3.1 TGF-Beta signalling

TGF-Beta signal transduction is initiated by heterodimerization of two cell surface serine/threonine kinase receptors (TßRI and TßRII). Subsequent phosphorylation of the SMAD proteins act as the primary intracellular effector of TGF-Beta signalling (347), which activate a wide variety of downstream targets, all of which have antiproliferative or pro-apoptotic effects. For example, there is increased expression of the cyclin dependent kinase inhibitor $p27^{Kip1}$, up regulation of BAX, down regulation of BCL-2, activation of caspase-1 (348, 349) and of IGFBP-3 (the protein involved in sequestration of IGF-1) (350). Additionally, normal prostatic fibroblasts also express the TGF-Beta receptor and are highly responsive to its actions (351). Indeed, mice in which the TGFß2 receptor has been inactivated specifically in prostatic stromal

fibroblasts develop preneoplastic lesions in the prostate (352). Putative mechanisms by which the absence of TGF-Beta activation in the stroma may have this action on prostatic epithelial cellular growth include paracrine Hepatocyte Growth Factor (HGF) production (352), inhibiting androgen signalling, and a relocation of androgen receptor localisation from the nucleus to cytoplasm (353). During carcinogenesis epithelial cells gain resistance to the growth suppressive effects of TGF-Beta, possibly through loss of the relevant receptors by methylation (354, 355). Subsequently, dysfunctional signalling may lead to pro-carcinogenic actions leading to the induction of proteases (356).

Finally, there is evidence from microarray expression studies to suggest that TGF-Beta secreted by tumor cells acts on stromal cells to promote tissue remodelling and wound healing that assists tumor growth and invasion (357) via the production of the angiogenic mediator, connective tissue growth factor (CTGF) in the extracellular matrix (358).

1.7.3.2 Insulin Growth Factor family

There are 2 types of IGFs, IGF-1 and IGF-2 with associated receptors, as well as 6 IGF binding proteins (IGFBPs), which are involved in modulating the effects of these growth factors (359). Of these, IGF-1 and IGFBP-3 are the most important in prostatic carcinogenesis (360). The two downstream pathways involved in IGF action are the mitogen activated protein kinase (MAPK) pathway and the phosphatidylinositol-3 (PI3K) pathway, both of which promote cell proliferation and inhibit cellular apoptosis (361). The consensus is that IGF-1 acts in a paracrine fashion in the prostate, with production in the stroma and activity in the epithelial cells (362) although it remains unclear at what stage of carcinogenesis it is of greatest importance (363-365). Insulin growth factor binding proteins (IGFBPs) also influence IGF signalling; for example, IGFBP-5 appears to potentiate IGF-1 signalling (366) and is stimulated by androgen

(364), whilst levels of IGFBP-3 may determine the overall activity of the IGFs (367) in that it attenuates the subsequent activation of the AKT pathway (368, 369). The IGFBP-3 gene is often inactivated by methylation (370) in prostate cancer and the protein is also degraded by PSA (368). IGFBP-3 may also have suppressive actions on tumor growth that are independent of its actions through the IGF axis, adding further complexity to the role of this growth factor (371).

1.7.4 Evasion of Apoptosis

There are two main mammalian pathways of apoptosis; the "extrinsic" pathway involves signals transduced through cell surface death receptors such as TNF-R1, TRAMP or TRAIL, while the "intrinsic" pathway is triggered by various forms of stress such as radiation (372, 373) before activation of the common caspases. These pathways interact with many of the signalling pathways described above. For example, Akt activation appears to inhibit apoptosis at a number of points including the prevention of cytochrome c release from mitochondria, phosphorylation of the pro-apoptotic protein BAD, phosphorylation of procaspase-9 (305, 374, 375) and phosphorylation of the FKHR family of transcription factors (376, 377). An additional modulator of the apoptotic response is the Bcl-2 family. Bcl-2 is a critical anti-apoptotic mediator, along with Bcl-X_L that opposes the pro-apoptotic effects of the BAX subfamily (Bax, Bak, Bok) and the BH3 subfamily (Bad, Bid, Bik, Blk, Hrk, BNIP3 and BimL). Nevertheless, prostate cell lines all contain intact cell death programs that become activated in response to different apoptotic stimuli (378, 379).

Expression of apoptosis related genes have not been evaluated rigorously in prostate cancer. For example, for Bcl-2, some reports indicate increases in expression from low but detectable levels in benign epithelium (380) to at least 50% of HPIN cases (381, 382) to near universal staining in androgen independent disease (383) with an association with tumor grade

(384, 385). Other studies have suggested significantly higher expression of Bcl-2 in HPIN compared to cancer (380, 386).

Generally, apoptotic indices when measured in prostate specimens show an increase from benign to cancerous cells (386). Whilst there is some evidence that the phosphorylation of BAD may be crucial in protecting prostate cancer cells from apoptosis, the heterogeneity seen *in vivo* is likely to limit the applicability of these findings (387).

1.8 INTEGRATED MODEL

There are at least 2 major limitations in proposing a pathway to prostatic carcinogenesis. First, prostate cancer is a heterogeneous disease, with multiple pathways to the malignant phenotype. For example, both the "outlier" based subclassification (described above) and other studies suggest that at least 3 distinct subtypes of prostate cancer can be defined, although the overlap between definitions remains unclear (388, 389). Secondly, the studies available to guide hypothesis generation are limited to evidence from static rather than longitudinal human studies. Nevertheless, a general overview is worthwhile to put the evidence into a temporal and conceptual context (Figure 1.4).

It is reasonable to assume that the aetiology of the epigenetic field effect in prostatic carcinogenesis is the forebear to further carcinogenic change. The underlying aetiology is likely to involve oxidant stress either via inflammatory mediators or dietary insufficiency (see review by (37, 390)). Attempts at cellular repair at this stage may lead to the emergence of the PIA phenotype accompanied by proliferative defects in genes such as C-MYC and p27. Epigenetic changes further inactivate genes such as those encoding TGF-Beta receptors (that regulate epithelial-stromal dependency) or NKX3.1 (predisposing the epithelium to further oxidant stress) and susceptibility to genomic damage (possibly via progressive telomere shortening) as

well as leading to increased androgen driven proliferation. At this stage, the presence of an intact p53/ RB/ p27 pathway may prevent lesions from progressing to a more invasive phenotype by inducing a senescence/ apoptosis response, although abrogation of this response by increased BCL-2 levels may occur. ETS factors are likely up regulated through undefined mechanisms in this earlier stage of carcinogenesis. Further cellular replication in the presence of shortened telomeres leads to the onset of chromosomal instability with the emergence of characteristic changes such as 8p and 6q loss that have as yet undefined implications. All of the aforementioned changes would be potentiated by *PTEN* abnormalities that simultaneously increase cellular proliferation (possibly via augmenting androgen signalling), increase instability and modulate apoptotic mechanisms. With the reactivation of telomerase (see Figure 1.3), the relevant cells are immortalised but physiological regulatory mechanisms restrain the cellular phenotype until selective pressure leads to the emergence of an ETS related translocation likely through an anomalous repair event. The co-opted tumor associated stroma likely facilitates tumor growth and invasion through the secretion of soluble factors to increase invasion. Subsequently, increasing expression of embryonic signalling pathways and epigenetic regulators likely further de-differentiate the cellular phenotype in early malignancy facilitating the development of an invasive aggressive phenotype. Ultimately, this lessens the dependency on androgen signalling as other pathways drive cell cycle progression and tumor evolution. (see Figure 1.5).

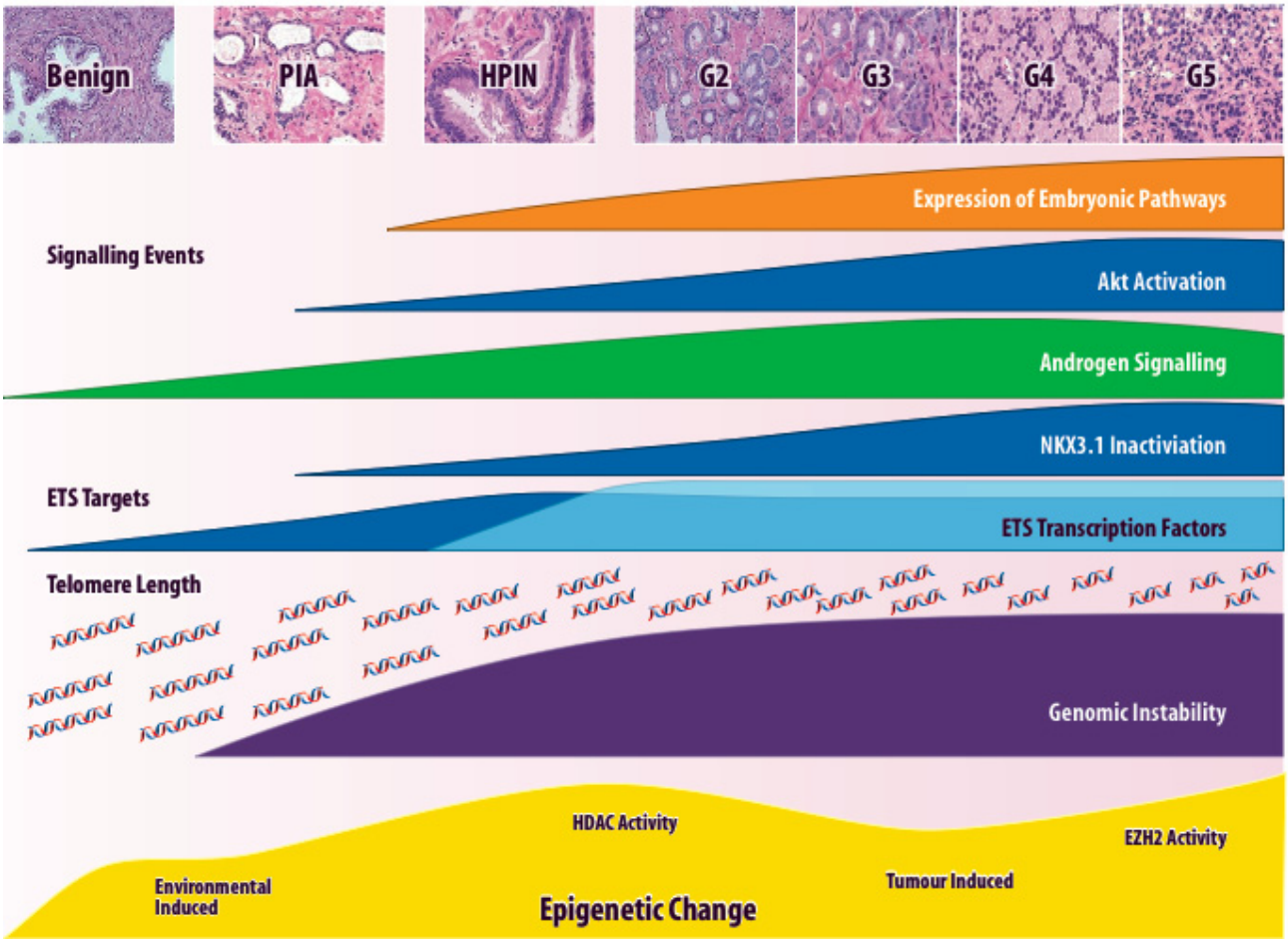

Figure 1.4 An integrative illustration of a proposed model in prostatic carcinogenesis incorporating themes discussed in the text. Events align along the vertical axis with the histology along the uppermost row. PIA – Prostatic Inflammatory Atrophy. HPIN – High Grade Prostatic Intrapeithelial Neoplasia. G – Gleason Score. Reproduced from Joshua et al., Prostatic preneoplasia and beyond, Biochim Biophys Acta. 2008 Apr;1785(2):156-81.

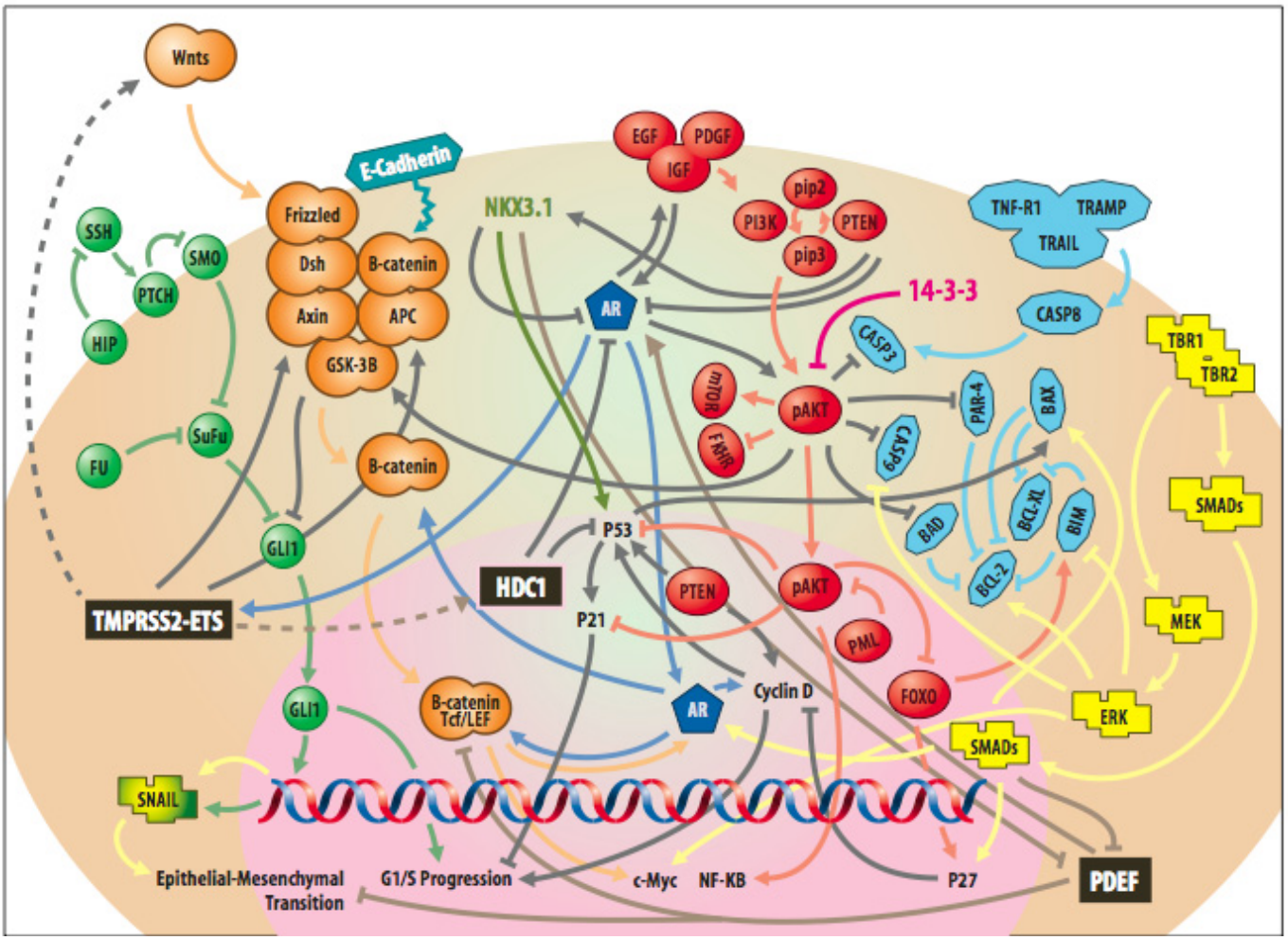

Figure 1.5 An illustration of the significant pathways and interactions mentioned in the text. Each pathway is illustrated by a particular colour and shape. Interactions within a particular pathway are illustrated by a different shade of the same colour. Grey lines indicate interactions that interact amongst signalling pathways. Positive interactions are indicated by arrowheads whereas bars illustrate inhibitory interactions. Jagged lines indicate binding/ sequestration interactions. Reproduced from Joshua et al., Prostatic preneoplasia and beyond, Biochim Biophys Acta. 2008 Apr;1785(2):156-81.

1.9 RATIONALE

The multi-step acquisition of oncogenic hits over several decades of life is thought to underlie genetic events leading to prostatic carcinogenesis. Recent studies have suggested that at least one of the hits affects genes involved in maintenance of genomic stability. Indeed, cytogenetic studies of prostate preneoplastic lesions and CaP tumors show evidence of phenotypic and genotypic heterogeneity such as ETS alterations concurrent with multifocal histology in early disease. However, the mechanism driving such instability process during prostate carcinogenesis has not been described. Telomere dysfunction has emerged as a plausible source of chromosomal abnormalities in epithelial carcinogenesis. Short, dysfunctional telomeres can initiate chromosomal instability through repetitive chromosome end-to-end fusion and breakage (BFB cycle) and have been shown to promote tumorigenesis. Immortalization through stabilization of telomeres via telomerase is thought to be a key step in tumor formation. Analysis of telomere length and chromosomal abnormalities in CaP will allow for a better characterization of genomic instability process underlying prostatic cancer initiation and progression.

1.10 HYPOTHESIS

I postulate that telomere dysfunction is a significant driving force behind the chromosomal instability process in prostatic carcinogenesis. Thus, excessive shortening of telomeres and chromosomal instability could be correlated during prostate tumorigenesis. Furthermore, the resulting chromosomal instability might influence tumor biology and have prognostic importance. Finally, the causes of telomere dysfunction should be evident as a definable field effect in prostatic carcinogenesis.

2. TELOMERE LENGTH AS A PROGNOSTIC MARKER IN HPIN

SUMMARY

The onset of chromosomal instability in the development of prostate cancer is likely to facilitate the formation of crucial genomic aberrations both in the precursor lesion high-grade prostatic intraepithelial neoplasia (HPIN) and in CaP. Instability generated by telomere attrition is one potential mechanism that could initiate chromosomal rearrangements. In this study, variation in normalized telomere length was examined in a cohort of 68 men without CaP who had HPIN only on prostatic biopsies. Coherent with our primary hypothesis, significant associations between telomere attrition and eventual diagnosis of CaP in the HPIN and in the surrounding stroma were found. Kaplan-Meier analysis of telomere length demonstrated a significantly increased risk for the development of cancer with short telomeres in the surrounding stroma [P = .035; hazard ratio (HR) = 2.12; 95% confidence interval (95% CI) = 0.231-0.956], and a trend in HPIN itself (P = 0.126; HR = 1.72; 95% CI = 0.287-1.168). Cox regression also demonstrated a significant relationship between the time from the original biopsy to the diagnosis of cancer and telomere length in HPIN and the surrounding stroma (both alone and in combination with baseline prostate-specific antigen). Together, these analyses lend support to the hypothesis that telomere attrition in prostatic preneoplasia may be fundamental to the generation of chromosomal instability and to the emergence of CaP.

BASED ON WORK IN;

Joshua AM, Vukovic B, Braude I, Hussein S, Zielenska M, Srigley J, Evans A, Squire JA. Telomere attrition in isolated high-grade prostatic intraepithelial neoplasia and surrounding stroma is predictive of prostate cancer. Neoplasia. 2007 Jan;9(1):81-9.

2.1 Introduction

As discussed in Chapter 1, prostate cancer exhibits genotypic and phenotypic heterogeneity with multifocal distribution in the gland. Each malignant focus must proceed through the multistep nature of carcinogenesis, involving the acquisition of the malignant characteristics of cancer cells (reviewed in (391)). Given the slow development of CaP, it is likely that the acquisition of genomic instability is a means by which more aggressive neoplastic characteristics are acquired, as it will accelerate the evolution of the malignant clone(s). Previous cytogenetic studies in both HPIN and CaP suggest that chromosomal instability appears to be a major contributor to genomic instability in prostatic carcinogenesis (10, 43, 46, 244, 392). Telomere dysfunction is a mechanism of chromosomal instability (see section 1.6.3.2), it is technically difficult to demonstrate pathognomic intermediaries of the telomere dysfunction such as BFB figures in paraffin embedded material, although it has been noted in prostatic cell lines (393). Additionally, other mechanisms driving genomic instability may be present in prostatic tissue such as chromosomal segregation defects (e.g. Aurora B overexpression (394)) and DNA replication defects (e.g. PSMA overexpression (395)) that may obscure correlative analyses.

The importance of chromosomal instability is that it is predicted to accelerate the rate at which preneoplastic cells acquire the characteristics of overt cancer cells. Provocatively, telomere dysfunction has been demonstrated to have prognostic value in a number of preneoplastic lesions such as Barretts oesophagus (396), ulcerative colitis (397, 398), DCIS (Ductal carcinoma in situ of the breast) (399) and bronchial dysplasias (400). It has also been demonstrated to have prognostic ability for time to recurrence of prostate cancer following prostatectomy (401). However, as a potentially relevant biomarker, greater clinical relevance

needs to be demonstrated in a scenario where it would alter clinical management such as the stratification of prostatic biopsies with HPIN into low or high risk, thus perhaps allowing patients to avoid the morbidity associated with repeated biopsies. Developing an assay for measurement of the length of telomeres in prostatic biopsies and evaluating its prognostic potential for the development of CaP from HPIN are described here.

The occurrence of multifocal HPIN and CaP in up to 80% of prostatectomies suggests a field effect in the peripheral zone of the prostate (43). The molecular nature of this field effect is thought only to involve the prostatic epithelium. We reasoned that telomere length in the prostatic stroma might also be altered in the peripheral zone for two reasons. Firstly, etiological agents involved in prostatic carcinogenesis may affect telomeres in the whole gland rather than just the epithelium. Secondly, it is conceivable that inheritance of shorter constitutional telomere length (affecting both epithelium and stroma) may itself be a risk factor for neoplastic progression in the prostate, as has been demonstrated in other malignancies (402).

To explore these concepts, we examined normalised telomere length in a cohort of men who had isolated HPIN on prostatic biopsies with follow-up of up to 5.5 years. In this study the amount of telomeric attrition in HPIN was accompanied by a proportional shortening in the surrounding stroma. We conclude that the extent of telomere attrition in such tissues may allow for improved prognostication of HPIN lesions into low and high-risk for development of eventual CaP, and provide insights into the genomic mechanism of carcinogenesis in prostatic preneoplasia.

2.2 Materials and Methods

2.2.1 Tissue accrual

Patient samples used in this study comprised a retrospective cohort obtained from prostatic biopsies obtained through UroPath Canadian Pathology Speciality Services over the period 1998-2000. The Research Ethics Board of the University Health Network, Toronto, Canada, approved this study.

2.2.2 Description of Cohort

Men were biopsied using a sextant technique with 6 possible sites for biopsy. 7/34 (21%) men had the cancer diagnosed at the site of the HPIN biopsy available for study, 12/34 (35%) had cancer diagnosed on the same side, whilst 19/34 (56%) had cancer diagnosed on the opposite side. The characteristics of the cohort are described in Table 2.1.

	Mean	Standard Deviation	Median	Range
PSA	8.8	6.95	8	0.7-51
Age	66	6.7	67	51-82
Time from first to final biopsy	19m	17	14.5	1-69
Time to diagnosis of cancer (n=34)	15.5m	12	14	1-42
Number of biopsies until cancer diagnosed (n=34)	1.5	1	1	1-5
Gleason Score (n=34)	6	0.5	6	5-8

Table 2.1
Description of clinical and pathological variables of the study cohort.

2.2.3 Pathology

Biopsy samples were formalin fixed and paraffin embedded. One biopsy was analysed from each man. The biopsies usually consisted of a slither of tissue (approx 1-2mm by up to 15mm). The initial cohort comprised 94 patients, all of whom had a diagnosis recorded of HPIN upon initial pathology review of prostatic biopsies. Following re-evaluation of deeper sections by Dr Andrew Evans, a cohort of 68 patients was identified for inclusion in this study that had evidence of HPIN and adequate stroma on deeper sectioning. There were 2-4 deeper slides available from the original hematoxylin and eosin (H&E) slide used for HPIN identification, orientation and further analyses. These regions, and surrounding areas of matching stroma were examined for telomeric and centromeric content using quantitative fluorescence in-situ hybridisation (QFISH). All investigators were blinded to patient outcome during the study period.

2.2.4 QFISH

QFISH was performed using pan-telomeric and pan-centromeric peptide nucleic acid (PNA) probes on unstained 5 μm sections. Telomere $(C_3TA_2)_3$ and centromere (16-mer α-repeat DNA) specific (403) probes were directly labelled with Cy3 and FITC fluorescent dyes respectively, and were obtained from Applied Biosystems (Foster City, CA, USA). A standard technique for PNA FISH (404) was applied with minor modifications as described previously (216). Slides were counterstained with DAPI/antifade (Vectashield, Burlingame, CA, USA) and analysed.

2.2.5 Image capture

Regions of interest were identified and marked on the overlying H&E section. Corresponding pathology was identified on the FISH slides. Slides were analysed with a Leica

DMRA2 epifluorescence microscope (Leica Microsystems, Wetzlar, Germany) equipped with appropriate filter sets, a 100W mercury lamp and a 100X/1.4 NA oil immersion lens. Twelve-bit grey scale image were produced with a Hamatasu ORCA ER-17 camera (Hamatasu, Bridgewater, NJ, USA) and the OpenLab 4.0.3 software package (Improvision, MA, USA). Filter Set 43HE (For Cy3; Excitation 550/25, Emission 605/70), Filter Set 17 (For FITC; Excitation 485/20, Emission 535/40) and Filter Set 01(For DAPI; Excitation 365, Emission 420) were used (Carl Zeiss, USA). Optimized exposure times were 300 ms (Cy3), 150 ms (FITC) and 10 ms (DAPI).

In order to compensate for different focal depths, 10 consecutive images were z-stacked using an automated Leica CTRMIC interface (Leica Microsystems, Wetzlar, Germany) into a composite image that was used for quantification. Images were saved and exported to the ImageJ software package (405) . Exposure times of the telomere and centromere signals were optimised to be within the linear range of fluorescence assessment. Once these times were optimised, they were kept constant for all further experiments. An average of 50 cells were examined from each HPIN and stroma in every slide to quantify the telomeric and centromeric signals by QFISH. Stromal cells were selected for analysis, avoiding areas of photobleaching and lipofuscin autofluorescence, typically within 1mm of HPIN.

2.2.6 Image Assessment

Quantitative assessment of the telomere/ centromere signal intensity was performed on the captured images and used to determine the relative changes in telomere length and DNA ploidy. After export to ImageJ, non-overlapping nuclei were defined in a region of interest. Subsequently, quantitative analysis was performed on a per nucleus basis, on Cy3 (telomere) and FITC (pan-centromere) images using visual thresholding to outline the relevant signals (406). The intensities of all pixels outlined within a predefined nuclear boundary were summed

on a per cell basis and tabulated. The absolute values for the pan-centromeric QFISH indicate partial ploidy change, polysomies, hybridisation differences or amount of nuclear material in a section. For example, theoretically there will be a doubling of telomere signal per centromere as a result of every extra chromosome per HPIN cell. Thus, to control for differences in ploidy and hybridisation, all telomere intensities were expressed as a ratio of telomeric to centromere intensity ratios for each nucleus. These ratios were then averaged across the whole slide. An example of the approach taken in this study is illustrated in Figure 2.1.

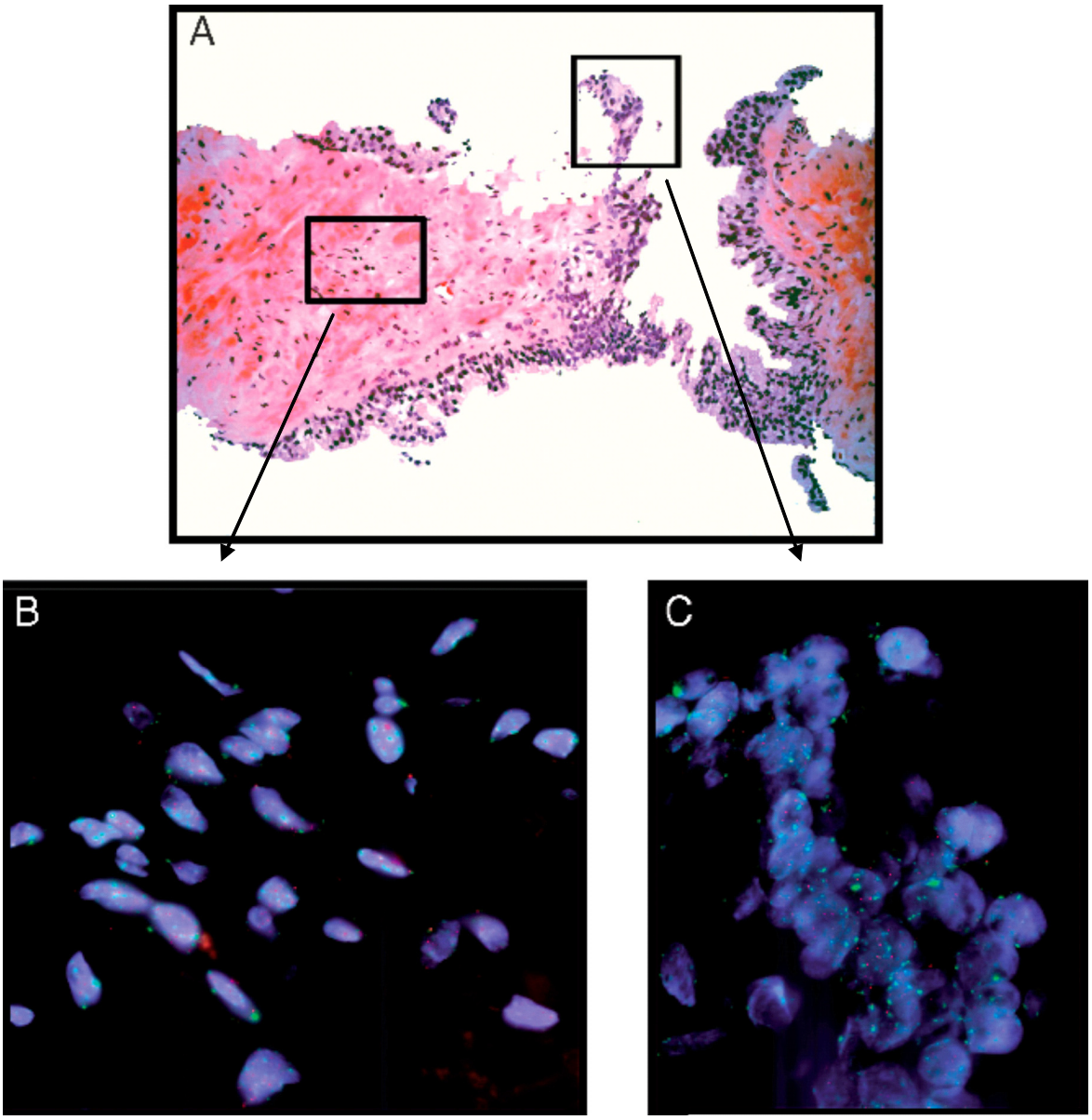

Figure 2.1 A representative example of the analysis utilised in HPIN biopsies. (A) Areas of interest were identified and corresponding QFISH images were generated on a deeper slice of tissue, with corresponding areas of stroma (B) and HPIN (C) analysed. The images have been coloured to facilitate visual inspection with telomere PNA probe (Cy3-red) and centromere PNA probe (FITC-green).

2.2.7 Statistical Assessment

All statistical assessments were carried out with the "R" software package (407). This software package is an open-source language and environment for statistical (linear and nonlinear modelling, classical statistical tests, time-series analysis, classification, clustering) and graphical techniques, and is highly extensible as it allows users to add additional functionality by defining new functions.

All correlations were examined with normalised telomere lengths. Statistical analyses for correlations for outcome to CaP were carried out using logistic regression and likelihood ratio tests for significance. P values are considered significant at the 0.05 level for the association of telomere length and the development of prostate cancer only, the other P values presented are subject to errors of multiple comparison testing and are hypothesis generating only. Standard t-tests were used to detect differences between mean telomere values of those men that did and did not develop cancer. Cox regression modelling was used to determine the association of time to diagnosis with normalised telomere length as well as the calculation of hazard ratios and confidence intervals for Kaplan-Meier analysis. Standard Kaplan-Meier analysis was carried out to explore the time to diagnosis of cancer stratified by telomere length in HPIN.

2.3 Results

2.3.1 Fluorescence Variables

2.3.1.1 Absolute Fluorescence Values

Overall combined centromeric intensity in HPIN revealed that centromeric fluorescence was 22% greater compared to the surrounding stroma (SD 31%) (Figure 2.2A). In comparison, overall combined telomeric intensity measured in HPIN divided by that of the surrounding

stroma revealed that the telomeres in HPIN had an intensity that was on average 36% of the surrounding stroma (SD 21%) (Figure 2.2B). The positions of the centromeric and telomeric signals within the cells were not recorded, and their analysis was beyond the capabilities of the software used.

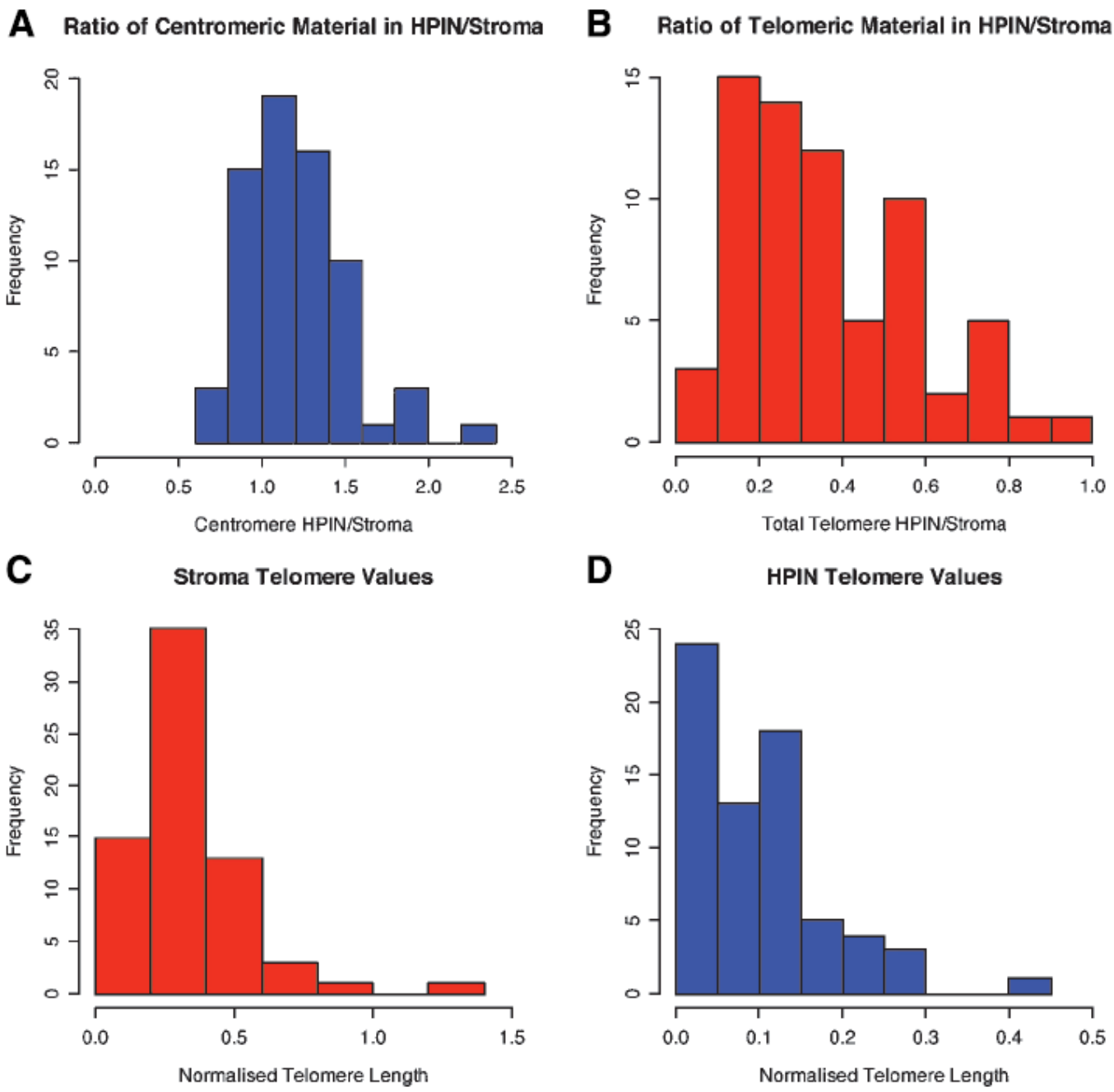

Figure 2.2 - To examine the relative amount of chromosomal material in HPIN versus surrounding stroma we plotted (A) the frequency distribution of the ratio of centromeric fluorescence intensity measurements in HPIN compared to the surrounding stroma. On average fluorescence was 22% greater (SD 31%) in HPIN compared to the surrounding stroma. To examine the relative amount of telomere attrition in the prostate we plotted (B) the frequency distribution of the ratio of the telomeric fluorescence in HPIN divided by that of the surrounding stroma. As described in the text, the average in the surrounding stroma was 64% less (SD 21%). (C) Frequency distribution of the normalised telomere values (telomeric fluorescence/ centromeric fluorescence) in HPIN and (D) in stroma for study cohort.

2.3.1.2 Normalised Fluorescence Values

Inspection of the normalised QFISH values alone for both HPIN and stroma did not reveal any population of uniform telomere length amongst the cells (Figure 2.2C, 2.2D). There did not appear to be any relationship between telomere length in HPIN or stroma and patient age at initial biopsy (Adjusted $R^2 = 0.052, 0.104$ respectively). Additionally, there was also no correlation between prostate specific antigen (PSA) level and telomere length, suggesting that these may be independent phenomena (Adjusted $R^2 = -0.007, 0.006$ respectively).

2.3.2 Statistical Correlations

2.3.2.1 Analysis for outcome to CaP

As the cohort of men did not have time or event mandated biopsies, we initially calculated logistic regression statistics for the diagnosis of CaP after particular time points had elapsed. The time variable corrects for men who were lost to follow-up after a negative biopsy subsequent to the time indicated in Table 2.2.

Time	Men at Risk	HPIN	Stroma	PSA	HPIN + PSA	Stroma + PSA
Immediately	68	0.026	0.029	0.021	0.012	0.010
3 months	64	0.050	0.038	0.032	0.019	0.015
6 months	61	0.075	0.046	0.046	0.036	0.026
12 months	56	0.056	0.043	0.107	0.049	0.046

Table 2.2 P values for logistic regression between outcome to CaP at various time points and telomere length in HPIN and Stroma as well as PSA at baseline

Multivariate modelling at these time points, combining telomere length measurements and PSA, also showed high levels of significance e.g. at 3 months, PSA + HPIN (p=0.019), PSA + Stroma (p=0.015). P values calculated for the association between telomere length and PSA by logistic and multivariate analysis are in Table 2.2. Alternatively, standard t-test analysis and accompanying boxplots for telomere length in both HPIN (t-test, p=0.03, 95% CI 0.004-0.080) and stroma (t-test, p=0.04, 95% CI 0.004-0.188) with final diagnosis are illustrated in Figure 2.3A and 2.3B.

2.3.2.2 Cox Regression modelling for time to diagnosis

Cox regression modelling demonstrated that telomere length of HPIN and surrounding stroma also predicted the time to diagnosis of cancer from the initial biopsy, both alone (p=0.015 and p=0.021 respectively) and in combination with PSA (HPIN and PSA, p=0.006; Stroma and PSA, p=0.010; PSA and HPIN and Stroma, p=0.015).

2.3.2.3 Site of cancer and Gleason score

There did not appear to be any relationship between the telomere length of the biopsy and the ultimate Gleason score of the prostate tumours (Figure 2.4B). To determine whether the relative telomere length within different regions of the gland at the time of biopsy was predictive of the site that was diagnosed subsequently with cancer, a comparison between the sites biopsied, and the side of the gland that was diagnosed with cancer was performed (Figure 2.4C). Whilst the numbers are limited, trends in both HPIN and stromal telomere length suggest that biopsy sites that eventually had cancer detected had shorter telomeres than those in whom cancer was detected on the same side but at a different site or on the opposite side of the gland.

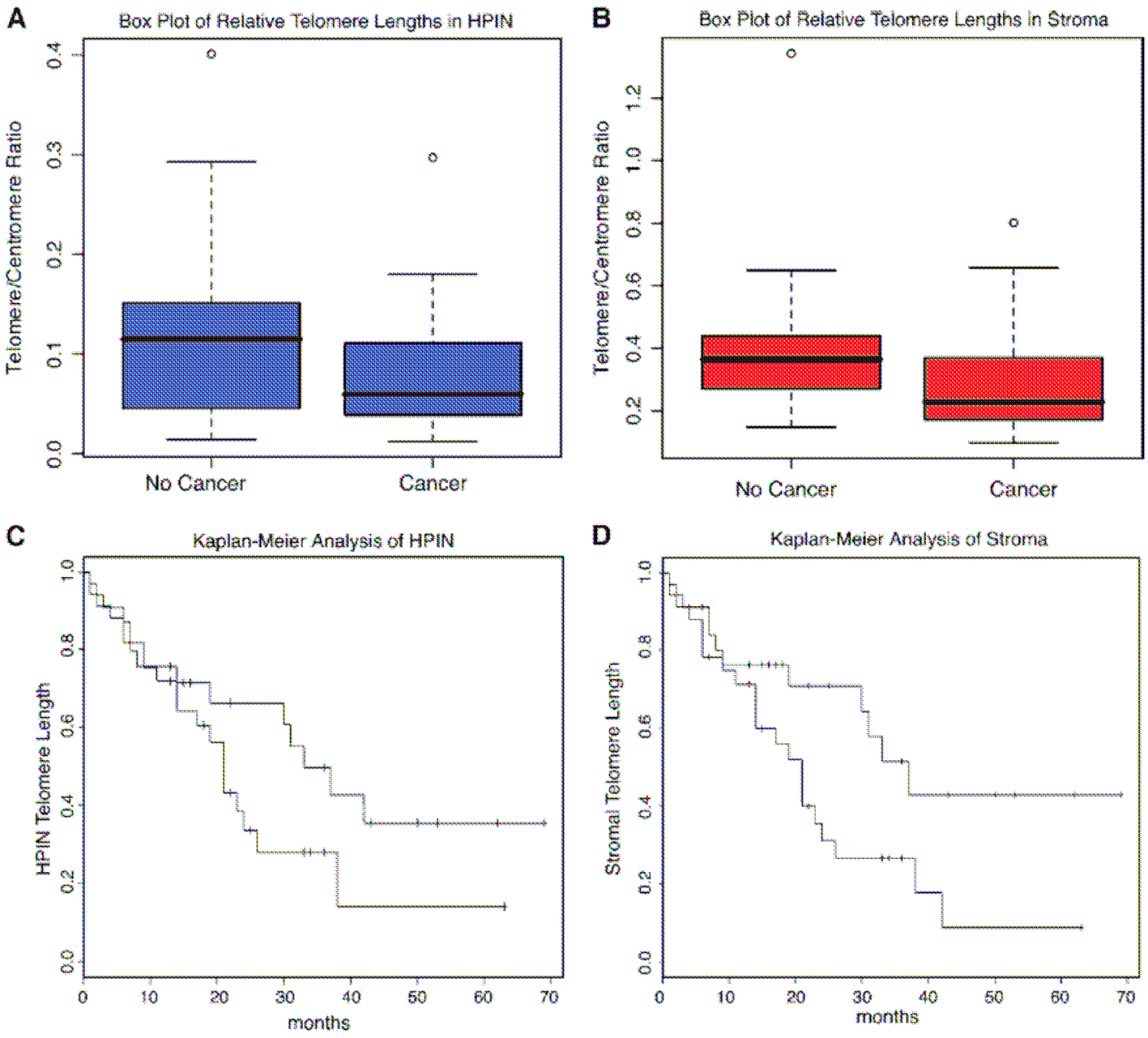

Figure 2.3 (A) Boxplot of relative telomere length in HPIN comparing groups of men who did and did not develop cancer. Thick black line represents median value. Upper border of blue rectangle represents 25% percentile, Lower border represents 75% percentile. Circles represent outliers based on 1.5X Inter-quartile range. Bars extending above and below represent upper and lower limits of data. (t-test, p=0.03, 95% CI 0.004-0.080) (B) Boxplot of relative telomere length in Stroma comparing groups of men who did and did not develop cancer. (t-test, p=0.04, 95% CI 0.004-0.188) (C) Kaplan-Meier Analysis of HPIN Telomere length, stratified by median value for the time to develop cancer (p=0.126, HR=1.72, 95% CI 0.287-1.168). (D) Kaplan-Meier Analysis of Stromal Telomere length, stratified by median value for the time to develop cancer (p=0.0346, HR=2.12, 95% CI 0.231-0.956).

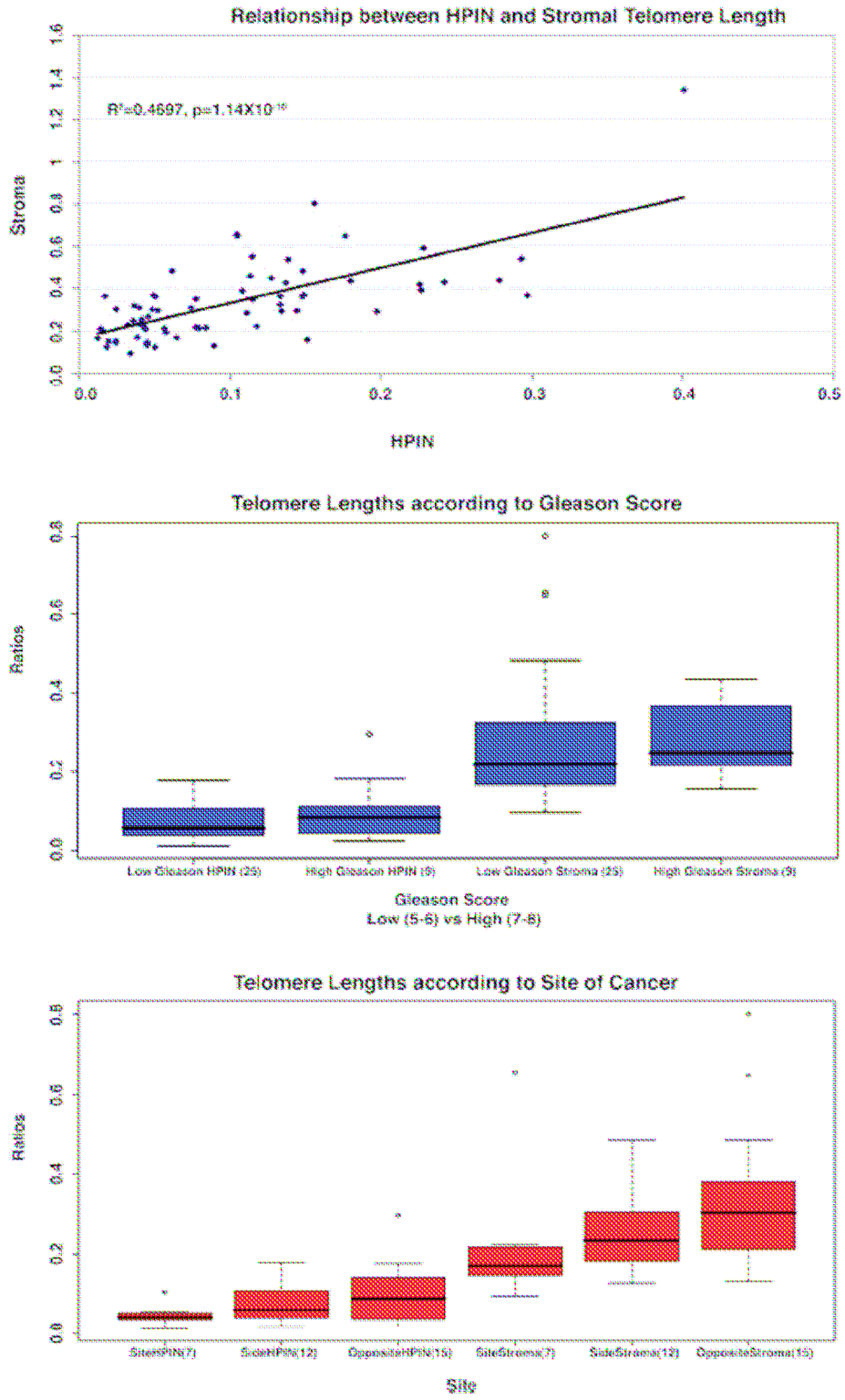

Figure 2.4 (A) Relationship between normalised HPIN and Stromal Telomere Length in prostatic biopsies. (B) Boxplots of normalised telomere lengths in HPIN and stroma according to Gleason score of eventual cancer. Numbers in brackets adjacent to labels on X axis represent the number of cases with that outcome in the cohort.(C) Boxplots represent sites of diagnosis of CaP grouped by their relationship to where the biopsy was taken. X axis labels refer to the type of analysis, with the first letters referring to the site of the eventual cancer; either the same site, the same side or the opposite side of the prostate gland the subsequent lettering indicates either HPIN or surrounding stroma. The numbers in brackets refer to the number of men in those groups.

2.3.2.4 Analyses from correlation of telomere length in HPIN and stroma

A notable finding was the significant association between the telomere length in the HPIN and that in the surrounding stroma (Adjusted R^2=0.4697, p=1.14X10^{-10}) (Figure 2.4A).

2.3.2.5 Analyses from Stratification of Telomere Length

As a further exploratory analysis, telomere length was stratified into "short" and "long" with the cut-off point at the median value. Kaplan-Meier analysis of the time to diagnosis of cancer stratified by telomere length in HPIN and stroma reveal trends to significance (p=0.126, HR=1.72, 95% CI 0.287-1.168) and (p=0.035, HR=2.12, 95% CI 0.23-0.96) respectively (Figures 3C, 3D). A trend was also noted for PSA (p=0.093, HR=1.8, 95% CI 0.89-3.63) but not for age (p=0.522, HR=0.8, 95%CI 0.63-2.57).

2.4 Discussion

Understanding the molecular processes driving prostatic carcinogenesis has important clinical consequences, as studies of biopsies and autopsies suggest that PIN may precede cancer by about a decade (11). Previously, our laboratory demonstrated a decreasing gradient of telomere length in radical prostatectomy samples from benign epithelium to HPIN far from the cancer to HPIN close to the cancer to CaP itself (216) (see Figure 1.3). The present QFISH study was the first to examine normalised telomere length measurements using cell-by-cell analyses of both pre-neoplastic epithelial tissue and stromal components of the prostate in a large enough cohort to detect a correlation between epithelial and stromal telomere lengths (Figure 2.1).

The results presented reveal insights concerning both telomere biology and the process of prostatic preneoplasia. The 22% increase in centromeric intensity in HPIN compared to the stroma (Figure 2.1A) is consistent with previous studies from our laboratory, indicating that in early HPIN gross ploidy change is rare, although subsets of patients have characteristic chromosomal gains (215). The 64% reduction of telomere length in the same tissue (Figure 2.1B) might be a surrogate marker for the number of times the pre-neoplastic epithelium has replicated compared to the surrounding stroma. The left shifted distribution of this ratio (Figure 2.2B) may indicate that there is variable timing to the reactivation of telomere maintenance in HPIN. Additionally, other factors may influence telomere length, since change in ploidy, concurrent telomerase expression, (408, 409) and additive oxidative stress (410) are all likely to influence the relative rates of attrition. The findings of the present study are coherent with that of Meeker *et al*., who examined 11 HPIN lesions from 6 patients after radical prostatectomy. Similar telomeric fluorescence in prostatic stromal and basal epithelial cells was found, with a 73% decrease of telomere length in luminal HPIN compared to the basal cells, comparable to our finding of a 64% decrease compared to surrounding stroma.

Overall, the data suggest that those men with biopsies showing shorter telomeres have a greater likelihood of being diagnosed with cancer. Shorter telomeres may either have been inherited as a constitutional trait, or have been acquired somatically because of induction of attrition by tissue-specific environmental factors. In either case, in HPIN lesions where cells have longer telomeres, there may be a tumour suppressor mechanism active, as the prostatic cells do not possess enough permissive mutations for continued proliferation to take place in the setting of a telomere induced DNA damage signal (261). As discussed in section 1.6.3.2, telomere length may act as a mitotic clock. It follows that areas of HPIN with shorter telomeres may have replicated more and/or been subjected to greater oxidative stress thereby leading to a greater potential for stochastic events such as defects in p53 or p27 that ultimately contribute to

the genomic instability and acquisition of the chromosomal rearrangements that are associated with the emergence of carcinoma (216).

Our findings lend support to the hypothesis that there may be broadly two types of HPIN; one arrested in oncogene induced senescence (with longer telomeres) and another that has bypassed OIS, continued to proliferate, and generated critically short telomeres (see Figure 1.3). Support for this model comes from; (1) the *PTEN* knock-out model of prostate cancer which found heterozygous *PTEN* deletion lead to a p53 dependent senescence barrier that would likely occur to early in the evolution of HPIN for a telomere induced barrier (411), (2) High levels of ATM, CHk2 and gH2AX activation in HPIN (258) indicating the presence of an activated DNA damage response, (3) Telomerase expression at varying levels in HPIN and high levels in prostate cancer (408, 409, 412).

Whilst current evidence suggests that histologically normal prostatic tissue adjacent to a CaP may harbour subtle oncogenic change(401, 413, 414) there are only limited data suggesting that the surrounding stroma is also subject to oncogenic modification (56). Preliminary evidence of such a phenomenon was first reported by Fordyce *et al*., (401) who found reduced telomere length in histologically normal prostate tissue (containing both epithelium and stroma) in tissue adjacent to foci of CaP. The findings in the present study indicate that telomere attrition also occurs in the stroma. As the prostatic stroma is not thought to replicate to any significant degree during the process of prostatic carcinogenesis, these data suggest that aetiological factors possibly related to prostatic carcinogenesis may affect both compartments of the prostatic microarchitecture. Dietary antioxidant deficiency and chronic inflammation are considered candidates for this effect, as they both act though oxidative stress to which telomeres are known to be particularly susceptible (204, 415). Corroborative evidence (416) suggests that senescent prostatic fibroblasts (which are likely to be those with short telomeres), secrete a number of growth factors such as HGF that may facilitate prostatic carcinogenesis through mechanisms

such as co-activation of androgen receptor signalling (417). Taken together, these studies suggest a link between the well-established role of tumour-stromal interaction (339) and telomere dysfunction in prostatic carcinogenesis.

Despite the intriguing observations made, there are limitations to this analysis. The patient biopsies originated from different community practices throughout Ontario, Canada and did not have consistent time/event-mandated further biopsies. We were limited in only analysing one HPIN containing biopsy site in the sextant biopsy set from every man rather than a thorough analyses of telomere length in every biopsy site which would allow a greater understanding of the evolution of telomere dysfunction in the three dimensional anatomy of the prostate gland. Additionally, ascertaining telomerase expression would have been useful in our cohort, but there are no reliable methodologies to do this in paraffin embedded sections (418). Our patient numbers were limited, which likely accounts for the differences in significance between the Kaplan-meier assessments of the HPIN and stroma. Unfortunately, normal peripheral blood was not available to further explore the contribution of constitutional telomere length in this study. Finally, it is possible that a proportion of the men who were diagnosed with CaP during the study period had foci of neoplasia that were missed on the initial biopsy.

In conclusion, this study suggests that analysis of telomere attrition might assist with diagnosis and prognosis in prostatic neoplasia. Further studies may examine the potential for greater prognostic value with other emerging markers of HPIN and prostate cancer (419-421).

3. THE ROLE OF *TMPRSS2-ERG* GENE FUSIONS IN THE EVOLUTION OF PROSTATE CANCER

SUMMARY

The description of novel recurrent ETS – related gene fusions in up to 80% of prostate cancer cases has emphasized the importance of understanding the origins and biologic implications of genomic instability in prostatic carcinogenesis. In this study, analysis of 15 prostate cancer cases by reverse transcription-polymerase chain reaction was used to detect six ERG-related gene fusion transcripts with TMPRSS2. No TMPRSS2/ETV1 chimeric fusion was detected in this series. Three-color fluorescence in situ hybridization confirms that TMPRSS2/ERG fusion may be accompanied by a small hemizygous sequence deletion on chromosome 21 between the ERG and TMPRSS2 genes. Analysis of genomic architecture in the region of genomic rearrangement suggests that tracts of microhomology could facilitate TMPRSS2/ERG fusion events.

BASED ON;

Three-Color FISH analysis of *TMPRSS2/ERG* fusions in prostate cancer indicates genomic microdeletion of chromosome 21 is associated with rearrangement, Yoshimoto M, Joshua AM, Chilton-Macneill S, Bayani J, Selvarajah S, Evans AJ, Zielenska M, Squire JA., Neoplasia. 2006 Jun;8(6):465-9.

Note: M. Yoshimoto and A.M. Joshua contributed equally to this work.

3.1 Introduction

Whilst well recognized in the haematological cancers, structural aberrations were thought to be rare in common solid tumours until the discovery in late 2005 of the TMPRRS2-ETS fusion genes in CaP. Initially alluded to by Petrovics *et al.* (188) who described the high level of overexpression of the *ETS*-related gene (*ERG1*) in the prostate Cancer (CaP) transcriptome it was Tomlins *et al*. (159) who described novel gene fusions involving either *ERG* or related genes, *ETV1*, *ETV4* (164) and *ETV5* (422) that underlie their previously described overexpression.

Here we provided independent confirmation of the translocation by FISH, demonstrated its presence in 6 of 15 (40%) CaP specimens and described two novel variant transcripts in a multi-centric tumour. In addition, break-apart three-color FISH was used to confirm that a deletion between *TMPRSS2* and *ERG* on chromosome 21 was associated with gene fusion events. This three-colour analysis was necessary to unravel the mechanisms involved in the translocation as dual colour FISH (as used in the original paper by Tomlins *et al*. (159)) is unable to distinguish between 3 possible scenarios of alterations at the *TMPRSS2-ERG* locus on chromosome 21(423), one of which may have been telomere mediated as it involved a repeat amplification (see Figure 3.1).

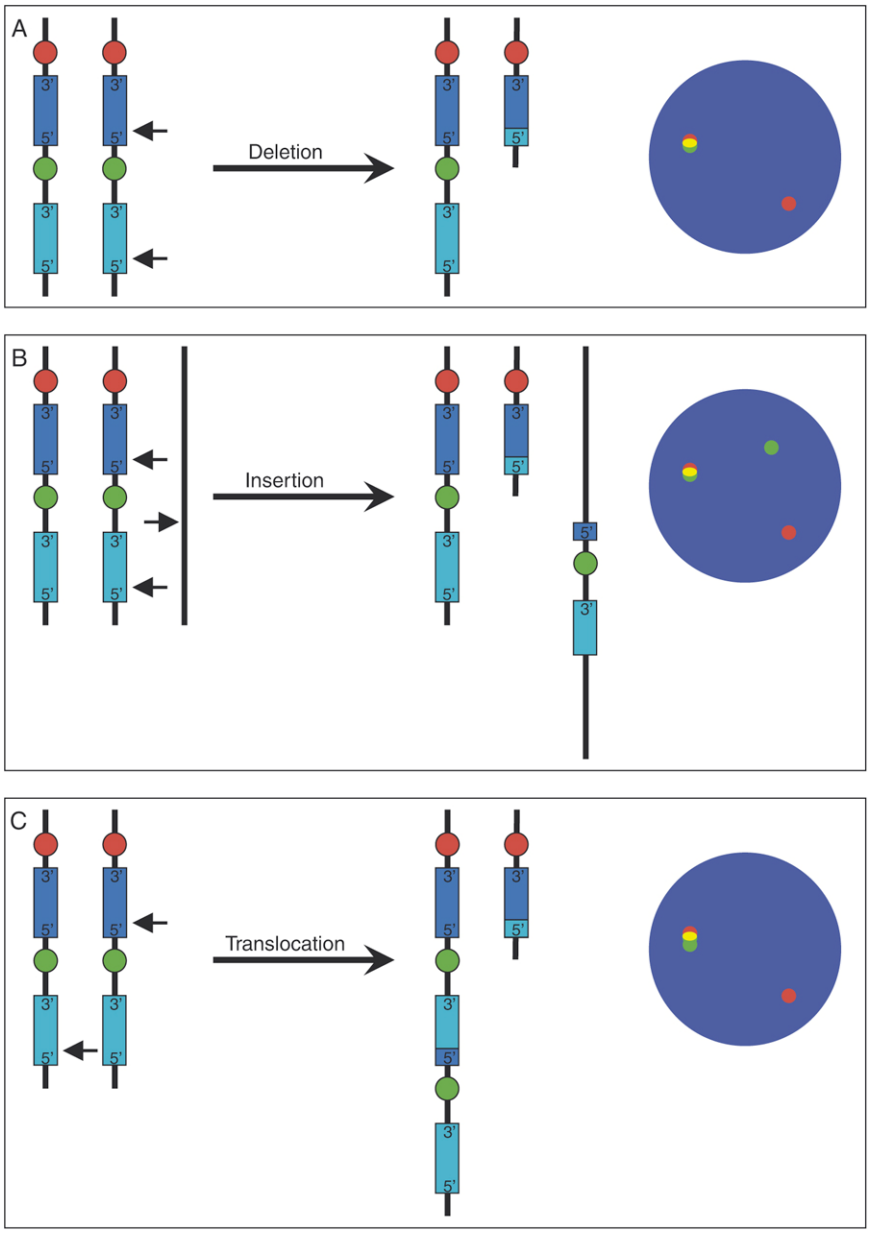

Figure 3.1. Schematic representation of possible chromosome mechanisms that can give rise to the TMPRSS2-ERG fusion oncogene in prostate carcinogenesis, and the expected FISH signal pattern in interphase nuclei using a dual-color, break-apart assay with 2 probes flanking the ERG gene (the normal pattern would be 2 pairs of colocalized red and green signals). A, TMPRSS2-ERG fusion obtained by a deletion between the 2 genes, resulting in 1 isolated red signal (corresponding to the 3'ERG probe) owing to the loss of one green signal (corresponding to the 5'ERG probe). B, TMPRSS2-ERG fusion obtained by insertion of DNA material between the 2 genes into a third chromosome, identified by the splitting apart of 1 red and 1 green signal. C, TMPRSS2-ERG fusion obtained by a translocation between the 2 chromosome 21 homologs, resulting in 1 isolated red signal and the juxtaposition of the corresponding green signal with the colocalized red and green signal from the other chromosome 21 (hardly distinguishable from the deletion mechanism illustrated in A, but clearly different from the insertion FISH pattern). Box with darker shade blue indicates ERG gene; box with lighter shade blue, TMPRSS2 gene; dark blue circle, interphase nuclei; green circle, 5'ERG probe; red circles, 3'ERG probe. Figure adapted from; Teixeira: Am J Surg Pathol, 32(4), 2008.640-644

3.2 Materials and Methods

3.2.1 Pathology

Fifteen CaP tissue samples were obtained from radical prostatectomies. Part of the tissue was embedded in frozen section medium and stored at -80˚C until tumor-rich tissue was selected for RNA extraction. FISH analysis was performed on adjacent sections. Tissue sections were also stained with hematoxylin and eosin and subjected to standard histopathological evaluation to determine pathological grade, tumor content and whether single or multifocal CaP was present. Gleason scores ranged from 6-9 and one tumor sample (78-01) was considered to have multicentric histology.

3.2.2 PCR/ Sequencing

To determine the prevalence of *ETS* rearrangement, reverse transcription and PCR (RT-PCR) amplification (GeneAmp RNA PCR Core Kit, Applied Biosystems) was carried out as described by Tomlins *et al*. (159). Duplicated RT-PCR products from 15 CaP cases were sized by electrophoresis on a 1.5% agarose gel and by a DNA 1000 LabChip Kit (Agilent 2100 Bioanalyzer, Agilent Technologies, Inc., Palo Alto, CA, USA). These products were then gel purified and sequenced directly using an ABI PRISM 377 sequencer (Figure 3.2).

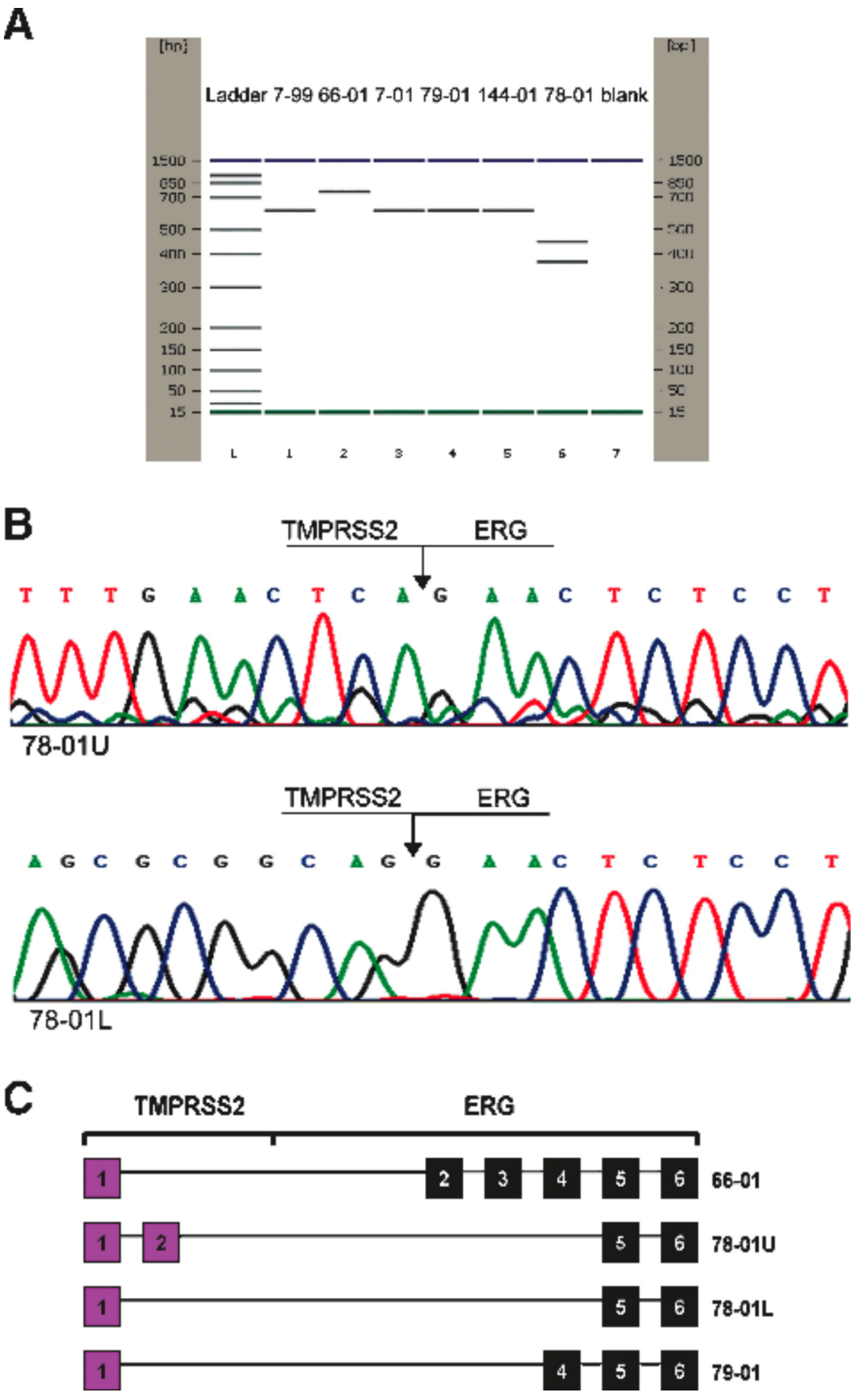
A
[bp]
Ladder 7-99 66-01 7-01 79-01 144-01 78-01 blank
1500
650
700
500
400
300
200
150
100
50
15
L 1 2 3 4 5 6 7
B
TMPRSS2
ERG
T T T G A A C T C A G A A C T C T C C T
78-01U
TMPRSS2
ERG
A G C G C G G C A G G A A C T C T C C T
78-01L
C
TMPRSS2
ERG
1 2 3 4 5 6 66-01
1 2 5 6 78-01U
1 5 6 78-01L
1 4 5 6 79-01

Figure 3.2 Rearrangement of the *TMPRSS2* and *ERG* genes in CaP. **A.** RT-PCR products from six CaP cases were sized using the Agilent 2100 Bioanalyzer. The fragments were analyzed with a ladder marker to determine the size of each variant *TMPRSS2*/*ERG* transcript. Depending on the breakpoints within each, the fragments were 800, 600, ~430, and ~350 base pairs. **B.** Sequence electropherograms of the mutant *TMPRSS2*/*ERG* transcripts from case 78-01. Two unique variant transcripts were found to be present in this case; one containing exons 1 and 2 of the *TMPRSS2* gene and exons 5 and 6 of the *ERG* gene, and the other containing exon 1 of the *TMPRSS2* gene joined to exons 5 and 6 of the *ERG* gene. The arrows indicate gene breakpoint. **C.** Schematic representation of the exon composition of the *TMPRSS2*/*ERG* gene fusion products from variants CaP cases.

3.2.3 FISH

To confirm the presence of *TMPRSS2*/*ERG* fusions we used interphase FISH assays on corresponding frozen sections. A break-apart FISH strategy was employed in the analysis of the *ERG* gene rearrangement using BAC DNA probes published previously (159). This approach consisted of two DNA probes positioned at opposite sides of the breakpoint region of the *ERG* gene, *ERG* 5' and *ERG* 3' loci, and differential labeling using the Ulysis, Nucleic Acid Labeling kit (Molecular Probes, Eugene, OR, USA). The OregonGreen-labeled RP11-95I21 BAC probe spans the *ERG* 5' and extends inward into exon 10. The red-fluorescein labeled RP11-476D17 BAC probe spans the *ERG* 3' locus and extends inward past exon 4. There is a 35 kb gap between the 3' and 5' *ERG* probes. The *TMPRSS2* gene was identified using the Pacific-blue labeled RP11-35C4 BAC probe, which starts 2.7 Mb from 5' end of the *ERG* gene (Figure 3.3). The FISH criteria to evaluate *TMPRSS2*/*ERG* rearrangement were: (1) visualization of separate green 5' *ERG* and red 3' *ERG* signals, and (2) enumeration of each green, red and blue signal.

The DAPI-stained tumor nuclei (dark blue) were identified in the adjacent H&E stained frozen tissue. The normal signal patterns of the probes were confirmed by the co-localization of Oregon Green labeled 5' *ERG* (green signals), Alexa Fluor 594 labeled 3' *ERG* (red signals) and Pacific-Blue labeled *TMPRSS2* (pale blue signals) in normal peripheral lymphocyte metaphase and normal interphase cells (Figure 3.4A). The *ERG* rearrangement was confirmed by the split of one of the co-localized signals in addition to a fused signal of the unaffected chromosome 21 (Figure 3.4B). A minimum of 300 signals per probe was counted to confirm the *TMPRSS2*/*ERG* rearrangement in CaP specimens previously analyzed by RT-PCR. A decreased ratio for the 5' *ERG* probe mapping to the genomic interval between the *TMPRSS2* region and 3' *ERG* (Figure 3.3) was indicative of a hemizygous deletion. These experiments were optimized using FISH

ratios present in normal adjacent tissue and deletion cut-off values were defined as a ratio of green 5' *ERG* signal over red 3' *ERG* ≤ 0.80 (424) when break-apart FISH analysis indicated a fusion genomic rearrangement was present.

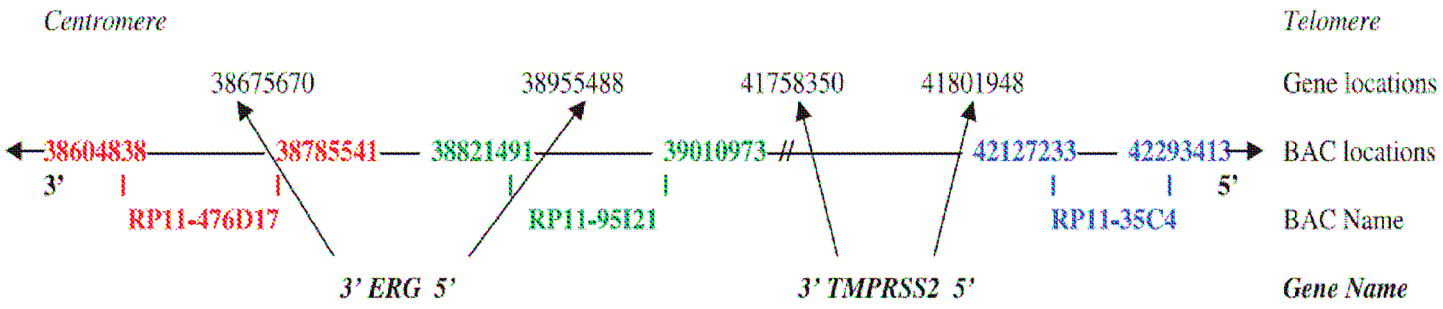

Figure 3.3 Location and names of the BAC probes and gene locations used in the analysis. Gene locations are taken from the May 2004 assembly of the UCSC Genome Browser. Numbers indicate base pair location along the chromosome. Colors correspond to the fluorochromes used in the fluorescence *in situ* hybridization experiments.

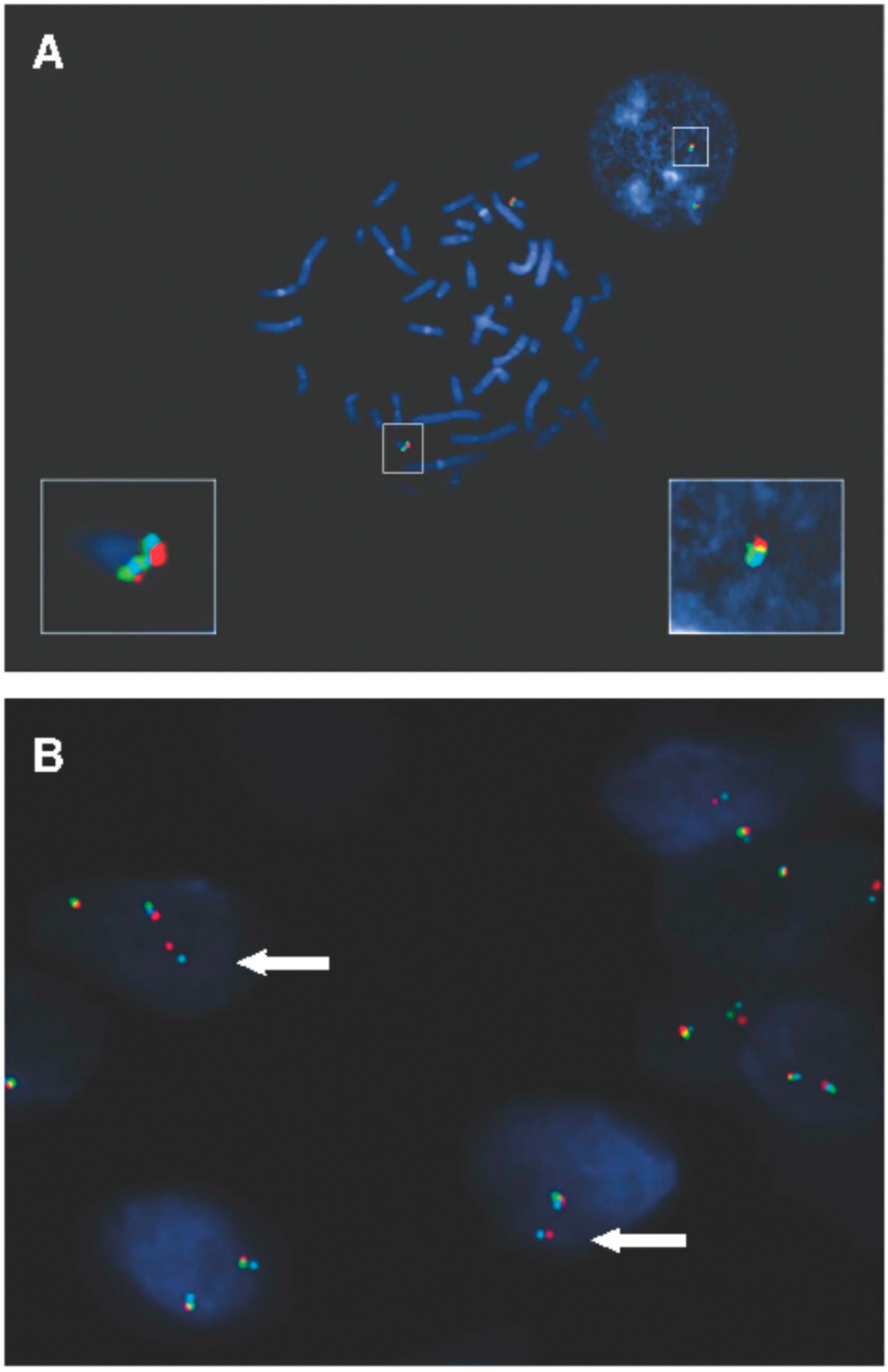

Figure 3.4. FISH analysis showing rearrangement of *TMPRSS2* and *ERG* genes in CaP. **A.** FISH confirms the co-localization of OregonGreen labeled 5' *ERG* (green signals), AlexaFluor 594 labeled 3' *ERG* (red signals) and Pacific-Blue labeled *TMPRSS2* (light blue signals) in normal peripheral lymphocyte metaphase and normal interphase cells. **B.** In CaP cells, the break-apart FISH results in a split of the co-localized 5' green/3' red signals in addition to a fused signal (comprising green, red and blue signals) of the unaffected chromosome 21. Using the *TMPRSS2/ERG* set of probes on CaP frozen sections, *TMPRSS2* (blue signal) remains juxtaposed to *ERG* 3' (red signal) (see white arrows), while co-localized 5' *ERG* signal (green) is lost, indicating the presence of *TMPRSS2*/*ERG* fusion and concomitant deletion of 5' *ERG* region.

3.3 Results and Discussion

3.3.1 Analysis

Of the 15 tumors analyzed, 6 (40%) possessed an *ERG* rearrangement, confirming the FISH findings of the original study (55%; 16/29) (159). Although none of our samples had an ETV1 rearrangement, this observation is not surprising since the original paper only detected the ETV1 fusion transcript in a small proportion of samples (25%; 7/29). More recent data suggest that this may be because ETV1 has numerous upstream partners that may not have been detected using our FISH or PCR probes (174). Using the Agilent Bioanalyzer, the fragment lengths were precisely determined. Five of the six positive *ERG*/*TMPRSS2* fusions had lengths consistent with published findings, however one tumor sample (CaP 78-01) contained two variant *TMPRSS2*/*ERG* transcripts of 430 base pairs and 350 base pairs. Automated DNA sequencing of gel purified transcripts from CaP 66-01 and CaP 79-01 (both typical *TMPRSS2*/*ERG* fusions), and from CaP 78-01 (upper and lower fragments) confirmed fusions of the *TMPRSS2* with the *ERG* gene. Sequence analysis of both gel purified fragments from CaP 78-01 revealed two distinct in-frame rearrangements generating novel *TMPRSS2*/*ERG* fusion transcripts. The variant *TMPRSS2*/*ERG* transcript of 430 bp resulted in the fusion of exons 1 and 2 of the *TMPRSS2* gene and exons 5 and 6 of the *ERG* gene, and the smaller variant *TMPRSS2/ERG* transcript of 350 bp resulted in the fusion of exon 1 of the *TMPRSS2* gene to exons 5 and 6 of the *ERG* gene (Figure 3.2C). It is conceivable that these fusion events represent protein splice variants or independent genomic alterations occurring within one clonal tumor outgrowth, or may represent independent fusions from this multicentric tumor. Applying the break-apart green (*ERG* 5' locus) and red (*ERG* 3' locus) FISH strategy allowed for the confirmation of *TMPRSS2*/*ERG* fusion in frozen sections from 6 different patients. Within these

6 patient samples, deletion between *TMPRSS2* and *ERG* was detected in 3 samples. In all cases, the enumeration with flanking *TMPRSS2* (pale blue) and 5' *ERG* (green) in tumors showed that the ratio was < 0.80 consistent with a deletion affecting the intervening genomic DNA. This high ratio was needed to ensure that the deletions seen are not due to cutting artefact secondary to sectioning or the large nuclei or differences in DNA condensation (425).

3.3.2 Genomic Architecture and Origin of Genetic Translocations

Whilst there are many transcripts recognized, the human *ETV1* gene has up to 14 exons with a DNA binding domain in the last exon, whereas the *ERG* gene has 11 exons with recognized functional domains occurring across exons 5,6 pointed (PNT) interaction domain and exon 11 (*ETS* DNA binding domain). *TMPRSS2* has 14 exons with functional domains in the latter half of the protein only. Both *ERG* and *TMPRSS2* lie on chromosome 21 at cytobands 21q22.3 and 21q22.2 respectively, with approximately 3 Mb between them and lie in the same transcriptional orientation, with *TMPRSS2* localized more telomeric than *ERG*. As can be seen in Figure 3.3 the 5' end of both genes faces the telomere. Given this genomic organization, and the observation that 5' *TMPRSS2* fuses in-frame with 3' *ERG,* an interstitial deletion of the intervening 3 Mb of DNA must take place. Indeed, our three-color FISH analysis confirms loss of genomic content from this region of chromosome 21. This finding raises the question of concomitant haploinsufficiency of one or more genes mapping to this deleted interval. Deletion of the *TMPRSS2* coding region resulting from the fusion rearrangement may lead to the haploinsufficiency of the gene. However, a *TMPRSS2* knockout mouse with no apparent abnormal phenotype was recently reported (426). Examination of the 13 genes within this region of chromosome 21 (*ETS2, DSCR, BRWD1, HMGN1, C21orf13, SH3BGR, B3GALT5, PCP4, DSCAM, BACE2, FAM3, MX2, MX1*) identified two candidate loci, *HMGN1* and *ETS2*. Knock-out models of *HMGN1* demonstrated that loss increased N-cadherin expression (427)

(which has been noted in high-grade CaP (428)) and alters the G2/M checkpoint (429). Additionally, underexpression of the ETS family member, *ETS-2*, has been associated with reduction of the antiapoptotic protein bcl-x(L) and growth regulatory factors Cyclin D1 and C-myc in prostate cancer cell lines (430). Whilst recent transfection experiments with the *TMPRSS2-ERG* fusion gene alone have suggested that it confers malignant characteristics (186) whether this is valid *in vivo* is still a valid issue.

Similar rearrangements involving *ETS* family members in the Ewings family of tumors and haematological malignancies have been shown to involve classic, complex or variant translocations. Interstitial deletions have been described in leukemias (431) and congenital syndromes, and are thought to be due to defective homologous recombination (432), perhaps related to areas of microhomology. For every case of the *ERG* fusion transcripts, there is at least one area of up to 300bp on the intron following the transcribed *TMPRSS2* exon that displays microhomology with up to 90% identity to multiple areas on the intron preceding the relevant *ERG* exon of the relevant transcript. These areas have recently been identified to be Alu repeats (169).

3.3.3 Functional Implications

The *ETS*-family of transcription factors encode nuclear transcription factors with an evolutionarily conserved *ETS* domain of 85 amino acids that mediate binding to purine-rich DNA residues. There are more than 400 target genes in the genome that are either positively or negatively regulated by them (178), so the consequences of ETS fusions could be diverse. To date (see section 1.6.3.1.1), the most relevant evidence suggests that overexpression of the ETS family of genes increases the invasiveness of prostate cancer cells and initiates a signaling program that leads to their dedifferentiation (186, 187), phenomena that fit with their occurrence at the HPIN-CaP transition point and be consistent with the “ETS conversion” process as a

means of epithelial to mesenchymal transition in prostatic epithelium. It also highlights the necessity for genomic instability to drive the process of carcinogenesis as an early change in the emergence of a neoplastic clone.

3.3.4 Clinical Implications

The clinical implications of the translocations remain unclear. In our small cohort, clinical characteristics were distributed unremarkably; tumor stages ranged from T2a-T3b and five tumors were Gleason 7, and 1 was Gleason 9. However, other cohorts provide inconsistent information (188, 190, 191, 433) although several larger studies are tending to suggest a poorer prognosis especially in tumors with a duplication of the *TMPRSS2-ERG* fusion (192, 193). In a recent autopsy study, all metastatic sites of disease demonstrated the *TMPRSS2-ERG* gene deletion (434) suggesting it may directly or indirectly promote the metastatic process and have an important prognostic role. The role the gene deletion plays in androgen refractory disease is also unclear, and is discussed further in Appendix 2.

4. TOPOGRAPHICAL ANALYSIS OF TELOMERE LENGTH AND CORRELATION WITH GENOMIC INSTABILITY IN WHOLE MOUNT PROSTATECTOMIES

SUMMARY

Many critical events in prostatic carcinogenesis appear to relate to the emergence of genomic instability. Characteristic abnormalities such as 8p loss, 8q gain, trisomy 7, *PTEN* microdeletions and *TMPRSS2-ERG* gene fusions appear to mediate mechanisms to increase neoplastic transformation. Evidence suggests that telomere dysfunction is a likely causative factor for some of these abnormalities on the basis of its prognostic importance and the break-fusion-bridge cycle that can lead to manifestations of genomic instability. In this study, we correlate telomere length in various prostatic histologies with markers of genomic instability and immunohistochemical measures of proliferation. We find that telomere shortening is correlated with abnormalities on chromosome 8, but not with trisomy 7 or abnormalities of the *PTEN* locus. Additionally, there were associations with *C-MYC* aberrations in stroma with greater proximity to cancer and a correlation between telomere length in a number of prostatic histologies and the adjacent stroma, suggesting the importance of microenvironmental effects on telomere maintenance in the prostate.

CONTRIBUTORS;

Joshua, A.M., Yoshimoto, M., Marrano, P., Zielenska, M., Minkin, S., Evans, A., Van der Kwast, T., Squire, JA

4.1 Introduction

As discussed in Chapter 2, telomere attrition appears to be an important prognostic factor in the progression of HPIN to CaP. The most plausible explanation for this is that telomere attrition causes the acquisition of genomic instability (see section 1.6.3) (see Figure 1.3). The forms of genomic instability that have been documented in prostatic carcinogenesis include both numerical (trisomy 7 and gains of 8q) as well as structural instability (*TMPRSS2-ETS* (see section 3) and *PTEN* (see Appendix 1)). The contribution of telomere dysfunction to either form has remained unclear.

The etiology of genomic instability remains unclear. Telomere shortening might occur due to factors discussed in section 1.6.3.2 such as hypoxia/ oxidative stress (205, 435, 436), cell replication (437) and defects in DNA repair (438, 439). Subsequent instability acts through intermediaries such as break-fusion-bridge cycles and anaphase bridges. However, it is difficult to demonstrate these intermediaries using prostate paraffin embedded material (given the slow doubling time of prostate cancer), although it is possible to evaluate them in prostatic cell lines (393).

Evidence for the causes of structural instability is limited. Extrapolation from genetic instability syndromes (440) and other malignancies (441) suggest that defects in DNA repair, in particular double strand break repair may contribute, possibly in association with recombinogenic DNA elements such as Alu repeats or tracts of microhomology (442). These mechanisms may co-segregate with telomere attrition in a molecular model of prostatic carcinogenesis since common mechanisms such as defects in DNA double strand break repair may occur concurrently.

As described in section 1.7.1, an oncogene induced senescence checkpoint (258) may act in the prostate to arrest pre-neoplastic cellular growth before the appearance of telomere crisis

(443). OIS might therefore act as an important tumour suppressor mechanism in a complementary fashion to that of early telomere shortening. Mouse models have suggested p53 dependency of this checkpoint in a *PTEN* knockout phenotype (411), but its relevance and occurrence *in vivo* is unclear. Recently, Majumder *et al*., have suggested that this checkpoint is mediated by p27 in HPIN; however neither its relationship to telomere attrition nor its effect on the emergence of genomic instability have been clarified (298).

To explore the aetiology and relationship of telomere attrition to the emergence of genomic instability, we planned a correlative study of; the causative factors of telomere attrition such as proliferation (measured by Ki67) and factors that may contribute to senescence and telomere attrition such as oxidative stress (measured by 8-Hydroxydeoxyguanosine) with telomere length and markers of instability (7CEP, 8p, 8CEP, 8q), microdeletions (*PTEN*) as well as expression of a senescence marker ($p27^{KIP}$) in prostatic whole mounts.

Our hypothesis was that Ki67 index and markers of oxidative stress would correlate with telomere attrition, which in turn would be correlated with markers of chromosomal instability in chromosomes 7 and 8. The inclusion of PTEN would act both as an important internal control and assist in the interpretation of $p27^{KIP}$ staining as AKT activation may contribute to tumour cell proliferation by phosphorylation and cytosolic retention of $p27^{KIP}$(444).

In addition, by studying cell-to-cell variations within extensive regions of whole mount sections, these analyses represent a survey of the genomic architecture within the prostatic tissues to help understand the causes and consequences of the field effect in prostatic carcinogenesis (see section 1.4). To this end, we hypothesis further that HPIN further away from cancer is more likely to express high levels of $p27^{KIP}$ consistent with its role as a marker of prostatic cellular senescence (298).

4.2 Materials and Methods

4.2.1 Tissue Accrual

Patient samples used in this study were obtained prospectively as part of a collaborative research project with Dr John Trachtenberg (Department of Urology, UHN) and Dr Masoom Haider (Department of Radiology, UHN). The Research Ethics Board of the University Health Network, Toronto, Canada, approved this study.

4.2.2 Pathology

The prostatectomy samples were formalin fixed and paraffin embedded. Formalin was injected into the whole prostate to preserve tissue architecture before sectioning. Prostates were sectioned as whole mounts, and cut into blocks at approximately 3mm intervals. From the top of each block, 10 sections were cut, each section being approximately 5 microns in thickness. The top section was stained with hematoxylin and eosin to provide histological information. Subsequent sections were used for quantitative FISH, Chromosome 8 FISH and *PTEN*/ Chromosome 7 FISH, Ki67 and p27 staining respectively. Each prostate contained 8 blocks, which allowed examination of the most relevant part of the prostate gland. Their clinical and pathological characteristics are summarised in Table 4.1

Case	Age	Pathological Stage	Pre-op PSA	Weight (grams)	BPH	HPIN	Cancer	Gleason	% of Prostate involved by Cancer
1	59	T2c	2.93	72	+++	Bilateral ++	Bilateral, predominantly left posterior.	7 (3 + 4) Tertiary 5	2
2	63	T2c	10.99	50	++	Bilateral minimal	Bilateral, predominantly left posterior	6 (3 + 3)	2.5
3	49	T2c	4.18	48	++	Bilateral +++	Bilateral, predominantly right lateral	6 (3+3)	5

Table 4.1 – Clinical and Histological characteristics of prostates analysed

4.2.3 FISH

QFISH was performed as outlined in section 2.2.4. FISH for chromosome 8 (8p22 (LPL)(Spectrum Orange™), CEP® 8 (8p11.1-q11.1)(Spectrum Aqua™), 8q24.12-24.13 (C-MYC)(Spectrum Green™) were carried out with a multi-color probe (Vysis Provysion, Abbott Molecular, Downers Grove, IL, USA) as per manufacturers instructions. Similarly, FISH for *PTEN* (CEP 10 (10p11.1-q11.1)(Spectrum Green™), *PTEN* (10q23)(Spectrum Orange™)) and chromosome 7 (CEP 7 (7p11.1-q11.1)(Spectrum Aqua™) were combined and hybridised as per

manufacturers instructions. All slides were counterstained with DAPI/antifade (Vectashield, Burlingame, CA, USA) and analysed.

4.2.4 Image Capturing

Following FISH, corresponding areas to those annotated on the H&E image were identified on the FISH slides using an epifluorescence microscope (AxioImager Z1, Carl Zeiss Microimaging, Thornwood, NY, USA) equipped with narrow band pass Cy3, FITC and DAPI filter sets, a 100W mercury lamp and 63X/1.4NA and 100X/1.4 NA oil immersion lenses. Filter Set 43HE (For Cy3; Excitation 550/25, Emission 605/70), Filter Set 17 (For FITC; Excitation 485/20, Emission 535/40) and Filter Set 01(For DAPI; Excitation 365, Emission 420) were used (Carl Zeiss, USA). Optimized exposure times were 200 ms (Cy3), 150 ms (FITC) and 5 ms (DAPI).Telomere imaging was undertaken using a 100X lens/1.4 NA and chromosomal imaging over the same glandular areas was carried out with the 63X lens/1.4 NA in order to maximise the number of cells assessable. A Zeiss AxioCam MRm was used for imaging. Sixteen-bit grey scale images were produced. In order to compensate for different focal depths for both quantitative FISH and numerical chromosome evaluation studies, images were z-stacked at 0.5um intervals before being combined into 1 image in a maximum intensity projection (Axiovision version 4.6 (Carl Zeiss Microimaging, Thornwood, NY, USA)). Exposure times of the telomere and centromere signals were optimised to be within the linear range of fluorescence assessment. Once optimisation times were determined, they were kept constant for all further analyses.

4.2.5 Image Assessment

Quantitative assessment of the FISH signal intensity was performed as described in section 2.2.6. Subsequently, automated “macros” were written with the open source program,

ImageJ (405) to allow high-throughput quantitative analyses to be performed on a per nucleus basis, using predetermined thresholding algorithms to define relevant signal; Cy3 (telomeric) fluorescence that exceeded the average + 2.5SD of the fluorescence signal in the non-overlapping nuclei and Cy5 (pan-centromeric) signal that exceeded the top 6.25% of the fluorescence signal in the non-overlapping nuclei were enumerated. These cut-offs differed as the centromeric signal is more diffuse given the larger number of centromeric repeats per chromosome compared to the telomere repeat sequences. The intensities of all pixels outlined within a predefined nuclear boundary were automatically summed, normalised on a per cell basis, and tabulated for analysis on a glandular basis. Since tissue sectioning can result in the truncation of nuclei, which will lead to loss of FISH signals in a subset of nuclei, it is important to rigorously optimize sample processing and scoring criteria (425). To avoid bias associated with truncation artefact; all samples were analysed independently, no analyses were planned that compared non-neoplastic to neoplastic cells (to minimize bias associated with differing nuclear size) and no dichotomous statistical analyses were undertaken, only correlative trends were analysed.

In total, approximately 8000 cells of various histologies were analysed for telomere length, 8500 cells for chromosome 8 abnormalities and 9350 for *PTEN* abnormalities.

4.2.6 Immunohistochemistry

Annotated sections from each block were stained with Hematoxylin and Eosin sections and then scanned into the Aperio ScanScope system (Aperio Technologies, Vista, CA, USA) at 20X magnification. Two pathologists (A.E., T.VdK) annotated the images for a variety of prostatic histologies. Other information, such as distance measurements within the prostates were derived from these sections. Ki67 staining was carried out with heat-retrieval with a 10 mM Citrate buffer pH 6.0 followed by 1 hr incubation at 1 in 300 using the avidin-biotin

technique and staining with a commercial antibody (Ki67 clone SP6, Lab Vision, Freemont, CA, USA). P27 staining was also carried out with the above method, at a 1 in 300 concentration ($P27^{KIP}$, clone 57, BD Biosciences, San Jose, CA). Both stained Ki67 and p27 images were scanned into the ScanScope system and quantified and standardised to an area of interest using the default Nuclear intensity quantification algorithm (Aperio Technologies, Vista, CA, USA) excluding the glandular lumens or other areas of irrelevant pathology.

4.2.7 Statistics

In order to examine the associations between telomere length and measures of genomic instability a number of indices of chromosomal instability were derived from the FISH data. For the chromosome 8 probes, two separate algorithms evaluated each probe locus. Initially, the percentage of cells within each gland that were abnormal (% of abnormalities) and the average number of signals in the nuclei were evaluated. These were combined into measures such as the percentage of total aberrations in a gland and the average signal count for a gland for all probes combined respectively. Monosomy was defined as a single signal for all 3 FISH probes and was recorded as a percentage of monosomic cells per gland evaluated. C-MYC gain was defined as diploid chromosome 8 centromere signals in combination with 3-4 C-MYC loci signals. C-MYC amplification was defined as 5+ C-MYC loci signals with diploid chromosome 8 centromere signals. Simple aneusomy was defined as 3-5 ploidy on the basis of C-MYC and CEP 8 loci whereas complicated aneusomy was defined as any other combination of genomic loci abnormalities at the CEP and C-MYC loci with greater than 3 signals. These measures were combined into a measure of total genomic aberrations. Variance was defined as the square root of the sum of the absolute differences from the diploid state for all 3 loci on the FISH probe divided by the number of cells -1. Similar methods were used for *PTEN* and chromosome 7 analyses; All single probes were evaluated as above; *PTEN* simple aneusomy was defined as 3

or greater centromeric signals from chromosomes 7 and 10. *PTEN* deletion was defined as any loss of 1 or more *PTEN* loci in combination with 2 or more centromeric loci.

All statistical assessments were carried out with the "R" software package (407). Because of limitations imposed by truncation artifacts, we did not attempt to obtain an absolute measure of chromosome instability in sections, but rather examined correlations between measures of instability and telomere length. All correlations were examined with normalised telomere lengths. Wilcoxon tests were used to examine for the difference between telomere lengths. Spearman correlation was used to determine the association of telomere length with measures of instability. Pearson correlation was used to determine the association between telomere length in prostatic epithelial histologies and adjacent stroma. As multiple comparisons were carried out on the same data set for associations between measures of chromosomal instability and telomere length, all these P values are hypothesis generating only and require further validation in additional data sets. P values are otherwise considered significant less then 0.05.

4.3 Results

There are three aspects of telomere pathophysiology reflected in the analyses of these prostatectomies (see Figure 4.1)

4.3.1 Relationship of prostatic pathology to telomere length

As shown in Figure 4.2, we noted significant telomere shortening in all tumours in comparison to normal epithelium, consistent with previous findings. Two of our 3 cases also had telomere shortening in regions of BPH in comparison to normal epithelium (case 1 ($p = 0.0003$, 95% CI -0.28 to -0.08) and case 2 ($p= 0.001$, 95% CI -0.44 to 0.09). None of our cases had telomere shortening in areas of cystic atrophy when compared to normal epithelium. The

telomere length of atrophic lesions might depend on the proximity of the cellular atrophy to the cancer (37), but such a relationship was not evident in the cases we analysed.

4.3.2 Relationship of stromal telomere length with adjacent epithelium

Given the findings of an association between telomere length in HPIN and the surrounding stroma in section 2.3.1.2, we explored whether a similar relationship existed in this cohort. There was a correlation between the telomere length in the stroma and that of the epithelial pathology to which it was adjacent for nearly all histologies (see Table 4.2) in particular for normal and atrophic epithelium. The relationships in cancer and HPIN were evident in 2 of 3 cases, likely limited by numerical power.

4.3.3 Association of genomic instability with telomere length and prostatic histologies

There was an association between genomic aberrations on chromosome 8 with telomere length whilst surprisingly, a consistent lack of any association across the *PTEN* locus. (see Table 4.3 (all neoplastic pathologies including HPIN, Gleason 3,4,5) and Table 4.4 (HPIN only)). Intriguingly, there were no associations of abnormalities seen at the chromosome 7 centromere with telomere length for either cancer or HPIN. There were no associations of any marker of instability with telomere length in stroma or normal epithelium.

To examine the effects of telomere attrition in stroma adjacent to cancer, we also assessed the relationship of the genomic abnormalities in the stroma with their proximity to cancer (see Figure 4.3). They show that with few exceptions, the probability of any aberration at the C-MYC locus, including C-MYC gain or amplification was higher in the stroma close to cancer than further away (see Table 4.5).

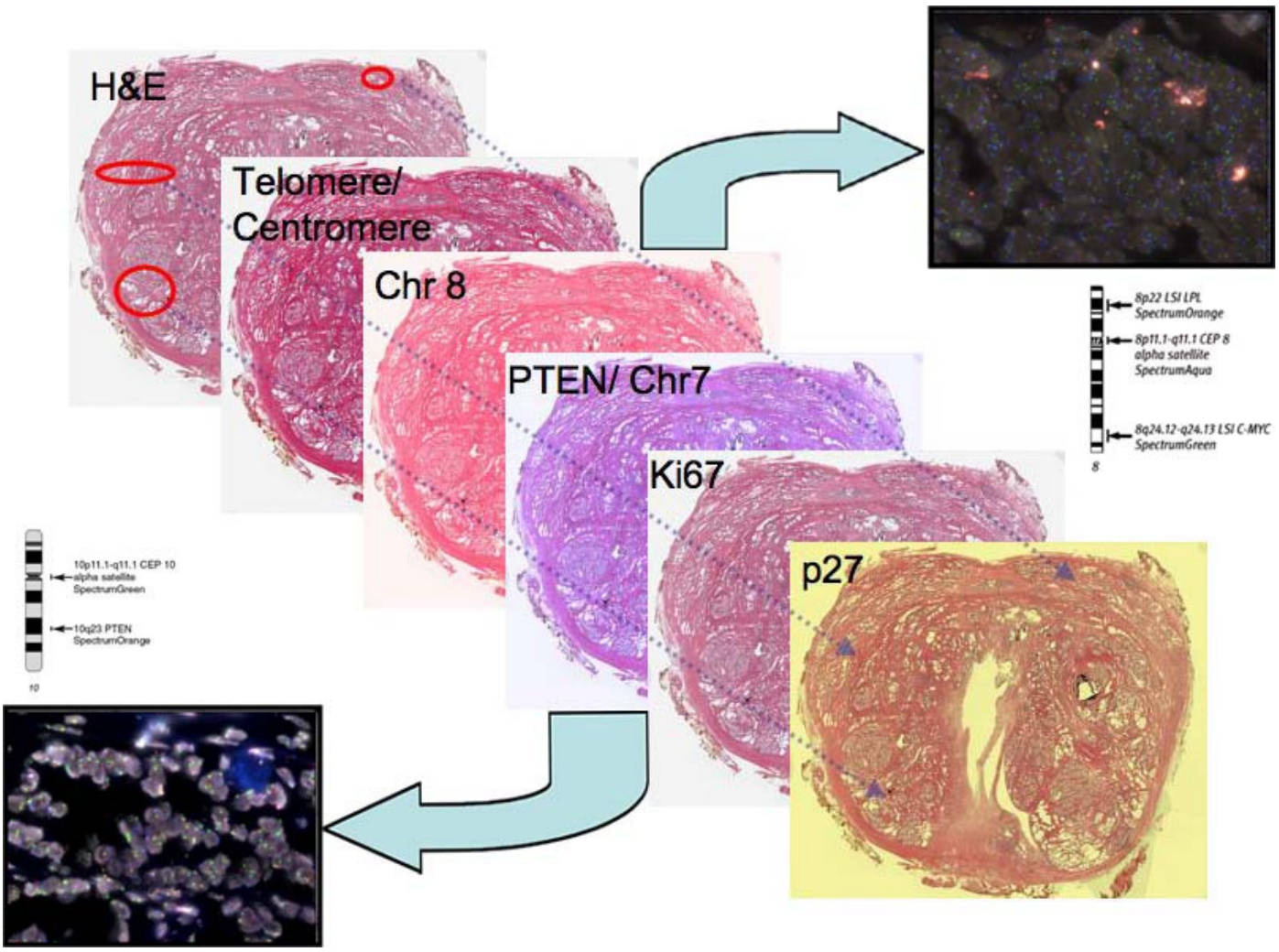

Figure 4.1 An illustration of the methodology in this study. Prostate whole mounts were serially sectioned, with the top section being annotated electronically by a pathologist after slide scanning. Subsequently, exact glands on deeper sections were identified and imaged with telomere/ centromere quantitative FISH, chromosome 8 probes (illustrated in the top right hand corner), PTEN and chromosome 7 probes (illustrated in the bottom right hand corner), as well as immunohistochemistry for Ki67 and p27.

4.3.4 Relationship of Ki67 and P27 with telomere length and histologies

Ki67 staining is illustrated in Figure 4.4. For all prostates there is a gradual increase in the computed Ki67 index as the histology becomes more malignant, with relatively similar scores in benign lesions.

In order to establish whether there was an inverse relationship between Ki67 index and telomere length, scatter plots were generated to examine the relationship between proliferation and telomere attrition. There were no consistent correlations between telomere lengths in pre-neoplastic or neoplastic histology and proliferation index. However, upon visual inspection, there were nearly no samples with high proliferation indices and long telomere lengths.

P27 staining may assist in the interpretation of senescence phenomena, telomere length in HPIN and the response to PTEN deletion in our sections. However, we are yet to complete p27 staining on our sections, although reproducible staining on preliminary sections has been noted.

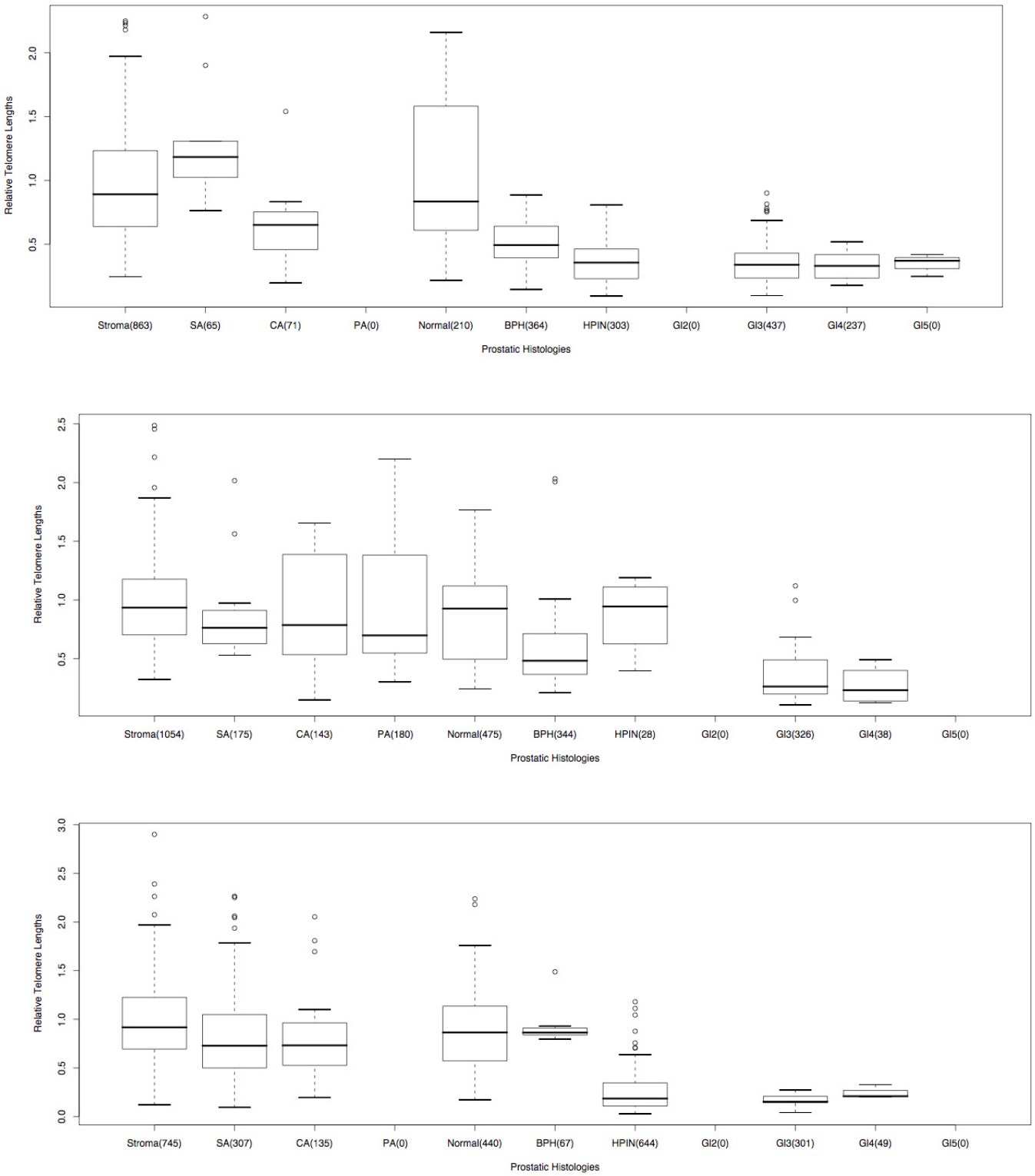

Figure 4.2 Comparison of prostatic histologies across cases analysed normalised to average stromal telomere values (for details see text)

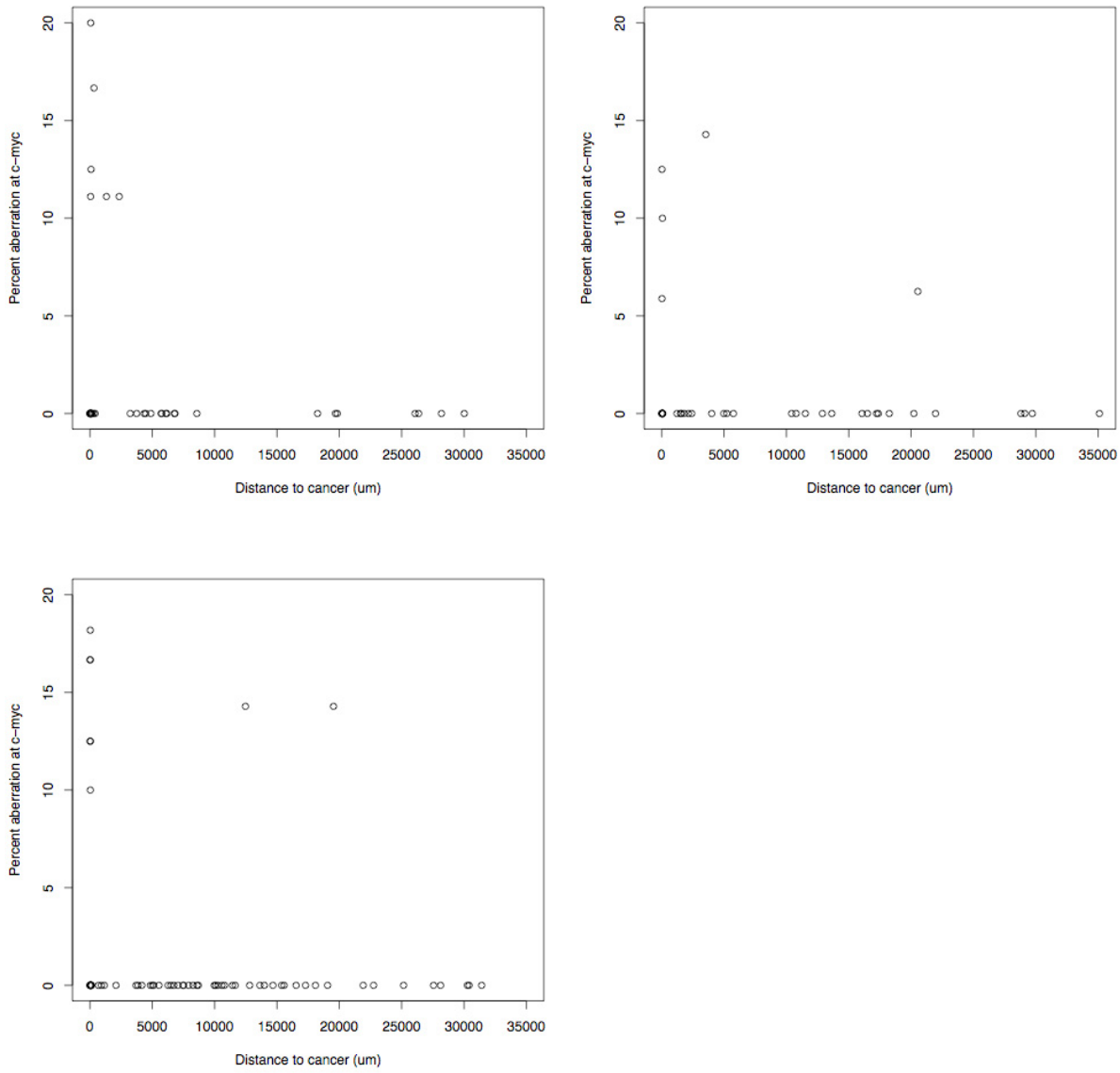

Figure 4.3 Association of the percent aberration at the C-MYC locus in peripheral zone stroma against the distance to cancer in 3 cases analysed. Case 1 (top left), Case 2 (top right) and Case 3 (bottom). For statistical tests, see text.

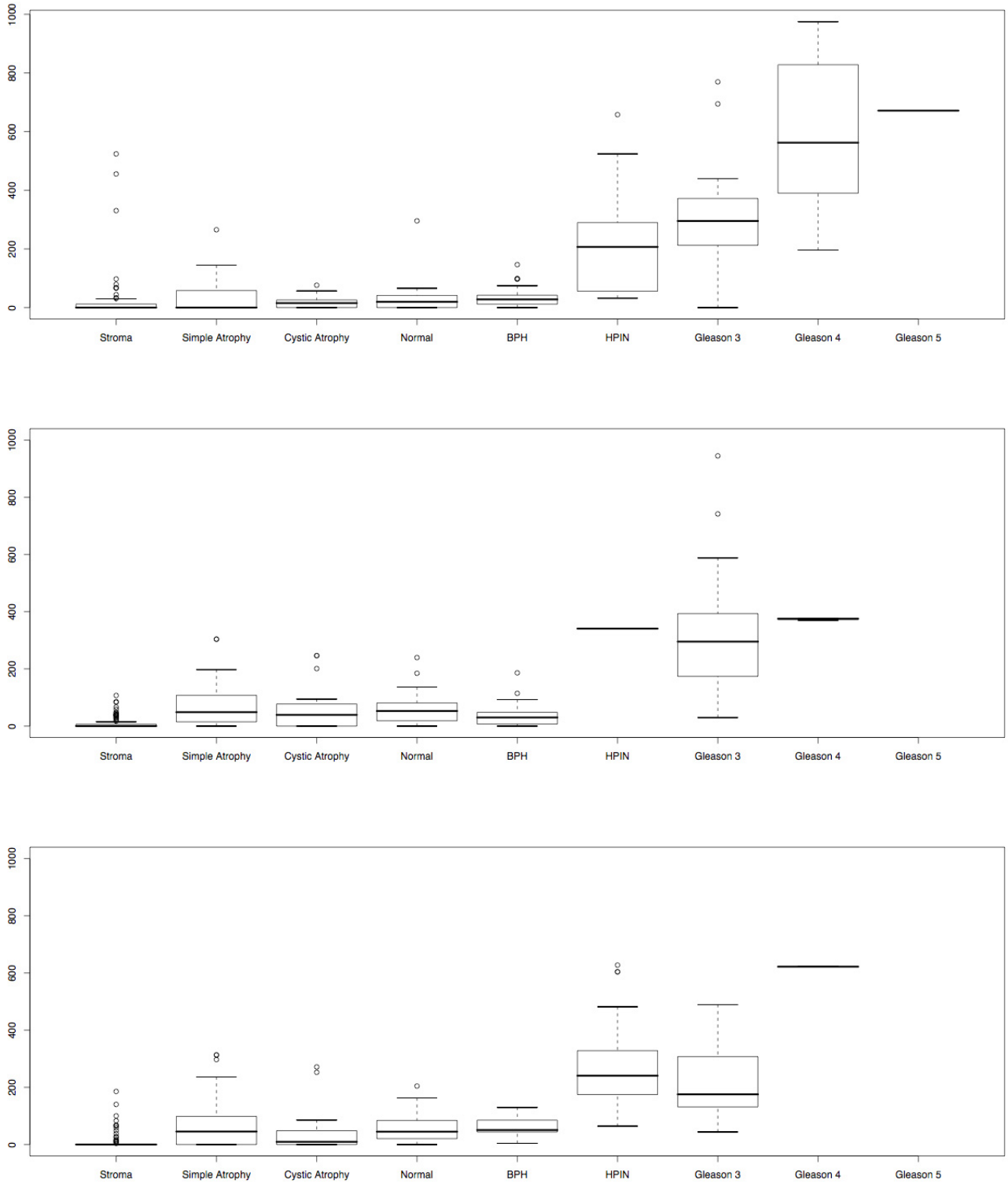

Figure 4.4 Normalised Ki67 Indices displayed by histology across the prostates analysed.

	Case 1	Matching pairs	Case 2	Matching pairs	Case 3	Matching pairs
Normal epithelium vs Adjacent stroma	**0.001 (0.35- 0.88)**	18	**0 (0.43-0.82)**	34	**0 (0.41-0.83)**	30
Atrophic epithelium (all types) vs Adjacent stroma	**0.04 (0.05-0.99)**	5	0.071 (-0.04-0.76)	17	**9.697e-05 (0.43-0.87)**	24
BPH vs Adjacent Stroma	0.12 (-0.08-0.63)	26	**0.004 (0.21-0.78)**	25	0.675 (-0.92- 0.98)	4
HPIN vs Adjacent Stroma	**0.04 (0.057-0.91)**	10	0.11 NA	3	**0.007 (0.14- 0.69)**	33
Cancer vs Adjacent Stroma	**0.01 (0.11-0.73)**	26	**0.005 (0.27-0.9)**	14	0.34 (-0.27-0.67)	16

Table 4.2 P values for the association of Telomere Length measurements between stroma and adjacent pathologies across the prostate glands examined by Pearson correlation. Values in brackets represent 95% confidence intervals. Significant p values are highlighted in bold and a shaded background.

		Case 1	Case 2	Case 3
Number of glandular areas assessed		62	42	78
Associations at 8p (LPL) (8p22)	% of abnormalities	r= 0.235 p=0.066	r= -0.262 p= 0.094	**r= -0.254** **p=0.025**
	Average number of signals	**r= -0.271** **p=0.033**	r= 0.235 p=0.134	**r= 0.318** **p=0.005**
Associations at 8 centromere	% of abnormalities	**r= 0.257** **p=0.044**	r= -0.259 p=0.097	r= -0.094 p=0.411
	Average number of signals	**r= 0.328** **p=0.009**	**r= 0.365** **p=0.018**	r= 0.119 p=0.301
Associations at 8q (C-MYC) (8q24)	% of abnormalities	r= 0.231 p=0.071	r= -0.223 p=0.155	r=-0.203 p=0.075
	Average number of signals	**r= 0.273** **p=0.031**	**r=0.357** **p=0.020**	**r=0.351** **p=0.002**
Chromosome 8 Overall measures	% Monosomy	r= -0.236 p=0.065	**r= -0.319** **p=0.039**	**r=-0.229** **p=0.044**
	Average number of signals	r= 0.197 p=0.125	**r= 0.327** **p=0.035**	**r= 0.33** **p=0.003**
	Total Genomic abnormalities	**r= 0.317** **p=0.012**	r= 0.259 p=0.097	**r= 0.228** **p=0.044**
	Total count abnormalities	**r=0.303** **p=0.017**	r= -0.016 p=0.918	r= -0.15 p=0.189
	Variance	**r= 0.333** **p=0.008**	r= -0.170 p=0.280	r= -0.201 p=0.077
Associations at	% of abnormalities	r= 0.039 p=0.757	r= 0.095 p=0.577	r= -0.037 p=0.746

Chromosome 7 centromere	Average number of signals	r= -0.208 p=0.093	r= 0.114 p=0.503	r=-0.0246 p=0.831
Associations at *PTEN* locus (10q23)	% of abnormalities	r= -0.007 p=0.957	r= -0.038 p=0.823	r= 0.025 p=0.826
	Average number of signals	r= -0.064 p=0.608	r= 0.284 p=0.089	r= -0.088 p=0.45
Associations chromosome 10 centromere	% of abnormalities	r= 0.021 p=0.869	r= 0.001 p=0.994	r= 0.061 p=0.598
	Average number of signals	r= -0.055 p=0.658	r= -0.047 p=0.780	r= -0.072 p=0.534
Any *PTEN* deletion abnormalities		r= -0.043 p=0.733	r= 0.017 p=0.922	r= 0.087 p=0.45
PTEN %Monosomy		r= 0.068 p=0.587	r= -0.057 p=0.737	r= 0.081 p=0.483

Table 4.3 P Values for the association of telomere length with markers of instability across neoplastic pathologies only for Spearman correlation analyses. % of abnormalities refers to any non-diploid signal count. Average signal count refers to the total number of signals for that probe divided by the number of cells in that glandular area. Significant p values are highlighted in bold and a shaded background

		Case 1	Case 2	Case 3
Number of glandular areas assessed		17	4	50
Associations at 8p (LPL) (8p22)	% of abnormalities	r= 0.068 p=0.796	r= 0.8 p=0.3333	**r= -0.406** **p=0.003**
	Average number of signals	r= -0.044 p=0.869	r=-0.8 p=0.3333	**r= 0.449** **p=0.001**
Associations at 8 centromere	% of abnormalities	r= 0.302 p=0.238	r= 0.4 p=0.75	r= -0.012 p=0.937
	Average number of signals	r= -0.034 p=0.898	r=0 p=1	r= 0.033 p=0.822
Associations at 8q (C-MYC) (8q24)	% of abnormalities	r= 0.247 p=0.34	r=-0.8 p=0.3333	r= -0.216 p=0.131
	Average number of signals	**r= -0.643** **p=0.005**	r=0.2 p=0.9167	**r= 0.404** **p=0.004**
Overall measures	% Monosomy	r= 0.026 p=0.921	r=-1 p=0.08333	r= -0.269 p=0.0588
	Average number of signals	r= -0.208 p=0.421	r=0 p=1	**r= 0.390** **p=0.005**
	Total Genomic abnormalities	r= -0.224 p=0.388	r=-0.8 p=0.3333	**r= 0.345** **p=0.014**
	Total count abnormalities	r= 0.125 p=0.632	r= -0.2 p=0.9167	r= -0.164 p=0.255
	Variance	r= -0.022 p=0.933	r= -0.2 p=0.9167	r= -0.175 p=0.224
Associations at chromosome 7 centromere	% of abnormalities	r= 0.103 p=0.657	r=1 p=1	r= -0.012 p=0.937
	Average number of signals	r= -0.01 p=0.967	r=-1 p=1	r= -0.076 p=0.604

Any *PTEN* deletion abnormalities	r= -0.08 p=0.738	r=1 p=1	r= 0.011 p=0.943
PTEN %Monosomy	r= 0.278 p=0.222	r=-1 p=1	r= 0.23 p=0.112

Table 4.4 R and P Values for the association of telomere length with markers of instability across HPIN only for Spearman correlation analyses. % of abnormalities refers to any non-diploid signal count. Average signal count refers to the total number of signals for that probe divided by the number of cells in that glandular area. Significant p values are highlighted in bold and a shaded background

	P Value
Case 1	0.011
Case 2	0.565
Case 3	0.009

Table 4.5 Wilcoxon statistics for differences in the percent aberration at the c-myc locus in peripheral zone stroma when comparing stroma greater or less than 1000 um from a cancer focus

4.4 Discussion

In this study, we examined approximately 25000 cells within 3 prostatectomy samples to understand the role of telomere attrition within various prostatic histologies and the emergence of chromosomal instability in prostatic carcinogenesis. We hypothesised that telomere attrition would increase the probability of chromosomal instability in neoplastic pathology, whilst a field effect of telomere attrition would be evident across stroma adjacent to these lesions.

BPH hyperplastic nodules are composed primarily of stromal components and to a lesser degree, epithelial cells. Generally, stroma comprises approximately 60 percent of the volume, epithelium 15 percent, and glandular lumens 25 percent (445). The finding of telomere shortening (compared to normal) in BPH in 2 of our 3 cases is surprising given the benign nature of this lesion. In the third case, the relative lack of BPH meant that this pathology was sampled less than in the previous two cases (see Figure 4.2) perhaps accounting for the differences seen. There has only been limited analysis of telomere length in BPH in the literature; some trends to reduced telomere length in BPH compared to normal epithelium have been noted previously (446). Most recently, Heaphy *et al*., reported telomere shortening in BPH associated with a tumour is comparable to the tumour telomere lengths (447). However, a similar relationship with telomere length was not evident in our dataset although we did not sample BPH adjacent to cancer specifically.

In one of our cases, the BPH telomere length was not significantly different to HPIN (case 2, p=0.223, 95% CI -0.7 to 0.2) however in all three cases BPH telomere length was significantly longer than in neoplastic epithelium. These findings might reflect the telomere shortening that occurs with cellular proliferation inherent to BPH, however there was no correlation with Ki67 index and telomere length in these samples. Therefore it is more likely

that this shortening is related to the microenvironment surrounding the BPH influencing telomere length. An alternative explanation is that the telomere length seen represents a reflection of the proliferative history of the lesion whilst the Ki67 index is only a snapshot of the lesions current behaviour. The well accepted lack of association of BPH with prostate carcinoma, even in the presence of telomere shortening might reflect the presence of an intact DNA damage checkpoint, related to p27 or 14-3-3sigma status (448-450), or the fact that BPH is primarily a stromal proliferation with relatively little increase in epithelial mass. Our findings support the previously reported hypothesis that one mechanism driving BPH in older men is the accumulation of senescent cells expressing IL-1alpha, which in turn increases FGF7 secretion and proliferation of non-senescent epithelial cells (451). Further markers of prostatic fibroblast senescence that could be examined to support this hypothesis are discussed in section 5.2.4.2.

The remainder of our telomere length measurements were consistent with our previous findings, although case 2 demonstrated relatively longer telomere lengths in HPIN than would be anticipated. This case demonstrated only 2 foci of HPIN, and 1 of these foci (with the longer telomere length) was the "flat" variant of HPIN. Whether the different histological variants of HPIN have any relationship to their telomere length is unknown, but flat HPIN has been noted to persist after androgen ablation so may be genomically different to other forms (452-454). Of note, this patient did not have endocrine therapy before his prostatectomy. Therefore, it is possible that "flat" HPIN may represent either a "stem-cell variant" of HPIN or that this HPIN variant represents an alternative path to neoplasia distinct from telomere attrition and the ensuing molecular consequences.

The relationship between telomere length in various histologies and the surrounding stroma was noted previously in section 2.3 for HPIN. A similar finding was evident in a number of other histologies within the gland. As discussed in section 2.4, microenvironmental changes affecting telomere length within the prostate (such as oxidative stress and hypoxia (436, 455))

may contribute to these findings. Indeed, the prostate is known to be hypoxic (456, 457) and serum markers of oxidative stress are found more commonly in men with prostate cancer than age-matched controls (458).

Genomic aberrations within cancer-associated stroma have not been reported commonly in prostate cancer but there is substantial evidence that cancer-associated fibroblasts are phenotypically different from normal prostatic fibroblasts. For example, Olumi *et al*., evaluated explanted tumour growth derived from fully transformed prostate epithelial cells mixed with fibroblasts isolated from prostate stroma or normal prostatic stroma (339). They found that only prostate associated fibroblasts were able to support the tumorigenic growth of fully transformed prostate cells *in vivo*, indicating that non-transformed stromal cells derived from the tumour microenvironment have either lost the capacity to exert growth suppressive control over initiated epithelial cells and/or acquired new capabilities permissive for carcinogenesis. This concept is also supported by recent studies suggesting genomic and epigenomic abnormalities in cancer associated stroma (56, 157, 459).

An important finding of this work is the correlation between telomere length and selected markers of genomic instability. For example, there were no associations with any markers of instability at the *PTEN* locus, suggesting that the mechanisms of microdeletion are distinct from those involving telomere attrition. This finding is in agreement with known intermediaries and end products of telomere dysfunction such as break-fusion-bridge cycles and multipolar mitoses, which are not known to include interstitial microdeletions (212). It also suggests that a common underlying process such as a defect in DNA repair (155) does not cause both telomere induced chromosomal instability and microdeletions. Indeed, whilst telomere shortening is a universal phenomenon in prostatic carcinogenesis, *PTEN* deletion is only found in up to 40% of localised disease suggesting that these phenomena are likely to be independent. An important caveat to this conclusion is that the commercial PTEN probe used spans 368 Kb

and thus may be relatively insensitive to microdeletions of the PTEN locus as may occur in the PC3 cell line and xenografts (460) . Whilst detailed analyses of the extent of PTEN deletion and thus the sensitivity of the commercial probe have not been reported, data from our laboratory (461) and others (324) suggests that small microdeletions do exist *in vivo* although most deletions are large enough to be detected, and are correlated with protein expression by immunohistochemistry (see section APP 1.3.1).

The associations found with the other chromosomal loci, in particular the C-MYC region in both HPIN and cancer suggests that telomere dysfunction may underlie the frequent gain of this region in prostate cancer. Despite gain of the C-MYC locus being associated with telomere attrition, gain of centromere 7 was not. This may relate to the different mechanisms of chromosomal gain in neoplasia, with trisomy 7 being related to other mechanisms of instability such as centrosome aberrations (153) or trisomy 7 not being present in these samples. The variability seen in the associations of telomere length and these markers of instability is likely due to differences between cases with regards to pathogenesis, karyotype or sampling. Nevertheless, telomere generated instability is likely to play an important role in the generation of phenotypes of instability given the large number of cells analysed, the correlations in the changes seen with pre-neoplasia as well as neoplasia and the associations noted with markers of whole cell instability such as monosomy in our data set.

These data parallel the conclusions of Gisselson and others (462) who investigated the nature of chromosomal instability across diverse tumour types. These studies suggest that one mechanism alone, such as telomere dysfunction, is insufficient to account for the complete set of genomic aberrations found across human tumours such as urothelial (463), renal (464), ovarian (465, 466), head and neck (467), osteosarcomas and pancreatic carcinomas(213).
There remain methodological areas of improvement that improve the understanding of the mechanisms of telomere dysfunction in future studies. Full three-dimensional rendering of the

prostate could not be performed due to the large size of the H&E stained whole mount slides. If computationally possible in the future, it would clarify the nature of the field effect in three dimensions. Additionally, a number of antibody stains were attempted both alone and in conjunction with FISH during the preparation phases of this chapter. Despite numerous attempts, both 8-hydroxydeoxyguanosine (a marker of oxidative stress), gH2AX and P-ATM were unable to be optimised with standard immunohistochemical techniques. Indeed, there are very limited papers describing the use of these antibodies in prostate tissue, and non-specific staining has been noted in uterine tissue recently (468). Finally, these findings need to be validated in further samples, to ensure that none of the associations found were seconday to multiple comparison testing.

How these findings relate to the newly discovered *TMPRSS2-ETS* gene fusions and translocation is unclear from the samples analysed. However, one possibility is that telomere generated C-MYC amplification is a mutually exclusive phenomenon from the *TMPRSS2-ERG* fusions as these fusion genes have also been shown to activate C-MYC (187). Such a hypothesis is supported by CGH suggesting prostate cancers with C-MYC amplification are distinct from those with the *TMPRSS2-ERG* fusions (389). Therefore analysing C-MYC immunohistochemistry in these sections, now that a commercially available antibody has been validated (250), would be of great interest.

This work consolidates the role of telomere attrition as a driving force for chromosomal instability in the development of prostatic carcinoma. The suggestion that certain genomic aberrations, such as those on chromosome 8, are more likely to be due to telomere attrition and its consequences than centrosome aberrations or other mechanisms remains to be validated. It also suggests that the genomic architecture of the telomeres within the gland is far more complex than previously anticipated, with the lack of association between proliferation and telomere length suggesting other microenvironmental influences on telomere length.

5.CONCLUSIONS AND FUTURE DIRECTIONS

5.1 Conclusions

5.1.1 Introduction

Classically, cancerous cells are characterised by six acquired capabilities; evading apoptosis, self-sufficiency in growth signals, insensitivity to anti-growth signals, tissue invasion and metastases, sustained angiogenesis and limitless replicative potential. Genomic instability represents "the means that enables evolving populations of premalignant cells to reach these six biological endpoints" (391).

Traditional models of carcinogenesis have emphasised single genetic "hits" to key pathways in the emergence of carcinoma. However, these models have difficulty accounting for both the frequency of cancer in human populations and the emergence of the heterogeneity evident in so many tumour types. A revised model emphasising an early defect in mechanisms regulating genomic instability may more accurately reflect the *in vivo* situation as this would lead to higher than average rate of mutations and cell-to-cell heterogeneity that would accelerate tumorigenesis. To this end, this thesis has focussed on the role of genomic instability in the development of prostate cancer. Prostate cancer is a likely target for telomere dysregulation given the proliferative abnormalities characterizing early preneoplastic stages, the close link of CaP risk with aging and its characteristic cytogenetic profile of abnormalities indicating an instability phenotype.

It remains to be proven whether the emergence of genomic instability within a preneoplastic population is a cause or consequence of neoplasia (469, 470) but suggestive evidence from congenital syndromes involving defects in DNA damage proteins (471) suggests that these genome maintenance systems contribute significantly to causality. Evidence that the prostate has defects in DNA damage/ repair, checkpoint and senescent pathways is of renewed

interest (157, 290, 298, 472); indeed these defects may be further exacerbated by environmental effects such as intra-prostatic hypoxia (156, 473) or a genetic predisposition to chromosomal instability (474). This concept has particular relevance to this work, as a prerequisite for the perpetuation of genomic instability within a tumour population is the ongoing abrogation of the DNA damage response and its consequences.

5.1.2 Overview of Conclusions

My work concentrated on the emergence of genomic instability secondary to telomere dysfunction as well as the microdeletions that characterise deletions such as those found in the *PTEN* and *TMPRSS2-ERG* loci. As discussed in Chapter 1, telomeres have an important role both as a tumour suppressor mechanism, when DNA damage pathways are intact and then as a generator of genomic instability as cells pass through telomere "crisis" and ultimately reactivate telomerase. Chapter 2 of this work demonstrated the prognostic importance of telomere shortening in the occurrence of prostate cancer from HPIN, which is hypothesised to act via the generation of genomic instability. This finding, evident both in the stroma and the HPIN epithelium suggested a field effect in the generation of prostatic carcinogenesis and was in agreement with findings suggesting the poor prognosis of short telomere length in prostate cancer itself (401, 413). The results also revealed aspects of telomere attrition such as the 64% reduction in telomere length compared to the surrounding stroma. This study continued the previous work from our laboratory in this area, connecting the work of Al-Maghrabi *et al* (215) who defined the extent of chromosomal instability and prognosis in HPIN to Vukovic *et al*, (216) who defined the extent of telomere shortening and chromosomal instability in HPIN (see Figure 1.3).

Chapter 3 explored the phenomena of the *TMPRSS2-ERG* fusions to determine if this was a telomere related phenomena. At the time of publication, this issue was unresolved, but

crucial to understanding the emergence of prostate carcinoma, as it was originally not noted to be evident in HPIN. Our results validated the findings in the original paper (159) and found the presence of multiple variants of the fusion gene. However, the origin of crucial microdeletions such as *TMPRSS2-ERG* (see chapter 3) and *PTEN* (see Appendix 1) are unknown. As discussed in section 3.3.2, we have suggested that an Alu repeat might mediate the TMPRSS2 deletion but this would not account for the *PTEN* deletion or the other more complex translocations characteristic of the ERG locus, which may be subsequent to as yet undefined nuclear microarchitecture (475), unstable genomic sequences (476, 477) or erroneous non-homologous end joining (155, 156).

Chapter 2 suggested that further validation was required to understand the field effect in prostatic carcinogenesis in a whole mount model and relate the emergence of chromosomal instability to telomere shortening. Thus, chapter 4 (i) clarified further field effects, e.g. the apparent increase in copy number of the C-MYC locus in cancer associated stroma, (ii) provided an expansion of the initial finding of a relationship between prostatic stroma and HPIN to other types of prostatic epithelia, implying the existence of microenvironmental effects in prostatic cell homeostasis, (iii) demonstrated a correlation between telomere attrition and the emergence of markers of genomic instability. These correlations may also allow insights into which mechanisms of instability are responsible for which patterns of instability. For example, numerical aberrations of the arms of chromosome 8 appeared to be associated with telomere attrition, while those of chromosome 7 were not (section 4.3.3).

5.1.3 Other modulators of genomic instability

Other candidates with an established role in developing instability in prostate cancer include centrosome abnormalities and mitotic spindle defects (153). As organizers of microtubules, centrosomes play an important role in many microtubule-mediated processes,

such as establishing cell shape and cell polarity (478-481). Centrosomes also coordinate numerous intracellular activities in part by providing docking sites for regulatory molecules, including those that control cell cycle progression, spindle function, and cell cycle checkpoints (482-484). However, centrosome defects have only been detected in 28% of HPIN and their correlation with chromosomal instability is inconsistent (154). Overexpression of the Aurora kinases may have a role in the development of controsome related chromosomal instability (394, 485) and are found in HPIN (485, 486) but their contribution to genomic instability has remained uninvestigated. They have recently been targeted in drug development in prostate cancer (486) with encouraging results.

There are only limited reports of the role of mitotic spindle defects in prostatic carcinogenesis. Of interest is a recent report suggesting that the prostate membrane specific antigen (PMSA), an protein commonly found overexpressed in prostate cancers, associates with the anaphase-promoting complex, and when overexpressed induces aneuploidy (395).

5.1.4 Relevance to Age dependency of Prostatic Neoplasia

Another link between this work and prostate pathobiology is the age-dependency of this neoplasm. This may have relevance to both the epithelium itself and the prostatic stroma. Age dependent progressive CpG island methylation takes place in a subset of cells residing in normal tissues and has been found in prostatic tissue(487, 488). These changes may target cancer relevant pathways (489) that may predispose to further oncogenic change as discussed in section 1.6.2.1.

5.1.5 Relevance of Stromal-Epithelial Interactions

Stromal-epithelial interactions are crucial to the emergence of prostatic carcinoma (see section 1.7.3). Previous studies have demonstrated that only prostatic carcinoma associated

fibroblasts were able to support tumourigenic growth of fully transformed epithelial cells *in vivo* (339) – indicating that non transformed stromal cells derived from the tumour microenvironment have either lost the capacity to exert suppressive control over initiated epithelial cells and/ or acquired new capabilities permissive for tumourigenesis. Nevertheless, an age-dependent process such as telomere attrition could induce stromal cells to facilitate this growth. Fibroblasts senescence after defined population doublings; a phenomenon seen both *in vitro* (490) and *in vivo* (491, 492). The senescent phenotype has been shown to lead to an increase in their production of cytokines, proteases and other matrix-degrading enzymes (493, 494). This milieu produced by the fibroblasts has been hypothesised to support tumour growth (495, 496) with evidence from studies in both prostate and breast cancer that alteration of stromal gene expression supports tumour growth (497). The finding in chapter 4 of a correlation of telomere length between a variety of prostatic epithelia and stroma might suggest that these changes occur in parallel and either directly or indirectly affect telomere length.

5.1.6 Potential for Clinical Impact

With findings that relate both to the prognostic value of telomere assessment and its mechanism of promoting carcinogenesis, this work reinforces the argument for greater emphasis to be placed on chemo-preventative strategies for prostate cancer (498). Prostatic carcinogenesis likely has a latent period of 20 years before the development of HPIN and another 10 years before the emergence of overt carcinoma (499). Epidemiological studies suggest that patients with HGPIN and no detectable cancer progressed to a 40% incidence of cancer in 3 years and to 80% incidence in 10 years (500). This provides a useful period of time to examine strategies of chemoprevention that have only begun to be explored (501).

This work also suggests new avenues for drug discovery in the area focussing on genomic instability, in particular on the transition from HPIN to prostate cancer. Drugs targeting

components of the machinery that lead to genomic instability are only in the preliminary stages of development (502) although a yet to be reported Canadian phase 3 prostate chemoprevention trial utilising lycopene, vitamin E and soy extract may be evaluating agents that act partly through telomerase inhibition (503-505). Recent insights into the role of $p27^{KIP}$ as a barrier to prostatic neoplasia that occurs in HPIN suggests the potential utility of CDK inhibitors (298) whilst insights and approaches to reinforcing the bypassed DNA damage checkpoints that facilitate telomere dysfunction may be elucidated from the functional validation experiments described below. Finally, the mechanism that mediates the fusion of dysfunctional telomeres during crisis is unclear. Knowledge of this mechanism could suggest possible ways to minimize chromosome fusion and maximize apoptosis in response to dysfunctional telomeres.

The work presented in Appendix 2 of a trial of cytarabine as a potential inhibitor of ETS related transformation is an attempt to alter the consequences of the effect of genomic instability on prostate carcinogenesis. As discussed in section APP 2.5, despite the absence of significant PSA responses, a notable finding of this trial is the re-induction of hormone sensitivity in a subset of patients. I hypothesize that this might be due to a differentiation effect of cytarabine on ETS positive tumours (506), disrupting the balance between ETS-related oncogenes (e.g. ERG, ETV1, ETV4) and tumour suppressor genes (PDEF, ESE-3) in a given tumour. This hypothesis awaits validation through FISH analysis of tumours, which is in progress. This study is also attempting to isolate *TMPRSS2-ERG* cDNA from patient blood samples.

Drug trials focussing on pathways that may be relevant to the work presented in Appendix 1 have been carried out but have not been stratified by the presence or absence of *PTEN* deletions that would likely to influence response (507, 508). Similarly, retrospective studies of the value of *PTEN* or indeed *TMPRSS2-ETS* status in predicting the time to androgen independence have not been reported but remain pertinent to understanding the roles of these oncogenes in the natural history of prostate cancer.

5.1.7 Potential for Methodological Advances

The advances in imaging of florescence signalling demonstrated by this work have contributed to the field. Based on the open source software package ImageJ (405), macros were developed that allowed for the high throughput assessment of telomere and centromere fluorescence. Further advances will concentrate on automated nuclear identification, which would accelerate the ability to carry out studies such as this. A unique aspect of the methodology presented in this work is the correlative nature of the assessments in chapter 4. The heterogeneity inherent in prostate cancer implies that bulk assessment of tumour biomarkers through tissue microarray or other evaluation techniques is unlikely to isolate populations of tumour cells that could reveal insights into carcinogenesis. The gland-by-gland assessment evaluated in chapter 4 through serial sections has been attempted infrequently (215) and full implementation awaits the more widespread use of techniques such as quantum dot technology to evaluate multiple biomarkers in the same section. Finally, the use of automated scanning and evaluation technologies as described in section 4.2 are promising pathological tools, in the evaluation of prostate pathology (509). The use of quantitation algorithms with this commercial package is new to the scientific literature (510) and needs further validation before diagnostic (as opposed to research) use.

5.1.8 Summary and Model of Genomic Instability in Prostatic Carcinogenesis

In conclusion, a model for the emergence of genomic instability in prostatic carcinogenesis is proposed that suggests that in the aging prostate there is a coordinate reduction of constitutional telomere length in foci of epithelium and adjacent stroma, secondary to a combination of (likely diet-induced) proliferative, genotoxic and oxidative stress (511, 512).

These early alterations may lead to epigenetic change such as the methylation of p16, a checkpoint protein that normally would arrest further proliferation (513). Ultimately, the ongoing selective pressure leads to early oncogene activation, resulting in oncogene-induced senescence in a proportion of proliferative foci. This senescence checkpoint is commonly associated with widespread DNA double strand breaks, some of which may facilitate the emergence of microdeletions such as *PTEN* and *TMPRSS2-ETS*, in particular in the presence of impaired recognition and repair of DNA damage (258). Certain foci probably escape this p27 related checkpoint through altered up regulation of C-MYC (250, 514), altered cell cycle checkpoint profiles or p53/Rb defects (257, 515). It is likely that these same checkpoint defects facilitate critical telomere shortening as cellular proliferation continues. For example, C-MYC can directly or indirectly induce telomere shortening (516) and p53 defects are required in multiple models for cells to proceed through telomere crisis (517). Other mechanisms of genomic instability such as multi-polar mitoses may contribute to centrosome and mitotic spindle dysfunction. Ultimately, through mechanisms that remain unclear but may include C-MYC activation (518), telomerase is reactivated and partially suppresses telomere-generated instability, stabilising the neoplastic clone and preventing mitotic catastrophe. Ongoing development of genomic evolution within the cancer is likely due to both the selective pressure of the environment and ongoing instability generated by multiple mechanisms.

Understanding of the basis of both cancer initiation and progression is crucial in development of meaningful diagnostic, prognostic and predictive markers in cancer treatment. To this end the work presented here contributes to the understanding and evaluation of genomic instability.

5.2 Future Directions

5.2.1 Introduction

Whilst this work has clarified mechanisms surrounding the evolution of genomic instability in prostatic carcinogenesis, a greater appreciation of its ultimate clinical impact requires more research on the two barriers to the progression of prostatic preneoplasia; oncogene-induced senescence and telomere-induced senescence.

5.2.2 Functional Validation of Telomere Mediated Instability

The latter has been previously investigated in our lab, which has demonstrated the presence of the BFB cycle as a mechanism of chromosomal instability concordant with loss of telomeric sequence in prostate cancer cell lines. It remains unclear whether the BFB cycle originates directly from a phenomena related to telomere dysfunction, an alternate source of sister chromatid fusions or whether there are alternative sources of double stranded breaks such as those that may occur during oncogene induced DNA damage. If observed levels of chromosomal instability are a consequence of telomere dysfunction, upregulation of telomerase expression should stabilize the telomeric ends and decrease the levels of chromosomal instability. Suppression of telomerase expression in prostate cancer cell lines DU 145 and LNCaP has been shown previously to initiate a severe crisis-like process, chromosome rearrangement and apoptosis (519). Upregulation of telomerase across a panel of benign and malignant prostate cell lines could be achieved with cDNA transfection. Given the possibility that hTERT transfection may affect telomere protection primarily rather than telomere length in those cell lines with defective checkpoint pathways (219), these pathways will also have to be carefully quantified and to understand the effect of the transfection on telomere length and “t-

stumps" (see section 1.6.3.3) telomere FISH for signal free ends and STELA analysis of telomere ends may have to be undertaken.

Ultimately, the emergence of telomere dysfunction could be monitored through the enumeration of telomere-induced DNA damage foci (assessed by immunofluorescence colocalisation) and anaphase bridges with overall instability assessed by techniques such as SKY and FISH for multiple chromosomal loci.

Subsequently, an expansion of this work could help address the issue of whether dysfunctional telomeres initiate genomic instability in the absence of mutations in checkpoint genes, or whether the main role of telomere dysfunction in ongoing chromosomal instability is after the loss of checkpoint proteins. To achieve this, we plan to examine the role of the DNA damage response in modulating or enhancing the emergence of genomic instability through siRNA knockout of critical DNA damage proteins (e.g. ATM, CHK2, p53 and p21) or pharmacological enhancers of p53 action (e.g. PRIMA-1 or Nutlin) in the above cell lines. Alterations in some of the genes associated with DNA repair pathways could perpetuate further karyotypic changes. For example, proteins such as NBS1 (520) and WRN (521) bind to telomeric protection proteins (e.g. TRF2) and can influence telomere loss. Additionally, defects in a large number of proteins involved in telomere maintenance also can promote chromosome fusion, including Ku, DNA-PKcs, the MRE11-RAD50-NBS1 complex and the WRN helicase. For example, Ku is localized to telomeres in humans and lack of Ku function leads to telomere-telomere fusions in mammals (522). This protein forms a complex that is thought to process broken DNA ends in preparation for their repair. It would be of interest to functionally investigate the DNA damage defects that have been suggested to occur in normal prostatic epithelium (Wee-1) and in early carcinogenesis (14-3-3) to see if their knockout in normal prostatic epithelial cell lines predisposes to the emergence of instability (157, 523). To verify that these DNA damage response protein(s) co-localize specifically at the telomere, chromatin

immunoprecipitation (ChiP) and dot-blot hybridisation to telomeric DNA with appropriate antibodies would be carried out.

5.2.3 Functional Validation of Oncogene Induced Senescence

An understanding of this issue will require experimentation to assess whether the same checkpoint proteins necessary for oncogene-induced senescence bypass are also those necessary for telomere induced senescence bypass. To investigate this, a model of prostate oncogene induced senescence will need to be established. This is likely to occur with the overexpression of oncogenes such as AKT or C-MYC in a benign prostate epithelial cell line such as PrEC (240). Alternatively, siRNA knockdown of tumour suppressors such as *PTEN* may achieve the same effect (411, 524, 525). If there is difficulty creating these cell lines then models may have to be created that involve pre-existing p16 inactivation, a phenomenon that seems to occur *in vivo* and may facilitate early proliferation (526, 527). The cell lines will be monitored for proliferation indices, apoptotic indices and cell cycle analysis to determine the onset of senescence. This onset will be correlated with putative markers of prostatic senescence (528) such as HP1 (529), p27 (298) and IFI 16 (530) as well as general markers of senescence such as heterochromatin formation (531). Telomere length would also be monitored (both by qFISH and TRF analysis) to ensure that the senescent state induced is not secondary to telomere-induced senescence. Markers of DNA damage such as gamma-H2AX could also be monitored to determine if there is a DNA damage threshold that occurs secondary to the oncogene driven aberrant replication forks (532) that lead to senescence induction. After this has been established, the role of abrogators or enhancers of this senescent state could be explored. For example, as recently described, the *TMPRSS2-ERG* protein activates C-MYC and leads to prostatic dedifferentiation *in vitro* (187). C-MYC in turn, may repress p27 and abrogate the oncogene induced senescence checkpoint (514).

5.2.4 Human Tissue Validation

5.2.4.1 Laser Capture Microdissection

Ultimately, these results from cell line experiments described above should be validated in human tissue. For example, laser-capture microdissection (LCM) may reveal insights into the relationship of telomerase with TMPRRS2, which can activate C-MYC, that in turn can activate telomerase (533). LCM will also allow the exploration of a large number of genes related to the DNA damage response and repair on focussed microarrays to determine aberrations of these pathways and how they may relate to telomere biology. Microarray technology in this setting may require whole-genome amplification techniques given the small amounts of HPIN that may be able to be isolated, a technique with which this laboratory has considerable experince (534). Isolating a small number of overexpressed genes may also require the use of computational techniques in analysis such as COPA (based on an outlier analysis) that led to the discovery of the *TMPRSS2-ERG* fusion (535).

5.2.4.2 Immunohistochemistry

Paraffin embedded tissue might reveal further insights into telomere biology in prostatic carcinogenesis. For example, a recently validated C-MYC antibody (250) may allow simultaneous assessment of C-MYC status and p27 status. For example, while the research presented suggests a correlation between telomere shortening and genomic instability, this was by association only. The detection of intermediaries of telomere dysfunction such as anaphase or internuclear bridges would strengthen the case for the role of telomere dysfunction in the generation of instability. Given the relatively slow doubling time of prostate cancer compared to other neoplasms such as osteosarcoma where the BFB mechanism is more clearly established,

this will likely require further high throughput imaging techniques on DAPI stained sections to detect and quantify these phenomena.

The integrity of the telomere is dependent on the six protective proteins, the "telosome" (536) or "shelterin" (537) whose altered expression can affect telomere length and telomerase function. These proteins have not been investigated in the setting of prostatic carcinogenesis. Telomere repeat binding factor 1 (TRF1), protection of telomeres 1 (POT1), and Tankyrase 1 (TRF1-interacting ankyrin-related ADP ribose polymerase) have essential roles in telomere length regulation (11). TRF1 binds to TTAGGG double stranded repeats of telomeres and has been identified as a negative regulator (538, 539). Tankyrase 1 interacts with TRF1 and its overexpression releases TRF1 from the telomeres and induces telomere elongation (540). POT1 is recruited to the 3 single-stranded portion of the telomeric DNA and it was found to employ telomerase for telomere elongation (541). Findings relating abnormal expression of these genes with telomerase, telomere length and even prognosis have been made in a number of cancers (542-548) and need to be clarified in prostate cancer. Such a study should be validated for the cell lines described above to validate their role.

As discussed above, the age dependency of the neoplasm and its relationship to the stroma requires further investigation. The most reliable, but not universal, marker of cell senescence is β-galactosidase, which requires frozen tissue. Markers of senescence that may be more amenable to immunohistochemistry have been suggested in prostatic fibroblasts such as HGF, FGF7 and AREG (416). They remain to be fully investigated in prostatic cancer samples, but we hypothesise that these markers would be more intense surrounding foci of HPIN before the transition to cancer associated fibroblasts surrounding foci of carcinoma should the contribution of fibroblasts to prostatic carcinogenesis be via an age-related senescence phenomena.

5.2.5 Role of the Microenvironment

The complexity found in regulation of telomere length within the prostate in this work suggests the importance of microenvironmental influences on telomere length. Primary amongst these is hypoxia or oxidative stress. Directly correlating the presence of hypoxia or a surrogate thereof (such as HIF) in prostatic tissue with telomere length appears feasible in paraffin embedded tissue (549) and might elucidate the cause of the regional variation found. Direct measures of partial pressures of oxygen with an eppendorf probe have also been reported (473) and could verify the immunohistochemical findings, although the final correlation with histology and would be approximate only.

5.2.6 Clinical Optimisation of Findings

Once these planned studies are undertaken, a greater understanding of modulators of instability in prostate carcinogenesis will be achieved. Ultimate validation of these changes is required to verify the proposed temporal sequence of events. To date, this evolution has been inferred from the proximity of HPIN to cancer in paraffin embedded specimens. An expanded cohort of men who have had HPIN on initial diagnosis and were subsequently followed with biopsies and blood samples would offer the opportunity to track the changes, or absence thereof, that predict for the ultimate appearance of prostate cancer. These experiments will have to be done in a prospective manner, with mandated time or event directed biopsies and with analysis of telomere length in all cores of the prostate biopsy. The blood samples would allow an assessment of both the consitutional telomere length in the individual, both also their baselines levels of oxidate stress (possibly by use of markers such as 8-hydroxydihydroguanosine) and prediposition to genomic instability (474, 550) – all of which might contribute to the emergence of an age related cancer such as in the prostate. The prostatic analyses may prove difficult to achieve with fluorescence based peptide nucleic acid probes and may require more clinically

adaptable techniques such as Chromogenic In situ hybridisation (CISH), which can be assessed under a light microscope. This technique has been used for telomere analysis (468) but has yet to be validated in prostatic tissue, although it has been used in other clinical settings such as HER-2 assessment, with comparable results to FISH (551, 552). Other markers that hold promise in this setting include AMACR (553) and *TMPRSS2-ERG* (554). Combinations of these biomarkers with integration into existing clinical models in this setting (555) may hold the potential for even greater accuracy.

Finally, the knowledge from the functional experiments described above might enhance the introduction of anti-telomerase therapies for prostate cancer. There are a number of telomerase inhibitors that are in pre-clinical development (e.g. GRN163L, BRACO-19) that have shown activity in prostatic cell lines (556, 557) and xenograft models (558) as well as other neoplasms (559). These drugs ability to induce mitotic catastrophe or apoptosis may be enhanced by a more complete understanding of the DNA damage response consequent to telomere attrition. For example, it may be necessary to combine the telomerase inhibitor with chemotherapy (560) as the inhibition of telomerase alone may initially exacerbate chromosomal instability or lead to a prolonged latency before telomere attrition to a critical length occurs (561). Alternatively, if the protective role of hTERT is more important in telomere pathophysiology than telomere lengthening by telomerase, anti-hTERT therapeutics may have to be developed.

APPENDIX 1. THE ROLE OF *PTEN* AND *TMPRSS2-ERG* MICRODELETIONS IN PROSTATIC CARCINOGENESIS

SUMMARY

The identification of prognostic molecular biomarkers is recognized as critically important in the future clinical management of prostate cancer. Despite the clinical utility of Gleason score, pathological stage and serum PSA in assessing prognosis and guiding management, further molecular determinants are needed that more accurately address pathways that underlie tumorigenesis and progression of CaP. Two leading biomarker candidates are *PTEN* gene deletion and the *TMPRSS2-ETS* gene aberrations, but their prevalence in prostatic neoplasia and prognostic importance remain unclear. In this appendix, we clarify the extent of *PTEN* gene deletion in 35 radical prostatectomy specimens and clarify both the extent and prognostic importance of the combination of the *PTEN* and *TMPRSS2-ERG* gene aberrations in a Brazilian tissue microarray (TMA) cohort of 125 samples. Our findings suggest that *PTEN* haploinsufficency is common and that in combination with *TMPRSS2-ERG* gene aberrations, both biomarkers offer the potential to define a subset of patients with a high risk of biochemical recurrence.

BASED ON;

Yoshimoto M, Cutz JC, Nuin PA, Joshua AM, Bayani J, Evans AJ, Zielenska M, Squire JA., Interphase FISH analysis of *PTEN* in histologic sections shows genomic deletions in 68% of primary prostate cancer and 23% of high-grade prostatic intra-epithelial neoplasias, Cancer Genetics Cytogenetics. 2006 Sep;169(2):128-37

Yoshimoto M, Joshua AM, Cunha IW, Coudry RA, Fonseca FP, Ludkovski O, Zielenska M, Soares FA, Squire JA., Absence of TMPRSS2:ERG fusions and *PTEN* losses in prostate cancer is associated with a favorable outcome. Modern Pathology. 2008 (in press)

AP1.1 Introduction

As previously discussed, chromosomal deletions of 10q23 suggest that the *PTEN* gene is strongly associated with the neoplastic evolution of CaP (18, 562) as it plays an important role in the modulation of the phosphatidylinositol-3-kinase (PI3K) pathway (see section 1.7.2.3). Previous studies have suggested that *PTEN* deletion is associated with tumour progression (327, 563, 564) and is predictive of a short time to biochemical recurrence of disease (330).

The occurrence of *PTEN* deletion in CaP is relatively common, with reported frequencies of 30-62% (317, 565), underscoring the probable importance of this event in prostatic carcinogenesis. However, at the time of this research, both the timing of the *PTEN* deletion and its relationship to other biomarkers in CaP progression were unclear. Furthermore there had been no previous large scale FISH study of *PTEN* deletion in CaP. Of the various means of determining genomic deletion, FISH offers the advantage of being highly specific, quantitative, and the assay permits determination of gene copy number within individual cells in tissue sections. Thus, the first part of this study was designed to assess the overall frequency of *PTEN* genomic deletion by FISH, and to determine whether such deletions were present in preneoplastic lesions.

The discovery of recurrent translocations in ~ 40 to 60% of prostate carcinomas (18, 161, 176, 190, 419, 566), involving members of the ETS transcription factor family (see section 3), has provided a promising new biomarker which helps to stratify men for treatment.

Thus, the second major aim of this study was to clarify both the clinical and importance of the co-occurrence of the *PTEN* and *TMPRSS2-ERG* abnormalities. Given the evidence that additional oncogenic mutations aside from those involving the ERG family need to take place to lead to a neoplastic phenotype in both cell culture and mouse models of the fusion genes, *PTEN*

abnormalities are a leading candidate for this critical transition i.e. it is unclear whether the *TMPRSS2-ERG* rearrangements might be accompanied by *PTEN* genomic loss, or in contrast, whether these are mutually exclusive events.

APP 1.2 Materials and Methods

APP 1.2.1 *PTEN* cohort

All specimens were obtained and handled according to the University Health Network Research Ethics guidelines. Archival formalin-fixed, paraffin embedded tissues from 35 radical prostatectomy specimens were used in this study. Nine of these specimens were evaluated using whole tissue sections obtained from the original paraffin blocks. The remaining 26 cases were sampled using two or three tissue cores (3 mm diameter) distributed on four tissue microarray slides. Haematoxylin and eosin (H&E) stained sections were reviewed by a pathologist (J-C.C. or A.J.E.) to determine the presence and extent of CaP, low-grade prostatic intra-epithelial neoplasia (LGPIN), HGPIN, benign glandular epithelium, and stroma in each tissue section or core. The clinico-pathological (TNM) stage for each case was obtained from the surgical pathology reports and medical records. The size of tumor was based on assessment of total surface area of gland examined histologically involved by carcinoma.

APP 1.2.2 *PTEN*/ ETS cohort

The collection of all tissue specimens, clinical and patient follow-up data were obtained after informed consent in accordance with the Hospital do Câncer Research Ethics guidelines (São Paulo, Brazil). Archival formalin-fixed, paraffin embedded tissues were obtained from 125 radical prostatectomies performed between 1997 and 2000 at the Hospital do Câncer, AC Camargo, São Paulo, Brazil. For control purposes, ten non-neoplastic prostate tissue samples

were obtained from patients undergoing surgery solely for benign prostate hyperplasia. The CaP cohort and control specimens were sampled using a 0.6-mm diameter tissue core distributed on a TMA slide. Adjacent hematoxylin and eosin (H&E) stained section was reviewed by two pathologists to determine the presence and extent of morphologically representative areas of the original tumors in each tissue core. Reassessment of Gleason grading in a contiguous H&E stained TMA section assured the presence of prostate adenocarcinoma and the fidelity of the intended TMA core. The size of the tumor was based on assessment of total surface area of gland examined histologically involved by carcinoma. Preoperative PSA levels were available for all patients. PSA failure was defined as PSA above 0.2 ng/ml after radical prostatectomy.

APP 1.2.3 Fluorescence in situ hybridization

Break-apart FISH was employed in the analysis of the *TMPRSS2-ERG* gene rearrangement using bacterial artificial chromosome (BAC) DNA probes as previously described in section 3.2.3 (330). Subsequently, the following bacterial artificial chromosome (BAC) clones were used for verification and diagnostic purposes. BACs located at: (a) the 3' *ERG* gene locus (RP11-476D17, 3'*ERG* sequence extending inward past exon 4), (b) the 5' *ERG* gene locus (RP11-95I21, 5'*ERG* sequence extending inward into exon 10), (c) the *TMPRSS2* locus (RP11-535H11), and (d) the telomeric BACs to the 5' end of *TMPRSS2* locus (RP11-35C4, RP11-891L10 and RP11-260O11, 325 kb downstream from the 5' end of the *TMPRSS2* gene) (See figure App1.1).

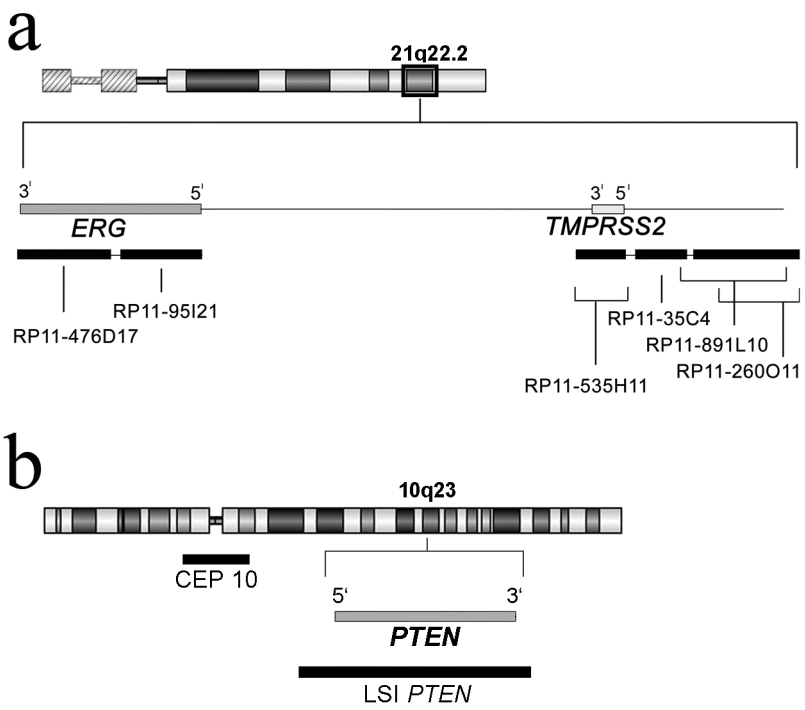

Figure App1.1 FISH probes used to detect the genomic alteration in CaP. **(a)** Location and names of the BAC probes spanning the genomic region of the *ERG* and *TMPRSS2* loci at chromosome 21q22.2 and. The linear order and approximate distances of the BAC clones are based on the Human March 2006 assembly of the UCSC Genome Browser. **(b)** Genomic localization of the commercially-available locus-specific *PTEN* probe and alpha-satellite DNA sequences of chromosome 10 probe (Vysis Inc, Illinois, USA).

In the first *PTEN* cohort, two observers (M.Y. and J-C.C) evaluated independently at least 100 non-overlapped, intact interphase nuclei in each area of interest, which was identified by DAPI-staining of nuclei with reference to the corresponding H&E stained tissue. Deletion at the *PTEN* locus in each case was determined by statistical comparison of the number of fluorescent signals in each cell type. Significant differences were determined using the Chi-squared method ($p<0.01$). Hemizygous deletions were identified in nuclei showing one red signal (*PTEN* locus) and 2 green signals (control locus) while homozygous deletions exhibited only the green control signals (567-569). Homozygous deletion was deemed significant when present in >30% of cells (568)

In the second cohort, the sequential dual-color FISH method was applied to the TMA to investigate the occurrence of *PTEN* genomic deletion in addition to *TMPRSS2-ERG* gene rearrangements in 82 of the125 patient cohort. Dual-color FISH on paraffin-embedded TMA tissue was performed using commercially available DNA probes as previously described in section 4.2.3. Five μm histologic TMA tissue sections were deparaffinized with a series of xylene washes prior to immersion in 100% ethanol. Fluorescence in situ hybridization was carried out as described (330).

APP 1.2.4 Immunohistochemistry

Immunohistochemical staining for total *PTEN* protein was carried out using heat-induced antigen retrieval and the labeled streptavidin-biotin (LSAB) method (LSAB-kit, DakoCytomation, CA, USA). Prior to antibody incubation, tissue sections were blocked in 3% skim milk (BD Biosciences Canada, Mississauga, ON, Canada) in 1x PBS for 1 hour at room temperature. Sections were incubated with polyclonal rabbit anti-*PTEN* antibody (Zymed Laboratories, Inc., Burlington, ON, Canada) diluted 1:100 in buffer with background reducing

components (DakoCytomation, CA, USA) and washed according to manufacturer's instructions. Negative control sections were treated identically but without primary antibody. Benign glandular epithelium served as an internal positive control.

Cytoplasmic and/or nuclear *PTEN* immunoreactivity was scored by 2 blinded independent observers (M.Y. and J-C.C.) according to the product of staining intensity (1-3) multiple by the proportion of immunoreactive cells in the areas of interest (1-4) (271). The overall score range was from 1 to 12. Immunoreactivity scores were then dichotomized using a cutoff value of 6 (i.e. weak *versus* moderate to strong) and this overall score was compared with the FISH score using Welch t-test statistical method.

APP 1.2.5 Data Analysis

The *TMPRSS2-ERG* fusion was evaluated for each probe by spot visualization and enumeration in a range from 50 to 100 nonoverlapped, intact interphase nuclei per tumor tissue core using a Zeiss Imager.Z1 microscope equipped with a digital camera AxioCam MRm and AxioVision 4.3 capturing software (Carl Zeiss Canada Ltd, Canada). The ERG rearrangement in tumor nuclei was detected by either the split of one of the colocalized 3' and 5' ERG signals in addition to a fused signal of the unaffected chromosome 21 or the hemizygous loss of 5' ERG (RP11-95I21—green signal), whereas the homologue signal colocalized to the fused signal of the apparently unaffected loci at chromosome 21. The telomeric BACs to the 5' end of TMPRSS2 locus signal colocalized with the signal of the 3' ERG BAC, confirming the presence of the typical 5' TMPRSS2-3' ERG rearrangements. When the BAC telomeric to the 5' end of TMPRSS2 (blue signal) was well separated from the 3' ERG BAC (red signal), the *TMPRSS2-ERG* rearrangement was confirmed using the TMPRSS2 BAC (RP11-535H11—blue), 5' ERG (RP11-95I21—green) and 3' ERG BAC (RP11-476D17—red). Based on hybridization in 10 control cores (data not shown) and the tumor cohort, the detection of *TMPRSS2-ERG*

rearrangement was defined the presence of the rearrangement in greater than 10% of cells when the distance between signals was >3 times the estimated signal diameter (425).

PTEN copy number was evaluated for each probe by counting spots in a range from 50 to 100 nonoverlapped, intact interphase nuclei per tumor tissue core. Based on hybridization in 10 control cores (data not shown), hemizygous deletion of *PTEN* were defined as >20% (mean+3 SD in non-neoplastic controls) of tumor nuclei containing one *PTEN* locus signal and by the presence of centromere 10 signals. Homozygous deletion of *PTEN* was exhibited by the simultaneous lack of the both *PTEN* locus signals and by the presence of control signals in greater than 30% of cells sampled (425, 567-569).

APP 1.2.6 Statistical Analysis

FISH findings for the first *PTEN* FISH cohort were analyzed for associations using the Welch t-test. FISH findings for *TMPRSS2-ERG* fusion were correlated in a univariate and multivariate fashion with clinical and pathologic measures of disease aggressiveness. A comprehensive description of the clinical parameters associated with the adenocarcinomas having the *TMPRSS2-ERG* fusion is summarized in Table App1.1.

Clinicopathological parameters	Number of cases	*TMPRSS2-ERG*		P
		Not fused (%)	Fusion (%)	
Preoperative PSA (ng/mL)*				0.61
0.9-4.0	9	3 (33)	6 (67)	
4.0-10.0	58	31 (53)	27 (47)	
10.1-20.0	37	21 (57)	16 (43)	
20.1-84.0	15	7 (47)	8 (53)	
Median tumor volume (%)*				0.89
0-10.0	35	19 (54)	16 (45)	
10.1-20.0	28	14 (50)	14 (50)	
20.1-85.0	49	24 (49)	25 (51)	
Gleason score				0.64
Gleason score 4-6	74	39 (53)	35 (47)	
Gleason score 7	35	18 (51)	17 (49)	
Gleason score 8-9	13	5 (38)	8 (62)	
Pathologic stage				0.97
pT2a	10	6 (60)	4 (40)	
pT2b	58	30 (52)	28 (48)	
pT3a	39	19 (49)	20 (51)	
pT3b	9	4 (44)	5 (56)	
pT4	6	3 (50)	3 (50)	
Seminal vesicle invasion*				0.34
Negative	108	54 (50)	54 (50)	
Positive	9	6 (67)	3 (33)	
Perineural infiltration				0.34
Negative	18	11 (61)	7 (39)	
Positive	104	51 (49)	53 (51)	
Angiolymphatic invasion*				0.4
Negative	89	43 (48.31)	46 (81)	
Positive	26	15 (58)	11 (19)	
Capsular invasion*				0.39
Negative	52	29 (56)	23 (44)	
Positive	69	33 (48)	36 (52)	
Extraprostatic extension*				0.84
Negative	92	46 (50)	50 (50)	
Positive	19	9 (47)	10 (53)	
Lymphonodal invasion*				0.15
Negative	108	53 (49)	55 (51)	
Positive	2	2 (100)	0 (0)	
Biochemical recurrence				0.05
Negative	62	37 (60)	25 (40)	
Positive	60	25 (42)	35 (58)	

Table App1.1. Clinicopathological parameters from 122 of the 125 prostatic adenocarcinoma patients. The three atypical tumors with complex fusions were excluded from the analysis. * Values not available for all 122 cases. Median overall survival was 87.4 months (11.5 - 161.6). *P* value= Chi square analysis

The frequency of *TMPRSS2-ERG* rearrangements was correlated with *PTEN* genomic deletions and to determinants of disease mortality and morbidity, such as PSA, and

extraprostatic extension, time to biochemical relapse, PSA doubling time, and the time to the development of metastases following definitive treatment. Univariate and multivariate analyses for the risk of biochemical failure were studied by the cox proportional hazard model. A significant correlation between two parameters was taken at the 95% confidence interval. For this exploratory analysis, P values <0.05 were considered significant, although it is recognised that multiple comparison testing occurred. The survival rate was estimated by applying the Kaplan-Meier method. Endpoints were defined by the time from radical prostatectomy until the occurrence of metastasis or PSA determined biochemical recurrence, i.e. the date of first PSA increase above 0.2 ng/ml. (median follow-up time 87.4 months, range 11.5 to 161.6). All calculations were performed using Stata 9.1 (StataCorp LP).

APP 1.3 Results

APP 1.3.1 *PTEN*

In the first *PTEN* cohort, archival tissue from 35 patients who underwent radical prostatectomy was analyzed. Using FISH, samples of benign glandular epithelium (n= 6) or LGPIN (n= 12) showed no *PTEN* deletion. *PTEN* deletion was found in 3/13 (23%) of HGPIN and 24/35 (68%) of CaP ($p<0.01$). Furthermore, of the 24 cases of CaP showing *PTEN* deletion, 2 were homozygous. Representative images of FISH and immunohistochemistry are shown in Figures App1.2 and 1.3, respectively. The frequency of *PTEN* gene deletion did not correlate significantly with patient age (range 45 to 75) ($p= 0.37$, Welch t-test), tumor size or stage ($p= 0.47$, Fisher Exact test), Gleason score (range 6 to 8) ($p= 0.72$, Fisher Exact test) or pre-operative PSA level (range 2.1 to 48) ($p= 0.17$, Welch t-test).

Concordance was observed between *PTEN* deletion and total *PTEN* protein expression

assessed by immunohistochemistry ($p= 2.2x10^{-16}$, Welch t-test). Informative immunohistochemical results were obtained from 33 of 35 CaP, 13 HGPIN, 10 LGPIN cases and 8 benign glands. The pattern of immunoreactivity was predominantly cytoplasmic with occasional nuclear staining. In general, moderate to strong *PTEN* staining was seen in cancer, HGPIN, LGPIN and benign cells not containing the *PTEN* deletion (Figure App1.4). Of the 24 CaP samples showing *PTEN* deletion, 100% (24/24) demonstrated variable weak cytoplasmatic and/or nuclear *PTEN* immunoreactivity. Overall, the immunostaining was weaker in tumor cells with homozygous *PTEN* deletions.

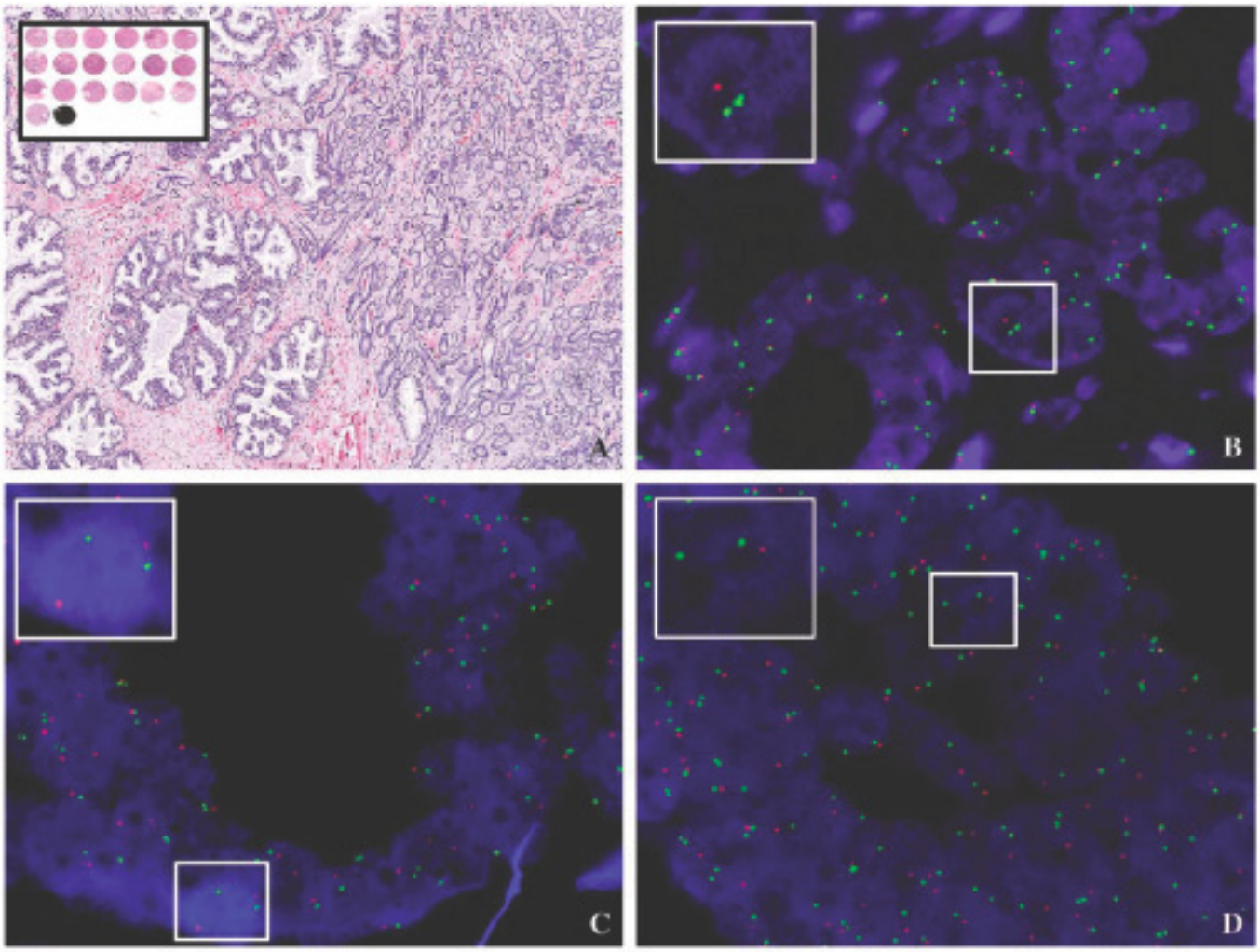

Figure App1.2. Representative images of dual-color FISH using LSI *PTEN*/CEP 10 on paraffin-embedded tissue sections. Haematoxylin and eosin stained section shows an area of CaP and adjacent PIN (A). FISH image shows tumor cells with single red signals for 10q23/*PTEN* locus in most of the nuclei and paired green signals for CEP10 indicating hemizygous deletion of 10q23/*PTEN* locus in CaP (B) and HGPIN cells (D). Two signals of each color in most of the nuclei indicate no deletion of *PTEN* in tumor cells from CaP (C).

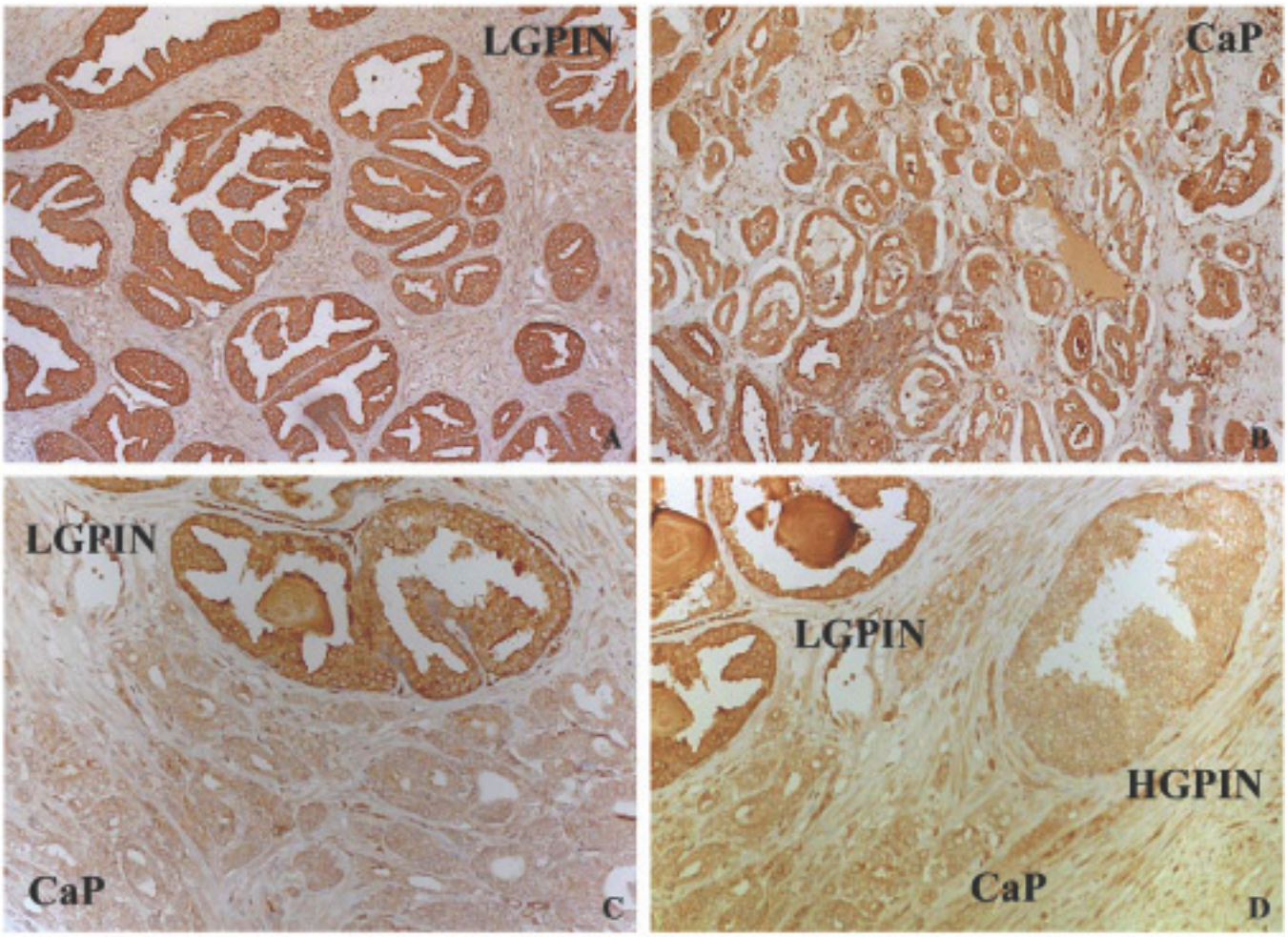

Figure App1.3. Immunohistochemical staining with anti-PTEN antibody of paraffin-embedded tissue sections. Strong immunoreactivity of PTEN protein in LGPIN (A) and cancer (B). Weak immunoreactivity of PTEN protein in cancer (C) and in HGPIN (D) compared to LGPIN foci (A, C, and D).

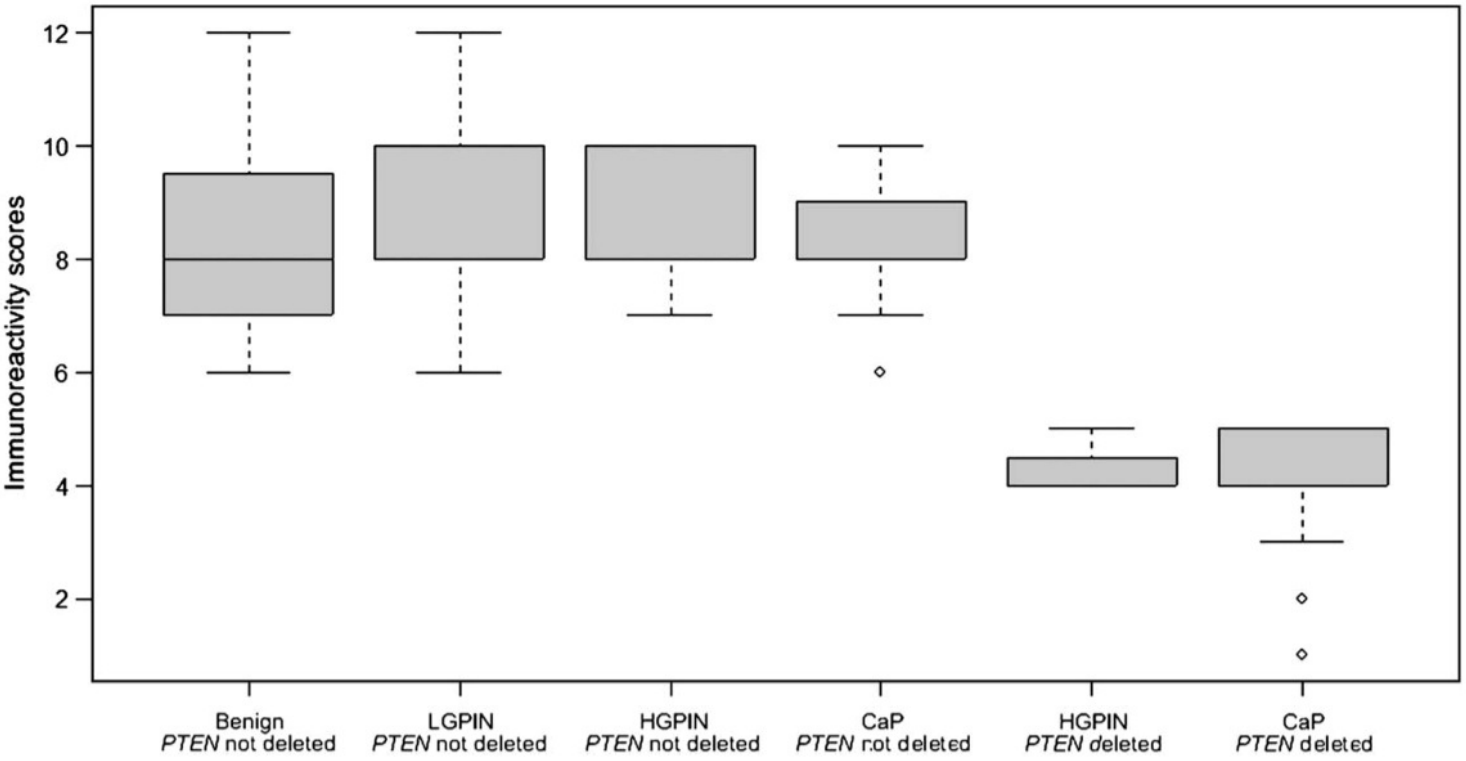

Figure App1.4. Relationship between immunohistochemical PTEN expression and *PTEN* deletion status. Two distinct distributions are shown: weak PTEN immunoreactivity is observed in HGPIN and CaP showing the *PTEN* deletion. Moderate or strong immunoreactivity is observed in benign prostate epithelium, LGPIN, HGPIN and CaP regions without the *PTEN* deletion. The box plot shows the median, upper and lower quartiles and minimum and maximum values for IHC scores.

APP 1.3.2 *TMPRSS2-ERG* fusion

A total of 125 archival tissues with anonymous clinical annotation were analyzed for *TMPRSS2-ERG* rearrangements by interphase tri-color FISH. *TMPRSS2-ERG* rearrangement was found in 60 of 125 (48%) of prostatic adenocarcinomas samples. There was evidence of *TMPRSS2-ERG* fusion with deletion of 5' *ERG* probe in 43 of 125 (34%) cases. As previously characterized (173), sequential FISH analysis using the BAC set telomeric to the 5' end of *TMPRSS2* (RP11-35C4, RP11-891L10 and RP11-260O11 - blue) identified a split of the typical co-localized 5' end of *TMPRSS2- 3' ERG* probe signals in 3 of these 43 samples. This extreme nuclear separation is indicative of a more complex genomic alteration, involving an unknown chromosomal partner(s). Confirmation of the *TMPRSS2-ERG* fusion in these 3 samples showing the atypical FISH pattern was obtained by the BAC set consisting of the 3' *ERG* BAC (RP11-476D17), 5' *ERG* (RP11-95I21) and the *TMPRSS2* locus (RP11-535H11). Interestingly, an extra copy of *TMPRSS2-ERG* fusion associated with deletion of 5' *ERG* probe was observed in 7 of the 43 samples showing *TMPRSS2-ERG* fusion with deletion of 5' *ERG* (See Table App1.2). There was evidence of FISH *TMPRSS2-ERG* fusion with no deletion of 5' *ERG* probe in 17 of 125 (14%) cases. Only 1 of the 17 cases showed the BAC set telomeric to the 5' end of *TMPRSS2* (RP11-35C4, RP11-891L10 and RP11-260O11 - blue) well separated from the 3' *ERG* BAC (RP11-476D17-red) (See Table App1.2).

***TMPRSS2-ERG* status**	**Number of cases (%)**
TMPRSS2-ERG fusion via translocation	17 (14%)
TMPRSS2-ERG fusion via genomic deletion of 5' *ERG*	43 (34%)*
Other rearrangements	3 (2.4%)
Not fused	62 (49.6%)
Total	125

Table App1.2. Summary of the *TMPRSS2-ERG* fusion status by tri-color FISH
* Duplication of *TMPRSS2-ERG* fusion was observed in 7 of the 43 samples showing *TMPRSS2-ERG* fusion via genomic deletion of the 5' end of the *ERG* gene

In addition to the 60 *TMPRSS2-ERG* fused cases, 3 atypical cases had abnormal *TMPRSS2-ERG* FISH co-localization pattern. The 3' *ERG* RP11-476D17 (red signal) remained juxtaposed to the 5' *ERG* RP11-95I21 (green signal), but failed to exhibit the expected co-localization of the *TMPRSS2* locus (RP11-535H11 - blue) with the *ERG* gene probes. We were not able to detect FISH fusions between *TMPRSS2* and *ETV1* or *ETV4* in any of these three cases with abnormal FISH *TMPRSS2-ERG* break-apart results. Furthermore, extra copies of the *TMPRSS2* locus (RP11-535H11 - blue) were observed in the atypical samples. Such findings indicate that: (a) fusion events between *TMPRSS2* and other genes are possible, and (b) *TMPRSS2-ERG* fusions may sometimes have concurrent complex genomic rearrangements within the ~2.9 Mb that separates these two genes. However, the 3 atypical cases were excluded from the clinicopathological correlation analysis given that complex genomic rearrangement involving an unknown chromosomal partner(s) could not be elucidated.

Among the 60 rearranged *TMPRSS2-ERG* tumors detected, Gleason scores were 4-6 (35 tumors), 7 (17 tumors) and 8-9 (8 tumors). A median tumor volume of >20% of the prostate was found in 25/60, and biochemical recurrence based on PSA level was present in 35 of the 60 the rearranged *TMPRSS2-ERG* tumors. In addition, early biochemical recurrence was detected

in all 7 samples with an extra copy of *TMPRSS2-ERG* fusion associated with deletion of 5' *ERG* probe.

APP 1.3.3 Presence of *TMPRSS2-ERG* fusion and *PTEN* genomic deletion

After acquisition of FISH data, the cases were reviewed to search for potential associations between *PTEN* deletion (330), and *TMPRSS2-ERG* rearrangements. Therefore, we examined the status of *PTEN* (deleted or not deleted) and presence of *TMPRSS2-ERG* fusion in 82 of the 125 tumor samples to assess the utility of a possible association as a biomarker of prognosis. *PTEN* deletion in addition to the presence of *TMPRSS2-ERG* rearrangement was observed in 23 of 82 (28%) prostatic adenocarcinomas. *PTEN* deletion was also found in 14 prostate adenocarcinoma samples showing absence of *TMPRSS2-ERG* rearrangement (14/82, 17%). There was evidence of no copy change of *PTEN* locus with *TMPRSS2-ERG* fusion in 21 of 82 (26%) cases and no copy change of *PTEN* locus with absence of *TMPRSS2-ERG* fusion in 24 of 82 (29%) cases. *TMPRSS2-ERG* fusion and *PTEN* deletion are summarized in Table App1.3, although no clear statistical relationship is evident.

	***TMPRSS2-ERG* fusion**	**No fusion**
***PTEN* deletion**	23 (28%)	14 (17%)
***PTEN* not deleted**	21 (26%)	24 (29%)

Table App1.3. Distribution of the CaP samples showing *TMPRSS2-ERG* fusion and *PTEN* deletion in 82 prostatic adenocarcinomas. A comprehensive description of the clinicopathological parameters associated with 47 adenocarcinomas (23 cases showing both *PTEN* deletion and *TMPRSS2-ERG* fusion, and 24 cases in which neither rearrangement was present) is summarized in Table App 1.4.Representative images of *TMPRSS2-ERG* rearrangement and *PTEN* deletion are shown in Figure App 1.5.

	***TMPRSS2-ERG* fusion and *PTEN* deletion**	***TMPRSS2-ERG* not fused and *PTEN* not deleted**
Preoperative PSA (ng/mL) *		
0.9-4.0	1	0
4.0-10.0	10	14
10.1-20.0	6	7
20.1-84.0	4	3
Median tumor volume (%) *		
0-10.0	4	10
10.1-20.0	5	6
20.1-85.0	13	11
Gleason score		
Gleason score 4-6	12	16
Gleason score 7	7	7
Gleason score 8-9	4	1
Pathologic stage		
pT2a	1	1
pT2b	12	11
pT3a	6	9
pT3b	3	1
pT4	1	2
Seminal vesicle invasion *		
Negative	18	22
Positive	2	2
Perineural infiltration		
Negative	2	5
Positive	21	19
Angiolymphatic invasion *		
Negative	17	17
Positive	5	5
Capsular invasion *		
Negative	8	9
Positive	13	14
Extraprostatic extension		
Negative	17	16
Positive	6	8
Lymphonodal invasion *		
Negative	21	20
Positive	1	1
Biochemical recurrence		
Negative	5	15
Positive	18	9

Table App1.4. Clinicopathological parameters from 47 of the 82 prostatic adenocarcinoma patients analyzed for the differential status of *PTEN* (deleted or not deleted) and presence of *TMPRSS2-ERG* fusions*values not available for all 47 samples. Median overall survival was 109 months (49.3-161.3)

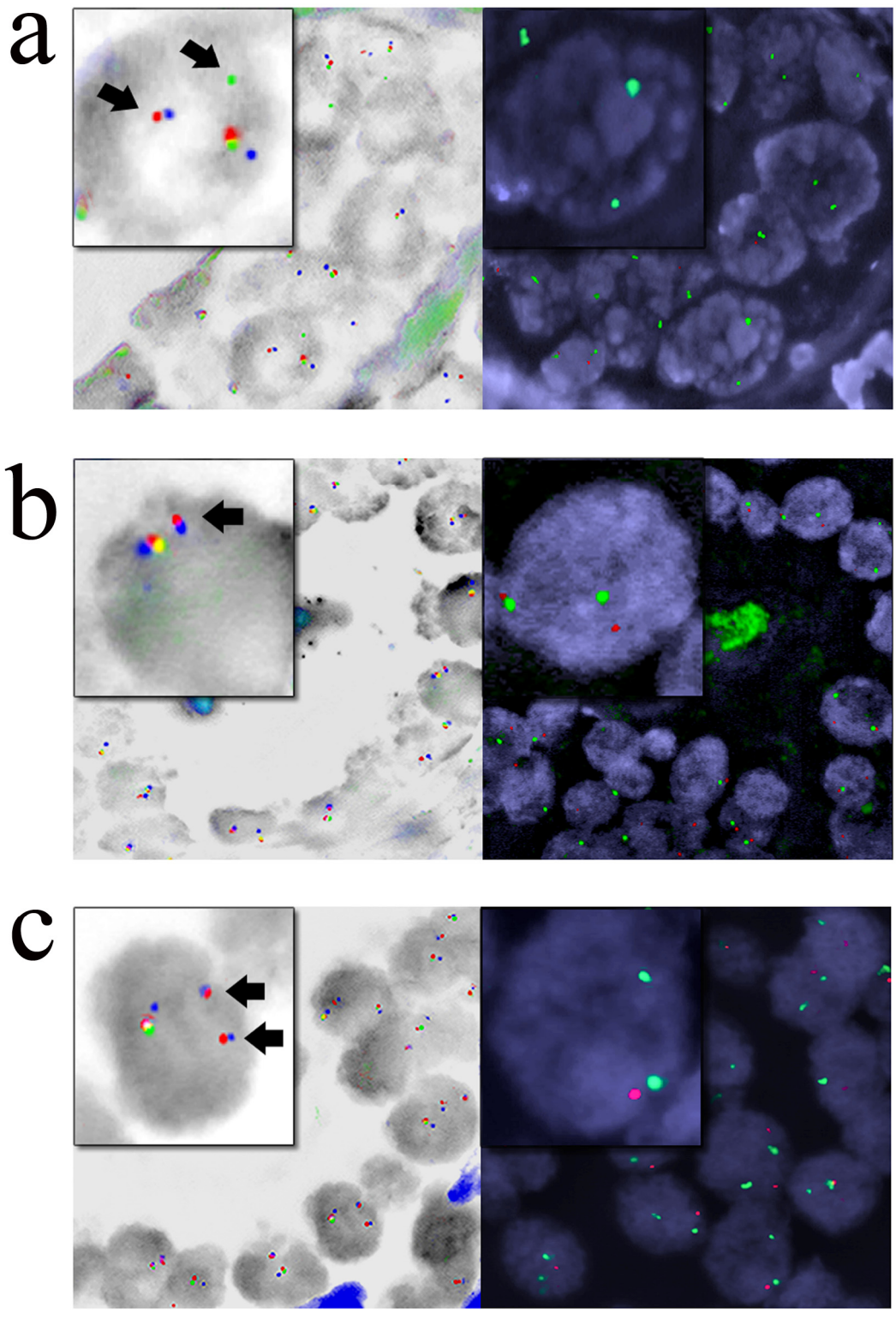
a
b
c

Figure App1.5. Different patterns of genomic alterations detected by interphase FISH in CaP. Representative FISH images are shown for CaP tissue microarray applying *TMPRSS2:ERG* (left panel) and *PTEN* (right panel). **(a-c)** A representative FISH image of *TMPRSS2:ERG* rearrangements (left panel) is displayed in a tissue core with accompanying FISH for the *PTEN* locus (right panel). The left panel shows a representative pseudo-color image with the inverted-DAPI counterstained nuclei as a grey tone overlay to facilitate interpretation. The right panel shows a representative pseudo-color image with the DAPI counterstained nuclei. The rectangles show an enlarged nucleus FISH image. (**a)** Representative break-apart tri-color FISH strategy identifies the 5' *ERG* BAC (RP11-95I21-green) well separated from the 3'*ERG* BAC (RP11-476D17-red) (arrow). The fused signal of the 3' *ERG* (red) and *TMPRSS2* gene locus (blue) that confirms the probes used detect *TMPRSS2:ERG* fusions (arrows). The BAC probes hybridising to the unaffected *TMPRSS2:ERG* locus show the normal red-green (yellow) and blue co-localization pattern. This extreme nuclear separation is indicative of *TMPRSS2:ERG* rearrangements via genomic translocation mechanisms. Representative *PTEN* FISH image of homozygous deletion in CaP shows absence of red signal for 10q23/*PTEN* locus in most of the nuclei and retained green signals for CEP 10. **(b)** The fused signal of the 3' *ERG* (red) and *TMPRSS2* gene locus (blue) that confirms the *TMPRSS2:ERG* fusion is arrowed. In addition, the hemizygous loss of 5' *ERG* BAC (green) indicates an intervening genomic microdeletion of chromosome 21. The BAC probes hybridizing to the unaffected *TMPRSS:ERG* locus show the normal tri-color (red, green and blue) co-localization pattern. Representative *PTEN* FISH image of two signals of both red signals (10q23/*PTEN* locus) and green signals (CEP 10) in most of the nuclei indicating no deletion of *PTEN* in tumor cells. **(c)** Duplication of the fused signal of the 3' *ERG* (red) and *TMPRSS2* gene locus (blue) that confirms the *TMPRSS2:ERG* fusion is arrowed. In addition, the hemizygous loss of 5' *ERG* BAC (green) indicates an intervening genomic microdeletion of chromosome 21. The BAC probes hybridizing to the unaffected *TMPRSS:ERG* locus show the normal tri-color (red, green and blue) co-localization pattern. The *PTEN* FISH image shows tumor cells with single red signal for 10q23/*PTEN* locus in most of the nuclei and paired green signals for CEP 10 indicating hemizygous deletion of 10q23/*PTEN* locus in CaP.

APP 1.3.4 Statistical analysis of clinical parameters and genomic alterations

Clinical parameters of aggressive disease such as extraprostatic extension (P=0.0002), seminal vesicle invasion (P=0.0023), margin status (P=0.0008), Gleason grade (P=0.0002)/score (P=0.001), median tumor volume (P=0.0024), preoperative PSA (P=0.001) as well as genetic factors such as *PTEN* deletion (P=0.009), concurrent *TMPRSS2-ERG* fusion and *PTEN* deletion (0.001) and perineural invasion (P=0.0304) were significantly associated with biochemical recurrence by univariate analysis with *TMPRSS2-ERG* approaching significance (P=0.052; Table App1.5). By multivariate analysis, relevant factors associated with biochemical failure included Gleason score (7 and 8–10, P=0.001 and P=0.015, respectively), concurrent *TMPRSS2-ERG* fusion and *PTEN* deletion (0.036) and *PTEN* homozygous deletion (0.013). The *PTEN* findings reflect those previously reported for this cohort (Table App1.6) (330).

Further analysis of the Kaplan-Meier estimated disease-free survival curves demonstrated association between *TMPRSS2-ERG* fusion and short time based to PSA recurrence (Figure App1.6a). Duplication of the *TMPRSS2-ERG* fusion was associated with an earlier onset of biochemical recurrence (Figure App1.6b). Furthermore, the estimated disease-free survival Kaplan-Meier curves demonstrated an association of concurrent *PTEN* deletion and *TMPRSS2-ERG* rearrangements with short time to PSA recurrence (Figure App1.6c). This analysis allowed for three broad groupings of differential patient outcome based on genetic characteristics; (1) a poor prognostic group characterized by both *PTEN* deletion and *TMPRSS2-ERG* fusions; (2) an intermediate group with either *PTEN* deletion or *TMPRSS2-ERG* fusion and (3) a favorable prognostic group with neither event.

Variables	***Category***	***BRFS****		***HR***	***95% CI***
		5 years	**P-*value***		
Perineural invasion	Negative	77.04	0.0304	1.0	Reference
	Positive	49.94		2.91	1.05–8.04
Extraprostatic extension	Negative	63.45	0.0002	1.0	Reference
	Positive	26.78		3.10	1.67–5.76
Margins	Negative	62.99	0.0008	1.0	Reference
	Positive	25.70		2.40	1.41–4.07
Seminal vesicle invasion	Negative	57.33	0.0023	1.0	Reference
	Positive	20.00		3.28	1.46–7.36
Neoadjuvant hormonotherapy	Negative	59.49	0.0004	1.0	Reference
	Positive	33.33		1.59	1.21–2.08
Primary gleason grade	2–3	48.01	0.0002	1.0	Reference
	4	15.43		1.48	1.74–6.95
Gleason score	4–6	69.90	<0.001	1.0	Reference
	7	32.58		3.14	1,79–5.49
	8	19.94		3.42	1.63–7.16
Median tumor volume	0–10.0	71.43	0.0024	1.0	Reference
	10.1–20.0	62.95		1.10	0.46–2.60
	20.1–85.0	39.63		2.67	1.35–5.30
Preoperative PSA	0.9–4.0	77.78	<0.001	1.0	Reference
	4.1–10.0	62.85		2.38	0.56–10.08
	10.1–20.0	55.52		2.86	0.66–12.37
	20.1–84.0	6.67		13.08	2.93–58.26
TMPRSS2-ERG fusion	Negative	61.77	0.0523	1.0	Reference
	Positive	45.72		1.99	1.21–3.27
PTEN deletion	Negative	57.04	0.0009	1.0	Reference
	Hemizygous	50.00		1.53	0.82–2.85
	Homozygous	0.0		5.93	2.12–16.84
PTEN deletion and	Negative	59.35	0.001	1.0	Reference
TMPRSS2-ERG fusion	Positive	30.43		2.49	1.43–4.35

Table App 1.5. Univariate Cox proportional hazard analysis of biochemical failure risks (each variable predictor analyzed separately). BRFS – Biochemical Recurrence Free Survival

Variables	***Category***	***HR***	**P-*value***	***95% CI***
Gleason score	4–6	1.0		Reference
	7	3.07	<0.001	1.75–5.37
	8–10	2.65	0.015	1.21–5.81
PTEN status	Negative	1.0		Reference
	Hemizygous deletion	1.30	0.433	0.67–2.54
	Homozygous deletion	4.43	0.013	1.36–14.40
PTEN deletion and *TMPRSS2-ERG* fusion	Negative	1.0		Reference
	Positive	1.87	0.036	1.04–3.36

Table App 1.6. Multivariate model to biochemical failure risks by Cox logistic regression analysis. CI, confidence interval; HR, hazard ratio.

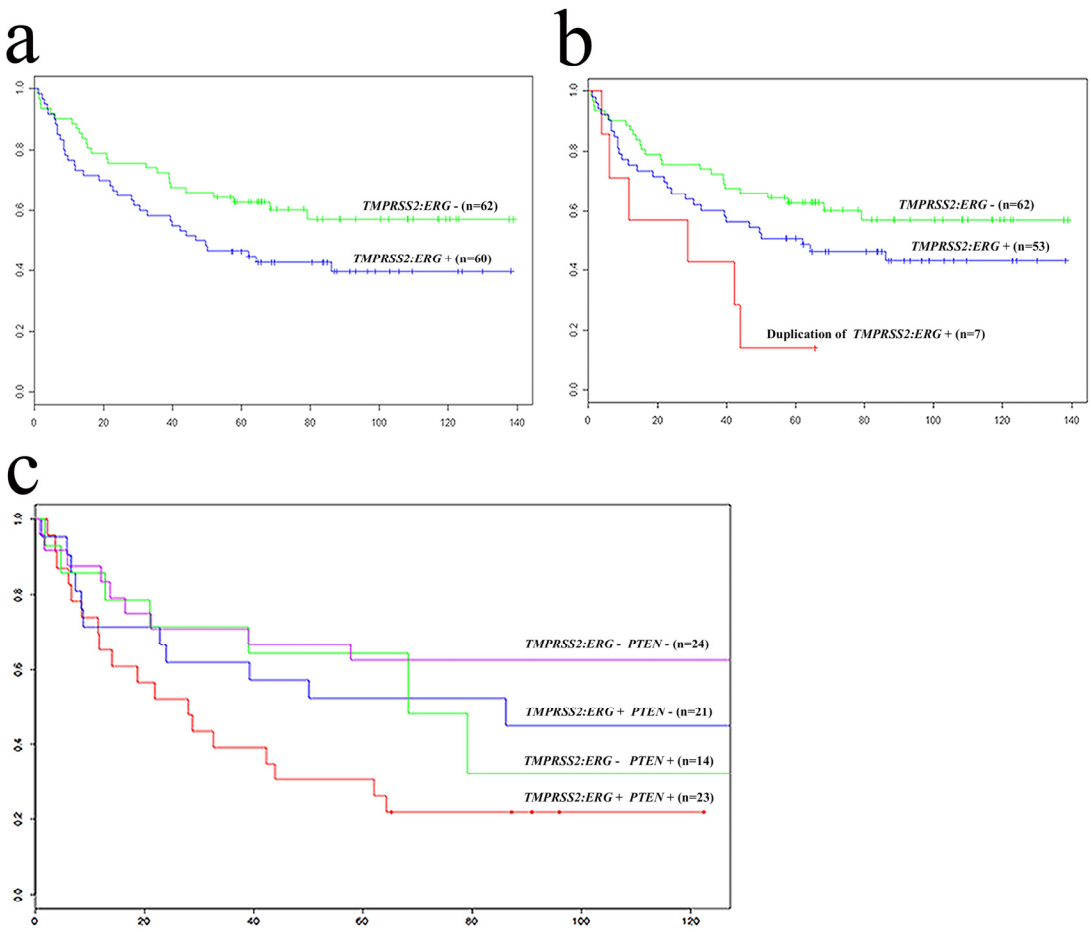

Figure App 1.6 Kaplan–Meier curves illustrating biochemical recurrence-free survival among prostate cancer patients defined by the status of selected clinicopathological parameters, *TMPRSS2:ERG* rearrangements and *PTEN* copy number changes; (+) presence, (-) absence. (**a**) PSA recurrence-free survival curve stratified by the *TMPRSS2:ERG* rearrangements (absence or presence of gene fusion) on 122 prostate cancer patients and (**b**) when duplicate *TMPRSS2:ERG* FISH fusion signals were present (red curve) the outcome was the least favorable. (**c**) PSA recurrence-free survival analysis stratified by *TMPRSS2:ERG* rearrangements and *PTEN* copy number changes in 82 prostate cancer patients.

APP 1.4 Discussion

The reported frequency of *PTEN* deletion in CaP varies widely, most likely as a result of differences in tissue preparation, stage of disease and the methodology used to detect molecular aberrations (Table App1.7). The heterogeneous nature of these studies has probably obscured the role of *PTEN* in human prostate cancer. Previous investigations have generally indicated a role of *PTEN* deletion in advanced disease, although more thorough studies have suggested higher rates of altered expression. Our findings, in both cohorts, along with studies using *in vivo* mouse models and cell lines (316, 318, 570), support the concept of *PTEN* deletion as a frequent and important event in prostatic carcinogenesis; they were facilitated by the ability of FISH to detect clonal deletions in a subset of tumor cells. In contrast, most previous studies employed loss of heterozygosity (LOH) analysis of either microdissected or bulk-extracted tissue and could not detect small populations of cells containing these clonal deletions.

In examining the first cohort, the occurrence of hemizygous deletions in a small proportion of pre-neoplastic HGPIN lesions, but with a marked increase in frequency of *PTEN* deletion in CaP, suggests that the acquisition of the deletion and concomitant loss of *PTEN* functional activity is an important early step in prostatic tumorigenesis. Conclusions drawn from studies in mice suggest that *PTEN* haploinsufficiency is pathogenic (411). The relative deficiency of *PTEN* cellular protein levels is likely to produce a net activation of the *AKT* pathway and acquisition of a more malignant phenotype. Consequences of *AKT* activation such as angiogenesis, and increased cell mobility and breakdown of cellular junctions (571) are also likely to occur. Previous authors have demonstrated an association between decreased *PTEN* protein expression and a higher Gleason grade and advanced tumor stage (326, 327). However, within our first study group there was no statistically significant relationship between *PTEN*

deletion status and clinicopathologic parameters. This observation is likely a consequence of the small sample size and the relatively narrow range of Gleason scores of the samples (97% of samples were Gleason score 6 or 7) studied.

The knowledge that early heterozygous deletion of *PTEN* is frequent in CaP is an important consideration for novel therapeutic trials where biological efficacy is influenced by the activity level of *PTEN* and its downstream targets. Potential therapeutic opportunities for control of tumors in the context of *PTEN* pathways have been reviewed recently (411, 572). Additionally, preclinical studies have provided a rationale for combining AKT inhibition with other pathways (573), chemotherapy (574, 575) and hormonal therapy (576) although clinical studies to date with an AKT inhibitor (perifosine) showed limited clinical activity (508).

Our second cohort of patient samples evaluated *PTEN* and the *TMPRSS2-ERG* rearrangements for their contribution to prostate cancer prognosis in a large Brazilian TMA. Although limited by multiple comparison testing, Figure App 1.6C illustrates these two genomic biomarkers which appeared to segregate prostate cancer cases into three broad groupings based on biochemical recurrence as an endpoint: (1) 'poor genomic grade' characterized by both *PTEN* deletion and *TMPRSS2-ERG* fusions; (2) 'intermediate genomic grade' with either *PTEN* deletion or *TMPRSS2-ERG* fusion and (3) 'favorable genomic grade' in which neither rearrangement was present. However, the multi-variate analysis indicates that the hazard ratio imparted by a high Gleason score (5) remained greater than any other factor in the analysis, although as mentioned the tumours analysed had a relatively narrow range of Gleason scores for analysis, suggesting the need for further confirmatory studies.

The proportion of prostatic adenocarcinoma samples with *TMPRSS2-ERG* rearrangement (48%) is in agreement with similar cohorts that included diverse stage and Gleason scores (190, 193) whereas subsets with earlier stage disease tend to have lower incidence (192, 193). This association of the gene rearrangement with more advanced disease

has been suggested previously (171, 193) and might explain the suggestion of poorer survival in patients with the fusion genes. The confirmation of the finding of poorest prognosis associated with the duplication of gene fusion via 5' ERG deletion (171) variant also likely highlight important aspects of the pathophysiology of prostate cancer. The ERG gene duplication associated with this variant is likely to contribute to an increased rate of biochemical recurrence seen in our and other cohorts (19, 186, 192). Collectively, our data indicate that the duplication of gene fusion via 5' ERG deletion is predictive of a shorter time to biochemical recurrence of disease. However, some authors have suggested that duplication of the fusion may be a manifestation of general polyploidy rather than a specific duplication event (577), which has likewise been associated with poor prognosis in CaP (578-580).

As *PTEN* deletion and *TMPRSS2-ERG* abnormalities could be additive or mutually exclusive, we evaluated the prognostic information gained by *TMPRSS2-ERG* analysis alone and in combination with genomic *PTEN* deletions (see Figure App 1.6). The additive effect seen may relate to increased cellular motility, a phenotype that can be attributable to both ETS fusion (581) and *PTEN* deletion (582, 583). Thus together, activation of these pathways might facilitate epithelial–mesenchymal transition that is characteristic of malignant transformation (584). To further explore the potential for synergy between these genomic events, we used Oncomine (585) to interrogate two publicly available microarray studies of prostate cancer progression for differentially expressed genes between ETS overexpressing and nonoverexpressing prostate cancers (388, 586).The ETS overexpressing prostate cancers demonstrated dysregulation of genes particularly involved in the Wnt pathway. *PTEN* deletion and its sequel are also likely to affect the same pathways and synergize with the consequences of ETS-related overexpression. Akt activation is also known to inhibit GSK3β, (587) The combination of these two events would theoretically lead to extra translocation of β-catenin to the nucleus further assisting

cellular motility and epithelial to mesenchymal transition (588), a phenomena that could be explored further in our samples. Additionally, we found a theorectical up-regulation of the B-RAF gene in ETS over expressing tumors, such that combined signalling through ERK is also likely to increase cellular migration phenomenon.

Our findings suggests that the subgroup of prostate cancers with absence of both TMPRS2:ERG fusions and genomic *PTEN* alterations might have a favourable prognosis. Kaplan–Meier and multivariate analysis indicate that *TMPRSS2-ERG* fusion and *PTEN* loss together are a predictor of earlier biochemical recurrence of disease. The acquisition of the *TMPRSS2-ERG* fusion and concomitant *PTEN* deletion at an early phase in prostatic oncogenesis appear to be determinants of a more aggressive tumor phenotype. Further studies should validate this concept to allow better stratification of care in prostate cancer.

First Author, Year	Source Material	Techniques	Findings (HGPIN)	Findings (CaP)	Conclusions relevant to this study
Cairns *et al.* (589)	80 RP specimens (frozen tissue)	LOH analysis, sequencing, methylation-specific PCR FISH (1 sample)	Not done	LOH through *PTEN*: 23/80 (6/23 exhibited homozygous deletion). Of the 23 cases of CaP with LOH: 11 were localized and 12 pelvic nodes[1] Mutations: 4/17 Methylation: 0/13	*PTEN* is the main inactivation target of 10q loss in CaP
Pesche *et al.* (590)	22 CaP specimens	LOH analysis, sequencing No FISH	Not done	LOH at 10q22-23: 12/22 (55%). Of the 12 cases of CaP with LOH, 6 showed LOH within *PTEN*. Mutation: 1/6	Deletion of 10q22-q24, including *PTEN*, appears prominent in CaP
Gray *et al.* (591)	37 TURP specimens (microdissection)	Mutation analysis, northern blotting, Immunofluorescence	Not done	Alteration or loss of at least one *PTEN* copy: 26/37 (21 containing allele loss only, 3 with allele loss	Supportive evidence that *PTEN* acts as a tumour suppressor gene in

		No FISH		and mutation, 2 with mutation only)	prostate
Feilotter *et al.* (592)	51 RP and FFPE CaP specimens (microdissection)	LOH analysis, SSCP, sequencing No FISH	Not done	LOH: 25/51 (49%) Mutations: 1/51	*PTEN* maps to region of LOH in CaP
Wang *et al.* (593)	60 RP specimens containing ate least 50% of tumour	Southern blotting, LOH analysis, sequencing, No FISH	Not done	Deletions: 10/60 Homozygous by Southern: 8/60 *PTEN* mutations: 0/10	Inactivation of *PTEN* occurs in 10-15% of primary stage B CaP
Suzuki *et al.* (594)	50 metastatic CaP specimens from 19 patients	SSCP, sequencing, microsatellite analysis FISH (2 samples)	Not done	Deletions/point mutations: at least 1 metastatic site in 12/19 Homozygous deletions: 2/19 Point mutations: 4/19 LOH: 10/18 Loss of the same allele was found in all metastases in a given patient	*PTEN* gene alterations occur frequently in lethal CaP; substantial mutational heterogeneity is found among different metastatic sites within the same patient

				in 9/10 cases	
Dong *et al.* (595)	40 RP samples (macrodissection: at least 70% of tumour)	LOH analysis, PCR for homozygous deletion, sequencing No FISH	Not done	LOH using intragenic markers: 0/40 Mutation: 1/40 Homozygous deletions: 0/40	*PTEN* plays an insignificant role in low stage CaPs
Orikasa *et al.* (596)	45 RP specimens: 18 FFPE and 27 frozen	LOH analysis FISH (12 samples)	Not done	LOH: 2/18 (11.1%) FISH single allele loss: 2/12 (16.7%) Mutations: 0/27	Mutation of *PTEN* does not play a major role in prostatic carcinogenesis in Japan
McMenamin *et al.* (326)	109 RP and FFPE CaP specimens	IHC No FISH	*PTEN* expression Positive: 58/58	*PTEN* expression Positive: 17/109 (16%) Mixed: 70/109 (64%) Absence: 22/109 (20%)	Absence of staining correlated with increased stage, size
Muller *et al.* (597)	40 CaP samples[2] (microdissection)	LOH and mutation analysis No FISH	Not done	LOH: 14/40 (35%) Mutations: 8/14 (5 coding, 3 intronic)	LOH data on 10q affects *PTEN* region

Dong *et al.* (598)	32 RP and FFPE CaPs (Asian), 6 metastases (USA) (microdissection)	SSCP, sequencing No FISH	Not done	*PTEN* mutations: 5/32 (16%) of RP and 2/6 (33%) of metastases	*PTEN* mutations likely more common in higher grade tumours
Halvorsen *et al.* (599)	104 RP specimens	IHC on tissue microarray No FISH	Not done	Absence of *PTEN* expression: 28/103 (27%)	Loss of *PTEN* / p27 associated with adverse pathology, proliferation and risk of recurrence
Lieberfarb *et al.* (600)	52 RP and FFPE CaP specimens (microdissection)	SNP analysis No FISH	Not done	LOH of 10q23: 5/52	Microarray based LOH detection is feasible and robust
Koksal *et al.* (327)	15 RP specimens, 18 TURP for malignant disease (microdissection)	Western blotting/ Densitometry No FISH	Not done	86% reduction in *PTEN* protein in advanced disease	*PTEN* status appears to be useful as an independent marker to predict progression
Fenic *et al.*	58 CaP specimens	ISH, RT-PCR,	*PTEN*	*PTEN* expression	*PTEN* protein and

(524)	(31 RP and 27 TURP) 26 PIN and 15 metastases	Western, IHC No FISH	expression ++mRNA: 26/26 (100%) ++IHC: 21/26 (81%) +IHC: 3/26 (11.5%) -IHC: 2/26(7.7%)	++mRNA: 40/58 (69%) +mRNA: 16/58 (27.6%) -mRNA: 2/58 (3.4%) ++IHC: 27/58 (46.5%) +IHC: 24/58 (41.3%) -IHC: 8/58(13.8%)	tumour progression - inconclusive
Verhagen *et al*. (324)	40 locally progressive CaP (macrodissection, 80% tumour)	Allelotype analysis, FISH, array-CGH, PCR-SSCP, Sequencing, WPR analysis	Not done	3/40 mutations by sequencing; 8/37 homozygous *PTEN* deletion by FISH; 7/37 loss of one *PTEN* copy by FISH; 11/19 LOH; 15/38 negative by IHC; 15/38 biallelic deletion, 15/38 single allele loss by WPR analysis	Bi-allelic deletion is a major mechanism of *PTEN* inactivation in locally progressive CaP

Schmitz *et al*. (329)	Biopsies at first diagnosis (Study I, 112 patients) and patients with confirmed metastasis (Study II, 42 patients)	IHC	Not done	In Study I, loss of *PTEN* in 26/112 patients (23%). In Study II, 25/42 patients (59%) with lymph node metastasis had complete loss of *PTEN* expression in both tissues, of these 13 (52%) exhibited loss of *PTEN* expression at first diagnosis.	Patients with a low Gleason score and negative *PTEN* expression are might progress to metastatic disease.
Pourmand *et al.* (601)	51 formalin-fixed paraffin-embedded specimens	Tissue microdissection and polymerase chain reaction/single-strand conformation polymorphism methods	Not done	6/51 cases (11.6%) showed mutation in *PTEN* involved exons 1, 2, and 5. 2/51 had localized and others had advanced CaP.	Patients with prostate cancer and *PTEN* mutation had greater GS, poorer prognosis, and higher rate of metastasis. However, this mutation cannot predict the

					prognosis and the GS is a more precise factor.
Hellwinkel *et al.* (602)	20 patients with varying stages of prostate cancer	Microdissected tumour tissues via qRT-PCR	Not done	Significant downregulation of *PTEN* expression in Gleason 5-6 vs Gleason 7-10	Down-regulation of the PIK3/PKB pathway could represent a marker for the formation of highly de-differentiated prostate cancers from low-grade tumour foci

Table App 1.7. Summary of the *PTEN* analysis literature to date in prostatic neoplasia and preneoplasia

[1]Authors consider results an underestimate as did not search for promoter, regulatory region mutations, did not sequence tumors without loss of heterozygosity, likely missed small homozygous deletions; [2]type unclear; CaP- prostate cancer; PIN- prostatic intra-epithelial neoplasia; RP- radical prostatectomy; TURP- transurethral resection of the prostate; FFPE- formaldehyde-fixed paraffin-embedded; LOH- loss of heterozygosity; ++ moderate to strong expression; + low expression; - negative expression; WPR- wild-type:pseudogene ratio analysis

APPENDIX 2. A PHASE 2 TRIAL OF CYTARABINE (ARA-C) IN METASTATIC HORMONE REFRACTORY PROSTATE CANCER

APP 2.1 Background

APP 2.1.1 Prostate Cancer

Prostate cancer is primarily treated by surgery (radical prostatectomy) or radiotherapy if diagnosed when still localised. Advanced prostate cancer, either that which has failed local therapy or is metastatic, requires systemic therapy, usually with anti-testosterone hormone medication or castration. However the median response to androgen deprivation therapy is approximately 18-24 months, and all men eventually progress to androgen independence (unless they die of other causes). Once the disease becomes hormone refractory and therapy is indicated, then the standard of care is chemotherapy (docetaxel) (603, 604) but there is no standard of care following tumour progression after chemotherapy and further treatment options are needed.

APP 2.1.2 ETS Family Relationship to Prostatic Carcinogenesis

As referred to throughout this thesis, the ETS transcription factors appear to demarcate an important juncture into from the preneoplastic HPIN lesion to overt prostatic carcinoma. The ETS family encodes nuclear transcription factors with an evolutionarily conserved ETS domain of 85 amino acids that mediates binding to purine-rich DNA residues; more than 400 target genes are either positively or negatively regulated by them. There are currently 27 ETS related transcription factors that have been characterised amongst them ERG, ETV1, ETV4 and FLI1. The concept of "ETS conversion" (the overexpression of ETS transcription factors) as a mechanism of epithelial to mesenchymal transition, and thus malignant transformation, is well established and indeed, recent evidence appears to corroborate this mechanism in ETS overexpressing models (186).

APP 2.1.3 Ara-C (Cytarabine)

Ara-C is an analog of deoxycytidine and has multiple effects on DNA synthesis. Ara-C undergoes phosphorylation to form arabinosylcytosine triphosphate (Ara-CTP), which competitively inhibits DNA polymerase - in opposition to the normal substrate deoxycytidine 5-triphosphate (dCTP) (605). More importantly, Ara-C is incorporated into DNA, a feature that correlates closely with cytotoxicity (606); evidence suggests that this is the major cytotoxic lesion in Ara-C–treated cells. Other biochemical actions of Ara-C have been described, including inhibition of ribonucleotide reductase (607) and formation of Ara-CDP-choline, an analogue of cytidine 5- diphosphocholine (CDP-choline) that inhibits synthesis of membrane glycoproteins and glycolipids. Nevertheless, the molecular mechanisms of cell death after Ara-C exposure are unclear. For example, some investigators report that induction of pRb phosphatase activity by DNA-damaging drugs, including Ara-C, is at least one of the mechanisms responsible for p53-independent, Rb-mediated G1 arrest and apoptosis (608). The resulting hypo-phosphorylated pRb binds to and inactivates the E2F transcription factor, which inhibits the transcription of numerous genes involved in cell-cycle progression (609).

APP 2.1.4 Relationship between Ara-C and the ETS family of transcription factors

In recently published data (610), high-throughput drug screening (611) identified Ara-C as a drug that inhibits production of a characteristic 14-gene mRNA signature found in Ewings sarcoma cells with the characteristic EWS-FLI1 fusion, with effects analogous to transfection with FLI1 RNAi. This fusion gene is pathognomonic of the malignant phenotype in Ewings sarcoma (612-614). FLI1 is a member of the ETS family of transcription factors. FLI1, and the ETS family member most relevant to prostatic carcinogenesis (ERG), are known to interact

directly (615) and have identical effects on molecular pathways such as TGF-Beta that are of established importance in prostatic carcinogenesis. In addition, their overexpression in Ewings sarcoma results in a common phenotype suggesting overlapping transcript profiles.

APP 2.2 Hypothesis and Aims

The hypothesis of this study is that Ara-C (cytarabine) blocks the effect of ETS-related translocations in prostatic carcinogenesis and has unrecognised activity in prostate cancer. The specific aims are;

1. To assess the PSA (Primary endpoint) and palliative response rate (Secondary endpoint) of Ara-C in men with HRPC (Hormone Refractory Prostate Cancer) who have received prior therapy with docetaxel.
2. To assess the toxicity of Ara-C in men with HRPC.
3. To assess the relationship between ETS translocations in prostate cancer and response to Ara-C.
4. To assess the relationship between serum ETS fusion genes and PSA response.

APP 2.3 Preliminary Studies

In order to verify the presence of the 14-gene mRNA signature in prostate cancer we used the two largest publicly available expression microarray studies of prostate cancer that compare normal prostate tissue to localized cancer and metastatic disease through the Oncomine resource (49, 388, 585). This signature appears to be largely intact in localized and metastatic prostate cancer, (See Table App2.1) with the majority of genes showing a similar or related pattern of dysregulation in prostate cancer when compared to Ewings sarcoma. This suggests potential activity of Ara-C in treating this neoplasm. Additionally, we have been encouraged by xenograft

work suggesting that more advanced hormone refractory disease is associated with greater activation of non-ERG ETS family members, in particular FLI1, which is relevant to this proposal (165).

Study(s)→	Ewings data		Prostate Studies					
Gene(s) ↓	CONTROL RNAI	RNAI to FLI1	Lapointe *et al* (N vs L)	Lapointe *et al* (LND vs L)	Lapointe *et al* (LND vs N+L)	Yu *et al* (N vs L)	Yu *et al* (M vs L)	Yu *et al* (M vs N+L)
SP100	LOW	HIGH	LOW- 6.5E-6	LOW- 0.008	LOW- 3.2E-7	LOW- 0.011	LOW- 0.037	LOW- 7.4E-4
FHL2	LOW	HIGH	LOW- 1.7E-10	LOW- 0.001	LOW- 1.8E-16	LOW- 3.7E-6	LOW- 2.4E-14	LOW- 3.5E-18
SCA1	LOW	HIGH	NOCHANGE -0.147	LOW- 0.007	LOW- 4.6E-4	NOCHANGE -0.893	LOW- 7.6E-5	LOW- 0.001
IGFBP7	LOW	HIGH	NOCHANGE - 0.056	NOCHANGE- 0.375	NOCHANGE- 0.335	LOW- 0.038	LOW- 0.001	LOW- 2.1E-5
HSBP3	LOW	HIGH	N/A	N/A	N/A	LOW- 0.012	LOW- 0.027	LOW- 4.6E-4
CDH12	HIGH	LOW	N/A	N/A	N/A	HIGH- 1E-4	HIGH- 7E-15	HIGH- #
IL8	LOW	HIGH	NOCHANGE - 0.215	LOW- 0.009	LOW- 0.003	N/A	N/A	N/A
SSX2	HIGH	LOW	N/A	N/A	N/A	NOCHANGE -0.686	HIGH- 0.009	HIGH- 2E-4
SSX3	HIGH	LOW	N/A	N/A	N/A	NOCHANGE -0.389	HIGH- 0.013	HIGH- 0.004
FCGRT	HIGH	LOW	LOW- 1E-5	NOCHANGE- 0.133	HIGH- 0.008	LOW- 3.2E-4	LOW- 7.9E-9	LOW- 3.3E-14
PDGFA	LOW	HIGH	HIGH-0.044	NOCHANGE- 0.105	NOCHANGE- 0.748	NOCHANGE -0.059	NOCHANGE- 0.016	NOCHANGE- 0.665
PP1R1A	HIGH	LOW	N/A	N/A	N/A	LOW- 0.046	NOCHANGE- 0.075	NOCHANGE- 0.65
GLI	HIGH	LOW	NOCHANGE -0.172	NOCHANGE- 0.541	NOCHANGE- 0.366	NOCHANGE -0.788	LOW- 5.2E-4	LOW- 3E-4
SERPINE1	LOW	HIGH	NOCHANGE - 0.106	NOCHANGE- 0.444	NOCHANGE- 0.382	NOCHANGE – 0.33&	HIGH- 0.047	HIGH- 0.014

Table App2.1 - Direction of gene expression is indicated in each box. Grey Shading indicates concurrence between Ewings sarcoma expression data and that of prostate cancer. Where data available, a p value of 0.05 considered significant. N/A – Not analysed in dataset. E= Exponential. HIGH-Upregulated. LOW-Downregulated. NOCHANGE- No change by above significance criteria. N= Normal prostate L= Localised disease LND = Lymph Node Disease M = Metastatic Disease #=Data point missing in database

Preliminary studies investigating *in vitro* sensitivity of prostate cancer cell lines to explore our hypothesis were carried out in Dr Jongstra's laboratory. We used a SulphoRhodamine B (SRB) assay to determine the potency of Ara-C to inhibit growth of three prostate cancer cell lines, DU-145, PC3 and 22rv1 (Unfortunately, after these experiments were carried out, it became apparent that none of these cell lines are known to possess the ERG fusion gene). The method is suitable for routine and very large-scale applications (616) and was carried out in standard fashion in 96 well plates. The results of 3 independent experiments are shown in Figure

App2.1A. Ara-C inhibits growth of PC3 and 22Rv1 cells with IC50 values of ~ 400 nM and of DU-145 cells with an IC50 of ~ 200 nM. To provide a comparison with other widely used anti-cancer agents the IC50s of doxorubicin and cisplatin were determined for growth inhibition of DU-145 cells (not shown). In agreement with published results we found IC50s for doxorubicin and cisplatin of 20 nM and 4 mM respectively. Mean plasma levels that can be achieved following an Ara-C dose of $2g/m^2$ decrease in a logarithmic fashion after infusion but remain above 1μM for the first 160 minutes post infusion (617). Thus levels of Ara-C that cause growth inhibition are likely to be achievable *in vivo*.

To determine the efficacy of Ara-C on cell survival, a standard clonogenic assay was performed with colony formation evaluated in 6-well plates. Results were compared with those for doxorubicin and cisplatin. Cells were treated with 0.25 uM Ara-C, 20 nM doxorubicin and 4 mM cisplatin. These concentrations are close to the IC50s for growth inhibition as determined in SRB assays described above. Fig.App2.1B shows that Ara-C inhibits clonogenic cell growth by > 100-fold. In contrast doxorubicin and cisplatin lowered the surviving fraction by only ~ 20 – 30 %. These results identify Ara-C as a potent inhibitor of growth of prostate cancer cell lines and an inhibitor of cell survival at clinically achievable doses.

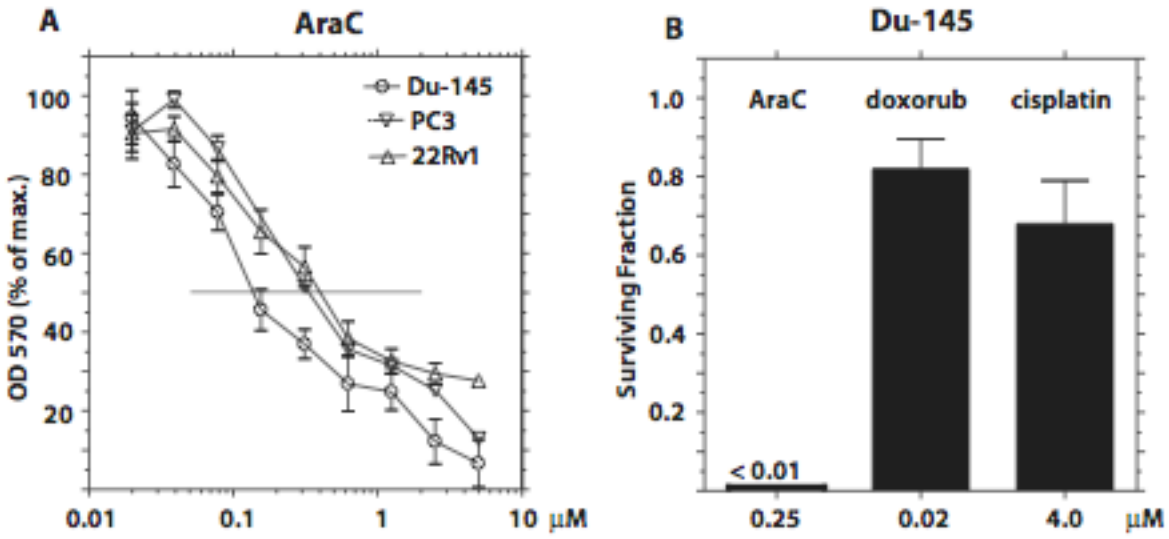

Figure App2.1. AraC Inhibits growth and clonogenicity of prostate cancer cell lines.A, growth inhibition of DU-145, PC3 and 22Rv1 cells by AraC using a SRB based assay. Cells were treated in 96-well plates for 72 hrs with AraC and the results of the SRB assay was expressed as the OD570 as a % of the OD570 determined from untreated control wells. The 50 % growth inhibition is indicated with a thin horizontal line. B, clonogenic activity of Arac, doxorubicin and cisplatin on DU-145 cells. Cells were plated in 6-well plates and treated with compound at a concentration corresponding to their respective IC50 values for growth inhibition on DU-145 cells as determined in SRB assays (results for doxorubicin and cisplatin not shown).

Finally, on review of the literature, there has been one man who has received Ara-C for metastatic prostate cancer during the course of treatment for ALL (618). He received 3 cycles of hyper-CVAD for his leukemia and his serum PSA was recorded. Coinciding with the administration of Ara-C in the second cycle his PSA fell precipitously (Figure APP 2.2) and at autopsy no metastases could be detected. The dose of Ara-C in Hyper-CVAD is $3g/m^2$ bid for 4 doses.

Thus the rationale for this proposal includes: (i) An extension of microarray signature work from Ewings sarcoma that suggests activity of Ara-C in malignancies with expression abnormalities in the ETS family of transcription factors. (ii) The existence of overlapping pathways of FLI1 and ERG overexpression in tumours (ii) Preliminary data that suggest potent activity of Ara-C in prostate cancer cell lines at concentrations likely to be achievable in vivo. (iii) A case report that indicates activity for high-dose Ara-C against HRPC in a patient who also had leukemia (iv) Xenograft studies suggesting the increased FLI1 expression in advanced HR CaP suggesting a more direct effect of Ara-C on inhibiting resulting transcriptional pathways (v) An unmet need for effective 2^{nd} line chemotherapy for men with HRPC since only 1^{st} line docetaxel has been shown to improve survival.

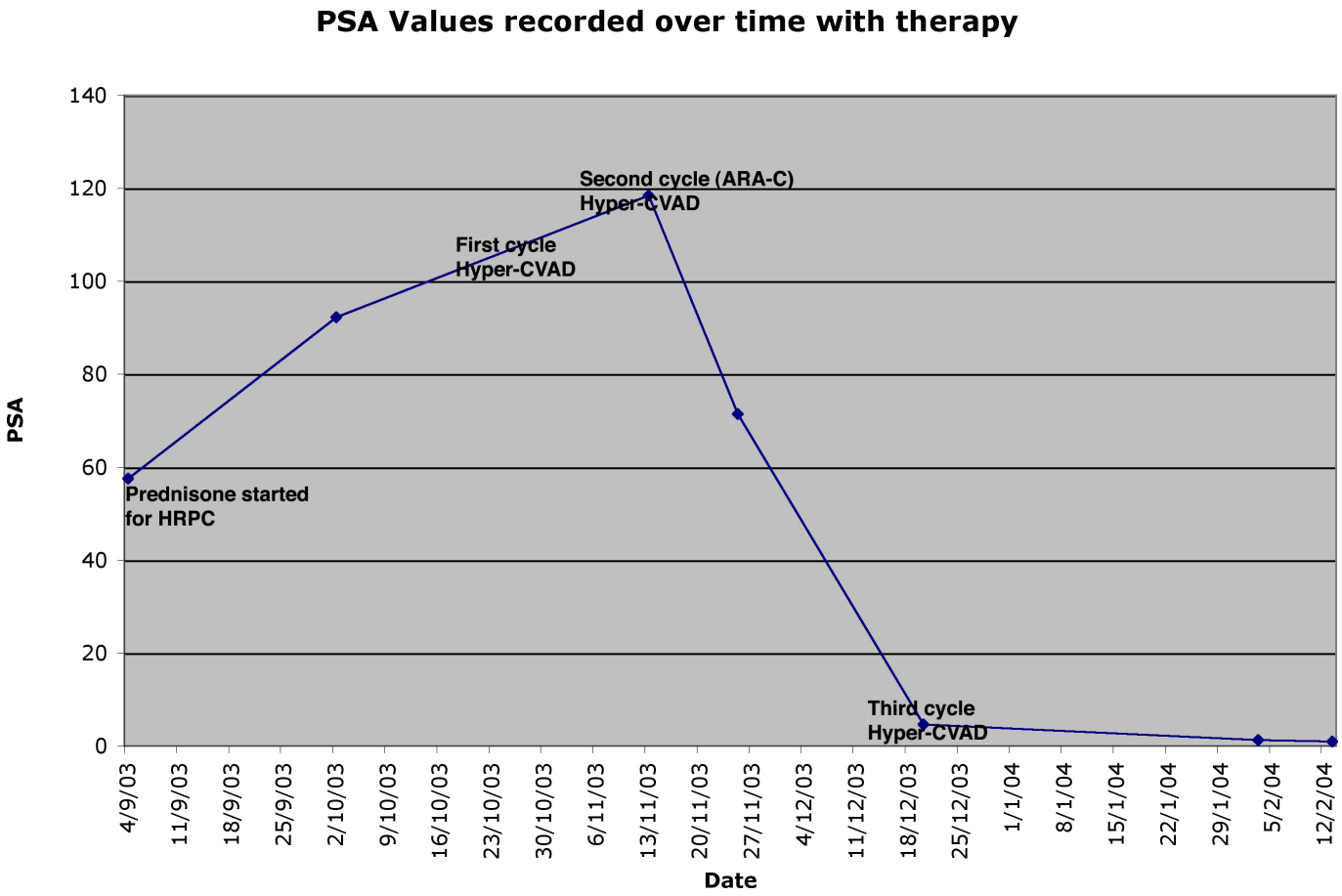

Figure App 2.2. Serum PSA levels from Gandhok *et al*., showing a fall in PSA coinciding with the administration of cytarabine with the second cycle of Hyper-CVAD for a patient suffering from both leukemia and hormone refractory prostate cancer

APP 2.4 Clinical trial Design and Methods

APP 2.4.1 Overview

Clinically, we are carrying out a phase 2 trial of Ara-C in men with metastatic hormone refractory prostate cancer (HRPC) who have progressed after first line therapy with docetaxel. The translational component of this work involves determination of the patients' status as *TMPRSS2-ETS* translocation carriers from analysis of their paraffin –embedded biopsies or radical proctatectomy sections and then the association between response and gene fusion status. The primary clinical endpoint of the study is PSA response (619) following Ara-C treatment. The secondary clinical endpoint is PSA progression free survival. The primary molecular endpoint is the association between the presence of FISH detected fusion transcripts and PSA response whilst the secondary endpoint is the relationship between levels of ETS transcripts in relation to PSA response.

An *a priori* hypothesis is that responses are more likely to occur in men with ETS translocations, although our preliminary data suggest that Ara-C might be active against prostate cancer cells without ETS translocations. Current estimates are that such translocations are present in 70% of men with prostate cancer. A PSA response rate of 30% among men with ETS translocations (response rate of 20% overall) would be regarded as clinically relevant and sufficient to proceed to further investigation of this agent.

Initial studies of high-dose Ara-C in leukemia examined dosing levels. No grade 3 or 4 toxicity was noted in 2 patients receiving the $3g/m^2$ dose in the absence of any additional chemotherapy (620). Nevertheless, this dose is likely to be profoundly immunosuppressive in a population of elderly men, many of whom may have limited marrow reserve due to previous chemotherapy and bony metastases. Additionally, an important side-effect of high-dose Ara-C is cerebral toxicity characterized by obtundation, somnolence and headache. Risk factors for this

include the age of the patient, dose of Ara-C and renal function (620).Thus a starting dose of 1g/m^2 increasing to 1.5 g/m2 every 12 hours for 4 doses is likely to be better tolerated than the traditional leukemic doses, and would offer an adequate therapeutic window with adequate serum levels to assess the response of men to this regimen.

In order to minimize the number of patients treated in the event that this regimen proves to be disappointing, a classical two stage Phase 2 "Fleming" design will be used. Only extreme results indicating poor efficacy will result in early study termination. If such extreme results are not observed, a maximum of 30 patients will be studied. This regimen will be assumed to be inactive if the PSA-response rate is at most 5% and potentially active if it is at least 20%. Therefore, we set P0 = 0.05 and P1= 0.20. In stage I we will accrue 15 evaluable patients; if at least 1 evaluable patient has a PSA-response, we will proceed to stage II and accrue an additional 15 evaluable patients. If 4 or more of the 30 evaluable patients have a PSA-response, the treatment will be deemed potentially active. If 3 or less of the 30 evaluable patients have a PSA-response, the treatment will be deemed inactive and uninteresting for further study. The true alpha using this design is 0.058 and the true beta is 0.135. The probability of stopping after the first stage is 0.463 if the treatment is inactive (i.e. true PSA-response rate is 0.05). The trial plans to accrue about 2 patients per month, and is thus expected to complete accrual in 15-18 months.

APP 2.4.2 Response Criteria

Criteria of PSA response will be as proposed by the recent Consensus group (619). Briefly, PSA progression free survival is defined as the time between randomization and the date of PSA progression or the date of death due to prostate cancer, whichever occurs first (with the caveat that early increases in PSA within the first 12 weeks are ignored if followed by subsequent decline). Patients are assessed by baseline CT of the abdomen and pelvis, and if measurable

disease is present, this is repeated after every 3rd cycle and on completion of study. Response is evaluated by RECIST criteria (621). The RECIST criteria are a simplified and conservative mechanism to extract of imaging data for wide application in clinical trials. They presume that linear measures are an adequate substitute for 2-D methods and registers four response categories; CR (complete response, disappearance of all target lesions), PR (partial response, 30% decrease in the sum of the longest diameter of target lesions), PD (progressive disease, 20% increase in the sum of the longest diameter of target lesions) and SD (stable disease, small changes that do not meet above criteria).

APP 2.4.3 Translational Components

The Squire laboratory has demonstrated the ability of tri-color fluorescence in-situ hybridization (FISH) to detect *TMPRSS2-ERG* translocations in clinically accessible archived prostate tissue. The generation and validation of PCR primers to detect the transcript in blood is in progress in limiting dilutions of VCaP cells. Other groups have reported the PCR-based detection of the transcript in urine suggesting the feasibility of this approach. Several approaches will be evaluated to increase the success of RT-PCR if needed.

The primary molecular endpoint of this phase 2 study will be the association between the PSA response and the presence of a fusion transcript detected by FISH on the patient biopsy or prostatectomy sections as determined by chi-squared analysis. Further logistic regression analysis for associations between % PSA reduction and the presence of a fusion transcript will also be carried out. Comparison between groups with and without the fusion gene with their PSA response rate will also be carried out with a student t-test. Secondary endpoints will be a linear regression analyses to seek any association between the levels of the fusion transcript detected in the blood (Taqman $\Delta\Delta$CT method) and PSA response, logistic regression to determine the association between response and presence of various levels of fusion transcripts

in the blood and an examination of any association between subsequent androgen response and the presence of the fusion genes.

APP 2.5 Results

To date, 6 patients have been enrolled, with a median age of 72 (range 53-74), median baseline PSA of 160 (range 85-2992), median Gleason score 8.5 (range 6-9), median performance status 1 (range 0-2). All patients have completed 2-3 cycles of treatment and have been removed from the study. Reasons for removal from the study protocol include; Progressive disease (3), Grade 4 neutropenia (1), Grade 3 thrombocytopenia (1), recurrent Grade 2 anaemia (1). Median time on study is 70 days (range 56-86 days).

Generally, patients have demonstrated an increase in their PSA from baseline (median PSA rise 210% from baseline). Given the absence of third-line prostate clinical trials, patients were generally treated with tertiary hormonal manipulations upon exit from the trial. Two patients achieved a PSA nadir after approximately 90 days of hormone treatment. These nadirs have been 0.16% and 14% of the baseline PSA at entry; two further patients have a falling PSA, but have not reached a nadir, with one currently at 63% of entry PSA and another at 124% of baseline PSA. Another patient has experienced grade 4 thrombocytopenia from either diethylstilboestrol or disease progression in the post trial period.

FISH has not yet been carried out on the patient's original tumour samples. Blood for mRNA analysis has been collected and stored, but not yet subjected to RT-PCR.

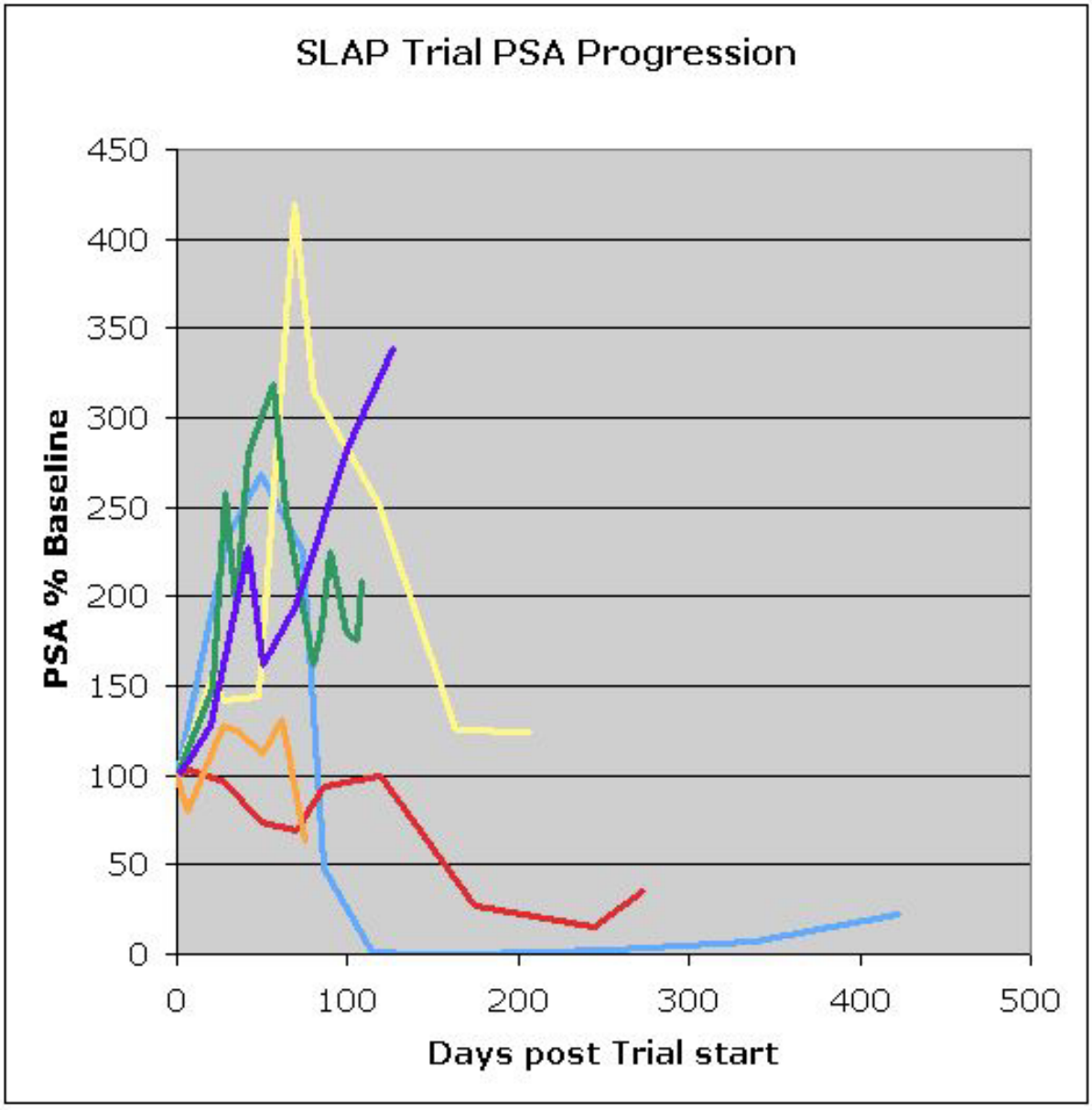

Figure App 2.3 PSA progression graph for patients participating in the study of cytarabine for hormone refractory metastatic prostate cancer. Chart represents % PSA change from baseline at entry and PSA followed on 1 line of anti-hormonal treatment post trial. Data ends at commencement of 2nd therapy (1 patient), last PSA measurement (4 patients) or transfer to palliative care (1 patient). Patients were commenced on anti-hormonal treatment they had not had previously including ketoconazole, nilutamide and DES.

APP 2.6 Discussion

Whilst the primary therapy seems not to be active, the profound fall in the PSA with hormone treatment post cytarabine might suggest a reinduction of hormone sensitivity in these patients. Such a hypothesis is supported by laboratory data suggesting a differentiation effect of ETS family knockdown in prostate cell line models (186, 187). The ultimate effect of the ETS related fusion events might relate to the balance of ETS acting transcription factors in the cell. The role of the PDEF and ESE-3 and tumour suppressing ETS transcription factors may be relevant (see section 1.6.3.1.1).

A small molecule that targets ERG, the most commonly dysregulated member of the ETS family might be the most efficacious course to target this fusion gene. However, there are a number of drawbacks to this approach; (1) ERG has been recently identified as essential for definitive hematopoiesis and the function of adult hematopoietic stem cells (622). (2) Whether the *TMPRSS2-ERG* protein is produced in advanced hormone-refractory metastatic disease given its androgen regulation is unclear and will await the validation of immunohistochemical approaches. (3) The approach would only target a subset of the tumours in which there is ETS dysregulation.

Alternatively, there may be a reciprocal balance between pro- and anti-oncogenic ETS factors in the progression to carcinogenesis (506). Therefore, an approach to avoid the disadvantages above is to reduce one of the oncogenic ETS proteins in an effort to restore this balance. FLI1 is an ideal candidate for this given both the xenograft work suggesting it is upregulated in hormone refractory disease (165) and an existing mechanism to reduce its protein level using existing therapeutics (610).

In conclusion, although patients receiving cytarabine in this phase 2 protocol have demonstrated PSA progression, an encouraging trend to increased hormone responsiveness has been observed (50% of patients demonstrating PSAs below baseline) after protocol cessation that might reflect the effects of treatment.

We will continue to enrol patients to this protocol as per the statistical design and will complete the translational component of the research. We will also evaluate the mechanism of the putative increased hormone responsiveness in *in vitro* and *in vivo* models.

REFERENCES

1. Canadian Cancer Society & National Cancer Institute of Canada Canadian Cancer Statistics 2008. Canadian Cancer Society & National Cancer Institute of Canada, 2007.
2. The American Cancer Society Cancer Facts and Figures, 2008. The American Cancer Society, 2007.
3. Jemal, A., Siegel, R., Ward, E., Hao, Y., Xu, J., Murray, T., and Thun, M. J. Cancer statistics, 2008. CA Cancer J Clin, *58:* 71-96, 2008.
4. Isaacs, J. T. and Coffey, D. S. Etiology and disease process of benign prostatic hyperplasia. Prostate Suppl, *2:* 33-50, 1989.
5. Ziada, A., Rosenblum, M., and Crawford, E. D. Benign prostatic hyperplasia: an overview. Urology, *53:* 1-6, 1999.
6. McNeal, J. E., Redwine, E. A., Freiha, F. S., and Stamey, T. A. Zonal distribution of prostatic adenocarcinoma. Correlation with histologic pattern and direction of spread. Am J Surg Pathol, *12:* 897-906, 1988.
7. Qian, J., Wollan, P., and Bostwick, D. G. The extent and multicentricity of high-grade prostatic intraepithelial neoplasia in clinically localized prostatic adenocarcinoma. Hum Pathol, *28:* 143-148, 1997.
8. Sakr, W. A., Grignon, D. J., Crissman, J. D., Heilbrun, L. K., Cassin, B. J., Pontes, J. J., and Haas, G. P. High grade prostatic intraepithelial neoplasia (HGPIN) and prostatic adenocarcinoma between the ages of 20-69: an autopsy study of 249 cases. In Vivo, *8:* 439-443, 1994.
9. Sakr, W. A., Haas, G. P., Cassin, B. F., Pontes, J. E., and Crissman, J. D. The frequency of carcinoma and intraepithelial neoplasia of the prostate in young male patients. J Urol, *150:* 379-385, 1993.
10. Beheshti, B., Vukovic, B., Marrano, P., Squire, J. A., and Park, P. C. Resolution of genotypic heterogeneity in prostate tumors using polymerase chain reaction and comparative genomic hybridization on microdissected carcinoma and prostatic intraepithelial neoplasia foci. Cancer Genet Cytogenet, *137:* 15-22, 2002.
11. Bostwick, D. G. and Qian, J. High-grade prostatic intraepithelial neoplasia. Mod Pathol, *17:* 360-379, 2004.
12. Qian, J. and Bostwick, D. G. The extent and zonal location of prostatic intraepithelial neoplasia and atypical adenomatous hyperplasia: relationship with carcinoma in radical prostatectomy specimens. Pathol Res Pract, *191:* 860-867, 1995.
13. Bishara, T., Ramnani, D. M., and Epstein, J. I. High-grade prostatic intraepithelial neoplasia on needle biopsy: risk of cancer on repeat biopsy related to number of involved cores and morphologic pattern. Am J Surg Pathol, *28:* 629-633, 2004.
14. Kronz, J. D., Allan, C. H., Shaikh, A. A., and Epstein, J. I. Predicting cancer following a diagnosis of high-grade prostatic intraepithelial neoplasia on needle biopsy: data on men with more than one follow-up biopsy. Am J Surg Pathol, *25:* 1079-1085, 2001.
15. Sakr, W. A. and Partin, A. W. Histological markers of risk and the role of high-grade prostatic intraepithelial neoplasia. Urology, *57:* 115-120, 2001.
16. Bostwick, D. G., Montironi, R., and Sesterhenn, I. A. Diagnosis of prostatic intraepithelial neoplasia: Prostate Working Group/consensus report. Scand J Urol Nephrol Suppl*:* 3-10, 2000.
17. Nupponen, N. N. and Visakorpi, T. Molecular cytogenetics of prostate cancer. Microsc Res Tech, *51:* 456-463, 2000.

18. Hughes, S., Yoshimoto, M., Beheshti, B., Houlston, R. S., Squire, J. A., and Evans, A. The use of whole genome amplification to study chromosomal changes in prostate cancer: insights into genome-wide signature of preneoplasia associated with cancer progression. BMC Genomics, *7:* 65, 2006.
19. Tomlins, S. A., Mehra, R., Rhodes, D. R., Cao, X., Wang, L., Dhanasekaran, S. M., Kalyana-Sundaram, S., Wei, J. T., Rubin, M. A., Pienta, K. J., Shah, R. B., and Chinnaiyan, A. M. Integrative molecular concept modeling of prostate cancer progression. Nat Genet, *39:* 41-51, 2007.
20. Ruska, K. M., Sauvageot, J., and Epstein, J. I. Histology and cellular kinetics of prostatic atrophy. Am J Surg Pathol, *22:* 1073-1077, 1998.
21. Cheville, J. C. and Bostwick, D. G. Postatrophic hyperplasia of the prostate. A histologic mimic of prostatic adenocarcinoma. Am J Surg Pathol, *19:* 1068-1076, 1995.
22. De Marzo, A. M., Platz, E. A., Sutcliffe, S., Xu, J., Gronberg, H., Drake, C. G., Nakai, Y., Isaacs, W. B., and Nelson, W. G. Inflammation in prostate carcinogenesis. Nat Rev Cancer, *7:* 256-269, 2007.
23. De Marzo, A. M., DeWeese, T. L., Platz, E. A., Meeker, A. K., Nakayama, M., Epstein, J. I., Isaacs, W. B., and Nelson, W. G. Pathological and molecular mechanisms of prostate carcinogenesis: implications for diagnosis, detection, prevention, and treatment. J Cell Biochem, *91:* 459-477, 2004.
24. Anton, R. C., Kattan, M. W., Chakraborty, S., and Wheeler, T. M. Postatrophic hyperplasia of the prostate: lack of association with prostate cancer. Am J Surg Pathol, *23:* 932-936, 1999.
25. Billis, A. Prostatic atrophy: an autopsy study of a histologic mimic of adenocarcinoma. Mod Pathol, *11:* 47-54, 1998.
26. Billis, A. and Magna, L. A. Inflammatory atrophy of the prostate. Prevalence and significance. Arch Pathol Lab Med, *127:* 840-844, 2003.
27. Putzi, M. J. and De Marzo, A. M. Morphologic transitions between proliferative inflammatory atrophy and high-grade prostatic intraepithelial neoplasia. Urology, *56:* 828-832, 2000.
28. Franks, L. M. Atrophy and hyperplasia in the prostate proper. J Pathol Bacteriol, *68:* 617-621, 1954.
29. Liavag, I. The localization of prostatic carcinoma. An autopsy study. Scand J Urol Nephrol, *2:* 65-71, 1968.
30. Faith, D., Han, S., Lee, D. K., Friedl, A., Hicks, J. L., De Marzo, A. M., and Jarrard, D. F. p16 Is upregulated in proliferative inflammatory atrophy of the prostate. Prostate, *65:* 73-82, 2005.
31. Nakayama, M., Bennett, C. J., Hicks, J. L., Epstein, J. I., Platz, E. A., Nelson, W. G., and De Marzo, A. M. Hypermethylation of the human glutathione S-transferase-pi gene (GSTP1) CpG island is present in a subset of proliferative inflammatory atrophy lesions but not in normal or hyperplastic epithelium of the prostate: a detailed study using laser-capture microdissection. Am J Pathol, *163:* 923-933, 2003.
32. Parsons, J. K., Nelson, C. P., Gage, W. R., Nelson, W. G., Kensler, T. W., and De Marzo, A. M. GSTA1 expression in normal, preneoplastic, and neoplastic human prostate tissue. Prostate, *49:* 30-37, 2001.
33. Zha, S., Gage, W. R., Sauvageot, J., Saria, E. A., Putzi, M. J., Ewing, C. M., Faith, D. A., Nelson, W. G., De Marzo, A. M., and Isaacs, W. B. Cyclooxygenase-2 is up-regulated in proliferative inflammatory atrophy of the prostate, but not in prostate carcinoma. Cancer Res, *61:* 8617-8623, 2001.

34. Bethel, C. R., Faith, D., Li, X., Guan, B., Hicks, J. L., Lan, F., Jenkins, R. B., Bieberich, C. J., and De Marzo, A. M. Decreased NKX3.1 protein expression in focal prostatic atrophy, prostatic intraepithelial neoplasia, and adenocarcinoma: association with gleason score and chromosome 8p deletion. Cancer Res, *66:* 10683-10690, 2006.
35. Shah, R., Mucci, N. R., Amin, A., Macoska, J. A., and Rubin, M. A. Postatrophic hyperplasia of the prostate gland: neoplastic precursor or innocent bystander? Am J Pathol, *158:* 1767-1773, 2001.
36. De Marzo, A. M., Marchi, V. L., Epstein, J. I., and Nelson, W. G. Proliferative inflammatory atrophy of the prostate: implications for prostatic carcinogenesis. Am J Pathol, *155:* 1985-1992, 1999.
37. De Marzo, A. M., Smearman, E., Meeker, A. K., and Iwata, T. Telomere Shortening in Prostate Atrophy Lesions. American Urological Association. Anaheim, California, 2007.
38. Slaughter, D. P., Southwick, H. W., and Smejkal, W. Field cancerization in oral stratified squamous epithelium; clinical implications of multicentric origin. Cancer, *6:* 963-968, 1953.
39. Garcia, S. B., Park, H. S., Novelli, M., and Wright, N. A. Field cancerization, clonality, and epithelial stem cells: the spread of mutated clones in epithelial sheets. J Pathol, *187:* 61-81, 1999.
40. Braakhuis, B. J., Tabor, M. P., Kummer, J. A., Leemans, C. R., and Brakenhoff, R. H. A genetic explanation of Slaughter's concept of field cancerization: evidence and clinical implications. Cancer Res, *63:* 1727-1730, 2003.
41. Villers, A., McNeal, J. E., Freiha, F. S., and Stamey, T. A. Multiple cancers in the prostate. Morphologic features of clinically recognized versus incidental tumors. Cancer, *70:* 2313-2318, 1992.
42. Greene, D. R., Wheeler, T. M., Egawa, S., Dunn, J. K., and Scardino, P. T. A comparison of the morphological features of cancer arising in the transition zone and in the peripheral zone of the prostate. J Urol, *146:* 1069-1076, 1991.
43. Bostwick, D. G., Shan, A., Qian, J., Darson, M., Maihle, N. J., Jenkins, R. B., and Cheng, L. Independent origin of multiple foci of prostatic intraepithelial neoplasia: comparison with matched foci of prostate carcinoma. Cancer, *83:* 1995-2002, 1998.
44. Ruijter, E. T., Miller, G. J., van de Kaa, C. A., van Bokhoven, A., Bussemakers, M. J., Debruyne, F. M., Ruiter, D. J., and Schalken, J. A. Molecular analysis of multifocal prostate cancer lesions. J Pathol, *188:* 271-277, 1999.
45. Macintosh, C. A., Stower, M., Reid, N., and Maitland, N. J. Precise microdissection of human prostate cancers reveals genotypic heterogeneity. Cancer Res, *58:* 23-28, 1998.
46. Cheng, L., Song, S. Y., Pretlow, T. G., Abdul-Karim, F. W., Kung, H. J., Dawson, D. V., Park, W. S., Moon, Y. W., Tsai, M. L., Linehan, W. M., Emmert-Buck, M. R., Liotta, L. A., and Zhuang, Z. Evidence of independent origin of multiple tumors from patients with prostate cancer. J Natl Cancer Inst, *90:* 233-237, 1998.
47. Gao, C., Furusato, B., McLeod, D. G., Srivastava, S., Petrovics, G., and Sesterhenn, I. A. Mapping of TMPRSS2-ERG fusion in Multi-Focal Prostate Cancer. American Urological Association. Anaheim, California, 2007.
48. Mehra, R., Han, B., Tomlins, S. A., Wang, L., Menon, A., Wasco, M. J., Shen, R., Montie, J. E., Chinnaiyan, A. M., and Shah, R. B. Heterogeneity of TMPRSS2 Gene Rearrangements in Multifocal Prostate Adenocarcinoma: Molecular Evidence for an Independent Group of Diseases. Cancer Res, *67:* 7991-7995, 2007.
49. Yu, Y. P., Landsittel, D., Jing, L., Nelson, J., Ren, B., Liu, L., McDonald, C., Thomas, R., Dhir, R., Finkelstein, S., Michalopoulos, G., Becich, M., and Luo, J. H. Gene

expression alterations in prostate cancer predicting tumor aggression and preceding development of malignancy. J Clin Oncol, *22:* 2790-2799, 2004.
50. Ananthanarayanan, V., Deaton, R. J., Yang, X. J., Pins, M. R., and Gann, P. H. Alpha-methylacyl-CoA racemase (AMACR) expression in normal prostatic glands and high-grade prostatic intraepithelial neoplasia (HGPIN): association with diagnosis of prostate cancer. Prostate, *63:* 341-346, 2005.
51. Dhir, R., Vietmeier, B., Arlotti, J., Acquafondata, M., Landsittel, D., Masterson, R., and Getzenberg, R. H. Early identification of individuals with prostate cancer in negative biopsies. J Urol, *171:* 1419-1423, 2004.
52. Ayala, G., Thompson, T., Yang, G., Frolov, A., Li, R., Scardino, P., Ohori, M., Wheeler, T., and Harper, W. High levels of phosphorylated form of Akt-1 in prostate cancer and non-neoplastic prostate tissues are strong predictors of biochemical recurrence. Clin Cancer Res, *10:* 6572-6578, 2004.
53. Montironi, R., Hamilton, P. W., Scarpelli, M., Thompson, D., and Bartels, P. H. Subtle morphological and molecular changes in normal-looking epithelium in prostates with prostatic intraepithelial neoplasia or cancer. Eur Urol, *35:* 468-473, 1999.
54. Ananthanarayanan, V., Deaton, R. J., Yang, X. J., Pins, M. R., and Gann, P. H. Alteration of proliferation and apoptotic markers in normal and premalignant tissue associated with prostate cancer. BMC Cancer, *6:* 73, 2006.
55. Bartels, P. H., da Silva, V. D., Montironi, R., Hamilton, P. W., Thompson, D., Vaught, L., and Bartels, H. G. Chromatin texture signatures in nuclei from prostate lesions. Anal Quant Cytol Histol, *20:* 407-416, 1998.
56. Hanson, J. A., Gillespie, J. W., Grover, A., Tangrea, M. A., Chuaqui, R. F., Emmert-Buck, M. R., Tangrea, J. A., Libutti, S. K., Linehan, W. M., and Woodson, K. G. Gene promoter methylation in prostate tumor-associated stromal cells. J Natl Cancer Inst, *98:* 255-261, 2006.
57. Cavalieri, E. L., Devanesan, P., Bosland, M. C., Badawi, A. F., and Rogan, E. G. Catechol estrogen metabolites and conjugates in different regions of the prostate of Noble rats treated with 4-hydroxyestradiol: implications for estrogen-induced initiation of prostate cancer. Carcinogenesis, *23:* 329-333, 2002.
58. Laczko, I., Hudson, D. L., Freeman, A., Feneley, M. R., and Masters, J. R. Comparison of the zones of the human prostate with the seminal vesicle: morphology, immunohistochemistry, and cell kinetics. Prostate, *62:* 260-266, 2005.
59. Pardal, R., Clarke, M. F., and Morrison, S. J. Applying the principles of stem-cell biology to cancer. Nat Rev Cancer, *3:* 895-902, 2003.
60. Clarke, M. F. and Fuller, M. Stem cells and cancer: two faces of eve. Cell, *124:* 1111-1115, 2006.
61. Cohnheim, J. Ueber entzundung und eiterung. Path. Anat. Physiol. Klin. Med., *40:* 1-79, 1867.
62. Virchow, R. Editorial. Virchows Arch. Pathol. Anat. Physiol. Klin. Med., *3*, 1855.
63. Till, J. E. and Mc, C. E. A direct measurement of the radiation sensitivity of normal mouse bone marrow cells. Radiat Res, *14:* 213-222, 1961.
64. Bonnet, D. and Dick, J. E. Human acute myeloid leukemia is organized as a hierarchy that originates from a primitive hematopoietic cell. Nat Med, *3:* 730-737, 1997.
65. Al-Hajj, M., Wicha, M. S., Benito-Hernandez, A., Morrison, S. J., and Clarke, M. F. Prospective identification of tumorigenic breast cancer cells. Proc Natl Acad Sci U S A, *100:* 3983-3988, 2003.

66. Singh, S. K., Clarke, I. D., Terasaki, M., Bonn, V. E., Hawkins, C., Squire, J., and Dirks, P. B. Identification of a cancer stem cell in human brain tumors. Cancer Res, *63:* 5821-5828, 2003.
67. Singh, S. K., Hawkins, C., Clarke, I. D., Squire, J. A., Bayani, J., Hide, T., Henkelman, R. M., Cusimano, M. D., and Dirks, P. B. Identification of human brain tumour initiating cells. Nature, *432:* 396-401, 2004.
68. O'Brien, C. A., Pollett, A., Gallinger, S., and Dick, J. E. A human colon cancer cell capable of initiating tumour growth in immunodeficient mice. Nature, *445:* 106-110, 2007.
69. Tang, D. G., Patrawala, L., Calhoun, T., Bhatia, B., Choy, G., Schneider-Broussard, R., and Jeter, C. Prostate cancer stem/progenitor cells: identification, characterization, and implications. Mol Carcinog, *46:* 1-14, 2007.
70. Leong, K. G., Wang, B. E., Johnson, L., and Gao, W. Q. Generation of a prostate from a single adult stem cell. Nature, *456:* 804-808, 2008.
71. Lawson, D. A. and Witte, O. N. Stem cells in prostate cancer initiation and progression. J Clin Invest, *117:* 2044-2050, 2007.
72. Collins, A. T. and Maitland, N. J. Prostate cancer stem cells. Eur J Cancer, *42:* 1213-1218, 2006.
73. Maitland, N. J. and Collins, A. A tumour stem cell hypothesis for the origins of prostate cancer. BJU Int, *96:* 1219-1223, 2005.
74. Taipale, J. and Beachy, P. A. The Hedgehog and Wnt signalling pathways in cancer. Nature, *411:* 349-354, 2001.
75. Liu, S., Dontu, G., and Wicha, M. S. Mammary stem cells, self-renewal pathways, and carcinogenesis. Breast Cancer Res, *7:* 86-95, 2005.
76. Glinsky, G. V., Berezovska, O., and Glinskii, A. B. Microarray analysis identifies a death-from-cancer signature predicting therapy failure in patients with multiple types of cancer. J Clin Invest, *115:* 1503-1521, 2005.
77. Verras, M. and Sun, Z. Roles and regulation of Wnt signaling and beta-catenin in prostate cancer. Cancer Lett, *237:* 22-32, 2006.
78. Thiyagarajan, S., Bhatia, N., Reagan-Shaw, S., Cozma, D., Thomas-Tikhonenko, A., Ahmad, N., and Spiegelman, V. S. Role of GLI2 transcription factor in growth and tumorigenicity of prostate cells. Cancer Res, *67:* 10642-10646, 2007.
79. Kasper, M., Regl, G., Frischauf, A. M., and Aberger, F. GLI transcription factors: mediators of oncogenic Hedgehog signalling. Eur J Cancer, *42:* 437-445, 2006.
80. Barnett, D. H., Huang, H. Y., Wu, X. R., Laciak, R., Shapiro, E., and Bushman, W. The human prostate expresses sonic hedgehog during fetal development. J Urol, *168:* 2206-2210, 2002.
81. Fan, L., Pepicelli, C. V., Dibble, C. C., Catbagan, W., Zarycki, J. L., Laciak, R., Gipp, J., Shaw, A., Lamm, M. L., Munoz, A., Lipinski, R., Thrasher, J. B., and Bushman, W. Hedgehog signaling promotes prostate xenograft tumor growth. Endocrinology, *145:* 3961-3970, 2004.
82. Sanchez, P., Hernandez, A. M., Stecca, B., Kahler, A. J., DeGueme, A. M., Barrett, A., Beyna, M., Datta, M. W., Datta, S., and Ruiz i Altaba, A. Inhibition of prostate cancer proliferation by interference with SONIC HEDGEHOG-GLI1 signaling. Proc Natl Acad Sci U S A, *101:* 12561-12566, 2004.
83. Wang, B. E., Shou, J., Ross, S., Koeppen, H., De Sauvage, F. J., and Gao, W. Q. Inhibition of epithelial ductal branching in the prostate by sonic hedgehog is indirectly mediated by stromal cells. J Biol Chem, *278:* 18506-18513, 2003.

84. Karhadkar, S. S., Bova, G. S., Abdallah, N., Dhara, S., Gardner, D., Maitra, A., Isaacs, J. T., Berman, D. M., and Beachy, P. A. Hedgehog signalling in prostate regeneration, neoplasia and metastasis. Nature, *431:* 707-712, 2004.
85. Shaw, A. and Bushman, W. Hedgehog signaling in the prostate. J Urol, *177:* 832-838, 2007.
86. Yauch, R. L., Gould, S. E., Scales, S. J., Tang, T., Tian, H., Ahn, C. P., Marshall, D., Fu, L., Januario, T., Kallop, D., Nannini-Pepe, M., Kotkow, K., Marsters, J. C., Rubin, L. L., and de Sauvage, F. J. A paracrine requirement for hedgehog signalling in cancer. Nature, *455:* 406-410, 2008.
87. Sheng, T., Li, C., Zhang, X., Chi, S., He, N., Chen, K., McCormick, F., Gatalica, Z., and Xie, J. Activation of the hedgehog pathway in advanced prostate cancer. Mol Cancer, *3:* 29, 2004.
88. Sun, J., Liu, W., Adams, T. S., Sun, J., Li, X., Turner, A. R., Chang, B., Kim, J. W., Zheng, S. L., Isaacs, W. B., and Xu, J. DNA copy number alterations in prostate cancers: A combined analysis of published CGH studies. Prostate, *67:* 692-700, 2007.
89. Wodarz, A. and Nusse, R. Mechanisms of Wnt signaling in development. Annu Rev Cell Dev Biol, *14:* 59-88, 1998.
90. Yang-Snyder, J., Miller, J. R., Brown, J. D., Lai, C. J., and Moon, R. T. A frizzled homolog functions in a vertebrate Wnt signaling pathway. Curr Biol, *6:* 1302-1306, 1996.
91. Willert, K., Shibamoto, S., and Nusse, R. Wnt-induced dephosphorylation of axin releases beta-catenin from the axin complex. Genes Dev, *13:* 1768-1773, 1999.
92. Ikeda, S., Kishida, S., Yamamoto, H., Murai, H., Koyama, S., and Kikuchi, A. Axin, a negative regulator of the Wnt signaling pathway, forms a complex with GSK-3beta and beta-catenin and promotes GSK-3beta-dependent phosphorylation of beta-catenin. Embo J, *17:* 1371-1384, 1998.
93. Kobayashi, M., Honma, T., Matsuda, Y., Suzuki, Y., Narisawa, R., Ajioka, Y., and Asakura, H. Nuclear translocation of beta-catenin in colorectal cancer. Br J Cancer, *82:* 1689-1693, 2000.
94. Roose, J. and Clevers, H. TCF transcription factors: molecular switches in carcinogenesis. Biochim Biophys Acta, *1424:* M23-37, 1999.
95. He, T. C., Sparks, A. B., Rago, C., Hermeking, H., Zawel, L., da Costa, L. T., Morin, P. J., Vogelstein, B., and Kinzler, K. W. Identification of c-MYC as a target of the APC pathway. Science, *281:* 1509-1512, 1998.
96. Mann, B., Gelos, M., Siedow, A., Hanski, M. L., Gratchev, A., Ilyas, M., Bodmer, W. F., Moyer, M. P., Riecken, E. O., Buhr, H. J., and Hanski, C. Target genes of beta-catenin-T cell-factor/lymphoid-enhancer-factor signaling in human colorectal carcinomas. Proc Natl Acad Sci U S A, *96:* 1603-1608, 1999.
97. Tetsu, O. and McCormick, F. Beta-catenin regulates expression of cyclin D1 in colon carcinoma cells. Nature, *398:* 422-426, 1999.
98. Gounari, F., Signoretti, S., Bronson, R., Klein, L., Sellers, W. R., Kum, J., Siermann, A., Taketo, M. M., von Boehmer, H., and Khazaie, K. Stabilization of beta-catenin induces lesions reminiscent of prostatic intraepithelial neoplasia, but terminal squamous transdifferentiation of other secretory epithelia. Oncogene, *21:* 4099-4107, 2002.
99. de la Taille, A., Rubin, M. A., Chen, M. W., Vacherot, F., de Medina, S. G., Burchardt, M., Buttyan, R., and Chopin, D. Beta-catenin-related anomalies in apoptosis-resistant and hormone-refractory prostate cancer cells. Clin Cancer Res, *9:* 1801-1807, 2003.
100. Chen, G., Shukeir, N., Potti, A., Sircar, K., Aprikian, A., Goltzman, D., and Rabbani, S. A. Up-regulation of Wnt-1 and beta-catenin production in patients with advanced

metastatic prostate carcinoma: potential pathogenetic and prognostic implications. Cancer, *101:* 1345-1356, 2004.
101. Kwabi-Addo, B., Chung, W., Shen, L., Ittmann, M., Wheeler, T., Jelinek, J., and Issa, J. P. Age-related DNA methylation changes in normal human prostate tissues. Clin Cancer Res, *13:* 3796-3802, 2007.
102. Yegnasubramanian, S., Kowalski, J., Gonzalgo, M. L., Zahurak, M., Piantadosi, S., Walsh, P. C., Bova, G. S., De Marzo, A. M., Isaacs, W. B., and Nelson, W. G. Hypermethylation of CpG islands in primary and metastatic human prostate cancer. Cancer Res, *64:* 1975-1986, 2004.
103. Florl, A. R., Steinhoff, C., Muller, M., Seifert, H. H., Hader, C., Engers, R., Ackermann, R., and Schulz, W. A. Coordinate hypermethylation at specific genes in prostate carcinoma precedes LINE-1 hypomethylation. Br J Cancer, *91:* 985-994, 2004.
104. Herceg, Z. Epigenetics and cancer: towards an evaluation of the impact of environmental and dietary factors. Mutagenesis, *22:* 91-103, 2007.
105. Aitchison, A., Warren, A., Neal, D., and Rabbitts, P. RASSF1A promoter methylation is frequently detected in both pre-malignant and non-malignant microdissected prostatic epithelial tissues. Prostate, *67:* 638-644, 2007.
106. Henrique, R., Jeronimo, C., Teixeira, M. R., Hoque, M. O., Carvalho, A. L., Pais, I., Ribeiro, F. R., Oliveira, J., Lopes, C., and Sidransky, D. Epigenetic heterogeneity of high-grade prostatic intraepithelial neoplasia: clues for clonal progression in prostate carcinogenesis. Mol Cancer Res, *4:* 1-8, 2006.
107. Bedford, M. T. and van Helden, P. D. Hypomethylation of DNA in pathological conditions of the human prostate. Cancer Res, *47:* 5274-5276, 1987.
108. Dodge, J. E., Okano, M., Dick, F., Tsujimoto, N., Chen, T., Wang, S., Ueda, Y., Dyson, N., and Li, E. Inactivation of Dnmt3b in mouse embryonic fibroblasts results in DNA hypomethylation, chromosomal instability, and spontaneous immortalization. J Biol Chem, *280:* 17986-17991, 2005.
109. Schulz, W. A., Elo, J. P., Florl, A. R., Pennanen, S., Santourlidis, S., Engers, R., Buchardt, M., Seifert, H. H., and Visakorpi, T. Genomewide DNA hypomethylation is associated with alterations on chromosome 8 in prostate carcinoma. Genes Chromosomes Cancer, *35:* 58-65, 2002.
110. Li, L. C., Carroll, P. R., and Dahiya, R. Epigenetic changes in prostate cancer: implication for diagnosis and treatment. J Natl Cancer Inst, *97:* 103-115, 2005.
111. Pulukuri, S. M., Estes, N., Patel, J., and Rao, J. S. Demethylation-linked activation of urokinase plasminogen activator is involved in progression of prostate cancer. Cancer Res, *67:* 930-939, 2007.
112. Ogishima, T., Shiina, H., Breault, J. E., Tabatabai, L., Bassett, W. W., Enokida, H., Li, L. C., Kawakami, T., Urakami, S., Ribeiro-Filho, L. A., Terashima, M., Fujime, M., Igawa, M., and Dahiya, R. Increased heparanase expression is caused by promoter hypomethylation and up-regulation of transcriptional factor early growth response-1 in human prostate cancer. Clin Cancer Res, *11:* 1028-1036, 2005.
113. Schulz, W. A. and Hatina, J. Epigenetics of prostate cancer: beyond DNA methylation. J Cell Mol Med, *10:* 100-125, 2006.
114. Dobosy, J. R., Roberts, J. L., Fu, V. X., and Jarrard, D. F. The expanding role of epigenetics in the development, diagnosis and treatment of prostate cancer and benign prostatic hyperplasia. J Urol, *177:* 822-831, 2007.
115. Grover, A. C., Tangrea, M. A., Woodson, K. G., Wallis, B. S., Hanson, J. C., Chuaqui, R. F., Gillespie, J. W., Erickson, H. S., Bonner, R. F., Pohida, T. J., Emmert-Buck, M.

R., and Libutti, S. K. Tumor-associated endothelial cells display GSTP1 and RARbeta2 promoter methylation in human prostate cancer. J Transl Med, *4:* 13, 2006.
116. Mahajan, S. and Atkins, W. M. The chemistry and biology of inhibitors and pro-drugs targeted to glutathione S-transferases. Cell Mol Life Sci, *62:* 1221-1233, 2005.
117. Cheng, L., Pan, C. X., Zhang, J. T., Zhang, S., Kinch, M. S., Li, L., Baldridge, L. A., Wade, C., Hu, Z., Koch, M. O., Ulbright, T. M., and Eble, J. N. Loss of 14-3-3sigma in prostate cancer and its precursors. Clin Cancer Res, *10:* 3064-3068, 2004.
118. Henrique, R., Jeronimo, C., Hoque, M. O., Carvalho, A. L., Oliveira, J., Teixeira, M. R., Lopes, C., and Sidransky, D. Frequent 14-3-3 sigma promoter methylation in benign and malignant prostate lesions. DNA Cell Biol, *24:* 264-269, 2005.
119. Wilker, E. W., van Vugt, M. A., Artim, S. A., Huang, P. H., Petersen, C. P., Reinhardt, H. C., Feng, Y., Sharp, P. A., Sonenberg, N., White, F. M., and Yaffe, M. B. 14-3-3sigma controls mitotic translation to facilitate cytokinesis. Nature, *446:* 329-332, 2007.
120. Yang, H., Zhang, Y., Zhao, R., Wen, Y. Y., Fournier, K., Wu, H. B., Yang, H. Y., Diaz, J., Laronga, C., and Lee, M. H. Negative cell cycle regulator 14-3-3sigma stabilizes p27 Kip1 by inhibiting the activity of PKB/Akt. Oncogene, *25:* 4585-4594, 2006.
121. Hermeking, H., Lengauer, C., Polyak, K., He, T. C., Zhang, L., Thiagalingam, S., Kinzler, K. W., and Vogelstein, B. 14-3-3 sigma is a p53-regulated inhibitor of G2/M progression. Mol Cell, *1:* 3-11, 1997.
122. Gao, N., Zhang, Z., Jiang, B. H., and Shi, X. Role of PI3K/AKT/mTOR signaling in the cell cycle progression of human prostate cancer. Biochem Biophys Res Commun, *310:* 1124-1132, 2003.
123. Graff, J. R., Gabrielson, E., Fujii, H., Baylin, S. B., and Herman, J. G. Methylation patterns of the E-cadherin 5' CpG island are unstable and reflect the dynamic, heterogeneous loss of E-cadherin expression during metastatic progression. J Biol Chem, *275:* 2727-2732, 2000.
124. Graff, J. R., Herman, J. G., Lapidus, R. G., Chopra, H., Xu, R., Jarrard, D. F., Isaacs, W. B., Pitha, P. M., Davidson, N. E., and Baylin, S. B. E-cadherin expression is silenced by DNA hypermethylation in human breast and prostate carcinomas. Cancer Res, *55:* 5195-5199, 1995.
125. Ross, J. S., Figge, H. L., Bui, H. X., del Rosario, A. D., Fisher, H. A., Nazeer, T., Jennings, T. A., Ingle, R., and Kim, D. N. E-cadherin expression in prostatic carcinoma biopsies: correlation with tumor grade, DNA content, pathologic stage, and clinical outcome. Mod Pathol, *7:* 835-841, 1994.
126. Richmond, P. J., Karayiannakis, A. J., Nagafuchi, A., Kaisary, A. V., and Pignatelli, M. Aberrant E-cadherin and alpha-catenin expression in prostate cancer: correlation with patient survival. Cancer Res, *57:* 3189-3193, 1997.
127. Yang, F., Li, X., Sharma, M., Sasaki, C. Y., Longo, D. L., Lim, B., and Sun, Z. Linking beta-catenin to androgen-signaling pathway. J Biol Chem, *277:* 11336-11344, 2002.
128. Patra, S. K., Patra, A., Zhao, H., and Dahiya, R. DNA methyltransferase and demethylase in human prostate cancer. Mol Carcinog, *33:* 163-171, 2002.
129. Halkidou, K., Gaughan, L., Cook, S., Leung, H. Y., Neal, D. E., and Robson, C. N. Upregulation and nuclear recruitment of HDAC1 in hormone refractory prostate cancer. Prostate, *59:* 177-189, 2004.
130. Bandyopadhyay, D., Mishra, A., and Medrano, E. E. Overexpression of histone deacetylase 1 confers resistance to sodium butyrate-mediated apoptosis in melanoma cells through a p53-mediated pathway. Cancer Res, *64:* 7706-7710, 2004.
131. Lagger, G., O'Carroll, D., Rembold, M., Khier, H., Tischler, J., Weitzer, G., Schuettengruber, B., Hauser, C., Brunmeir, R., Jenuwein, T., and Seiser, C. Essential

function of histone deacetylase 1 in proliferation control and CDK inhibitor repression. Embo J, *21:* 2672-2681, 2002.
132. Zhou, Q., Melkoumian, Z. K., Lucktong, A., Moniwa, M., Davie, J. R., and Strobl, J. S. Rapid induction of histone hyperacetylation and cellular differentiation in human breast tumor cell lines following degradation of histone deacetylase-1. J Biol Chem, *275:* 35256-35263, 2000.
133. Gaughan, L., Logan, I. R., Cook, S., Neal, D. E., and Robson, C. N. Tip60 and histone deacetylase 1 regulate androgen receptor activity through changes to the acetylation status of the receptor. J Biol Chem, *277:* 25904-25913, 2002.
134. Ito, A., Kawaguchi, Y., Lai, C. H., Kovacs, J. J., Higashimoto, Y., Appella, E., and Yao, T. P. MDM2-HDAC1-mediated deacetylation of p53 is required for its degradation. Embo J, *21:* 6236-6245, 2002.
135. Li, X., Yin, S., Meng, Y., Sakr, W., and Sheng, S. Endogenous inhibition of histone deacetylase 1 by tumor-suppressive maspin. Cancer Res, *66:* 9323-9329, 2006.
136. Bracken, A. P., Kleine-Kohlbrecher, D., Dietrich, N., Pasini, D., Gargiulo, G., Beekman, C., Theilgaard-Monch, K., Minucci, S., Porse, B. T., Marine, J. C., Hansen, K. H., and Helin, K. The Polycomb group proteins bind throughout the INK4A-ARF locus and are disassociated in senescent cells. Genes Dev, *21:* 525-530, 2007.
137. Cha, T. L., Zhou, B. P., Xia, W., Wu, Y., Yang, C. C., Chen, C. T., Ping, B., Otte, A. P., and Hung, M. C. Akt-mediated phosphorylation of EZH2 suppresses methylation of lysine 27 in histone H3. Science, *310:* 306-310, 2005.
138. Gil, J. and Peters, G. Regulation of the INK4b-ARF-INK4a tumour suppressor locus: all for one or one for all. Nat Rev Mol Cell Biol, *7:* 667-677, 2006.
139. Yu, J., Yu, J., Rhodes, D. R., Tomlins, S. A., Cao, X., Chen, G., Mehra, R., Wang, X., Ghosh, D., Shah, R. B., Varambally, S., Pienta, K. J., and Chinnaiyan, A. M. A polycomb repression signature in metastatic prostate cancer predicts cancer outcome. Cancer Res, *67:* 10657-10663, 2007.
140. Varambally, S., Cao, Q., Mani, R. S., Shankar, S., Wang, X., Ateeq, B., Laxman, B., Cao, X., Jing, X., Ramnarayanan, K., Brenner, J. C., Yu, J., Kim, J. H., Han, B., Tan, P., Kumar-Sinha, C., Lonigro, R. J., Palanisamy, N., Maher, C. A., and Chinnaiyan, A. M. Genomic loss of microRNA-101 leads to overexpression of histone methyltransferase EZH2 in cancer. Science, *322:* 1695-1699, 2008.
141. Varambally, S., Dhanasekaran, S. M., Zhou, M., Barrette, T. R., Kumar-Sinha, C., Sanda, M. G., Ghosh, D., Pienta, K. J., Sewalt, R. G., Otte, A. P., Rubin, M. A., and Chinnaiyan, A. M. The polycomb group protein EZH2 is involved in progression of prostate cancer. Nature, *419:* 624-629, 2002.
142. Lengauer, C., Kinzler, K. W., and Vogelstein, B. Genetic instability in colorectal cancers. Nature, *386:* 623-627, 1997.
143. Modrich, P. Strand-specific mismatch repair in mammalian cells. J Biol Chem, *272:* 24727-24730, 1997.
144. Kolodner, R. D. Mismatch repair: mechanisms and relationship to cancer susceptibility. Trends Biochem Sci, *20:* 397-401, 1995.
145. Rajagopalan, H., Nowak, M. A., Vogelstein, B., and Lengauer, C. The significance of unstable chromosomes in colorectal cancer. Nat Rev Cancer, *3:* 695-701, 2003.
146. Rajagopalan, H. and Lengauer, C. Aneuploidy and cancer. Nature, *432:* 338-341, 2004.
147. Roudier, M. P., True, L. D., Higano, C. S., Vesselle, H., Ellis, W., Lange, P., and Vessella, R. L. Phenotypic heterogeneity of end-stage prostate carcinoma metastatic to bone. Hum Pathol, *34:* 646-653, 2003.

148. Shah, R. B., Mehra, R., Chinnaiyan, A. M., Shen, R., Ghosh, D., Zhou, M., Macvicar, G. R., Varambally, S., Harwood, J., Bismar, T. A., Kim, R., Rubin, M. A., and Pienta, K. J. Androgen-independent prostate cancer is a heterogeneous group of diseases: lessons from a rapid autopsy program. Cancer Res, *64:* 9209-9216, 2004.
149. Ribeiro, F. R., Diep, C. B., Jeronimo, C., Henrique, R., Lopes, C., Eknaes, M., Lingjaerde, O. C., Lothe, R. A., and Teixeira, M. R. Statistical dissection of genetic pathways involved in prostate carcinogenesis. Genes Chromosomes Cancer, *45:* 154-163, 2006.
150. Saramaki, O. and Visakorpi, T. Chromosomal aberrations in prostate cancer. Front Biosci, *12:* 3287-3301, 2007.
151. Chaib, H., MacDonald, J. W., Vessella, R. L., Washburn, J. G., Quinn, J. E., Odman, A., Rubin, M. A., and Macoska, J. A. Haploinsufficiency and reduced expression of genes localized to the 8p chromosomal region in human prostate tumors. Genes Chromosomes Cancer, *37:* 306-313, 2003.
152. Chin, K., de Solorzano, C. O., Knowles, D., Jones, A., Chou, W., Rodriguez, E. G., Kuo, W. L., Ljung, B. M., Chew, K., Myambo, K., Miranda, M., Krig, S., Garbe, J., Stampfer, M., Yaswen, P., Gray, J. W., and Lockett, S. J. In situ analyses of genome instability in breast cancer. Nat Genet, *36:* 984-988, 2004.
153. Pihan, G. A., Purohit, A., Wallace, J., Malhotra, R., Liotta, L., and Doxsey, S. J. Centrosome defects can account for cellular and genetic changes that characterize prostate cancer progression. Cancer Res, *61:* 2212-2219, 2001.
154. Pihan, G. A., Wallace, J., Zhou, Y., and Doxsey, S. J. Centrosome abnormalities and chromosome instability occur together in pre-invasive carcinomas. Cancer Res, *63:* 1398-1404, 2003.
155. Fan, R., Kumaravel, T. S., Jalali, F., Marrano, P., Squire, J. A., and Bristow, R. G. Defective DNA strand break repair after DNA damage in prostate cancer cells: implications for genetic instability and prostate cancer progression. Cancer Res, *64:* 8526-8533, 2004.
156. Meng, A. X., Jalali, F., Cuddihy, A., Chan, N., Bindra, R. S., Glazer, P. M., and Bristow, R. G. Hypoxia down-regulates DNA double strand break repair gene expression in prostate cancer cells. Radiother Oncol, *76:* 168-176, 2005.
157. Kiviharju-af Hallstrom, T. M., Jaamaa, S., Monkkonen, M., Peltonen, K., Andersson, L. C., Medema, R. H., Peehl, D. M., and Laiho, M. Human prostate epithelium lacks Wee1A-mediated DNA damage-induced checkpoint enforcement. Proc Natl Acad Sci U S A, *104:* 7211-7216, 2007.
158. Lobrich, M. and Jeggo, P. A. The impact of a negligent G2/M checkpoint on genomic instability and cancer induction. Nat Rev Cancer, *7:* 861-869, 2007.
159. Tomlins, S. A., Rhodes, D. R., Perner, S., Dhanasekaran, S. M., Mehra, R., Sun, X. W., Varambally, S., Cao, X., Tchinda, J., Kuefer, R., Lee, C., Montie, J. E., Shah, R. B., Pienta, K. J., Rubin, M. A., and Chinnaiyan, A. M. Recurrent fusion of TMPRSS2 and ETS transcription factor genes in prostate cancer. Science, *310:* 644-648, 2005.
160. Tomlins, S. A., Mehra, R., Rhodes, D. R., Cao, X., Wang, L., Dhanasekaran, S. M., Kalyana-Sundaram, S., Wei, J. T., Rubin, M. A., Pienta, K. J., Shah, R. B., and Chinnaiyan, A. M. Integrative molecular concept modeling of prostate cancer progression. Nat Genet, 2006.
161. Soller, M. J., Isaksson, M., Elfving, P., Soller, W., Lundgren, R., and Panagopoulos, I. Confirmation of the high frequency of the TMPRSS2/ERG fusion gene in prostate cancer. Genes Chromosomes Cancer, *45:* 717-719, 2006.

162. Yoshimoto, M., Joshua, A.M., Chilton-MacNeill, S., Bayani, J., Selvarajah, S., Evans, A.J., Zielenska, M., Squire, J.A. Three-Color FISH Analysis of TMPRSS2/ERG Fusions in Prostate Cancer Indicates That Genomic Microdeletion of Chromosome 21 is Associated with Rearrangement. Neoplasia, *8:* 465-469, 2006.
163. Wang, J., Cai, Y., Ren, C., and Ittmann, M. Expression of Variant TMPRSS2/ERG Fusion Messenger RNAs Is Associated with Aggressive Prostate Cancer. Cancer Res, *66:* 8347-8351, 2006.
164. Tomlins, S. A., Mehra, R., Rhodes, D. R., Smith, L. R., Roulston, D., Helgeson, B. E., Cao, X., Wei, J. T., Rubin, M. A., Shah, R. B., and Chinnaiyan, A. M. TMPRSS2:ETV4 gene fusions define a third molecular subtype of prostate cancer. Cancer Res, *66:* 3396-3400, 2006.
165. Hermans, K. G., van Marion, R., van Dekken, H., Jenster, G., van Weerden, W. M., and Trapman, J. TMPRSS2:ERG fusion by translocation or interstitial deletion is highly relevant in androgen-dependent prostate cancer, but is bypassed in late-stage androgen receptor-negative prostate cancer. Cancer Res, *66:* 10658-10663, 2006.
166. Cai, C., Hsieh, C. L., Omwancha, J., Zheng, Z., Chen, S. Y., Baert, J. L., and Shemshedini, L. ETV1 Is a Novel Androgen Receptor-Regulated Gene That Mediates Prostate Cancer Cell Invasion. Mol Endocrinol, 2007.
167. Clark, J., Merson, S., Jhavar, S., Flohr, P., Edwards, S., Foster, C. S., Eeles, R., Martin, F. L., Phillips, D. H., Crundwell, M., Christmas, T., Thompson, A., Fisher, C., Kovacs, G., and Cooper, C. S. Diversity of TMPRSS2-ERG fusion transcripts in the human prostate. Oncogene, 2006.
168. Joshua, A. M., Evans, A., Van der Kwast, T., Zielenska, M., Meeker, A. K., Chinnaiyan, A., and Squire, J. A. Prostatic preneoplasia and beyond. Biochim Biophys Acta, 2007.
169. Liu, W., Ewing, C. M., Chang, B. L., Li, T., Sun, J., Turner, A. R., Dimitrov, L., Zhu, Y., Sun, J., Kim, J. W., Zheng, S. L., Isaacs, W. B., and Xu, J. Multiple genomic alterations on 21q22 predict various TMPRSS2/ERG fusion transcripts in human prostate cancers. Genes Chromosomes Cancer, 2007.
170. Yoshimoto, M., Joshua, A. M., Chilton-Macneill, S., Bayani, J., Selvarajah, S., Evans, A. J., Zielenska, M., and Squire, J. A. Three-color FISH analysis of TMPRSS2/ERG fusions in prostate cancer indicates that genomic microdeletion of chromosome 21 is associated with rearrangement. Neoplasia, *8:* 465-469, 2006.
171. Mehra, R., Tomlins, S. A., Shen, R., Nadeem, O., Wang, L., Wei, J. T., Pienta, K. J., Ghosh, D., Rubin, M. A., Chinnaiyan, A. M., and Shah, R. B. Comprehensive assessment of TMPRSS2 and ETS family gene aberrations in clinically localized prostate cancer. Mod Pathol, 2007.
172. Dagher, R., Pham, T. A., Sorbara, L., Kumar, S., Long, L., Bernstein, D., Mackall, C., Raffeld, M., Tsokos, M., and Helman, L. Molecular confirmation of Ewing sarcoma. J Pediatr Hematol Oncol, *23:* 221-224, 2001.
173. Yoshimoto, M., Ludkovski, O., Bayani, J., Graham, C., Zielenska, M., and Squire, J. A. Microdeletion and concurrent translocation associated with a complex TMPRSS2:ERG prostate cancer gene fusion. Genes Chromosomes Cancer, 2007.
174. Tomlins, S. A., Laxman, B., Dhanasekaran, S. M., Helgeson, B. E., Cao, X., Morris, D. S., Menon, A., Jing, X., Cao, Q., Han, B., Yu, J., Wang, L., Montie, J. E., Rubin, M. A., Pienta, K. J., Roulston, D., Shah, R. B., Varambally, S., Mehra, R., and Chinnaiyan, A. M. Distinct classes of chromosomal rearrangements create oncogenic ETS gene fusions in prostate cancer. Nature, *448:* 595-599, 2007.
175. Attard, G., Clark, J., Ambroisine, L., Mills, I. G., Fisher, G., Flohr, P., Reid, A., Edwards, S., Kovacs, G., Berney, D., Foster, C., Massie, C. E., Fletcher, A., De Bono, J.

S., Scardino, P., Cuzick, J., and Cooper, C. S. Heterogeneity and clinical significance of ETV1 translocations in human prostate cancer. Br J Cancer, *99:* 314-320, 2008.
176. Cerveira, N., Ribeiro, F. R., Peixoto, A., Costa, V., Henrique, R., Jeronimo, C., and Teixeira, M. R. TMPRSS2-ERG gene fusion causing ERG overexpression precedes chromosome copy number changes in prostate carcinomas and paired HGPIN lesions. Neoplasia, *8:* 826-832, 2006.
177. Clark, J., Attard, G., Jhavar, S., Flohr, P., Reid, A., De-Bono, J., Eeles, R., Scardino, P., Cuzick, J., Fisher, G., Parker, M. D., Foster, C. S., Berney, D., Kovacs, G., and Cooper, C. S. Complex patterns of ETS gene alteration arise during cancer development in the human prostate. Oncogene, 2007.
178. Seth, A. and Watson, D. K. ETS transcription factors and their emerging roles in human cancer. Eur J Cancer, *41:* 2462-2478, 2005.
179. Yang, L., Mei, Q., Zielinska-Kwiatkowska, A., Matsui, Y., Blackburn, M. L., Benedetti, D., Krumm, A. A., Taborsky, G. J., Jr., and Chansky, H. A. An ERG (ets-related gene)-associated histone methyltransferase interacts with histone deacetylases 1/2 and transcription co-repressors mSin3A/B. Biochem J, *369:* 651-657, 2003.
180. Yi, H., Fujimura, Y., Ouchida, M., Prasad, D. D., Rao, V. N., and Reddy, E. S. Inhibition of apoptosis by normal and aberrant Fli-1 and erg proteins involved in human solid tumors and leukemias. Oncogene, *14:* 1259-1268, 1997.
181. Hart, A. H., Corrick, C. M., Tymms, M. J., Hertzog, P. J., and Kola, I. Human ERG is a proto-oncogene with mitogenic and transforming activity. Oncogene, *10:* 1423-1430, 1995.
182. Iljin, K., Wolf, M., Edgren, H., Gupta, S., Kilpinen, S., Skotheim, R. I., Peltola, M., Smit, F., Verhaegh, G., Schalken, J., Nees, M., and Kallioniemi, O. TMPRSS2 fusions with oncogenic ETS factors in prostate cancer involve unbalanced genomic rearrangements and are associated with HDAC1 and epigenetic reprogramming. Cancer Res, *66:* 10242-10246, 2006.
183. Cai, C., Hsieh, C. L., and Shemshedini, L. c-Jun has multiple enhancing activities in the novel cross talk between the androgen receptor and Ets variant gene 1 in prostate cancer. Mol Cancer Res, *5:* 725-735, 2007.
184. Chinnaiyan, A. M. Recurrent Gene Fusions in Prostate Cancer. IMPaCT (Innovative Minds in Prostate Cancer Today). Atlanta, Georgia: US Army Medical Research and Material Command, 2007.
185. Klezovitch, O., Risk, M., Coleman, I., Lucas, J. M., Null, M., True, L. D., Nelson, P. S., and Vasioukhin, V. A causal role for ERG in neoplastic transformation of prostate epithelium. Proc Natl Acad Sci U S A, *105:* 2105-2110, 2008.
186. Tomlins, S. A., Laxman, B., Varambally, S., Cao, X., Yu, J., Helgeson, B. E., Cao, Q., Prensner, J. R., Rubin, M. A., Shah, R. B., Mehra, R., and Chinnaiyan, A. M. Role of the TMPRSS2-ERG gene fusion in prostate cancer. Neoplasia, *10:* 177-188, 2008.
187. Sun, C., Dobi, A., Mohamed, A., Li, H., Thangapazham, R. L., Furusato, B., Shaheduzzaman, S., Tan, S. H., Vaidyanathan, G., Whitman, E., Hawksworth, D. J., Chen, Y., Nau, M., Patel, V., Vahey, M., Gutkind, J. S., Sreenath, T., Petrovics, G., Sesterhenn, I. A., McLeod, D. G., and Srivastava, S. TMPRSS2-ERG fusion, a common genomic alteration in prostate cancer activates C-MYC and abrogates prostate epithelial differentiation. Oncogene, 2008.
188. Petrovics, G., Liu, A., Shaheduzzaman, S., Furasato, B., Sun, C., Chen, Y., Nau, M., Ravindranath, L., Chen, Y., Dobi, A., Srikantan, V., Sesterhenn, I. A., McLeod, D. G., Vahey, M., Moul, J. W., and Srivastava, S. Frequent overexpression of ETS-related gene-1 (ERG1) in prostate cancer transcriptome. Oncogene, *24:* 3847-3852, 2005.

189. Nami, R. K., Sugar, L., Wang, Z., Yang, W., Kitching, R., Klotz, L. H., Venkateswaran, V., Narod, S. A., and Seth, A. Expression of TMPRSS2:ERG gene fusion in prostate cancer cells is an important prognostic factor for cancer progression. Cancer Biol Ther, *6:* 40-45, 2007.
190. Perner, S., Demichelis, F., Beroukhim, R., Schmidt, F. H., Mosquera, J. M., Setlur, S., Tchinda, J., Tomlins, S. A., Hofer, M. D., Pienta, K. G., Kuefer, R., Vessella, R., Sun, X. W., Meyerson, M., Lee, C., Sellers, W. R., Chinnaiyan, A. M., and Rubin, M. A. TMPRSS2:ERG Fusion-Associated Deletions Provide Insight into the Heterogeneity of Prostate Cancer. Cancer Res, *66:* 8337-8341, 2006.
191. Jenkins, R. B., Nakagawa, T., Kollmeyer, T., Morlan, B., Bergstrahl, E., Davis, B., Klee, G., and Ballman, K. V. Use of a tissue biomarker panel to predict which men with a rising PSA post-definitive prostate cancer therapy will have systemic progression. *In:* American Society of Clincal Oncology Proceedings Chicago, Illinois, June 20 2007.
192. Attard, G., Clark, J., Ambroisine, L., Fisher, G., Kovacs, G., Flohr, P., Berney, D., Foster, C. S., Fletcher, A., Gerald, W. L., Moller, H., Reuter, V., De Bono, J. S., Scardino, P., Cuzick, J., and Cooper, C. S. Duplication of the fusion of TMPRSS2 to ERG sequences identifies fatal human prostate cancer. Oncogene, 2007.
193. Demichelis, F., Fall, K., Perner, S., Andren, O., Schmidt, F., Setlur, S. R., Hoshida, Y., Mosquera, J. M., Pawitan, Y., Lee, C., Adami, H. O., Mucci, L. A., Kantoff, P. W., Andersson, S. O., Chinnaiyan, A. M., Johansson, J. E., and Rubin, M. A. TMPRSS2:ERG gene fusion associated with lethal prostate cancer in a watchful waiting cohort. Oncogene, *26:* 4596-4599, 2007.
194. Gu, X., Zerbini, L. F., Otu, H. H., Bhasin, M., Yang, Q., Joseph, M. G., Grall, F., Onatunde, T., Correa, R. G., and Libermann, T. A. Reduced PDEF Expression Increases Invasion and Expression of Mesenchymal Genes in Prostate Cancer Cells. Cancer Res, *67:* 4219-4226, 2007.
195. Oettgen, P., Finger, E., Sun, Z., Akbarali, Y., Thamrongsak, U., Boltax, J., Grall, F., Dube, A., Weiss, A., Brown, L., Quinn, G., Kas, K., Endress, G., Kunsch, C., and Libermann, T. A. PDEF, a novel prostate epithelium-specific ets transcription factor, interacts with the androgen receptor and activates prostate-specific antigen gene expression. J Biol Chem, *275:* 1216-1225, 2000.
196. Chen, H., Nandi, A. K., Li, X., and Bieberich, C. J. NKX-3.1 interacts with prostate-derived Ets factor and regulates the activity of the PSA promoter. Cancer Res, *62:* 338-340, 2002.
197. Sood, A. K., Saxena, R., Groth, J., Desouki, M. M., Cheewakriangkrai, C., Rodabaugh, K. J., Kasyapa, C. S., and Geradts, J. Expression characteristics of prostate-derived Ets factor support a role in breast and prostate cancer progression. Hum Pathol, 2007.
198. Cangemi, R., Mensah, A., Albertini, V., Jain, A., Mello-Grand, M., Chiorino, G., Catapano, C. V., and Carbone, G. M. Reduced expression and tumor suppressor function of the ETS transcription factor ESE-3 in prostate cancer. Oncogene, *27:* 2877-2885, 2008.
199. Kas, K., Finger, E., Grall, F., Gu, X., Akbarali, Y., Boltax, J., Weiss, A., Oettgen, P., Kapeller, R., and Libermann, T. A. ESE-3, a novel member of an epithelium-specific ets transcription factor subfamily, demonstrates different target gene specificity from ESE-1. J Biol Chem, *275:* 2986-2998, 2000.
200. Tomlins, S. A., Rhodes, D. R., Yu, J., Varambally, S., Mehra, R., Perner, S., Demichelis, F., Helgeson, B. E., Laxman, B., Morris, D. S., Cao, Q., Cao, X., Andren, O., Fall, K., Johnson, L., Wei, J. T., Shah, R. B., Al-Ahmadie, H., Eastham, J. A., Eggener, S. E., Fine, S. W., Hotakainen, K., Stenman, U. H., Tsodikov, A., Gerald, W. L., Lilja, H.,

Reuter, V. E., Kantoff, P. W., Scardino, P. T., Rubin, M. A., Bjartell, A. S., and Chinnaiyan, A. M. The role of SPINK1 in ETS rearrangement-negative prostate cancers. Cancer Cell, *13:* 519-528, 2008.
201. Moyzis, R. K., Buckingham, J. M., Cram, L. S., Dani, M., Deaven, L. L., Jones, M. D., Meyne, J., Ratliff, R. L., and Wu, J. R. A highly conserved repetitive DNA sequence, (TTAGGG)n, present at the telomeres of human chromosomes. Proc Natl Acad Sci U S A, *85:* 6622-6626, 1988.
202. Maser, R. S. and DePinho, R. A. Telomeres and the DNA damage response: why the fox is guarding the henhouse. DNA Repair (Amst), *3:* 979-988, 2004.
203. Griffith, J. D., Comeau, L., Rosenfield, S., Stansel, R. M., Bianchi, A., Moss, H., and de Lange, T. Mammalian telomeres end in a large duplex loop. Cell, *97:* 503-514, 1999.
204. Kawanishi, S. and Oikawa, S. Mechanism of telomere shortening by oxidative stress. Ann N Y Acad Sci, *1019:* 278-284, 2004.
205. Richter, T. and Proctor, C. The role of intracellular peroxide levels on the development and maintenance of telomere-dependent senescence. Exp Gerontol, *42:* 1043-1052, 2007.
206. Baird, D. M., Rowson, J., Wynford-Thomas, D., and Kipling, D. Extensive allelic variation and ultrashort telomeres in senescent human cells. Nat Genet, *33:* 203-207, 2003.
207. Ohki, R., Tsurimoto, T., and Ishikawa, F. In vitro reconstitution of the end replication problem. Mol Cell Biol, *21:* 5753-5766, 2001.
208. Harley, C. B., Futcher, A. B., and Greider, C. W. Telomeres shorten during ageing of human fibroblasts. Nature, *345:* 458-460, 1990.
209. Lindsey, J., McGill, N. I., Lindsey, L. A., Green, D. K., and Cooke, H. J. In vivo loss of telomeric repeats with age in humans. Mutat Res, *256:* 45-48, 1991.
210. McClintock, B. The stability of broken ends of chromosomes in Zea mays. Genetics, *1041:* 234-282, 1941.
211. Mathieu, N., Pirzio, L., Freulet-Marriere, M. A., Desmaze, C., and Sabatier, L. Telomeres and chromosomal instability. Cell Mol Life Sci, *61:* 641-656, 2004.
212. Murnane, J. P. and Sabatier, L. Chromosome rearrangements resulting from telomere dysfunction and their role in cancer. Bioessays, *26:* 1164-1174, 2004.
213. Gisselsson, D., Jonson, T., Petersen, A., Strombeck, B., Dal Cin, P., Hoglund, M., Mitelman, F., Mertens, F., and Mandahl, N. Telomere dysfunction triggers extensive DNA fragmentation and evolution of complex chromosome abnormalities in human malignant tumors. Proc Natl Acad Sci U S A, *98:* 12683-12688, 2001.
214. Gisselsson, D., Pettersson, L., Hoglund, M., Heidenblad, M., Gorunova, L., Wiegant, J., Mertens, F., Dal Cin, P., Mitelman, F., and Mandahl, N. Chromosomal breakage-fusion-bridge events cause genetic intratumor heterogeneity. Proc Natl Acad Sci U S A, *97:* 5357-5362, 2000.
215. Al-Maghrabi, J., Vorobyova, L., Toi, A., Chapman, W., Zielenska, M., and Squire, J. A. Identification of numerical chromosomal changes detected by interphase fluorescence in situ hybridization in high-grade prostate intraepithelial neoplasia as a predictor of carcinoma. Arch Pathol Lab Med, *126:* 165-169, 2002.
216. Vukovic, B., Park, P. C., Al-Maghrabi, J., Beheshti, B., Sweet, J., Evans, A., Trachtenberg, J., and Squire, J. Evidence of multifocality of telomere erosion in high-grade prostatic intraepithelial neoplasia (HPIN) and concurrent carcinoma. Oncogene, *22:* 1978-1987, 2003.
217. Artandi, S. E. and DePinho, R. A. A critical role for telomeres in suppressing and facilitating carcinogenesis. Curr Opin Genet Dev, *10:* 39-46, 2000.

218. Fujikawa, M., Katagiri, T., Tugores, A., Nakamura, Y., and Ishikawa, F. ESE-3, an Ets family transcription factor, is up-regulated in cellular senescence. Cancer Sci, *98:* 1468-1475, 2007.
219. Xu, L. and Blackburn, E. H. Human cancer cells harbor T-stumps, a distinct class of extremely short telomeres. Mol Cell, *28:* 315-327, 2007.
220. Zhu, J., Wang, H., Bishop, J. M., and Blackburn, E. H. Telomerase extends the lifespan of virus-transformed human cells without net telomere lengthening. Proc Natl Acad Sci U S A, *96:* 3723-3728, 1999.
221. Kim, M., Xu, L., and Blackburn, E. H. Catalytically active human telomerase mutants with allele-specific biological properties. Exp Cell Res, *288:* 277-287, 2003.
222. Li, S., Rosenberg, J. E., Donjacour, A. A., Botchkina, I. L., Hom, Y. K., Cunha, G. R., and Blackburn, E. H. Rapid inhibition of cancer cell growth induced by lentiviral delivery and expression of mutant-template telomerase RNA and anti-telomerase short-interfering RNA. Cancer Res, *64:* 4833-4840, 2004.
223. Masutomi, K., Possemato, R., Wong, J. M., Currier, J. L., Tothova, Z., Manola, J. B., Ganesan, S., Lansdorp, P. M., Collins, K., and Hahn, W. C. The telomerase reverse transcriptase regulates chromatin state and DNA damage responses. Proc Natl Acad Sci U S A, *102:* 8222-8227, 2005.
224. Sarin, K. Y., Cheung, P., Gilison, D., Lee, E., Tennen, R. I., Wang, E., Artandi, M. K., Oro, A. E., and Artandi, S. E. Conditional telomerase induction causes proliferation of hair follicle stem cells. Nature, *436:* 1048-1052, 2005.
225. Gelmann, E. P. Molecular biology of the androgen receptor. J Clin Oncol, *20:* 3001-3015, 2002.
226. Hayward, S. W., Rosen, M. A., and Cunha, G. R. Stromal-epithelial interactions in the normal and neoplastic prostate. Br J Urol, *79 Suppl 2:* 18-26, 1997.
227. Cunha, G. R., Cooke, P. S., and Kurita, T. Role of stromal-epithelial interactions in hormonal responses. Arch Histol Cytol, *67:* 417-434, 2004.
228. Cunha, G. R., Hayward, S. W., Wang, Y. Z., and Ricke, W. A. Role of the stromal microenvironment in carcinogenesis of the prostate. Int J Cancer, *107:* 1-10, 2003.
229. Cunha, G. R., Hayward, S. W., and Wang, Y. Z. Role of stroma in carcinogenesis of the prostate. Differentiation, *70:* 473-485, 2002.
230. Peehl, D. M. and Rubin, J. S. Keratinocyte growth factor: an androgen-regulated mediator of stromal-epithelial interactions in the prostate. World J Urol, *13:* 312-317, 1995.
231. Chang, C. Y. and McDonnell, D. P. Androgen receptor-cofactor interactions as targets for new drug discovery. Trends Pharmacol Sci, *26:* 225-228, 2005.
232. Dehm, S. M. and Tindall, D. J. Regulation of androgen receptor signaling in prostate cancer. Expert Rev Anticancer Ther, *5:* 63-74, 2005.
233. Dehm, S. M. and Tindall, D. J. Molecular regulation of androgen action in prostate cancer. J Cell Biochem, *99:* 333-344, 2006.
234. Heinlein, C. A. and Chang, C. The roles of androgen receptors and androgen-binding proteins in nongenomic androgen actions. Mol Endocrinol, *16:* 2181-2187, 2002.
235. Suh, J. and Rabson, A. B. NF-kappaB activation in human prostate cancer: important mediator or epiphenomenon? J Cell Biochem, *91:* 100-117, 2004.
236. Delfino, F. J., Boustead, J. N., Fix, C., and Walker, W. H. NF-kappaB and TNF-alpha stimulate androgen receptor expression in Sertoli cells. Mol Cell Endocrinol, *201:* 1-12, 2003.

237. Chen, C. D. and Sawyers, C. L. NF-kappa B activates prostate-specific antigen expression and is upregulated in androgen-independent prostate cancer. Mol Cell Biol, *22:* 2862-2870, 2002.
238. Foley, K. P. and Eisenman, R. N. Two MAD tails: what the recent knockouts of Mad1 and Mxi1 tell us about the MYC/MAX/MAD network. Biochim Biophys Acta, *1423:* M37-47, 1999.
239. Williams, K., Fernandez, S., Stien, X., Ishii, K., Love, H. D., Lau, Y. F., Roberts, R. L., and Hayward, S. W. Unopposed c-MYC expression in benign prostatic epithelium causes a cancer phenotype. Prostate, *63:* 369-384, 2005.
240. Gil, J., Kerai, P., Lleonart, M., Bernard, D., Cigudosa, J. C., Peters, G., Carnero, A., and Beach, D. Immortalization of primary human prostate epithelial cells by c-Myc. Cancer Res, *65:* 2179-2185, 2005.
241. Zhang, X., Lee, C., Ng, P. Y., Rubin, M., Shabsigh, A., and Buttyan, R. Prostatic neoplasia in transgenic mice with prostate-directed overexpression of the c-myc oncoprotein. Prostate, *43:* 278-285, 2000.
242. Ellwood-Yen, K., Graeber, T. G., Wongvipat, J., Iruela-Arispe, M. L., Zhang, J., Matusik, R., Thomas, G. V., and Sawyers, C. L. Myc-driven murine prostate cancer shares molecular features with human prostate tumors. Cancer Cell, *4:* 223-238, 2003.
243. Latil, A., Vidaud, D., Valeri, A., Fournier, G., Vidaud, M., Lidereau, R., Cussenot, O., and Biache, I. htert expression correlates with MYC over-expression in human prostate cancer. Int J Cancer, *89:* 172-176, 2000.
244. Jenkins, R. B., Qian, J., Lieber, M. M., and Bostwick, D. G. Detection of c-myc oncogene amplification and chromosomal anomalies in metastatic prostatic carcinoma by fluorescence in situ hybridization. Cancer Res, *57:* 524-531, 1997.
245. Sato, K., Qian, J., Slezak, J. M., Lieber, M. M., Bostwick, D. G., Bergstralh, E. J., and Jenkins, R. B. Clinical significance of alterations of chromosome 8 in high-grade, advanced, nonmetastatic prostate carcinoma. J Natl Cancer Inst, *91:* 1574-1580, 1999.
246. Ribeiro, F. R., Henrique, R., Martins, A. T., Jeronimo, C., and Teixeira, M. R. Relative copy number gain of MYC in diagnostic needle biopsies is an independent prognostic factor for prostate cancer patients. Eur Urol, *52:* 116-125, 2007.
247. Sato, H., Minei, S., Hachiya, T., Yoshida, T., and Takimoto, Y. Fluorescence in situ hybridization analysis of c-myc amplification in stage TNM prostate cancer in Japanese patients. Int J Urol, *13:* 761-766, 2006.
248. Reiter, R. E., Sato, I., Thomas, G., Qian, J., Gu, Z., Watabe, T., Loda, M., and Jenkins, R. B. Coamplification of prostate stem cell antigen (PSCA) and MYC in locally advanced prostate cancer. Genes Chromosomes Cancer, *27:* 95-103, 2000.
249. Bubendorf, L., Kononen, J., Koivisto, P., Schraml, P., Moch, H., Gasser, T. C., Willi, N., Mihatsch, M. J., Sauter, G., and Kallioniemi, O. P. Survey of gene amplifications during prostate cancer progression by high-throughout fluorescence in situ hybridization on tissue microarrays. Cancer Res, *59:* 803-806, 1999.
250. Gurel, B., Iwata, T., C, M. K., Jenkins, R. B., Lan, F., Van Dang, C., Hicks, J. L., Morgan, J., Cornish, T. C., Sutcliffe, S., Isaacs, W. B., Luo, J., and De Marzo, A. M. Nuclear MYC protein overexpression is an early alteration in human prostate carcinogenesis. Mod Pathol, 2008.
251. Yeager, M., Orr, N., Hayes, R. B., Jacobs, K. B., Kraft, P., Wacholder, S., Minichiello, M. J., Fearnhead, P., Yu, K., Chatterjee, N., Wang, Z., Welch, R., Staats, B. J., Calle, E. E., Feigelson, H. S., Thun, M. J., Rodriguez, C., Albanes, D., Virtamo, J., Weinstein, S., Schumacher, F. R., Giovannucci, E., Willett, W. C., Cancel-Tassin, G., Cussenot, O., Valeri, A., Andriole, G. L., Gelmann, E. P., Tucker, M., Gerhard, D. S., Fraumeni, J. F.,

Jr., Hoover, R., Hunter, D. J., Chanock, S. J., and Thomas, G. Genome-wide association study of prostate cancer identifies a second risk locus at 8q24. Nat Genet, *39:* 645-649, 2007.

252. Gudmundsson, J., Sulem, P., Manolescu, A., Amundadottir, L. T., Gudbjartsson, D., Helgason, A., Rafnar, T., Bergthorsson, J. T., Agnarsson, B. A., Baker, A., Sigurdsson, A., Benediktsdottir, K. R., Jakobsdottir, M., Xu, J., Blondal, T., Kostic, J., Sun, J., Ghosh, S., Stacey, S. N., Mouy, M., Saemundsdottir, J., Backman, V. M., Kristjansson, K., Tres, A., Partin, A. W., Albers-Akkers, M. T., Godino-Ivan Marcos, J., Walsh, P. C., Swinkels, D. W., Navarrete, S., Isaacs, S. D., Aben, K. K., Graif, T., Cashy, J., Ruiz-Echarri, M., Wiley, K. E., Suarez, B. K., Witjes, J. A., Frigge, M., Ober, C., Jonsson, E., Einarsson, G. V., Mayordomo, J. I., Kiemeney, L. A., Isaacs, W. B., Catalona, W. J., Barkardottir, R. B., Gulcher, J. R., Thorsteinsdottir, U., Kong, A., and Stefansson, K. Genome-wide association study identifies a second prostate cancer susceptibility variant at 8q24. Nat Genet, *39:* 631-637, 2007.
253. Beck-Engeser, G. B., Lum, A. M., Huppi, K., Caplen, N. J., Wang, B. B., and Wabl, M. Pvt1-encoded microRNAs in oncogenesis. Retrovirology, *5:* 4, 2008.
254. Huppi, K., Volfovsky, N., Runfola, T., Jones, T. L., Mackiewicz, M., Martin, S. E., Mushinski, J. F., Stephens, R., and Caplen, N. J. The identification of microRNAs in a genomically unstable region of human chromosome 8q24. Mol Cancer Res, *6:* 212-221, 2008.
255. Baudis, M. and Cleary, M. L. Progenetix.net: an online repository for molecular cytogenetic aberration data. Bioinformatics, *17:* 1228-1229, 2001.
256. Serrano, M., Lin, A. W., McCurrach, M. E., Beach, D., and Lowe, S. W. Oncogenic ras provokes premature cell senescence associated with accumulation of p53 and p16INK4a. Cell, *88:* 593-602, 1997.
257. Halazonetis, T. D., Gorgoulis, V. G., and Bartek, J. An oncogene-induced DNA damage model for cancer development. Science, *319:* 1352-1355, 2008.
258. Fan, C., Quan, R., Feng, X., Gillis, A., He, L., Matsumoto, E. D., Salama, S., Cutz, J. C., Kapoor, A., and Tang, D. ATM activation is accompanied with earlier stages of prostate tumorigenesis. Biochim Biophys Acta, *1763:* 1090-1097, 2006.
259. Braig, M., Lee, S., Loddenkemper, C., Rudolph, C., Peters, A. H., Schlegelberger, B., Stein, H., Dorken, B., Jenuwein, T., and Schmitt, C. A. Oncogene-induced senescence as an initial barrier in lymphoma development. Nature, *436:* 660-665, 2005.
260. Collado, M., Gil, J., Efeyan, A., Guerra, C., Schuhmacher, A. J., Barradas, M., Benguria, A., Zaballos, A., Flores, J. M., Barbacid, M., Beach, D., and Serrano, M. Tumour biology: senescence in premalignant tumours. Nature, *436:* 642, 2005.
261. Meeker, A. K. Telomeres and telomerase in prostatic intraepithelial neoplasia and prostate cancer biology. Urol Oncol, *24:* 122-130, 2006.
262. Tao, W. and Levine, A. J. P19(ARF) stabilizes p53 by blocking nucleo-cytoplasmic shuttling of Mdm2. Proc Natl Acad Sci U S A, *96:* 6937-6941, 1999.
263. Zindy, F., Eischen, C. M., Randle, D. H., Kamijo, T., Cleveland, J. L., Sherr, C. J., and Roussel, M. F. Myc signaling via the ARF tumor suppressor regulates p53-dependent apoptosis and immortalization. Genes Dev, *12:* 2424-2433, 1998.
264. Downing, S. R., Russell, P. J., and Jackson, P. Alterations of p53 are common in early stage prostate cancer. Can J Urol, *10:* 1924-1933, 2003.
265. Petrescu, A., Marzan, L., Codreanu, O., and Niculescu, L. Immunohistochemical detection of p53 protein as a prognostic indicator in prostate carcinoma. Rom J Morphol Embryol, *47:* 143-146, 2006.

266. Zeng, L., Rowland, R. G., Lele, S. M., and Kyprianou, N. Apoptosis incidence and protein expression of p53, TGF-beta receptor II, p27Kip1, and Smad4 in benign, premalignant, and malignant human prostate. Hum Pathol, *35:* 290-297, 2004.
267. Incognito, L. S., Cazares, L. H., Schellhammer, P. F., Kuban, D. A., Van Dyk, E. O., Moriarty, R. P., Wright, G. L., Jr., and Somers, K. D. Overexpression of p53 in prostate carcinoma is associated with improved overall survival but not predictive of response to radiotherapy. Int J Oncol, *17:* 761-769, 2000.
268. Merseburger, A. S., Kuczyk, M. A., Serth, J., Bokemeyer, C., Young, D. Y., Sun, L., Connelly, R. R., McLeod, D. G., Mostofi, F. K., Srivastava, S. K., Stenzl, A., Moul, J. W., and Sesterhenn, I. A. Limitations of tissue microarrays in the evaluation of focal alterations of bcl-2 and p53 in whole mount derived prostate tissues. Oncol Rep, *10:* 223-228, 2003.
269. Abaza, R., Diaz, L. K., Jr., Laskin, W. B., and Pins, M. R. Prognostic value of DNA ploidy, bcl-2 and p53 in localized prostate adenocarcinoma incidentally discovered at transurethral prostatectomy. J Urol, *176:* 2701-2705, 2006.
270. Stackhouse, G. B., Sesterhenn, I. A., Bauer, J. J., Mostofi, F. K., Connelly, R. R., Srivastava, S. K., and Moul, J. W. p53 and bcl-2 immunohistochemistry in pretreatment prostate needle biopsies to predict recurrence of prostate cancer after radical prostatectomy. J Urol, *162:* 2040-2045, 1999.
271. Al-Maghrabi, J. A. Chromosomal instability detected by interphase fluorescence in situ hybridization and its relation to p53 alteration in prostate carcinoma in Saudi patients. Saudi Med J, *26:* 379-384, 2005.
272. Fonseca, G. N., Srougi, M., Leite, K. R., Nesrallah, L. J., and Ortiz, V. The role of HER2/neu, BCL2, p53 genes and proliferating cell nuclear protein as molecular prognostic parameters in localized prostate carcinoma. Sao Paulo Med J, *122:* 124-127, 2004.
273. Sasor, A., Wagrowska-Danilewicz, M., and Danilewicz, M. Ki-67 antigen and P53 protein expression in benign and malignant prostatic lesions. Immunohistochemical quantitative study. Pol J Pathol, *51:* 31-36, 2000.
274. Kallakury, B. V., Jennings, T. A., Ross, J. S., Breese, K., Figge, H. L., Fisher, H. A., and Figge, J. Alteration of the p53 locus in benign hyperplastic prostatic epithelium associated with high-grade prostatic adenocarcinoma. Diagn Mol Pathol, *3:* 227-232, 1994.
275. Aprikian, A. G., Sarkis, A. S., Fair, W. R., Zhang, Z. F., Fuks, Z., and Cordon-Cardo, C. Immunohistochemical determination of p53 protein nuclear accumulation in prostatic adenocarcinoma. J Urol, *151:* 1276-1280, 1994.
276. Henke, R. P., Kruger, E., Ayhan, N., Hubner, D., Hammerer, P., and Huland, H. Immunohistochemical detection of p53 protein in human prostatic cancer. J Urol, *152:* 1297-1301, 1994.
277. Massenkeil, G., Oberhuber, H., Hailemariam, S., Sulser, T., Diener, P. A., Bannwart, F., Schafer, R., and Schwarte-Waldhoff, I. P53 mutations and loss of heterozygosity on chromosomes 8p, 16q, 17p, and 18q are confined to advanced prostate cancer. Anticancer Res, *14:* 2785-2790, 1994.
278. Myers, R. B., Oelschlager, D., Srivastava, S., and Grizzle, W. E. Accumulation of the p53 protein occurs more frequently in metastatic than in localized prostatic adenocarcinomas. Prostate, *25:* 243-248, 1994.
279. Mirchandani, D., Zheng, J., Miller, G. J., Ghosh, A. K., Shibata, D. K., Cote, R. J., and Roy-Burman, P. Heterogeneity in intratumor distribution of p53 mutations in human prostate cancer. Am J Pathol, *147:* 92-101, 1995.

280. Griewe, G. L., Dean, R. C., Zhang, W., Young, D., Sesterhenn, I. A., Shanmugam, N., McLeod, D. G., Moul, J. W., and Srivastava, S. p53 Immunostaining guided laser capture microdissection (p53-LCM) defines the presence of p53 gene mutations in focal regions of primary prostate cancer positive for p53 protein. Prostate Cancer Prostatic Dis, *6:* 281-285, 2003.
281. Troester, M. A., Herschkowitz, J. I., Oh, D. S., He, X., Hoadley, K. A., Barbier, C. S., and Perou, C. M. Gene expression patterns associated with p53 status in breast cancer. BMC Cancer, *6:* 276, 2006.
282. Miller, L. D., Smeds, J., George, J., Vega, V. B., Vergara, L., Ploner, A., Pawitan, Y., Hall, P., Klaar, S., Liu, E. T., and Bergh, J. An expression signature for p53 status in human breast cancer predicts mutation status, transcriptional effects, and patient survival. Proc Natl Acad Sci U S A, *102:* 13550-13555, 2005.
283. Leite, K. R., Franco, M. F., Srougi, M., Nesrallah, L. J., Nesrallah, A., Bevilacqua, R. G., Darini, E., Carvalho, C. M., Meirelles, M. I., Santana, I., and Camara-Lopes, L. H. Abnormal expression of MDM2 in prostate carcinoma. Mod Pathol, *14:* 428-436, 2001.
284. Girinsky, T., Koumenis, C., Graeber, T. G., Peehl, D. M., and Giaccia, A. J. Attenuated response of p53 and p21 in primary cultures of human prostatic epithelial cells exposed to DNA-damaging agents. Cancer Res, *55:* 3726-3731, 1995.
285. Sherr, C. J. Cancer cell cycles. Science, *274:* 1672-1677, 1996.
286. Greenberg, N. M., DeMayo, F., Finegold, M. J., Medina, D., Tilley, W. D., Aspinall, J. O., Cunha, G. R., Donjacour, A. A., Matusik, R. J., and Rosen, J. M. Prostate cancer in a transgenic mouse. Proc Natl Acad Sci U S A, *92:* 3439-3443, 1995.
287. Wang, Y., Hayward, S. W., Donjacour, A. A., Young, P., Jacks, T., Sage, J., Dahiya, R., Cardiff, R. D., Day, M. L., and Cunha, G. R. Sex hormone-induced carcinogenesis in Rb-deficient prostate tissue. Cancer Res, *60:* 6008-6017, 2000.
288. Lee, C. T., Capodieci, P., Osman, I., Fazzari, M., Ferrara, J., Scher, H. I., and Cordon-Cardo, C. Overexpression of the cyclin-dependent kinase inhibitor p16 is associated with tumor recurrence in human prostate cancer. Clin Cancer Res, *5:* 977-983, 1999.
289. Henshall, S. M., Quinn, D. I., Lee, C. S., Head, D. R., Golovsky, D., Brenner, P. C., Delprado, W., Stricker, P. D., Grygiel, J. J., and Sutherland, R. L. Overexpression of the cell cycle inhibitor p16INK4A in high-grade prostatic intraepithelial neoplasia predicts early relapse in prostate cancer patients. Clin Cancer Res, *7:* 544-550, 2001.
290. Jarrard, D. F., Modder, J., Fadden, P., Fu, V., Sebree, L., Heisey, D., Schwarze, S. R., and Friedl, A. Alterations in the p16/pRb cell cycle checkpoint occur commonly in primary and metastatic human prostate cancer. Cancer Lett, *185:* 191-199, 2002.
291. Jacobs, J. J., Kieboom, K., Marino, S., DePinho, R. A., and van Lohuizen, M. The oncogene and Polycomb-group gene bmi-1 regulates cell proliferation and senescence through the ink4a locus. Nature, *397:* 164-168, 1999.
292. Sharpless, N. E. and DePinho, R. A. Telomeres, stem cells, senescence, and cancer. J Clin Invest, *113:* 160-168, 2004.
293. Jarrard, D. F., Sarkar, S., Shi, Y., Yeager, T. R., Magrane, G., Kinoshita, H., Nassif, N., Meisner, L., Newton, M. A., Waldman, F. M., and Reznikoff, C. A. p16/pRb pathway alterations are required for bypassing senescence in human prostate epithelial cells. Cancer Res, *59:* 2957-2964, 1999.
294. Shaffer, D. R., Viale, A., Ishiwata, R., Leversha, M., Olgac, S., Manova, K., Satagopan, J., Scher, H., and Koff, A. Evidence for a p27 tumor suppressive function independent of its role regulating cell proliferation in the prostate. Proc Natl Acad Sci U S A, *102:* 210-215, 2005.

295. Li, R., Wheeler, T. M., Dai, H., Sayeeduddin, M., Scardino, P. T., Frolov, A., and Ayala, G. E. Biological correlates of p27 compartmental expression in prostate cancer. J Urol, *175:* 528-532, 2006.
296. Revelos, K., Petraki, C., Gregorakis, A., Scorilas, A., Papanastasiou, P., Tenta, R., and Koutsilieris, M. p27(kip1) and Ki-67 (MIB1) immunohistochemical expression in radical prostatectomy specimens of patients with clinically localized prostate cancer. In Vivo, *19:* 911-920, 2005.
297. De Marzo, A. M., Meeker, A. K., Epstein, J. I., and Coffey, D. S. Prostate stem cell compartments: expression of the cell cycle inhibitor p27Kip1 in normal, hyperplastic, and neoplastic cells. Am J Pathol, *153:* 911-919, 1998.
298. Majumder, P. K., Grisanzio, C., O'Connell, F., Barry, M., Brito, J. M., Xu, Q., Guney, I., Berger, R., Herman, P., Bikoff, R., Fedele, G., Baek, W. K., Wang, S., Ellwood-Yen, K., Wu, H., Sawyers, C. L., Signoretti, S., Hahn, W. C., Loda, M., and Sellers, W. R. A prostatic intraepithelial neoplasia-dependent p27 Kip1 checkpoint induces senescence and inhibits cell proliferation and cancer progression. Cancer Cell, *14:* 146-155, 2008.
299. Stokoe, D. Pten. Curr Biol, *11:* R502, 2001.
300. Li, J., Yen, C., Liaw, D., Podsypanina, K., Bose, S., Wang, S. I., Puc, J., Miliaresis, C., Rodgers, L., McCombie, R., Bigner, S. H., Giovanella, B. C., Ittmann, M., Tycko, B., Hibshoosh, H., Wigler, M. H., and Parsons, R. PTEN, a putative protein tyrosine phosphatase gene mutated in human brain, breast, and prostate cancer. Science, *275:* 1943-1947, 1997.
301. Myers, M. P., Stolarov, J. P., Eng, C., Li, J., Wang, S. I., Wigler, M. H., Parsons, R., and Tonks, N. K. P-TEN, the tumor suppressor from human chromosome 10q23, is a dual-specificity phosphatase. Proc Natl Acad Sci U S A, *94:* 9052-9057, 1997.
302. Cantley, L. C. and Neel, B. G. New insights into tumor suppression: PTEN suppresses tumor formation by restraining the phosphoinositide 3-kinase/AKT pathway. Proc Natl Acad Sci U S A, *96:* 4240-4245, 1999.
303. Vivanco, I., Palaskas, N., Tran, C., Finn, S. P., Getz, G., Kennedy, N. J., Jiao, J., Rose, J., Xie, W., Loda, M., Golub, T., Mellinghoff, I. K., Davis, R. J., Wu, H., and Sawyers, C. L. Identification of the JNK Signaling Pathway as a Functional Target of the Tumor Suppressor PTEN. Cancer Cell, *11:* 555-569, 2007.
304. Datta, S. R., Dudek, H., Tao, X., Masters, S., Fu, H., Gotoh, Y., and Greenberg, M. E. Akt phosphorylation of BAD couples survival signals to the cell-intrinsic death machinery. Cell, *91:* 231-241, 1997.
305. Cardone, M. H., Roy, N., Stennicke, H. R., Salvesen, G. S., Franke, T. F., Stanbridge, E., Frisch, S., and Reed, J. C. Regulation of cell death protease caspase-9 by phosphorylation. Science, *282:* 1318-1321, 1998.
306. Ashcroft, M., Ludwig, R. L., Woods, D. B., Copeland, T. D., Weber, H. O., MacRae, E. J., and Vousden, K. H. Phosphorylation of HDM2 by Akt. Oncogene, *21:* 1955-1962, 2002.
307. Graff, J. R., Konicek, B. W., McNulty, A. M., Wang, Z., Houck, K., Allen, S., Paul, J. D., Hbaiu, A., Goode, R. G., Sandusky, G. E., Vessella, R. L., and Neubauer, B. L. Increased AKT activity contributes to prostate cancer progression by dramatically accelerating prostate tumor growth and diminishing p27Kip1 expression. J Biol Chem, *275:* 24500-24505, 2000.
308. Scott, P. H. and Lawrence, J. C., Jr. Attenuation of mammalian target of rapamycin activity by increased cAMP in 3T3-L1 adipocytes. J Biol Chem, *273:* 34496-34501, 1998.

309. Ozes, O. N., Mayo, L. D., Gustin, J. A., Pfeffer, S. R., Pfeffer, L. M., and Donner, D. B. NF-kappaB activation by tumour necrosis factor requires the Akt serine-threonine kinase. Nature, *401:* 82-85, 1999.
310. Sharma, M., Chuang, W. W., and Sun, Z. Phosphatidylinositol 3-kinase/Akt stimulates androgen pathway through GSK3beta inhibition and nuclear beta-catenin accumulation. J Biol Chem, *277:* 30935-30941, 2002.
311. Puc, J., Keniry, M., Li, H. S., Pandita, T. K., Choudhury, A. D., Memeo, L., Mansukhani, M., Murty, V. V., Gaciong, Z., Meek, S. E., Piwnica-Worms, H., Hibshoosh, H., and Parsons, R. Lack of PTEN sequesters CHK1 and initiates genetic instability. Cancer Cell, *7:* 193-204, 2005.
312. Wu, Z., Cho, H., Hampton, G. M., and Theodorescu, D. Cdc6 and cyclin E2 are PTEN-regulated genes associated with human prostate cancer metastasis. Neoplasia, *11:* 66-76, 2009.
313. Blanco-Aparicio, C., Renner, O., Leal, J. F., and Carnero, A. Pten, More Than the Akt Pathway. Carcinogenesis, 2007.
314. Shen, W. H., Balajee, A. S., Wang, J., Wu, H., Eng, C., Pandolfi, P. P., and Yin, Y. Essential role for nuclear PTEN in maintaining chromosomal integrity. Cell, *128:* 157-170, 2007.
315. Lee, J. T., Lehmann, B. D., Terrian, D. M., Chappell, W. H., Stivala, F., Libra, M., Martelli, A. M., Steelman, L. S., and McCubrey, J. A. Targeting prostate cancer based on signal transduction and cell cycle pathways. Cell Cycle, *7*, 2008.
316. Di Cristofano, A., Pesce, B., Cordon-Cardo, C., and Pandolfi, P. P. Pten is essential for embryonic development and tumour suppression. Nat Genet, *19:* 348-355, 1998.
317. Kwabi-Addo, B., Giri, D., Schmidt, K., Podsypanina, K., Parsons, R., Greenberg, N., and Ittmann, M. Haploinsufficiency of the Pten tumor suppressor gene promotes prostate cancer progression. Proc Natl Acad Sci U S A, *98:* 11563-11568, 2001.
318. Di Cristofano, A., De Acetis, M., Koff, A., Cordon-Cardo, C., and Pandolfi, P. P. Pten and p27KIP1 cooperate in prostate cancer tumor suppression in the mouse. Nat Genet, *27:* 222-224, 2001.
319. Abate-Shen, C., Banach-Petrosky, W. A., Sun, X., Economides, K. D., Desai, N., Gregg, J. P., Borowsky, A. D., Cardiff, R. D., and Shen, M. M. Nkx3.1; Pten mutant mice develop invasive prostate adenocarcinoma and lymph node metastases. Cancer Res, *63:* 3886-3890, 2003.
320. You, M. J., Castrillon, D. H., Bastian, B. C., O'Hagan, R. C., Bosenberg, M. W., Parsons, R., Chin, L., and DePinho, R. A. Genetic analysis of Pten and Ink4a/Arf interactions in the suppression of tumorigenesis in mice. Proc Natl Acad Sci U S A, *99:* 1455-1460, 2002.
321. Ma, X., Ziel-van der Made, A. C., Autar, B., van der Korput, H. A., Vermeij, M., van Duijn, P., Cleutjens, K. B., de Krijger, R., Krimpenfort, P., Berns, A., van der Kwast, T. H., and Trapman, J. Targeted biallelic inactivation of Pten in the mouse prostate leads to prostate cancer accompanied by increased epithelial cell proliferation but not by reduced apoptosis. Cancer Res, *65:* 5730-5739, 2005.
322. Chen, M. L., Xu, P. Z., Peng, X. D., Chen, W. S., Guzman, G., Yang, X., Di Cristofano, A., Pandolfi, P. P., and Hay, N. The deficiency of Akt1 is sufficient to suppress tumor development in Pten+/- mice. Genes Dev, *20:* 1569-1574, 2006.
323. Covey, T. M., Edes, K., and Fitzpatrick, F. A. Akt activation by arachidonic acid metabolism occurs via oxidation and inactivation of PTEN tumor suppressor. Oncogene, *26:* 5784-5792, 2007.

324. Verhagen, P. C., van Duijn, P. W., Hermans, K. G., Looijenga, L. H., van Gurp, R. J., Stoop, H., van der Kwast, T. H., and Trapman, J. The PTEN gene in locally progressive prostate cancer is preferentially inactivated by bi-allelic gene deletion. J Pathol, *208:* 699-707, 2006.
325. Bedolla, R., Prihoda, T. J., Kreisberg, J. I., Malik, S. N., Krishnegowda, N. K., Troyer, D. A., and Ghosh, P. M. Determining risk of biochemical recurrence in prostate cancer by immunohistochemical detection of PTEN expression and Akt activation. Clin Cancer Res, *13:* 3860-3867, 2007.
326. McMenamin, M. E., Soung, P., Perera, S., Kaplan, I., Loda, M., and Sellers, W. R. Loss of PTEN expression in paraffin-embedded primary prostate cancer correlates with high Gleason score and advanced stage. Cancer Res, *59:* 4291-4296, 1999.
327. Koksal, I. T., Dirice, E., Yasar, D., Sanlioglu, A. D., Ciftcioglu, A., Gulkesen, K. H., Ozes, N. O., Baykara, M., Luleci, G., and Sanlioglu, S. The assessment of PTEN tumor suppressor gene in combination with Gleason scoring and serum PSA to evaluate progression of prostate carcinoma. Urol Oncol, *22:* 307-312, 2004.
328. Kreisberg, J. I., Malik, S. N., Prihoda, T. J., Bedolla, R. G., Troyer, D. A., Kreisberg, S., and Ghosh, P. M. Phosphorylation of Akt (Ser473) is an excellent predictor of poor clinical outcome in prostate cancer. Cancer Res, *64:* 5232-5236, 2004.
329. Schmitz, M., Grignard, G., Margue, C., Dippel, W., Capesius, C., Mossong, J., Nathan, M., Giacchi, S., Scheiden, R., and Kieffer, N. Complete loss of PTEN expression as a possible early prognostic marker for prostate cancer metastasis. Int J Cancer, *120:* 1284-1292, 2007.
330. Yoshimoto, M., Cunha, I. W., Coudry, R. A., Fonseca, F. P., Torres, C. H., Soares, F. A., and Squire, J. A. FISH analysis of 107 prostate cancers shows that PTEN genomic deletion is associated with poor clinical outcome. Br J Cancer, *97:* 678-685, 2007.
331. Vocke, C. D., Pozzatti, R. O., Bostwick, D. G., Florence, C. D., Jennings, S. B., Strup, S. E., Duray, P. H., Liotta, L. A., Emmert-Buck, M. R., and Linehan, W. M. Analysis of 99 microdissected prostate carcinomas reveals a high frequency of allelic loss on chromosome 8p12-21. Cancer Res, *56:* 2411-2416, 1996.
332. Kim, M. J., Bhatia-Gaur, R., Banach-Petrosky, W. A., Desai, N., Wang, Y., Hayward, S. W., Cunha, G. R., Cardiff, R. D., Shen, M. M., and Abate-Shen, C. Nkx3.1 mutant mice recapitulate early stages of prostate carcinogenesis. Cancer Res, *62:* 2999-3004, 2002.
333. Gao, H., Ouyang, X., Banach-Petrosky, W., Borowsky, A. D., Lin, Y., Kim, M., Lee, H., Shih, W. J., Cardiff, R. D., Shen, M. M., and Abate-Shen, C. A critical role for p27kip1 gene dosage in a mouse model of prostate carcinogenesis. Proc Natl Acad Sci U S A, *101:* 17204-17209, 2004.
334. Asatiani, E., Huang, W. X., Wang, A., Rodriguez Ortner, E., Cavalli, L. R., Haddad, B. R., and Gelmann, E. P. Deletion, methylation, and expression of the NKX3.1 suppressor gene in primary human prostate cancer. Cancer Res, *65:* 1164-1173, 2005.
335. Gelmann, E. and Markowski, M. C. Inflammatory Cytokines Induce Ubiquitination and Loss of Prostate Suppressor NKX3.1. IMPaCT (Innovative Minds in Prostate Cancer Today). Atlanta, Georgia: US Army Medical Research and Material Command, 2007.
336. Ouyang, X., DeWeese, T. L., Nelson, W. G., and Abate-Shen, C. Loss-of-function of Nkx3.1 promotes increased oxidative damage in prostate carcinogenesis. Cancer Res, *65:* 6773-6779, 2005.
337. Lei, Q., Jiao, J., Xin, L., Chang, C. J., Wang, S., Gao, J., Gleave, M. E., Witte, O. N., Liu, X., and Wu, H. NKX3.1 stabilizes p53, inhibits AKT activation, and blocks prostate cancer initiation caused by PTEN loss. Cancer Cell, *9:* 367-378, 2006.

338. Yan, G., Fukabori, Y., McBride, G., Nikolaropolous, S., and McKeehan, W. L. Exon switching and activation of stromal and embryonic fibroblast growth factor (FGF)-FGF receptor genes in prostate epithelial cells accompany stromal independence and malignancy. Mol Cell Biol, *13:* 4513-4522, 1993.
339. Olumi, A. F., Grossfeld, G. D., Hayward, S. W., Carroll, P. R., Tlsty, T. D., and Cunha, G. R. Carcinoma-associated fibroblasts direct tumor progression of initiated human prostatic epithelium. Cancer Res, *59:* 5002-5011, 1999.
340. Chang, S. M. and Chung, L. W. Interaction between prostatic fibroblast and epithelial cells in culture: role of androgen. Endocrinology, *125:* 2719-2727, 1989.
341. Stephenson, R. A., Dinney, C. P., Gohji, K., Ordonez, N. G., Killion, J. J., and Fidler, I. J. Metastatic model for human prostate cancer using orthotopic implantation in nude mice. J Natl Cancer Inst, *84:* 951-957, 1992.
342. Chung, L. W., Baseman, A., Assikis, V., and Zhau, H. E. Molecular insights into prostate cancer progression: the missing link of tumor microenvironment. J Urol, *173:* 10-20, 2005.
343. Sugimura, Y., Cunha, G. R., and Bigsby, R. M. Androgenic induction of DNA synthesis in prostatic glands induced in the urothelium of testicular feminized (Tfm/Y) mice. Prostate, *9:* 217-225, 1986.
344. Condon, M. S. and Bosland, M. C. The role of stromal cells in prostate cancer development and progression. In Vivo, *13:* 61-65, 1999.
345. Tlsty, T. D. and Hein, P. W. Know thy neighbor: stromal cells can contribute oncogenic signals. Curr Opin Genet Dev, *11:* 54-59, 2001.
346. Tuxhorn, J. A., Ayala, G. E., Smith, M. J., Smith, V. C., Dang, T. D., and Rowley, D. R. Reactive stroma in human prostate cancer: induction of myofibroblast phenotype and extracellular matrix remodeling. Clin Cancer Res, *8:* 2912-2923, 2002.
347. Feng, X. H. and Derynck, R. Specificity and versatility in tgf-beta signaling through Smads. Annu Rev Cell Dev Biol, *21:* 659-693, 2005.
348. Guo, Y. and Kyprianou, N. Restoration of transforming growth factor beta signaling pathway in human prostate cancer cells suppresses tumorigenicity via induction of caspase-1-mediated apoptosis. Cancer Res, *59:* 1366-1371, 1999.
349. Kyprianou, N. Activation of TGF-beta signalling in human prostate cancer cells suppresses tumorigenicity via deregulation of cell cycle progression and induction of caspase-1 mediated apoptosis: significance in prostate tumorigenesis. Prostate Cancer Prostatic Dis, *2:* S18, 1999.
350. Gajewska, M. and Motyl, T. IGF-binding proteins mediate TGF-beta 1-induced apoptosis in bovine mammary epithelial BME-UV1 cells. Comp Biochem Physiol C Toxicol Pharmacol, *139:* 65-75, 2004.
351. Peehl, D. M. and Sellers, R. G. Induction of smooth muscle cell phenotype in cultured human prostatic stromal cells. Exp Cell Res, *232:* 208-215, 1997.
352. Bhowmick, N. A., Chytil, A., Plieth, D., Gorska, A. E., Dumont, N., Shappell, S., Washington, M. K., Neilson, E. G., and Moses, H. L. TGF-beta signaling in fibroblasts modulates the oncogenic potential of adjacent epithelia. Science, *303:* 848-851, 2004.
353. Gerdes, M. J., Dang, T. D., Larsen, M., and Rowley, D. R. Transforming growth factor-beta1 induces nuclear to cytoplasmic distribution of androgen receptor and inhibits androgen response in prostate smooth muscle cells. Endocrinology, *139:* 3569-3577, 1998.
354. Guo, Y., Jacobs, S. C., and Kyprianou, N. Down-regulation of protein and mRNA expression for transforming growth factor-beta (TGF-beta1) type I and type II receptors in human prostate cancer. Int J Cancer, *71:* 573-579, 1997.

355. Zhao, H., Shiina, H., Greene, K. L., Li, L. C., Tanaka, Y., Kishi, H., Igawa, M., Kane, C. J., Carroll, P., and Dahiya, R. CpG methylation at promoter site -140 inactivates TGFbeta2 receptor gene in prostate cancer. Cancer, *104:* 44-52, 2005.
356. Bello-DeOcampo, D. and Tindall, D. J. TGF-betal/Smad signaling in prostate cancer. Curr Drug Targets, *4:* 197-207, 2003.
357. Verona, E. V., Elkahloun, A. G., Yang, J., Bandyopadhyay, A., Yeh, I. T., and Sun, L. Z. Transforming growth factor-beta signaling in prostate stromal cells supports prostate carcinoma growth by up-regulating stromal genes related to tissue remodeling. Cancer Res, *67:* 5737-5746, 2007.
358. Yang, F., Tuxhorn, J. A., Ressler, S. J., McAlhany, S. J., Dang, T. D., and Rowley, D. R. Stromal expression of connective tissue growth factor promotes angiogenesis and prostate cancer tumorigenesis. Cancer Res, *65:* 8887-8895, 2005.
359. Jones, J. I. and Clemmons, D. R. Insulin-like growth factors and their binding proteins: biological actions. Endocr Rev, *16:* 3-34, 1995.
360. Meinbach, D. S. and Lokeshwar, B. L. Insulin-like growth factors and their binding proteins in prostate cancer: cause or consequence? Urol Oncol, *24:* 294-306, 2006.
361. Baserga, R., Peruzzi, F., and Reiss, K. The IGF-1 receptor in cancer biology. Int J Cancer, *107:* 873-877, 2003.
362. Kaplan, P. J., Mohan, S., Cohen, P., Foster, B. A., and Greenberg, N. M. The insulin-like growth factor axis and prostate cancer: lessons from the transgenic adenocarcinoma of mouse prostate (TRAMP) model. Cancer Res, *59:* 2203-2209, 1999.
363. Foster, B. A., Kaplan, P. J., and Greenberg, N. M. Peptide growth factors and prostate cancer: new models, new opportunities. Cancer Metastasis Rev, *17:* 317-324, 1998.
364. Nickerson, T., Chang, F., Lorimer, D., Smeekens, S. P., Sawyers, C. L., and Pollak, M. In vivo progression of LAPC-9 and LNCaP prostate cancer models to androgen independence is associated with increased expression of insulin-like growth factor I (IGF-I) and IGF-I receptor (IGF-IR). Cancer Res, *61:* 6276-6280, 2001.
365. Mauro, L., Salerno, M., Morelli, C., Boterberg, T., Bracke, M. E., and Surmacz, E. Role of the IGF-I receptor in the regulation of cell-cell adhesion: implications in cancer development and progression. J Cell Physiol, *194:* 108-116, 2003.
366. Miyake, H., Nelson, C., Rennie, P. S., and Gleave, M. E. Overexpression of insulin-like growth factor binding protein-5 helps accelerate progression to androgen-independence in the human prostate LNCaP tumor model through activation of phosphatidylinositol 3'-kinase pathway. Endocrinology, *141:* 2257-2265, 2000.
367. Juul, A. Serum levels of insulin-like growth factor I and its binding proteins in health and disease. Growth Horm IGF Res, *13:* 113-170, 2003.
368. Djavan, B., Waldert, M., Seitz, C., and Marberger, M. Insulin-like growth factors and prostate cancer. World J Urol, *19:* 225-233, 2001.
369. Moschos, S. J. and Mantzoros, C. S. The role of the IGF system in cancer: from basic to clinical studies and clinical applications. Oncology, *63:* 317-332, 2002.
370. Perry, A. S., Loftus, B., Moroose, R., Lynch, T. H., Hollywood, D., Watson, R. W., Woodson, K., and Lawler, M. In silico mining identifies IGFBP3 as a novel target of methylation in prostate cancer. Br J Cancer, 2007.
371. Silha, J. V., Sheppard, P. C., Mishra, S., Gui, Y., Schwartz, J., Dodd, J. G., and Murphy, L. J. Insulin-like growth factor (IGF) binding protein-3 attenuates prostate tumor growth by IGF-dependent and IGF-independent mechanisms. Endocrinology, *147:* 2112-2121, 2006.
372. Okada, H. and Mak, T. W. Pathways of apoptotic and non-apoptotic death in tumour cells. Nat Rev Cancer, *4:* 592-603, 2004.

373. Lassus, P., Opitz-Araya, X., and Lazebnik, Y. Requirement for caspase-2 in stress-induced apoptosis before mitochondrial permeabilization. Science, *297:* 1352-1354, 2002.
374. Kennedy, S. G., Kandel, E. S., Cross, T. K., and Hay, N. Akt/Protein kinase B inhibits cell death by preventing the release of cytochrome c from mitochondria. Mol Cell Biol, *19:* 5800-5810, 1999.
375. Khwaja, A. Akt is more than just a Bad kinase. Nature, *401:* 33-34, 1999.
376. Brunet, A., Bonni, A., Zigmond, M. J., Lin, M. Z., Juo, P., Hu, L. S., Anderson, M. J., Arden, K. C., Blenis, J., and Greenberg, M. E. Akt promotes cell survival by phosphorylating and inhibiting a Forkhead transcription factor. Cell, *96:* 857-868, 1999.
377. Brownawell, A. M., Kops, G. J., Macara, I. G., and Burgering, B. M. Inhibition of nuclear import by protein kinase B (Akt) regulates the subcellular distribution and activity of the forkhead transcription factor AFX. Mol Cell Biol, *21:* 3534-3546, 2001.
378. Rokhlin, O. W., Bishop, G. A., Hostager, B. S., Waldschmidt, T. J., Sidorenko, S. P., Pavloff, N., Kiefer, M. C., Umansky, S. R., Glover, R. A., and Cohen, M. B. Fas-mediated apoptosis in human prostatic carcinoma cell lines. Cancer Res, *57:* 1758-1768, 1997.
379. Nimmanapalli, R., Perkins, C. L., Orlando, M., O'Bryan, E., Nguyen, D., and Bhalla, K. N. Pretreatment with paclitaxel enhances apo-2 ligand/tumor necrosis factor-related apoptosis-inducing ligand-induced apoptosis of prostate cancer cells by inducing death receptors 4 and 5 protein levels. Cancer Res, *61:* 759-763, 2001.
380. Tolonen, T. T., Tommola, S., Jokinen, S., Parviainen, T., and Martikainen, P. M. Bax and Bcl-2 are focally overexpressed in the normal epithelium of cancerous prostates. Scand J Urol Nephrol, *41:* 85-90, 2007.
381. Haussler, O., Epstein, J. I., Amin, M. B., Heitz, P. U., and Hailemariam, S. Cell proliferation, apoptosis, oncogene, and tumor suppressor gene status in adenosis with comparison to benign prostatic hyperplasia, prostatic intraepithelial neoplasia, and cancer. Hum Pathol, *30:* 1077-1086, 1999.
382. Baltaci, S., Orhan, D., Ozer, G., Tolunay, O., and Gogous, O. Bcl-2 proto-oncogene expression in low- and high-grade prostatic intraepithelial neoplasia. BJU Int, *85:* 155-159, 2000.
383. McDonnell, T. J., Troncoso, P., Brisbay, S. M., Logothetis, C., Chung, L. W., Hsieh, J. T., Tu, S. M., and Campbell, M. L. Expression of the protooncogene bcl-2 in the prostate and its association with emergence of androgen-independent prostate cancer. Cancer Res, *52:* 6940-6944, 1992.
384. Krajewska, M., Krajewski, S., Epstein, J. I., Shabaik, A., Sauvageot, J., Song, K., Kitada, S., and Reed, J. C. Immunohistochemical analysis of bcl-2, bax, bcl-X, and mcl-1 expression in prostate cancers. Am J Pathol, *148:* 1567-1576, 1996.
385. Stattin, P., Damber, J. E., Karlberg, L., Nordgren, H., and Bergh, A. Bcl-2 immunoreactivity in prostate tumorigenesis in relation to prostatic intraepithelial neoplasia, grade, hormonal status, metastatic growth and survival. Urol Res, *24:* 257-264, 1996.
386. Johnson, M. I., Robinson, M. C., Marsh, C., Robson, C. N., Neal, D. E., and Hamdy, F. C. Expression of Bcl-2, Bax, and p53 in high-grade prostatic intraepithelial neoplasia and localized prostate cancer: relationship with apoptosis and proliferation. Prostate, *37:* 223-229, 1998.
387. Sastry, K. S., Smith, A. J., Karpova, Y., Datta, S. R., and Kulik, G. Diverse antiapoptotic signaling pathways activated by vasoactive intestinal polypeptide, epidermal growth

factor, and phosphatidylinositol 3-kinase in prostate cancer cells converge on BAD. J Biol Chem, *281:* 20891-20901, 2006.
388. Lapointe, J., Li, C., Higgins, J. P., van de Rijn, M., Bair, E., Montgomery, K., Ferrari, M., Egevad, L., Rayford, W., Bergerheim, U., Ekman, P., DeMarzo, A. M., Tibshirani, R., Botstein, D., Brown, P. O., Brooks, J. D., and Pollack, J. R. Gene expression profiling identifies clinically relevant subtypes of prostate cancer. Proc Natl Acad Sci U S A, *101:* 811-816, 2004.
389. Lapointe, J., Li, C., Giacomini, C. P., Salari, K., Huang, S., Wang, P., Ferrari, M., Hernandez-Boussard, T., Brooks, J. D., and Pollack, J. R. Genomic profiling reveals alternative genetic pathways of prostate tumorigenesis. Cancer Res, *67:* 8504-8510, 2007.
390. Nelson, W. G., Yegnasubramanian, S., Agoston, A. T., Bastian, P. J., Lee, B. H., Nakayama, M., and De Marzo, A. M. Abnormal DNA methylation, epigenetics, and prostate cancer. Front Biosci, *12:* 4254-4266, 2007.
391. Hanahan, D. and Weinberg, R. A. The hallmarks of cancer. Cell, *100:* 57-70, 2000.
392. Wullich, B., Breitkreuz, T., Zwergel, T., Unteregger, G., Seitz, G., and Zang, K. D. Cytogenetic evidence of intratumoral focal heterogeneity in prostatic carcinomas. Urol Int, *48:* 372-377, 1992.
393. Vukovic, B., Beheshti, B., Park, P., Lim, G., Bayani, J., Zielenska, M., and Squire, J. A. Correlating breakage-fusion-bridge events with the overall chromosomal instability and in vitro karyotype evolution in prostate cancer. Cytogenet Genome Res, *116:* 1-11, 2007.
394. Chieffi, P., Cozzolino, L., Kisslinger, A., Libertini, S., Staibano, S., Mansueto, G., De Rosa, G., Villacci, A., Vitale, M., Linardopoulos, S., Portella, G., and Tramontano, D. Aurora B expression directly correlates with prostate cancer malignancy and influence prostate cell proliferation. Prostate, *66:* 326-333, 2006.
395. Rajasekaran, S. A., Christiansen, J. J., Schmid, I., Oshima, E., Sakamoto, K., Weinstein, J., Rao, N. P., and Rajasekaran, A. K. Prostate-specific membrane antigen associates with anaphase-promoting complex and induces chromosomal instability. Mol Cancer Ther, *7:* 2142-2151, 2008.
396. Gertler, R., Doll, D., Maak, M., Feith, M., and Rosenberg, R. Telomere length and telomerase subunits as diagnostic and prognostic biomarkers in Barrett carcinoma. Cancer, *112:* 2173-2180, 2008.
397. O'Sullivan, J. N., Bronner, M. P., Brentnall, T. A., Finley, J. C., Shen, W. T., Emerson, S., Emond, M. J., Gollahon, K. A., Moskovitz, A. H., Crispin, D. A., Potter, J. D., and Rabinovitch, P. S. Chromosomal instability in ulcerative colitis is related to telomere shortening. Nat Genet, *32:* 280-284, 2002.
398. Cottliar, A., Fundia, A., Boerr, L., Sambuelli, A., Negreira, S., Gil, A., Gomez, J. C., Chopita, N., Bernedo, A., and Slavutsky, I. High frequencies of telomeric associations, chromosome aberrations, and sister chromatid exchanges in ulcerative colitis. Am J Gastroenterol, *95:* 2301-2307, 2000.
399. Meeker, A. K., Hicks, J. L., Gabrielson, E., Strauss, W. M., De Marzo, A. M., and Argani, P. Telomere shortening occurs in subsets of normal breast epithelium as well as in situ and invasive carcinoma. Am J Pathol, *164:* 925-935, 2004.
400. Lantuejoul, S., Soria, J. C., Morat, L., Lorimier, P., Moro-Sibilot, D., Sabatier, L., Brambilla, C., and Brambilla, E. Telomere shortening and telomerase reverse transcriptase expression in preinvasive bronchial lesions. Clin Cancer Res, *11:* 2074-2082, 2005.

401. Fordyce, C. A., Heaphy, C. M., Joste, N. E., Smith, A. Y., Hunt, W. C., and Griffith, J. K. Association between cancer-free survival and telomere DNA content in prostate tumors. J Urol, *173:* 610-614, 2005.
402. Wu, X., Amos, C. I., Zhu, Y., Zhao, H., Grossman, B. H., Shay, J. W., Luo, S., Hong, W. K., and Spitz, M. R. Telomere dysfunction: a potential cancer predisposition factor. J Natl Cancer Inst, *95:* 1211-1218, 2003.
403. Tabori, U., Vukovic, B., Zielenska, M., Hawkins, C., Braude, I., Rutka, J., Bouffet, E., Squire, J., and Malkin, D. The role of telomere maintenance in the spontaneous growth arrest of pediatric low-grade gliomas. Neoplasia, *8:* 136-142, 2006.
404. Poon, S. S., Martens, U. M., Ward, R. K., and Lansdorp, P. M. Telomere length measurements using digital fluorescence microscopy. Cytometry, *36:* 267-278, 1999.
405. Abramoff, M. D., Magelhaes, P.J., Ram, S.J. Image Processing with ImageJ. Biophotonics International, *11:* 36-42, 2004.
406. Meeker, A. K. Improved Software for quantitative analysis of fluorescence microscopy images. Advancing practice, instruction and innovation through informatics. 2003.
407. Team, R. D. C. R: A Language and Environment for Statistical Computing. Vienna, Austria: R Foundation for Statistical Computing, 2006.
408. Koeneman, K. S., Pan, C. X., Jin, J. K., Pyle, J. M., 3rd, Flanigan, R. C., Shankey, T. V., and Diaz, M. O. Telomerase activity, telomere length, and DNA ploidy in prostatic intraepithelial neoplasia (PIN). J Urol, *160:* 1533-1539, 1998.
409. Zhang, W., Kapusta, L. R., Slingerland, J. M., and Klotz, L. H. Telomerase activity in prostate cancer, prostatic intraepithelial neoplasia, and benign prostatic epithelium. Cancer Res, *58:* 619-621, 1998.
410. von Zglinicki, T. Oxidative stress shortens telomeres. Trends Biochem Sci, *27:* 339-344, 2002.
411. Chen, Z., Trotman, L. C., Shaffer, D., Lin, H. K., Dotan, Z. A., Niki, M., Koutcher, J. A., Scher, H. I., Ludwig, T., Gerald, W., Cordon-Cardo, C., and Pandolfi, P. P. Crucial role of p53-dependent cellular senescence in suppression of Pten-deficient tumorigenesis. Nature, *436:* 725-730, 2005.
412. Bettendorf, O., Heine, B., Kneif, S., Eltze, E., Semjonow, A., Herbst, H., Stein, H., Bocker, W., and Poremba, C. Expression-patterns of the RNA component (hTR)and the catalytic subunit (hTERT) of human telomerase in nonneoplastic prostate tissue, prostatic intraepithelial neoplasia, and prostate cancer. Prostate, *55:* 99-104, 2003.
413. Donaldson, L., Fordyce, C., Gilliland, F., Smith, A., Feddersen, R., Joste, N., Moyzis, R., and Griffith, J. Association between outcome and telomere DNA content in prostate cancer. J Urol, *162:* 1788-1792, 1999.
414. Merseburger, A. S., Hennenlotter, J., Simon, P., Muller, C. C., Kuhs, U., Knuchel-Clarke, R., Moul, J. W., Stenzl, A., and Kuczyk, M. A. Activation of the PKB/Akt pathway in histological benign prostatic tissue adjacent to the primary malignant lesions. Oncol Rep, *16:* 79-83, 2006.
415. Oikawa, S., Tada-Oikawa, S., and Kawanishi, S. Site-specific DNA damage at the GGG sequence by UVA involves acceleration of telomere shortening. Biochemistry, *40:* 4763-4768, 2001.
416. Bavik, C., Coleman, I., Dean, J. P., Knudsen, B., Plymate, S., and Nelson, P. S. The gene expression program of prostate fibroblast senescence modulates neoplastic epithelial cell proliferation through paracrine mechanisms. Cancer Res, *66:* 794-802, 2006.
417. Nakashiro, K., Okamoto, M., Hayashi, Y., and Oyasu, R. Hepatocyte growth factor secreted by prostate-derived stromal cells stimulates growth of androgen-independent human prostatic carcinoma cells. Am J Pathol, *157:* 795-803, 2000.

418. Wu, Y. L., Dudognon, C., Nguyen, E., Hillion, J., Pendino, F., Tarkanyi, I., Aradi, J., Lanotte, M., Tong, J. H., Chen, G. Q., and Segal-Bendirdjian, E. Immunodetection of human telomerase reverse-transcriptase (hTERT) re-appraised: nucleolin and telomerase cross paths. J Cell Sci, *119:* 2797-2806, 2006.
419. Laxman, B., Tomlins, S. A., Mehra, R., Morris, D. S., Wang, L., Helgeson, B. E., Shah, R. B., Rubin, M. A., Wei, J. T., and Chinnaiyan, A. M. Noninvasive detection of TMPRSS2:ERG fusion transcripts in the urine of men with prostate cancer. Neoplasia, *8:* 885-888, 2006.
420. Paul, B., Dhir, R., Landsittel, D., Hitchens, M. R., and Getzenberg, R. H. Detection of prostate cancer with a blood-based assay for early prostate cancer antigen. Cancer Res, *65:* 4097-4100, 2005.
421. Stewart, J., Fleshner, N., Cole, H., Toi, A., and Sweet, J. Prognostic significance of alpha-methylacyl-coA racemase among men with high grade prostatic intraepithelial neoplasia in prostate biopsies. J Urol, *179:* 1751-1755; discussion 1755, 2008.
422. Helgeson, B. E., Tomlins, S. A., Shah, N., Laxman, B., Cao, Q., Prensner, J. R., Cao, X., Singla, N., Montie, J. E., Varambally, S., Mehra, R., and Chinnaiyan, A. M. Characterization of TMPRSS2:ETV5 and SLC45A3:ETV5 gene fusions in prostate cancer. Cancer Res, *68:* 73-80, 2008.
423. Teixeira, M. R. Chromosome mechanisms giving rise to the TMPRSS2-ERG fusion oncogene in prostate cancer and HGPIN lesions. Am J Surg Pathol, *32:* 642-644; author reply 644, 2008.
424. Staff, S., Isola, J. J., Johannsson, O., Borg, A., and Tanner, M. M. Frequent somatic loss of BRCA1 in breast tumours from BRCA2 germ-line mutation carriers and vice versa. Br J Cancer, *85:* 1201-1205, 2001.
425. Ventura, R. A., Martin-Subero, J. I., Jones, M., McParland, J., Gesk, S., Mason, D. Y., and Siebert, R. FISH analysis for the detection of lymphoma-associated chromosomal abnormalities in routine paraffin-embedded tissue. J Mol Diagn, *8:* 141-151, 2006.
426. Kim, T. S., Heinlein, C., Hackman, R. C., and Nelson, P. S. Phenotypic analysis of mice lacking the Tmprss2-encoded protease. Mol Cell Biol, *26:* 965-975, 2006.
427. Rubinstein, Y. R., Furusawa, T., Lim, J. H., Postnikov, Y. V., West, K. L., Birger, Y., Lee, S., Nguyen, P., Trepel, J. B., and Bustin, M. Chromosomal protein HMGN1 modulates the expression of N-cadherin. Febs J, *272:* 5853-5863, 2005.
428. Jaggi, M., Nazemi, T., Abrahams, N. A., Baker, J. J., Galich, A., Smith, L. M., and Balaji, K. C. N-cadherin switching occurs in high Gleason grade prostate cancer. Prostate, *66:* 193-199, 2006.
429. Birger, Y., Catez, F., Furusawa, T., Lim, J. H., Prymakowska-Bosak, M., West, K. L., Postnikov, Y. V., Haines, D. C., and Bustin, M. Increased tumorigenicity and sensitivity to ionizing radiation upon loss of chromosomal protein HMGN1. Cancer Res, *65:* 6711-6718, 2005.
430. Carbone, G. M., Napoli, S., Valentini, A., Cavalli, F., Watson, D. K., and Catapano, C. V. Triplex DNA-mediated downregulation of Ets2 expression results in growth inhibition and apoptosis in human prostate cancer cells. Nucleic Acids Res, *32:* 4358-4367, 2004.
431. Kolomietz, E., Al-Maghrabi, J., Brennan, S., Karaskova, J., Minkin, S., Lipton, J., and Squire, J. A. Primary chromosomal rearrangements of leukemia are frequently accompanied by extensive submicroscopic deletions and may lead to altered prognosis. Blood, *97:* 3581-3588, 2001.

432. Kolomietz, E., Meyn, M. S., Pandita, A., and Squire, J. A. The role of Alu repeat clusters as mediators of recurrent chromosomal aberrations in tumors. Genes Chromosomes Cancer, *35:* 97-112, 2002.
433. Nam, R. K., Sugar, L., Yang, W., Srivastava, S., Klotz, L. H., Yang, L. Y., Stanimirovic, A., Encioiu, E., Neill, M., Loblaw, D. A., Trachtenberg, J., Narod, S. A., and Seth, A. Expression of the TMPRSS2:ERG fusion gene predicts cancer recurrence after surgery for localised prostate cancer. Br J Cancer, *97:* 1690-1695, 2007.
434. Mehra, R., Tomlins, S. A., Yu, J., Cao, X., Wang, L., Menon, A., Rubin, M. A., Pienta, K. J., Shah, R. B., and Chinnaiyan, A. M. Characterization of TMPRSS2-ETS gene aberrations in androgen-independent metastatic prostate cancer. Cancer Res, *68:* 3584-3590, 2008.
435. Cattan, V., Mercier, N., Gardner, J. P., Regnault, V., Labat, C., Maki-Jouppila, J., Nzietchueng, R., Benetos, A., Kimura, M., Aviv, A., and Lacolley, P. Chronic oxidative stress induces a tissue-specific reduction in telomere length in CAST/Ei mice. Free Radic Biol Med, *44:* 1592-1598, 2008.
436. Houben, J. M., Moonen, H. J., van Schooten, F. J., and Hageman, G. J. Telomere length assessment: biomarker of chronic oxidative stress? Free Radic Biol Med, *44:* 235-246, 2008.
437. Allsopp, R. C., Chang, E., Kashefi-Aazam, M., Rogaev, E. I., Piatyszek, M. A., Shay, J. W., and Harley, C. B. Telomere shortening is associated with cell division in vitro and in vivo. Exp Cell Res, *220:* 194-200, 1995.
438. Grandin, N. and Charbonneau, M. Protection against chromosome degradation at the telomeres. Biochimie, *90:* 41-59, 2008.
439. Callen, E. and Surralles, J. Telomere dysfunction in genome instability syndromes. Mutat Res, *567:* 85-104, 2004.
440. Meyn, M. S. Chromosome instability syndromes: lessons for carcinogenesis. Curr Top Microbiol Immunol, *221:* 71-148, 1997.
441. Jeffs, A. R., Benjes, S. M., Smith, T. L., Sowerby, S. J., and Morris, C. M. The BCR gene recombines preferentially with Alu elements in complex BCR-ABL translocations of chronic myeloid leukaemia. Hum Mol Genet, *7:* 767-776, 1998.
442. Aplan, P. D. Causes of oncogenic chromosomal translocation. Trends Genet, *22:* 46-55, 2006.
443. Michaloglou, C., Vredeveld, L. C., Soengas, M. S., Denoyelle, C., Kuilman, T., van der Horst, C. M., Majoor, D. M., Shay, J. W., Mooi, W. J., and Peeper, D. S. BRAFE600-associated senescence-like cell cycle arrest of human naevi. Nature, *436:* 720-724, 2005.
444. Shin, I., Yakes, F. M., Rojo, F., Shin, N. Y., Bakin, A. V., Baselga, J., and Arteaga, C. L. PKB/Akt mediates cell-cycle progression by phosphorylation of p27(Kip1) at threonine 157 and modulation of its cellular localization. Nat Med, *8:* 1145-1152, 2002.
445. Shapiro, E., Becich, M. J., Hartanto, V., and Lepor, H. The relative proportion of stromal and epithelial hyperplasia is related to the development of symptomatic benign prostate hyperplasia. J Urol, *147:* 1293-1297, 1992.
446. Sommerfeld, H. J., Meeker, A. K., Piatyszek, M. A., Bova, G. S., Shay, J. W., and Coffey, D. S. Telomerase activity: a prevalent marker of malignant human prostate tissue. Cancer Res, *56:* 218-222, 1996.
447. Heaphy, C. M., Treat, E. G., Fleet, T. M., Bisoffi, M., Smith, A. Y., Davis, M. S., Fischer, E. G., and Griffith, J. K. Field effect revealed by 3D-mapping of Telomere DNA Content and Allelic Imbalance in Whole Mount Prostates. American Urological Association. Orlando, 2008.

448. Lodygin, D., Diebold, J., and Hermeking, H. Prostate cancer is characterized by epigenetic silencing of 14-3-3sigma expression. Oncogene, *23:* 9034-9041, 2004.
449. Nikoleishvili, D., Pertia, A., Trsintsadze, O., Gogokhia, N., Managadze, L., and Chkhotua, A. Expression of p27((Kip1)), cyclin D3 and Ki67 in BPH, prostate cancer and hormone-treated prostate cancer cells. Int Urol Nephrol, 2008.
450. Nikoleishvili, D., Pertia, A., Tsintsadze, O., Gogokhia, N., and Chkhotua, A. Down-regulation of p27(Kip 1) cyclin-dependent kinase inhibitor in prostate cancer: distinct expression in various prostate cells associating with tumor stage and grades. Georgian Med News*:* 34-38, 2007.
451. Castro, P., Giri, D., Lamb, D., and Ittmann, M. Cellular senescence in the pathogenesis of benign prostatic hyperplasia. Prostate, *55:* 30-38, 2003.
452. Bullock, M. J., Srigley, J. R., Klotz, L. H., and Goldenberg, S. L. Pathologic effects of neoadjuvant cyproterone acetate on nonneoplastic prostate, prostatic intraepithelial neoplasia, and adenocarcinoma: a detailed analysis of radical prostatectomy specimens from a randomized trial. Am J Surg Pathol, *26:* 1400-1413, 2002.
453. van der Kwast, T. H., Labrie, F., and Tetu, B. Prostatic intraepithelial neoplasia and endocrine manipulation. Eur Urol, *35:* 508-510, 1999.
454. van der Kwast, T. H., Labrie, F., and Tetu, B. Persistence of high-grade prostatic intra-epithelial neoplasia under combined androgen blockade therapy. Hum Pathol, *30:* 1503-1507, 1999.
455. Anderson, C. J., Hoare, S. F., Ashcroft, M., Bilsland, A. E., and Keith, W. N. Hypoxic regulation of telomerase gene expression by transcriptional and post-transcriptional mechanisms. Oncogene, *25:* 61-69, 2006.
456. Milosevic, M., Chung, P., Parker, C., Bristow, R., Toi, A., Panzarella, T., Warde, P., Catton, C., Menard, C., Bayley, A., Gospodarowicz, M., and Hill, R. Androgen withdrawal in patients reduces prostate cancer hypoxia: implications for disease progression and radiation response. Cancer Res, *67:* 6022-6025, 2007.
457. Parker, C., Milosevic, M., Toi, A., Sweet, J., Panzarella, T., Bristow, R., Catton, C., Catton, P., Crook, J., Gospodarowicz, M., McLean, M., Warde, P., and Hill, R. P. Polarographic electrode study of tumor oxygenation in clinically localized prostate cancer. Int J Radiat Oncol Biol Phys, *58:* 750-757, 2004.
458. Miyake, H., Hara, I., Kamidono, S., and Eto, H. Oxidative DNA damage in patients with prostate cancer and its response to treatment. J Urol, *171:* 1533-1536, 2004.
459. Kekeeva, T. V., Popova, O. P., Shegai, P. V., Zavalishina, L. E., Andreeva, I., Zaletaev, D. V., and Nemtsova, M. V. [Frequent allelic losses in tumor-associated stromal cells and tumor epitelium of prostate cancer]. Mol Biol (Mosk), *42:* 96-101, 2008.
460. Hermans, K. G., van Alewijk, D. C., Veltman, J. A., van Weerden, W., van Kessel, A. G., and Trapman, J. Loss of a small region around the PTEN locus is a major chromosome 10 alteration in prostate cancer xenografts and cell lines. Genes Chromosomes Cancer, *39:* 171-184, 2004.
461. Watson, S. K., deLeeuw, R. J., Horsman, D. E., Squire, J. A., and Lam, W. L. Cytogenetically balanced translocations are associated with focal copy number alterations. Hum Genet, *120:* 795-805, 2007.
462. Poonepalli, A., Banerjee, B., Ramnarayanan, K., Palanisamy, N., Putti, T. C., and Hande, M. P. Telomere-mediated genomic instability and the clinico-pathological parameters in breast cancer. Genes Chromosomes Cancer, 2008.
463. Jin, Y., Stewenius, Y., Lindgren, D., Frigyesi, A., Calcagnile, O., Jonson, T., Edqvist, A., Larsson, N., Lundberg, L. M., Chebil, G., Liedberg, F., Gudjonsson, S., Mansson, W., Hoglund, M., and Gisselsson, D. Distinct mitotic segregation errors mediate

chromosomal instability in aggressive urothelial cancers. Clin Cancer Res, *13:* 1703-1712, 2007.
464. Gisselsson, D., Gorunova, L., Hoglund, M., Mandahl, N., and Elfving, P. Telomere shortening and mitotic dysfunction generate cytogenetic heterogeneity in a subgroup of renal cell carcinomas. Br J Cancer, *91:* 327-332, 2004.
465. Hoglund, M., Gisselsson, D., Hansen, G. B., Sall, T., and Mitelman, F. Ovarian carcinoma develops through multiple modes of chromosomal evolution. Cancer Res, *63:* 3378-3385, 2003.
466. Gisselsson, D., Lv, M., Tsao, S. W., Man, C., Jin, C., Hoglund, M., Kwong, Y. L., and Jin, Y. Telomere-mediated mitotic disturbances in immortalized ovarian epithelial cells reproduce chromosomal losses and breakpoints from ovarian carcinoma. Genes Chromosomes Cancer, *42:* 22-33, 2005.
467. Gisselsson, D., Jonson, T., Yu, C., Martins, C., Mandahl, N., Wiegant, J., Jin, Y., Mertens, F., and Jin, C. Centrosomal abnormalities, multipolar mitoses, and chromosomal instability in head and neck tumours with dysfunctional telomeres. Br J Cancer, *87:* 202-207, 2002.
468. Akbay, E. A., Contreras, C. M., Perera, S. A., Sullivan, J. P., Broaddus, R. R., Schorge, J. O., Ashfaq, R., Saboorian, H., Wong, K. K., and Castrillon, D. H. Differential roles of telomere attrition in type I and II endometrial carcinogenesis. Am J Pathol, *173:* 536-544, 2008.
469. Bayani, J., Selvarajah, S., Maire, G., Vukovic, B., Al-Romaih, K., Zielenska, M., and Squire, J. A. Genomic mechanisms and measurement of structural and numerical instability in cancer cells. Semin Cancer Biol, *17:* 5-18, 2007.
470. Murga, M. and Fernandez-Capetillo, O. Genomic instability: on the birth and death of cancer. Clin Transl Oncol, *9:* 216-220, 2007.
471. Hoeijmakers, J. H. Genome maintenance mechanisms for preventing cancer. Nature, *411:* 366-374, 2001.
472. Wang, J. Y., Ho, T., Trojanek, J., Chintapalli, J., Grabacka, M., Stoklosa, T., Garcia, F. U., Skorski, T., and Reiss, K. Impaired homologous recombination DNA repair and enhanced sensitivity to DNA damage in prostate cancer cells exposed to anchorage-independence. Oncogene, *24:* 3748-3758, 2005.
473. Chan, N., Milosevic, M., and Bristow, R. G. Tumor hypoxia, DNA repair and prostate cancer progression: new targets and new therapies. Future Oncol, *3:* 329-341, 2007.
474. El-Zein, R., Gu, Y., Sierra, M. S., Spitz, M. R., and Strom, S. S. Chromosomal instability in peripheral blood lymphocytes and risk of prostate cancer. Cancer Epidemiol Biomarkers Prev, *14:* 748-752, 2005.
475. Parada, L. A., McQueen, P. G., Munson, P. J., and Misteli, T. Conservation of relative chromosome positioning in normal and cancer cells. Curr Biol, *12:* 1692-1697, 2002.
476. Abeysinghe, S. S., Chuzhanova, N., Krawczak, M., Ball, E. V., and Cooper, D. N. Translocation and gross deletion breakpoints in human inherited disease and cancer I: Nucleotide composition and recombination-associated motifs. Hum Mutat, *22:* 229-244, 2003.
477. Chuzhanova, N., Abeysinghe, S. S., Krawczak, M., and Cooper, D. N. Translocation and gross deletion breakpoints in human inherited disease and cancer II: Potential involvement of repetitive sequence elements in secondary structure formation between DNA ends. Hum Mutat, *22:* 245-251, 2003.
478. Bornens, M. Cell polarity: intrinsic or externally imposed? New Biol, *3:* 627-636, 1991.
479. Whitehead, C. M. and Salisbury, J. L. Regulation and regulatory activities of centrosomes. J Cell Biochem, *Suppl 32-33:* 192-199, 1999.

480. Rizzolo, L. J. and Joshi, H. C. Apical orientation of the microtubule organizing center and associated gamma-tubulin during the polarization of the retinal pigment epithelium in vivo. Dev Biol, *157:* 147-156, 1993.
481. Meads, T. and Schroer, T. A. Polarity and nucleation of microtubules in polarized epithelial cells. Cell Motil Cytoskeleton, *32:* 273-288, 1995.
482. Brown, C. R., Doxsey, S. J., Hong-Brown, L. Q., Martin, R. L., and Welch, W. J. Molecular chaperones and the centrosome. A role for TCP-1 in microtubule nucleation. J Biol Chem, *271:* 824-832, 1996.
483. Brown, C. R., Hong-Brown, L. Q., Doxsey, S. J., and Welch, W. J. Molecular chaperones and the centrosome. A role for HSP 73 in centrosomal repair following heat shock treatment. J Biol Chem, *271:* 833-840, 1996.
484. Pines, J. Four-dimensional control of the cell cycle. Nat Cell Biol, *1:* E73-79, 1999.
485. Buschhorn, H. M., Klein, R. R., Chambers, S. M., Hardy, M. C., Green, S., Bearss, D., and Nagle, R. B. Aurora-A over-expression in high-grade PIN lesions and prostate cancer. Prostate, *64:* 341-346, 2005.
486. Lee, E. C., Frolov, A., Li, R., Ayala, G., and Greenberg, N. M. Targeting Aurora kinases for the treatment of prostate cancer. Cancer Res, *66:* 4996-5002, 2006.
487. Jones, P. A. and Laird, P. W. Cancer epigenetics comes of age. Nat Genet, *21:* 163-167, 1999.
488. Rodriguez-Canales, J., Hanson, J. C., Tangrea, M. A., Erickson, H. S., Albert, P. S., Wallis, B. S., Richardson, A. M., Pinto, P. A., Linehan, W. M., Gillespie, J. W., Merino, M. J., Libutti, S. K., Woodson, K. G., Emmert-Buck, M. R., and Chuaqui, R. F. Identification of a unique epigenetic sub-microenvironment in prostate cancer. J Pathol, *211:* 410-419, 2007.
489. Issa, J. P., Ottaviano, Y. L., Celano, P., Hamilton, S. R., Davidson, N. E., and Baylin, S. B. Methylation of the oestrogen receptor CpG island links ageing and neoplasia in human colon. Nat Genet, *7:* 536-540, 1994.
490. Shay, J. W. and Wright, W. E. Hayflick, his limit, and cellular ageing. Nat Rev Mol Cell Biol, *1:* 72-76, 2000.
491. Jeyapalan, J. C., Ferreira, M., Sedivy, J. M., and Herbig, U. Accumulation of senescent cells in mitotic tissue of aging primates. Mech Ageing Dev, *128:* 36-44, 2007.
492. Figueroa, R., Lindenmaier, H., Hergenhahn, M., Nielsen, K. V., and Boukamp, P. Telomere erosion varies during in vitro aging of normal human fibroblasts from young and adult donors. Cancer Res, *60:* 2770-2774, 2000.
493. Parrinello, S., Coppe, J. P., Krtolica, A., and Campisi, J. Stromal-epithelial interactions in aging and cancer: senescent fibroblasts alter epithelial cell differentiation. J Cell Sci, *118:* 485-496, 2005.
494. Martens, J. W., Sieuwerts, A. M., Bolt-deVries, J., Bosma, P. T., Swiggers, S. J., Klijn, J. G., and Foekens, J. A. Aging of stromal-derived human breast fibroblasts might contribute to breast cancer progression. Thromb Haemost, *89:* 393-404, 2003.
495. Krtolica, A. and Campisi, J. Cancer and aging: a model for the cancer promoting effects of the aging stroma. Int J Biochem Cell Biol, *34:* 1401-1414, 2002.
496. Krtolica, A. and Campisi, J. Integrating epithelial cancer, aging stroma and cellular senescence. Adv Gerontol, *11:* 109-116, 2003.
497. Sternlicht, M. D., Lochter, A., Sympson, C. J., Huey, B., Rougier, J. P., Gray, J. W., Pinkel, D., Bissell, M. J., and Werb, Z. The stromal proteinase MMP3/stromelysin-1 promotes mammary carcinogenesis. Cell, *98:* 137-146, 1999.
498. O'Shaughnessy, J. A., Kelloff, G. J., Gordon, G. B., Dannenberg, A. J., Hong, W. K., Fabian, C. J., Sigman, C. C., Bertagnolli, M. M., Stratton, S. P., Lam, S., Nelson, W. G.,

Meyskens, F. L., Alberts, D. S., Follen, M., Rustgi, A. K., Papadimitrakopoulou, V., Scardino, P. T., Gazdar, A. F., Wattenberg, L. W., Sporn, M. B., Sakr, W. A., Lippman, S. M., and Von Hoff, D. D. Treatment and prevention of intraepithelial neoplasia: an important target for accelerated new agent development. Clin Cancer Res, *8:* 314-346, 2002.

499. Bostwick, D. G. Prostatic intraepithelial neoplasia (PIN): current concepts. J Cell Biochem Suppl, *16H:* 10-19, 1992.
500. Sakr, W. A., Billis, A., Ekman, P., Wilt, T., and Bostwick, D. G. Epidemiology of high-grade prostatic intraepithelial neoplasia. Scand J Urol Nephrol Suppl*:* 11-18, 2000.
501. Price, D., Stein, B., Sieber, P., Tutrone, R., Bailen, J., Goluboff, E., Burzon, D., Bostwick, D., and Steiner, M. Toremifene for the prevention of prostate cancer in men with high grade prostatic intraepithelial neoplasia: results of a double-blind, placebo controlled, phase IIB clinical trial. J Urol, *176:* 965-970; discussion 970-961, 2006.
502. Gautschi, O., Heighway, J., Mack, P. C., Purnell, P. R., Lara, P. N., Jr., and Gandara, D. R. Aurora kinases as anticancer drug targets. Clin Cancer Res, *14:* 1639-1648, 2008.
503. Jagadeesh, S., Kyo, S., and Banerjee, P. P. Genistein represses telomerase activity via both transcriptional and posttranslational mechanisms in human prostate cancer cells. Cancer Res, *66:* 2107-2115, 2006.
504. Ouchi, H., Ishiguro, H., Ikeda, N., Hori, M., Kubota, Y., and Uemura, H. Genistein induces cell growth inhibition in prostate cancer through the suppression of telomerase activity. Int J Urol, *12:* 73-80, 2005.
505. Bermudez, Y., Ahmadi, S., Lowell, N. E., and Kruk, P. A. Vitamin E suppresses telomerase activity in ovarian cancer cells. Cancer Detect Prev, *31:* 119-128, 2007.
506. Turner, D. P. and Watson, D. K. ETS transcription factors: oncogenes and tumor suppressor genes as therapeutic targets for prostate cancer. Expert Rev Anticancer Ther, *8:* 33-42, 2008.
507. George, D. J., Armstrong, A. J., Creel, P., Morris, K., Madden, J., Turnbull, J., Dewhirst, M., Major, N., and Febbo, P. G. A phase II study of RAD001 in men with hormone-refractory metastatic prostate cancer (HRPC). *In:* American Society of Clinical Oncology Genito-Urinary Cancers Symposium, San Francisco, 2008.
508. Chee, K. G., Longmate, J., Quinn, D. I., Chatta, G., Pinski, J., Twardowski, P., Pan, C. X., Cambio, A., Evans, C. P., Gandara, D. R., and Lara, P. N., Jr. The AKT inhibitor perifosine in biochemically recurrent prostate cancer: a phase II California/Pittsburgh cancer consortium trial. Clin Genitourin Cancer, *5:* 433-437, 2007.
509. Fine, J. L., Grzybicki, D. M., Silowash, R., Ho, J., Gilbertson, J. R., Anthony, L., Wilson, R., Parwani, A. V., Bastacky, S. I., Epstein, J. I., and Jukic, D. M. Evaluation of whole slide image immunohistochemistry interpretation in challenging prostate needle biopsies. Hum Pathol, *39:* 564-572, 2008.
510. Cregger, M., Berger, A. J., and Rimm, D. L. Immunohistochemistry and quantitative analysis of protein expression. Arch Pathol Lab Med, *130:* 1026-1030, 2006.
511. Tang, D., Liu, J. J., Rundle, A., Neslund-Dudas, C., Savera, A. T., Bock, C. H., Nock, N. L., Yang, J. J., and Rybicki, B. A. Grilled meat consumption and PhIP-DNA adducts in prostate carcinogenesis. Cancer Epidemiol Biomarkers Prev, *16:* 803-808, 2007.
512. Lauber, S. N., Ali, S., and Gooderham, N. J. The cooked food derived carcinogen 2-amino-1-methyl-6-phenylimidazo[4,5-b] pyridine is a potent oestrogen: a mechanistic basis for its tissue-specific carcinogenicity. Carcinogenesis, *25:* 2509-2517, 2004.
513. Zhang, Y., Wang, Z., Ahmed, F., Banerjee, S., Li, Y., and Sarkar, F. H. Down-regulation of Jagged-1 induces cell growth inhibition and S phase arrest in prostate cancer cells. Int J Cancer, *119:* 2071-2077, 2006.

514. Chandramohan, V., Mineva, N. D., Burke, B., Jeay, S., Wu, M., Shen, J., Yang, W., Hann, S. R., and Sonenshein, G. E. c-Myc represses FOXO3a-mediated transcription of the gene encoding the p27(Kip1) cyclin dependent kinase inhibitor. J Cell Biochem, *104:* 2091-2106, 2008.
515. Courtois-Cox, S., Jones, S. L., and Cichowski, K. Many roads lead to oncogene-induced senescence. Oncogene, *27:* 2801-2809, 2008.
516. Mai, S. and Garini, Y. Oncogenic remodeling of the three-dimensional organization of the interphase nucleus: c-Myc induces telomeric aggregates whose formation precedes chromosomal rearrangements. Cell Cycle, *4:* 1327-1331, 2005.
517. Shay, J. W. and Wright, W. E. Senescence and immortalization: role of telomeres and telomerase. Carcinogenesis, *26:* 867-874, 2005.
518. Liu, J. P. Studies of the molecular mechanisms in the regulation of telomerase activity. Faseb J, *13:* 2091-2104, 1999.
519. Chen, Z., Koeneman, K. S., and Corey, D. R. Consequences of telomerase inhibition and combination treatments for the proliferation of cancer cells. Cancer Res, *63:* 5917-5925, 2003.
520. Zhu, X. D., Kuster, B., Mann, M., Petrini, J. H., and de Lange, T. Cell-cycle-regulated association of RAD50/MRE11/NBS1 with TRF2 and human telomeres. Nat Genet, *25:* 347-352, 2000.
521. Opresko, P. L., von Kobbe, C., Laine, J. P., Harrigan, J., Hickson, I. D., and Bohr, V. A. Telomere-binding protein TRF2 binds to and stimulates the Werner and Bloom syndrome helicases. J Biol Chem, *277:* 41110-41119, 2002.
522. Celli, G. B., Denchi, E. L., and de Lange, T. Ku70 stimulates fusion of dysfunctional telomeres yet protects chromosome ends from homologous recombination. Nat Cell Biol, *8:* 885-890, 2006.
523. Seimiya, H., Sawada, H., Muramatsu, Y., Shimizu, M., Ohko, K., Yamane, K., and Tsuruo, T. Involvement of 14-3-3 proteins in nuclear localization of telomerase. Embo J, *19:* 2652-2661, 2000.
524. Fenic, I., Franke, F., Failing, K., Steger, K., and Woenckhaus, J. Expression of PTEN in malignant and non-malignant human prostate tissues: comparison with p27 protein expression. J Pathol, *203:* 559-566, 2004.
525. Courtois-Cox, S., Genther Williams, S. M., Reczek, E. E., Johnson, B. W., McGillicuddy, L. T., Johannessen, C. M., Hollstein, P. E., MacCollin, M., and Cichowski, K. A negative feedback signaling network underlies oncogene-induced senescence. Cancer Cell, *10:* 459-472, 2006.
526. Shao, G., Balajee, A. S., Hei, T. K., and Zhao, Y. p16(INK4a) downregulation is involved in immortalization of primary human prostate epithelial cells induced by telomerase. Mol Carcinog, *47:* 775-783, 2008.
527. Kekeeva, T. V., Popova, O. P., Shegai, P. V., Alekseev, B., Adnreeva, I., Zaletaev, D. V., and Nemtsova, M. V. [Abberant methylation of p16, HIC1, N33 and GSTP1 genes in tumor epitelium and tumor-associated stromal cells of prostate cancer]. Mol Biol (Mosk), *41:* 79-85, 2007.
528. Untergasser, G., Koch, H. B., Menssen, A., and Hermeking, H. Characterization of epithelial senescence by serial analysis of gene expression: identification of genes potentially involved in prostate cancer. Cancer Res, *62:* 6255-6262, 2002.
529. Bartkova, J., Rezaei, N., Liontos, M., Karakaidos, P., Kletsas, D., Issaeva, N., Vassiliou, L. V., Kolettas, E., Niforou, K., Zoumpourlis, V. C., Takaoka, M., Nakagawa, H., Tort, F., Fugger, K., Johansson, F., Sehested, M., Andersen, C. L., Dyrskjot, L., Orntoft, T., Lukas, J., Kittas, C., Helleday, T., Halazonetis, T. D., Bartek, J., and Gorgoulis, V. G.

Oncogene-induced senescence is part of the tumorigenesis barrier imposed by DNA damage checkpoints. Nature, *444:* 633-637, 2006.
530. Xin, H., Curry, J., Johnstone, R. W., Nickoloff, B. J., and Choubey, D. Role of IFI 16, a member of the interferon-inducible p200-protein family, in prostate epithelial cellular senescence. Oncogene, *22:* 4831-4840, 2003.
531. Narita, M., Nunez, S., Heard, E., Narita, M., Lin, A. W., Hearn, S. A., Spector, D. L., Hannon, G. J., and Lowe, S. W. Rb-mediated heterochromatin formation and silencing of E2F target genes during cellular senescence. Cell, *113:* 703-716, 2003.
532. Di Micco, R., Fumagalli, M., Cicalese, A., Piccinin, S., Gasparini, P., Luise, C., Schurra, C., Garre, M., Nuciforo, P. G., Bensimon, A., Maestro, R., Pelicci, P. G., and d'Adda di Fagagna, F. Oncogene-induced senescence is a DNA damage response triggered by DNA hyper-replication. Nature, *444:* 638-642, 2006.
533. Greenberg, R. A., O'Hagan, R. C., Deng, H., Xiao, Q., Hann, S. R., Adams, R. R., Lichtsteiner, S., Chin, L., Morin, G. B., and DePinho, R. A. Telomerase reverse transcriptase gene is a direct target of c-Myc but is not functionally equivalent in cellular transformation. Oncogene, *18:* 1219-1226, 1999.
534. Hughes, S., Arneson, N., Done, S., and Squire, J. The use of whole genome amplification in the study of human disease. Prog Biophys Mol Biol, *88:* 173-189, 2005.
535. Rubin, M. A. and Chinnaiyan, A. M. Bioinformatics approach leads to the discovery of the TMPRSS2:ETS gene fusion in prostate cancer. Lab Invest, *86:* 1099-1102, 2006.
536. Liu, D., O'Connor, M. S., Qin, J., and Songyang, Z. Telosome, a mammalian telomere-associated complex formed by multiple telomeric proteins. J Biol Chem, *279:* 51338-51342, 2004.
537. de Lange, T. Shelterin: the protein complex that shapes and safeguards human telomeres. Genes Dev, *19:* 2100-2110, 2005.
538. Bilaud, T., Brun, C., Ancelin, K., Koering, C. E., Laroche, T., and Gilson, E. Telomeric localization of TRF2, a novel human telobox protein. Nat Genet, *17:* 236-239, 1997.
539. Broccoli, D., Smogorzewska, A., Chong, L., and de Lange, T. Human telomeres contain two distinct Myb-related proteins, TRF1 and TRF2. Nat Genet, *17:* 231-235, 1997.
540. Smith, S., Giriat, I., Schmitt, A., and de Lange, T. Tankyrase, a poly(ADP-ribose) polymerase at human telomeres. Science, *282:* 1484-1487, 1998.
541. Smogorzewska, A. and de Lange, T. Regulation of telomerase by telomeric proteins. Annu Rev Biochem, *73:* 177-208, 2004.
542. Hsu, C. P., Ko, J. L., Shai, S. E., and Lee, L. W. Modulation of telomere shelterin by TRF1 [corrected] and TRF2 interacts with telomerase to maintain the telomere length in non-small cell lung cancer. Lung Cancer, *58:* 310-316, 2007.
543. Salhab, M., Jiang, W. G., Newbold, R. F., and Mokbel, K. The expression of gene transcripts of telomere-associated genes in human breast cancer: correlation with clinico-pathological parameters and clinical outcome. Breast Cancer Res Treat, *109:* 35-46, 2008.
544. Lin, X., Gu, J., Lu, C., Spitz, M. R., and Wu, X. Expression of telomere-associated genes as prognostic markers for overall survival in patients with non-small cell lung cancer. Clin Cancer Res, *12:* 5720-5725, 2006.
545. Hsu, C. P., Lee, L. W., Shai, S. E., and Chen, C. Y. Clinical significance of telomerase and its associate genes expression in the maintenance of telomere length in squamous cell carcinoma of the esophagus. World J Gastroenterol, *11:* 6941-6947, 2005.
546. Yamada, M., Tsuji, N., Nakamura, M., Moriai, R., Kobayashi, D., Yagihashi, A., and Watanabe, N. Down-regulation of TRF1, TRF2 and TIN2 genes is important to maintain telomeric DNA for gastric cancers. Anticancer Res, *22:* 3303-3307, 2002.

547. Yajima, T., Yagihashi, A., Kameshima, H., Kobayashi, D., Hirata, K., and Watanabe, N. Telomerase reverse transcriptase and telomeric-repeat binding factor protein 1 as regulators of telomerase activity in pancreatic cancer cells. Br J Cancer, *85:* 752-757, 2001.
548. Garcia-Aranda, C., de Juan, C., Diaz-Lopez, A., Sanchez-Pernaute, A., Torres, A. J., Diaz-Rubio, E., Balibrea, J. L., Benito, M., and Iniesta, P. Correlations of telomere length, telomerase activity, and telomeric-repeat binding factor 1 expression in colorectal carcinoma. Cancer, *106:* 541-551, 2006.
549. Vergis, R., Corbishley, C. M., Norman, A. R., Bartlett, J., Jhavar, S., Borre, M., Heeboll, S., Horwich, A., Huddart, R., Khoo, V., Eeles, R., Cooper, C., Sydes, M., Dearnaley, D., and Parker, C. Intrinsic markers of tumour hypoxia and angiogenesis in localised prostate cancer and outcome of radical treatment: a retrospective analysis of two randomised radiotherapy trials and one surgical cohort study. Lancet Oncol, *9:* 342-351, 2008.
550. Chen, L., Stacewicz-Sapuntzakis, M., Duncan, C., Sharifi, R., Ghosh, L., van Breemen, R., Ashton, D., and Bowen, P. E. Oxidative DNA damage in prostate cancer patients consuming tomato sauce-based entrees as a whole-food intervention. J Natl Cancer Inst, *93:* 1872-1879, 2001.
551. van de Vijver, M., Bilous, M., Hanna, W., Hofmann, M., Kristel, P., Penault-Llorca, F., and Ruschoff, J. Chromogenic in situ hybridisation for the assessment of HER2 status in breast cancer: an international validation ring study. Breast Cancer Res, *9:* R68, 2007.
552. Pothos, A., Plastira, K., Plastiras, A., Vlachodimitropoulos, D., Goutas, N., and Angelopoulou, R. Comparison of chromogenic in situ hybridisation with fluorescence in situ hybridisation and immunohistochemistry for the assessment of her-2/neu oncogene in archival material of breast carcinoma. Acta Histochem Cytochem, *41:* 59-64, 2008.
553. Stewart, J., Fleshner, N., Cole, H., and Sweet, J. Comparison of annexin II, p63 and alpha-methylacyl-CoA racemase immunoreactivity in prostatic tissue: a tissue microarray study. J Clin Pathol, *60:* 773-780, 2007.
554. Mosquera, J. M., Perner, S., Genega, E. M., Sanda, M., Hofer, M. D., Mertz, K. D., Paris, P. L., Simko, J., Bismar, T. A., Ayala, G., Shah, R. B., Loda, M., and Rubin, M. A. Characterization of TMPRSS2-ERG fusion high-grade prostatic intraepithelial neoplasia and potential clinical implications. Clin Cancer Res, *14:* 3380-3385, 2008.
555. Yanke, B. V., Gonen, M., Scardino, P. T., and Kattan, M. W. Validation of a nomogram for predicting positive repeat biopsy for prostate cancer. J Urol, *173:* 421-424, 2005.
556. Folini, M., Brambilla, C., Villa, R., Gandellini, P., Vignati, S., Paduano, F., Daidone, M. G., and Zaffaroni, N. Antisense oligonucleotide-mediated inhibition of hTERT, but not hTERC, induces rapid cell growth decline and apoptosis in the absence of telomere shortening in human prostate cancer cells. Eur J Cancer, *41:* 624-634, 2005.
557. Incles, C. M., Schultes, C. M., Kempski, H., Koehler, H., Kelland, L. R., and Neidle, S. A G-quadruplex telomere targeting agent produces p16-associated senescence and chromosomal fusions in human prostate cancer cells. Mol Cancer Ther, *3:* 1201-1206, 2004.
558. Asai, A., Oshima, Y., Yamamoto, Y., Uochi, T. A., Kusaka, H., Akinaga, S., Yamashita, Y., Pongracz, K., Pruzan, R., Wunder, E., Piatyszek, M., Li, S., Chin, A. C., Harley, C. B., and Gryaznov, S. A novel telomerase template antagonist (GRN163) as a potential anticancer agent. Cancer Res, *63:* 3931-3939, 2003.
559. Shammas, M. A., Qazi, A., Batchu, R. B., Bertheau, R. C., Wong, J. Y., Rao, M. Y., Prasad, M., Chanda, D., Ponnazhagan, S., Anderson, K. C., Steffes, C. P., Munshi, N. C., De Vivo, I., Beer, D. G., Gryaznov, S., Weaver, D. W., and Goyal, R. K. Telomere

maintenance in laser capture microdissection-purified Barrett's adenocarcinoma cells and effect of telomerase inhibition in vivo. Clin Cancer Res, *14:* 4971-4980, 2008.
560. Canales, B. K., Li, Y., Thompson, M. G., Gleason, J. M., Chen, Z., Malaeb, B., Corey, D. R., Herbert, B. S., Shay, J. W., and Koeneman, K. S. Small molecule, oligonucleotide-based telomerase template inhibition in combination with cytolytic therapy in an in vitro androgen-independent prostate cancer model. Urol Oncol, *24:* 141-151, 2006.
561. Gryaznov, S. M., Jackson, S., Dikmen, G., Harley, C., Herbert, B. S., Wright, W. E., and Shay, J. W. Oligonucleotide conjugate GRN163L targeting human telomerase as potential anticancer and antimetastatic agent. Nucleosides Nucleotides Nucleic Acids, *26:* 1577-1579, 2007.
562. Yoshimoto, M., Cutz, J. C., Nuin, P. A., Joshua, A. M., Bayani, J., Evans, A. J., Zielenska, M., and Squire, J. A. Interphase FISH analysis of PTEN in histologic sections shows genomic deletions in 68% of primary prostate cancer and 23% of high-grade prostatic intra-epithelial neoplasias. Cancer Genet Cytogenet, *169:* 128-137, 2006.
563. Bertram, J., Peacock, J. W., Fazli, L., Mui, A. L., Chung, S. W., Cox, M. E., Monia, B., Gleave, M. E., and Ong, C. J. Loss of PTEN is associated with progression to androgen independence. Prostate, *66:* 895-902, 2006.
564. Schmitz, M., Grignard, G., Margue, C., Dippel, W., Capesius, C., Mossong, J., Nathan, M., Giacchi, S., Scheiden, R., and Kieffer, N. Complete loss of PTEN expression as a possible early prognostic marker for prostate cancer metastasis. Int J Cancer, 2006.
565. Whang, Y. E., Wu, X., Suzuki, H., Reiter, R. E., Tran, C., Vessella, R. L., Said, J. W., Isaacs, W. B., and Sawyers, C. L. Inactivation of the tumor suppressor PTEN/MMAC1 in advanced human prostate cancer through loss of expression. Proc Natl Acad Sci U S A, *95:* 5246-5250, 1998.
566. Ahlers, C. M. and Figg, W. D. ETS-TMPRSS2 fusion gene products in prostate cancer. Cancer Biol Ther, *5:* 254-255, 2006.
567. Kawai, T., Hiroi, S., Nakanishi, K., Sakurai, Y., and Torikata, C. Abnormalities in chromosome 17 and p53 in lung carcinoma cells detected by fluorescence in situ hybridization. Pathol Int, *54:* 413-419, 2004.
568. Korshunov, A., Sycheva, R., Gorelyshev, S., and Golanov, A. Clinical utility of fluorescence in situ hybridization (FISH) in nonbrainstem glioblastomas of childhood. Mod Pathol, *18:* 1258-1263, 2005.
569. Mezzelani, A., Alasio, L., Bartoli, C., Bonora, M. G., Pierotti, M. A., Rilke, F., and Pilotti, S. c-erbB2/neu gene and chromosome 17 analysis in breast cancer by FISH on archival cytological fine-needle aspirates. Br J Cancer, *80:* 519-525, 1999.
570. Trotman, L. C., Niki, M., Dotan, Z. A., Koutcher, J. A., Di Cristofano, A., Xiao, A., Khoo, A. S., Roy-Burman, P., Greenberg, N. M., Van Dyke, T., Cordon-Cardo, C., and Pandolfi, P. P. Pten dose dictates cancer progression in the prostate. PLoS Biol, *1:* E59, 2003.
571. Kotelevets, L., van Hengel, J., Bruyneel, E., Mareel, M., van Roy, F., and Chastre, E. Implication of the MAGI-1b/PTEN signalosome in stabilization of adherens junctions and suppression of invasiveness. Faseb J, *19:* 115-117, 2005.
572. Majumder, P. K. and Sellers, W. R. Akt-regulated pathways in prostate cancer. Oncogene, *24:* 7465-7474, 2005.
573. Liu, X. H., Kirschenbaum, A., Yu, K., Yao, S., and Levine, A. C. Cyclooxygenase-2 suppresses hypoxia-induced apoptosis via a combination of direct and indirect inhibition of p53 activity in a human prostate cancer cell line. J Biol Chem, *280:* 3817-3823, 2005.

574. Tanaka, M., Rosser, C. J., and Grossman, H. B. PTEN gene therapy induces growth inhibition and increases efficacy of chemotherapy in prostate cancer. Cancer Detect Prev, *29:* 170-174, 2005.
575. Wu, L., Birle, D. C., and Tannock, I. F. Effects of the mammalian target of rapamycin inhibitor CCI-779 used alone or with chemotherapy on human prostate cancer cells and xenografts. Cancer Res, *65:* 2825-2831, 2005.
576. Lin, H. K., Hu, Y. C., Lee, D. K., and Chang, C. Regulation of androgen receptor signaling by PTEN (phosphatase and tensin homolog deleted on chromosome 10) tumor suppressor through distinct mechanisms in prostate cancer cells. Mol Endocrinol, *18:* 2409-2423, 2004.
577. Gopalan, A., Leversha, M., Satagopan, J. M., Zhou, Q. C., Al-Ahmadie, H. A., Fine, S. W., Scardino, P., Tickoo, S. K., Reuter, V., and Gerald, W. Increased Copy Number of TMPRSS2-ERG Fusion, but Not Translocation Alone, Is Associated with Aggressive Disease in Patients Treated by Prostatectomy. *In:* United States and Canadian Academy of Pathology Annual Meeting, Denver, 2008.
578. Milcent, S., Lorenzato, M., Enaschescu, D., Enaschescu, C., Birembaut, P., and Staerman, F. [Cell ploidy: predictive factor of locally advanced prostate cancer]. Prog Urol, *17:* 819-823, 2007.
579. Haggarth, L., Auer, G., Busch, C., Norberg, M., Haggman, M., and Egevad, L. The significance of tumor heterogeneity for prediction of DNA ploidy of prostate cancer. Scand J Urol Nephrol, *39:* 387-392, 2005.
580. Deliveliotis, C., Skolarikos, A., Karayannis, A., Tzelepis, V., Trakas, N., Alargof, E., and Protogerou, V. The prognostic value of p53 and DNA ploidy following radical prostatectomy. World J Urol, *21:* 171-176, 2003.
581. Hsu, T., Trojanowska, M., and Watson, D. K. Ets proteins in biological control and cancer. J Cell Biochem, *91:* 896-903, 2004.
582. Shukla, S., Maclennan, G. T., Hartman, D. J., Fu, P., Resnick, M. I., and Gupta, S. Activation of PI3K-Akt signaling pathway promotes prostate cancer cell invasion. Int J Cancer, *121:* 1424-1432, 2007.
583. Kotelevets, L., van Hengel, J., Bruyneel, E., Mareel, M., van Roy, F., and Chastre, E. The lipid phosphatase activity of PTEN is critical for stabilizing intercellular junctions and reverting invasiveness. J Cell Biol, *155:* 1129-1135, 2001.
584. Larue, L. and Bellacosa, A. Epithelial-mesenchymal transition in development and cancer: role of phosphatidylinositol 3' kinase/AKT pathways. Oncogene, *24:* 7443-7454, 2005.
585. Rhodes, D. R., Kalyana-Sundaram, S., Mahavisno, V., Varambally, R., Yu, J., Briggs, B. B., Barrette, T. R., Anstet, M. J., Kincead-Beal, C., Kulkarni, P., Varambally, S., Ghosh, D., and Chinnaiyan, A. M. Oncomine 3.0: genes, pathways, and networks in a collection of 18,000 cancer gene expression profiles. Neoplasia, *9:* 166-180, 2007.
586. Glinsky, G. V., Glinskii, A. B., Stephenson, A. J., Hoffman, R. M., and Gerald, W. L. Gene expression profiling predicts clinical outcome of prostate cancer. J Clin Invest, *113:* 913-923, 2004.
587. Maira, S. M., Galetic, I., Brazil, D. P., Kaech, S., Ingley, E., Thelen, M., and Hemmings, B. A. Carboxyl-terminal modulator protein (CTMP), a negative regulator of PKB/Akt and v-Akt at the plasma membrane. Science, *294:* 374-380, 2001.
588. Polette, M., Mestdagt, M., Bindels, S., Nawrocki-Raby, B., Hunziker, W., Foidart, J. M., Birembaut, P., and Gilles, C. Beta-catenin and ZO-1: shuttle molecules involved in tumor invasion-associated epithelial-mesenchymal transition processes. Cells Tissues Organs, *185:* 61-65, 2007.

589. Cairns, P., Okami, K., Halachmi, S., Halachmi, N., Esteller, M., Herman, J. G., Jen, J., Isaacs, W. B., Bova, G. S., and Sidransky, D. Frequent inactivation of PTEN/MMAC1 in primary prostate cancer. Cancer Res, *57:* 4997-5000, 1997.
590. Pesche, S., Latil, A., Muzeau, F., Cussenot, O., Fournier, G., Longy, M., Eng, C., and Lidereau, R. PTEN/MMAC1/TEP1 involvement in primary prostate cancers. Oncogene, *16:* 2879-2883, 1998.
591. Gray, I. C., Stewart, L. M., Phillips, S. M., Hamilton, J. A., Gray, N. E., Watson, G. J., Spurr, N. K., and Snary, D. Mutation and expression analysis of the putative prostate tumour-suppressor gene PTEN. Br J Cancer, *78:* 1296-1300, 1998.
592. Feilotter, H. E., Nagai, M. A., Boag, A. H., Eng, C., and Mulligan, L. M. Analysis of PTEN and the 10q23 region in primary prostate carcinomas. Oncogene, *16:* 1743-1748, 1998.
593. Wang, S. I., Parsons, R., and Ittmann, M. Homozygous deletion of the PTEN tumor suppressor gene in a subset of prostate adenocarcinomas. Clin Cancer Res, *4:* 811-815, 1998.
594. Suzuki, H., Freije, D., Nusskern, D. R., Okami, K., Cairns, P., Sidransky, D., Isaacs, W. B., and Bova, G. S. Interfocal heterogeneity of PTEN/MMAC1 gene alterations in multiple metastatic prostate cancer tissues. Cancer Res, *58:* 204-209, 1998.
595. Dong, J. T., Sipe, T. W., Hyytinen, E. R., Li, C. L., Heise, C., McClintock, D. E., Grant, C. D., Chung, L. W., and Frierson, H. F., Jr. PTEN/MMAC1 is infrequently mutated in pT2 and pT3 carcinomas of the prostate. Oncogene, *17:* 1979-1982, 1998.
596. Orikasa, K., Fukushige, S., Hoshi, S., Orikasa, S., Kondo, K., Miyoshi, Y., Kubota, Y., and Horii, A. Infrequent genetic alterations of the PTEN gene in Japanese patients with sporadic prostate cancer. J Hum Genet, *43:* 228-230, 1998.
597. Muller, M., Rink, K., Krause, H., and Miller, K. PTEN/MMAC1 mutations in prostate cancer. Prostate Cancer Prostatic Dis, *3:* S32, 2000.
598. Dong, J. T., Li, C. L., Sipe, T. W., and Frierson, H. F., Jr. Mutations of PTEN/MMAC1 in primary prostate cancers from Chinese patients. Clin Cancer Res, *7:* 304-308, 2001.
599. Halvorsen, O. J., Haukaas, S. A., and Akslen, L. A. Combined loss of PTEN and p27 expression is associated with tumor cell proliferation by Ki-67 and increased risk of recurrent disease in localized prostate cancer. Clin Cancer Res, *9:* 1474-1479, 2003.
600. Lieberfarb, M. E., Lin, M., Lechpammer, M., Li, C., Tanenbaum, D. M., Febbo, P. G., Wright, R. L., Shim, J., Kantoff, P. W., Loda, M., Meyerson, M., and Sellers, W. R. Genome-wide loss of heterozygosity analysis from laser capture microdissected prostate cancer using single nucleotide polymorphic allele (SNP) arrays and a novel bioinformatics platform dChipSNP. Cancer Res, *63:* 4781-4785, 2003.
601. Pourmand, G., Ziaee, A. A., Abedi, A. R., Mehrsai, A., Alavi, H. A., Ahmadi, A., and Saadati, H. R. Role of PTEN gene in progression of prostate cancer. Urol J, *4:* 95-100, 2007.
602. Hellwinkel, O. J., Rogmann, J. P., Asong, L. E., Luebke, A. M., Eichelberg, C., Ahyai, S., Isbarn, H., Graefen, M., Huland, H., and Schlomm, T. A comprehensive analysis of transcript signatures of the phosphatidylinositol-3 kinase/protein kinase B signal-transduction pathway in prostate cancer. BJU Int, *101:* 1454-1460, 2008.
603. Tannock, I. F., de Wit, R., Berry, W. R., Horti, J., Pluzanska, A., Chi, K. N., Oudard, S., Theodore, C., James, N. D., Turesson, I., Rosenthal, M. A., and Eisenberger, M. A. Docetaxel plus prednisone or mitoxantrone plus prednisone for advanced prostate cancer. N Engl J Med, *351:* 1502-1512, 2004.
604. Petrylak, D. P., Tangen, C. M., Hussain, M. H., Lara, P. N., Jr., Jones, J. A., Taplin, M. E., Burch, P. A., Berry, D., Moinpour, C., Kohli, M., Benson, M. C., Small, E. J.,

Raghavan, D., and Crawford, E. D. Docetaxel and estramustine compared with mitoxantrone and prednisone for advanced refractory prostate cancer. N Engl J Med, *351:* 1513-1520, 2004.
605. Furth, J. J. and Cohen, S. S. Inhibition of mammalian DNA polymerase by the 5'-triphosphate of 1-beta-d-arabinofuranosylcytosine and the 5'-triphosphate of 9-beta-d-arabinofuranoxyladenine. Cancer Res, *28:* 2061-2067, 1968.
606. Kufe, D. W., Major, P. P., Egan, E. M., and Beardsley, G. P. Correlation of cytotoxicity with incorporation of ara-C into DNA. J Biol Chem, *255:* 8997-8900, 1980.
607. Moore, E. C. and Cohen, S. S. Effects of arabinonucleotides on ribonucleotide reduction by an enzyme system from rat tumor. J Biol Chem, *242:* 2116-2118, 1967.
608. Dou, Q. P., An, B., and Will, P. L. Induction of a retinoblastoma phosphatase activity by anticancer drugs accompanies p53-independent G1 arrest and apoptosis. Proc Natl Acad Sci U S A, *92:* 9019-9023, 1995.
609. Ikeda, M. A., Jakoi, L., and Nevins, J. R. A unique role for the Rb protein in controlling E2F accumulation during cell growth and differentiation. Proc Natl Acad Sci U S A, *93:* 3215-3220, 1996.
610. Stegmaier, K., Wong, J. S., Ross, K. N., Chow, K. T., Peck, D., Wright, R. D., Lessnick, S. L., Kung, A. L., and Golub, T. R. Signature-based small molecule screening identifies cytosine arabinoside as an EWS/FLI modulator in Ewing sarcoma. PLoS Med, *4:* e122, 2007.
611. Peck, D., Crawford, E. D., Ross, K. N., Stegmaier, K., Golub, T. R., and Lamb, J. A method for high-throughput gene expression signature analysis. Genome Biol, *7:* R61, 2006.
612. Toub, N., Bertrand, J. R., Tamaddon, A., Elhamess, H., Hillaireau, H., Maksimenko, A., Maccario, J., Malvy, C., Fattal, E., and Couvreur, P. Efficacy of siRNA nanocapsules targeted against the EWS-Fli1 oncogene in Ewing sarcoma. Pharm Res, *23:* 892-900, 2006.
613. Bernstein, M., Kovar, H., Paulussen, M., Randall, R. L., Schuck, A., Teot, L. A., and Juergens, H. Ewing's sarcoma family of tumors: current management. Oncologist, *11:* 503-519, 2006.
614. Matsunobu, T., Tanaka, K., Nakamura, T., Nakatani, F., Sakimura, R., Hanada, M., Li, X., Okada, T., Oda, Y., Tsuneyoshi, M., and Iwamoto, Y. The possible role of EWS-Fli1 in evasion of senescence in Ewing family tumors. Cancer Res, *66:* 803-811, 2006.
615. Carrere, S., Verger, A., Flourens, A., Stehelin, D., and Duterque-Coquillaud, M. Erg proteins, transcription factors of the Ets family, form homo, heterodimers and ternary complexes via two distinct domains. Oncogene, *16:* 3261-3268, 1998.
616. Skehan, P., Storeng, R., Scudiero, D., Monks, A., McMahon, J., Vistica, D., Warren, J. T., Bokesch, H., Kenney, S., and Boyd, M. R. New colorimetric cytotoxicity assay for anticancer-drug screening. J Natl Cancer Inst, *82:* 1107-1112, 1990.
617. Early, A. P., Preisler, H. D., Slocum, H., and Rustum, Y. M. A pilot study of high-dose 1-beta-D-arabinofuranosylcytosine for acute leukemia and refractory lymphoma: clinical response and pharmacology. Cancer Res, *42:* 1587-1594, 1982.
618. Gandhok, N. and Sartor, O. Unexpected response of hormone-refractory prostate cancer to treatment with an antileukemic chemotherapy regimen. Urology, *64:* 807-809, 2004.
619. Scher, H. I., Halabi, S., Tannock, I., Morris, M., Sternberg, C. N., Carducci, M. A., Eisenberger, M. A., Higano, C., Bubley, G. J., Dreicer, R., Petrylak, D., Kantoff, P., Basch, E., Kelly, W. K., Figg, W. D., Small, E. J., Beer, T. M., Wilding, G., Martin, A., and Hussain, M. Design and end points of clinical trials for patients with progressive

prostate cancer and castrate levels of testosterone: recommendations of the Prostate Cancer Clinical Trials Working Group. J Clin Oncol, *26:* 1148-1159, 2008.

620. Herzig, R. H., Wolff, S. N., Lazarus, H. M., Phillips, G. L., Karanes, C., and Herzig, G. P. High-dose cytosine arabinoside therapy for refractory leukemia. Blood, *62:* 361-369, 1983.

621. Therasse, P., Arbuck, S. G., Eisenhauer, E. A., Wanders, J., Kaplan, R. S., Rubinstein, L., Verweij, J., Van Glabbeke, M., van Oosterom, A. T., Christian, M. C., and Gwyther, S. G. New guidelines to evaluate the response to treatment in solid tumors. European Organization for Research and Treatment of Cancer, National Cancer Institute of the United States, National Cancer Institute of Canada. J Natl Cancer Inst, *92:* 205-216, 2000.

622. Loughran, S. J., Kruse, E. A., Hacking, D. F., de Graaf, C. A., Hyland, C. D., Willson, T. A., Henley, K. J., Ellis, S., Voss, A. K., Metcalf, D., Hilton, D. J., Alexander, W. S., and Kile, B. T. The transcription factor Erg is essential for definitive hematopoiesis and the function of adult hematopoietic stem cells. Nat Immunol, *9:* 810-819, 2008.